UNIVERSIDADE FEDERAL DO CEARÁ
CENTRO DE CIÊNCIAS
DEPARTAMENTO DE BIOLOGIA
PROGRAMA DE PÓS-GRADUAÇÃO EM SISTEMÁTICA, USO E CONSERVAÇÃO DA BIODIVERSIDADE

ANA KAMILA MEDEIROS LIMA

INTERAÇÕES DE MICROPARTÍCULAS DE TiO_2 COM OS SISTEMAS BIOLÓGICOS *Lactuca sativa* L., *Artemia salina* e *Danio rerio*

FORTALEZA
2025

ANA KAMILA MEDEIROS LIMA

INTERAÇÕES DE MICROPARTÍCULAS DE TiO_2 COM OS SISTEMAS BIOLÓGICOS

Lactuca sativa L., *Artemia salina* e *Danio rerio*

Tese apresentada ao Programa de Pós-graduação em Sistemática, Uso e Conservação da Biodiversidade da Universidade Federal do Ceará, como um dos requisitos para a obtenção do grau de Doutora. Linha de pesquisa: Interação de materiais nanoestruturados com sistemas biológicos.

Orientador: Prof. Dr. Emilio de Castro Miguel

FORTALEZA

2025

Dados Internacionais de Catalogação na Publicação
Universidade Federal do Ceará
Sistema de Bibliotecas
Gerada automaticamente pelo módulo Catalog, mediante os dados fornecidos pelo(a) autor(a)

L696i Lima, Ana Kamila Medeiros.
Interações de microparticulas de TiO2 com os sistemas biológicos Lactuca sativa L., Artemia salina e Danio rerio / Ana Kamila Medeiros Lima. – 2025.
148 f. : il. color.

Tese (doutorado) – Universidade Federal do Ceará, Centro de Ciências, Programa de Pós-Graduação em Sistemática, Uso e Conservação da Biodiversidade, Fortaleza, 2025.
Orientação: Prof. Dr. Emilio de Castro Miguel.

1. Ecotoxicologia. 2. Dióxido de titânio. 3. Microscopia. I. Título.

CDD 578.7

ANA KAMILA MEDEIROS LIMA

INTERAÇÕES DE MICROPARTÍCULAS DE TiO_2 COM OS SISTEMAS BIOLÓGICOS

Lactuca sativa L., *Artemia salina* e *Danio rerio*

Tese apresentada ao Programa de Pós-graduação em Sistemática, Uso e Conservação da Biodiversidade da Universidade Federal do Ceará, como um dos requisitos para a obtenção do grau de Doutora. Linha de pesquisa: Interação de materiais nanoestruturados com sistemas biológicos.

Aprovado em: 10/10/2025

BANCA EXAMINADORA:

Dr. Emilio de Castro Miguel (Orientador)

Universidade Federal do Ceará (UFC)

Dr. Vicente Vieira Faria

Universidade Federal do Ceará (UFC)

Dra. Erika Freitas Mota

Universidade Federal do Ceará (UFC)

Dra. Fernanda Gomes Trindade

Universidade Estadual do Norte Fluminense Darcy Ribeiro (UENF)

Dr. Renato Grillo

Universidade Estadual de São Paulo Júlio de Mesquita Filho (UNESP)

À minha mãe, Karina.

Ao meu avô, Seu Medeiros.

AGRADECIMENTOS

À minha mãe, Karina Medeiros, por ser o meu exemplo a seguir, de filha, mãe, profissional, amiga, de tudo. Por ser aquela que sempre foi a primeira pessoa a vibrar em cada conquista alcançada e nessa, não seria diferente. Por me dar um amor incondicional. E ao meu irmão Rodrigo, pelo apoio, pela torcida e por acreditar em mim.

Ao meu companheiro, Fernando, por acreditar em mim quando eu não conseguia, por dividir a vida comigo e ter estado presente durante todo esse tempo me encorajado a sempre seguir em frente e ir atrás do que eu acredito e desejo. Sorte a minha ter você pra dividir a vida.

À minha irmã Anna Clara, por me ouvir todas as vezes que precisei, me ajudar todas as vezes que eu pedi e acreditar no meu potencial quando eu não acreditei ou tive medo dos desafios.

À minha família, "Medeirada", pela torcida incondicional em qualquer projeto que eu decida realizar, pelo exemplo, valores e por me fazerem acreditar que sou capaz.

À Universidade Federal do Ceará, que é minha casa há mais de 10 anos. Aqui recebi mais que a minha formação e os meus diplomas. Fiz amigos que vou levar para além desses muros. A oportunidade de carregar o nome dessa instituição e tudo o que ela representa é um privilégio.

Ao meu orientador e amigo, Prof. Dr. Emilio de Castro Miguel. Eu não tenho palavras pra expressar a gratidão que eu sinto nesse momento. Obrigada prof, pela parceria, pelo aprendizado, oportunidade, orientação, conselhos e cafés. Sem o senhor eu definitivamente não seria a mesma profissional, tenho muito orgulho quando dizem que pareço com você.

Ao time do Laboratório de Biomateriais, sou muito feliz por fazer parte desse time com vocês, Emilio, Thaiz, Vinicius, Alexia, Jorge Henrique, Roberta, Luiz Gustavo, Kennedy, Ana, Davi, Bia, André e Léo. Obrigada a cada um pelo apoio, pelo incentivo, pela ajuda, ideias trocadas, aprendizados e companheirismo. Meu doutorado foi mais legal por causa de vocês.

Roberta, Alexia, Jorge e Vinicius, já disse várias vezes, mas sem vocês eu não teria conseguido, mil vezes obrigada por chegarem junto comigo em todas as horas que eu precisei, seja de ajuda com os experimentos, processamento de dados ou apenas de ombros e ouvidos amigos e por aguentarem cada um dos meus choros, eu sou muito grata. Saibam que sempre estarei aqui também quando vocês precisarem.

Aos amigos que fiz ao longo dessa jornada, desde a graduação e que permaneceram, Paulo, Karol e Brenda, aos que dividiram o PPGSis comigo, Renata, Yan, Heberson, Bruno e Giovanna, por dividirem a jornada e torná-la mais especial.

Aos amigos que fiz ao longo da vida e que permaneceram comigo até esse momento, obrigada pela torcida, palavras de incentivo, isso me deu força nos momentos que precisei.

À Central Analítica da UFC pelo espaço e aprendizado.

À Coordenação e Corpo Docente do PPGSis pela torcida e pelo empenho com o programa. À minha turma, por dividirmos essa jornada juntos.

Aos membros da minha banca avaliadora, Prof. Dr. Vicente Faria, Profa. Dra. Érika Freitas, Prof. Dr. Renato Grillo e Dra. Fernanda Trindade, minha banca avaliadora pela disponibilidade em fazer parte dessa etapa tão importante para mim e por contribuírem com o meu trabalho e com o meu crescimento profissional.

À Fernanda Trindade e ao Laboratório de Biologia Tecidual da Universidade Estadual do Norte Fluminense (UENF) pela colaboração nas análises de microscopia eletrônica de transmissão.

À Antje Biesemeier, ao Tom Wirtz e ao Luxembourg Institute of Science and Technology (LIST) pela oportunidade de realização de análises de espectrometria de massa de íons secundários pela disponibilidade.

Ao CNPEM e ao Laboratório Nacional de Nanotecnologia (LNNano) pela oportunidade de realizar análises de microscopia eletrônica de transmissão e aprendizado.

O presente trabalho foi realizado com apoio da Coordenação de Aperfeiçoamento de Pessoal de Nível Superior – Brasil (CAPES) – Código de Financiamento 001.

"Estou entre aqueles que acham que a Ciência
tem uma grande beleza."

- Marie Curie

RESUMO

Os materiais nanoestruturados revolucionaram a vida moderna. Inúmeros compostos passaram por processos de redução de tamanho e foram reintroduzidos em setores como saúde, cosméticos, alimentação, agricultura, tecnologia e outros. O composto utilizado neste trabalho são micropartículas de dióxido de titânio (TiO_2MPs). Ele é um metal produzido em larga escala e utilizado em formulações de filtro solar, em alimentos como corante em estratégias de despoluição aquática dentre outros. O objetivo do trabalho foi caracterizar os efeitos da toxicidade do dióxido de titânio em sistemas biológicos. Os três modelos escolhidos foram: *Lactuca sativa L*., *Artemia salina* e *Danio rerio*. Foram realizados experimentos de exposição dos modelos a diferentes concentrações, a alface à 50 $mg.L^{-1}$ TiO_2MPs, artemia à 12,5, 25, 50 e 100 $mg.L^{-1}$ TiO_2MPs e o peixe-zebra à 1, 10 e 100 $mg.L^{-1}$ TiO_2MPs. Os resultados foram analisados por meio de microscopia ótica convencional, eletrônica de varredura e eletrônica de transmissão. Danos anatômicos e ultra estruturais comprovaram a toxicidade do composto para a alface. Na artemia causou alta taxa de mortalidade além de dano celular nas concentrações de 25, 50 e 100 $mg.L^{-1}$ TiO_2MPs. No peixe zebra, no entanto, não houve mortalidade ou alta taxa de deformações. As TiO_2MPs apresentaram toxicidade dependente da concentração, tempo e modelo biológico. Mesmo sem absorção confirmada, o contato direto causa danos celulares e estruturais em plantas e animais. Os resultados ressaltam a importância de estudos crônicos e em condições ambientais realistas para avaliar o impacto das TiO_2MPs em ecossistemas e cadeias alimentares.

Palavras-chave: ecotoxicologia; dióxido de titânio; microscopia.

ABSTRACT

Nanostructured materials have revolutionized modern life. Numerous compounds have undergone size reduction processes and have been reintroduced into sectors such as health, cosmetics, food, agriculture, technology, and others. The compound used in this work is titanium dioxide microparticles (TiO_2MPs). It is a metal produced on a large scale and used in sunscreen formulations, in food as a colorant, in aquatic depollution strategies, among others. The objective of this work was to characterize the effects of titanium dioxide toxicity on biological systems. The three models chosen were: *Lactuca sativa L*., *Artemia salina*, and *Danio rerio*. Experiments were carried out exposing the models to different concentrations: lettuce to 50 mg.L-1 TiO_2MPs, artemia to 12.5, 25, 50, and 100 mg.L-1 TiO_2MPs, and zebrafish to 1, 10, and 100 mg.L-1 TiO_2MPs. The results were analyzed using conventional optical microscopy, scanning electron microscopy, and transmission electron microscopy. Anatomical and ultrastructural damage confirmed the compound's toxicity to lettuce. In artemia, it caused a high mortality rate in addition to cellular damage at concentrations of 25, 50, and 100 mg.L-1 TiO_2MPs. In zebrafish, however, there was no mortality or high rate of deformation. TiO_2MPs showed toxicity dependent on concentration, time, and biological model. Even without confirmed absorption, direct contact causes cellular and structural damage in plants and animals. The results highlight the importance of chronic studies under realistic environmental conditions to assess the impact of TiO_2MPs on ecosystems and food chains.

Keywords: ecotoxicology; titanium dioxide; microscopy.

SUMÁRIO

1 INTRODUÇÃO GERAL

O impacto da nanotecnologia na vida moderna proporcionou benefícios significativos com as aplicações práticas descobertas. As nanopartículas de dióxido de titânio (TiO_2NPs) estão entre aquelas produzidas em escala industrial e são muito utilizadas nos mais diversos segmentos na indústria para produtos utilizados frequentemente no cotidiano (Bevacqua *et al.*, 2022). Elas são aplicadas em cosméticos, tintas e revestimentos de superfície (Clément; Hurel; Marmier, 2013; Servin *et al.*, 2012). No entanto, a compreensão da interação, no nível molecular, desses compostos com sistemas biológicos não cresceu na mesma proporção que seu uso (Maynard *et al.*, 2006).

O dióxido de titânio (TiO_2) é um pó branco amplamente utilizado na purificação de água e alimentos, bem como na garantia da segurança industrial e ambiental e na proteção da pele contra radiação prejudicial em protetores solares, por exemplo (Racovita, 2022). Segundo (Hsu *et al.*, 2024), o dióxido de titânio está entre um dos mais produzidos nanomateriais manufaturados, além de ser um dos maiores poluentes emergentes. Em 2020 a taxa atual de produção industrial de dióxido de titânio, proveniente da ilmenita natural, era de cerca de 6.500 kT por ano (Rajakaruna *et al.*, tem 2020). Além de sua alta produção, estima-se o crescimento da produção anual do dióxido de titânio de 6% entre 2021 e 2028 (Firoozi *et al.*, 2021).

O conhecimento atual sobre os efeitos e consequências do uso regular de diferentes formulações contendo dióxido de titânio, tanto em humanos quanto no meio ambiente, evidencia que as TiO_2NPs apresentam toxicidade por múltiplos mecanismos, impactando a saúde humana e os ecossistemas (Minghui *et al.*, 2023). Estudos sobre fitotoxicidade (Emamverdian *et al.,* 2021) e sobre coexposição dessas partículas com outros contaminantes (Wang *et al.,* 2022) indicam que a presença combinada desses componentes no meio pode modificar a biodisponibilidade e a toxicidade das TiO_2NPs.

O uso crescente de formulações contendo dióxido de titânio resulta em maior geração de resíduos químicos introduzidos no meio ambiente. Nesse contexto, a avaliação dos efeitos desses produtos sobre sistemas biológicos e humanos tem sido foco de investigações, especialmente nas indústrias farmacêutica e cosmética. Testes dermatológicos indicam que NPs de TiO_2, quando presentes em formulações de filtros solares, não são tóxicas para a pele humana por contato direto (Nohynek; Dufour; Roberts, 2008). Um estudo subsequente também examinou as possíveis diferenças nos efeitos decorrentes do uso de partículas micro e nanométricas na produção desses filtros (Smijs; Pavel, 2011). Mais recentemente, Racovita (2022) ressaltou a importância de revisar os avanços em setores nos quais o TiO_2 é amplamente

utilizado, destacando, além das controvérsias sobre seu potencial carcinogênico em humanos, a ausência de uniformidade nos protocolos e nos resultados de testes de toxicidade.

Embora não seja possível afirmar sobre a possibilidade de ausência de riscos quanto ao uso de materiais com diâmetro reduzido em cosméticos e medicamentos, estudos como os de (Nohynek; Dufour; Roberts, 2008) mostram que o uso de nanopartículas de titânio (TiO_2NPs) não apresenta risco à pele ou à saúde humana quando presentes em formulações de protetores solares que além de serem eficazes na proteção contra raios UV, não penetram na pele.

No entanto, é necessário ampliar o estudo da interação desses tipos de partículas com outros grupos de organismos e o meio ambiente. Testes de toxicidade podem oferecer uma visão ecossistêmica dos possíveis impactos causados pelo titânio. As espécies escolhidas para este trabalho são apresentadas a seguir, bem como o motivo de sua escolha. Com o objetivo de fornecer uma visão holística da interação do titânio com modelos biológicos, foram escolhidas espécies de diferentes habitats. Uma espécie de planta terrestre, uma espécie de invertebrado filtrador, que é um dos alimentos vivos mais importantes e base da cadeia alimentar para espécies aquáticas (Al-Jaryan; Abd Al-Rezzaq; Al-Amari, 2024), e finalmente, um modelo vertebrado que pode ser usado como uma etapa intermediária entre testes em células e animais de laboratório convencionais.

A espécie de planta terrestre escolhida foi a alface (*L. sativa*), da família Asteraceae, por ser um modelo bem estabelecido na literatura, de fácil manutenção e rápido para testes de ecotoxicidade devido ao grande número de estudos na área com esses espécimes (Barrena *et al.*, 2009; Liu *et al.*, 2016; Zhang *et al.*, 2015).

Em seguida, a *Artemia salina*, um microcrustáceo zooplanctônico, que desempenha um papel essencial no fluxo de energia da cadeia alimentar em diversos ecossistemas de água salgada (Ates *et al*., 2013; Tang; Zhang; Zhu, 2019). A espécie foi escolhida porque o gênero Artemia é distribuído globalmente e é amplamente utilizado para avaliações toxicológicas (Nunes *et al.*, 2006). Representa o táxon com maior biomassa e serve como consumidor primário na cadeia alimentar ecológica (Sorgeloos; Remiche-Van Der Wielen; Persoone, 1978). Além de ter um ciclo de vida rápido, é fácil de obter, manejar e possui baixo custo de manutenção. O modelo foi usado em testes com nanopartículas metálicas (De Paiva Pinheiro *et al.,* 2023; Pinheiro *et al.,* 2024), em testes de veneno de cobra (Okumu *et al*., 2021) e em testes de bioacumulação (Mounier *et al*., 2020).

Finalmente, como um modelo de maior complexidade biológica, o peixe-zebra

(*Danio rerio*) tem várias vantagens inerentes para triagem de drogas: é pequeno, possui manutenção e criação de baixo custo e é facilmente criado em grandes números - uma única desova produz de 100 a 200 ovos. O peixe-zebra adulto tem 3 cm de comprimento. As larvas, que têm apenas 1-4 mm de comprimento, podem viver por sete dias em um único poço de uma placa de micro titulação sem alimentação por conta dos nutrientes armazenados no saco vitelínico. Além disso, a administração de drogas ou compostos potencialmente tóxicos é simples: as larvas do peixe-zebra absorvem pequenas moléculas diluídas na água ao redor através de sua pele e guelras. Seus órgãos e tecidos demonstraram ser semelhantes aos de seus equivalentes mamíferos nos níveis anatômico, fisiológico e molecular. Este modelo animal pode servir como uma etapa intermediária entre a avaliação baseada em células e os testes convencionais em animais.

O estudo realizado por Wang *et al*. (2022) destaca que a presença de NPs de TiO_2 influenciou a toxicidade do Decabromodifenil etano (DBDPE) em embriões/larvas de peixe-zebra, enfatizando a importância de entender as interações entre nanopartículas e poluentes em ambientes aquáticos. Nessa perspectiva, o estudo de Paiva Pinheiro e colaboradores (2023) destaca a importância de avaliar a toxicidade de micropartículas de dióxido de titânio (TiO_2MPs) em organismos aquáticos como *Artemia sp*. em náuplios de instar I e II, que são comumente usados como organismos modelo em pesquisas de ecotoxicologia.

Oliver *et. al.*, (2015) demonstraram que organismos aquáticos como o peixe-zebra são capazes de acumular TiO_2NPs, com variáveis como rotas de exposição e composições químicas desempenhando um papel fundamental na determinação de seu acúmulo (Oliver *et al*., 2015). Além disso, no trabalho de Asztemborska *et al*., (2018), as TiO_2NPs presentes em sedimentos de solo de ambientes aquáticos eram acessíveis a plantas e peixes, sendo que plantas aquáticas eram capazes de acumular nanopartículas (NPs) e potencialmente transferi-las para organismos superiores. Devido à alta relevância do titânio nos mais diversos segmentos, entender sua capacidade de bioacumulação é necessário tanto para o desenvolvimento de NPs mais seguras quanto pelos riscos que podem causar aos ecossistemas, além da segurança para o consumidor final.

Ademais, existe uma controvérsia acerca do uso e da proibição do dióxido de titânio em diferentes países. A União Europeia baniu o uso do composto em 2022 (European Food Safety Authority (EFSA), 2022). Enquanto o órgão Health Canada's Food Directorate, no Canadá, escolheu não banir o composto, porém alertar sobre as incertezas quanto à segurança do uso do TiO_2 (Health Canada's Food Directorate, 2023). No Brasil, a Agência Nacional de

Vigilância Sanitária (Anvisa) concluiu que o dióxido de titânio utilizado na indústria alimentícia não apresenta riscos toxicológicos (Brazil, 2023).

Nesse contexto, a relevância deste trabalho inclui a realização de testes toxicológicos e de passagem de nível tróficos são necessários para preencher lacunas no conhecimento sobre os efeitos das micropartículas de dióxido de titânio (TiO_2MPs) com uniformidade de protocolo para a obtenção de resultados agregadores. Além de fornecer subsídios para a tomada de decisões mais efetivas.

As micropartículas de dióxido de titânio (TiO_2MPs) recebem essa nomenclatura neste trabalho de acordo com novos achados científicos da Comissão Europeia (EC) e com a experiência regulatória, que adotaram uma definição atualizada de nanomaterial. Essa definição considera como nanomaterial qualquer material natural, incidental ou manufaturado, constituído por partículas sólidas presentes de forma isolada ou como partículas constituintes identificáveis em agregados ou aglomerados, nas quais uma ou mais dimensões externas das partículas se situam na faixa de tamanho entre 1 nm e 100 nm (Comissão Europeia, 2022).

Fatores como o acúmulo de resíduos provenientes de produtos com titânio em sua formulação e a importância de estudos de ecotoxicologia, que fornecem subsídios para o desenvolvimento de fórmulas mais seguras, devem ser considerados na criação de estratégias de biorremediação e conservação. Nesse sentido, é necessário aprofundar as pesquisas sobre a toxicidade do TiO_2 em diferentes grupos de organismos, devido aos potenciais riscos para os ecossistemas e para o bem-estar humano.

Este trabalho foi dividido em três capítulos abrangendo os modelos escolhidos em cada um deles. O primeiro capítulo foi dedicado aos estudos de toxicidade relacionados ao modelo vegetal *Lactuca sativa*, o segundo trás o estudo do modelo invertebrado *Artemia salina*, o terceiro capítulo trata dos ensaios de toxicidade realizados no modelo vertebrado *Danio rerio*. Os testes de toxicidade aguda foram realizados em embriões enquanto os testes de toxicidade subcrônica foram realizados em indivíduos adultos. Por fim, foi caracterizado o caracterizado o efeito da partícula na relação trófica existente entre a artêmia e o peixe zebra.

2 OBJETIVOS

2.1 Objetivo Geral

• Caracterizar os efeitos morfológicos, histológicos e celulares da interação entre micropartículas de dióxido de titânio (TiO_2MPs) e os modelos *Lactuca sativa*, *Artemia salina* e *Danio rerio*.

2.2.1 Objetivos Específicos

• Detalhar a anatomia de plântulas da alface (*Lactuca sativa*) após interação com as TiO_2MPs;

• Caracterizar alterações na anatomia das plântulas alface após interação com as TiO_2MPs, em terrários;

• Avaliar se as TiO_2MPs influenciam no crescimento e ganho de peso das plantas;

• Examinar a incorporação das TiO_2MPs na planta observando alterações estruturais;

• Localizar subcelularmente as TiO_2MPs em (*Lactuca sativa*) e explicar a dinâmica do processo de entrada e translocação da micropartícula;

• Investigar a ocorrência de translocação das TiO_2MPs em *Artemia salina* e explicar a dinâmica do processo de absorção da partícula;

• Investigar a ocorrência de absorção das TiO_2MPs em embriões de *Danio rerio*, avaliar a toxicidade e explicar a dinâmica do processo;

• Caracterizar a influência das TiO_2MPs na relação trófica entre *Artemia salina* e indivíduos adultos de *Danio rerio*.

• Avaliar a existência de toxicidade em adultos de *Danio rerio* através da mudança de nível trófico pelo consumo de *Artemia salina* previamente exposta às TiO_2MPs.

• Caracterizar alterações na anatomia e histologia do peixe-zebra após a alimentação com a *Artemia salina* que foram expostas àsaq111 TiO_2MPs.

3 REFERÊNCIAS

AL-JARYAN, Sara Khalid; ABD AL-REZZAQ, Adi Jassim; AL-AMARI, Moayed JY. Using algae and brine shrimp as food chain model for bioaccumulation and biomagnification of lead and cadmium. **Journal of Applied & Natural Science**, v. 16, n. 2, 2024

ASZTEMBORSKA, M. *et al.* Titanium Dioxide Nanoparticle Circulation in an Aquatic Ecosystem. **Water, Air, and Soil Pollution**, v. 229, n. 6, 1 jun. 2018.

ATES, M. *et al.* Comparative evaluation of impact of Zn and ZnO nanoparticles on brine shrimp (*Artemia salina*) larvae: Effects of particle size and solubility on toxicity. **Environmental Sciences: Processes and Impacts**, v. 15, n. 1, p. 225–233, 2013.

BARRENA, R. *et al.* Evaluation of the ecotoxicity of model nanoparticles. **Chemosphere**, v. 75, n. 7, p. 850–857, maio 2009.

BEVACQUA, E. *et al.* TiO_2 -NPs Toxicity and Safety: An Update of the Findings Published over the Last Six Years. **Mini-Reviews in Medicinal Chemistry**, v. 23, n. 9, p. 1050–1057, 30 set. 2022.

CLEMENT, L., HUREL, C., MARMIER, N., 2013. Toxicity of TiO_2 nanoparticles to cladocerans, algae, rotifers and plants - Effects of size and crystalline structure. **Chemosphere** 90 (3), 1083-1090.

DE PAIVA PINHEIRO, S. K. *et al.* Acute toxicity of titanium dioxide microparticles in *Artemia sp*. nauplii instar I and II. **Microscopy Research and Technique**, v. 86, n. 6, p. 636–647, 1 jun. 2023.

EMAMVERDIAN, A. *et al.* Different physiological and biochemical responses of bamboo to the addition of TiO_2 NPs under heavy metal toxicity. **Forests**, v. 12, n. 6, 2021.

EUROPEAN COMMISSION. Commission recommendation of 10.06.2022 on the definition of nanomaterial. Brussels, 2022.

LIU, Y. *et al.* Evaluating the Combined Toxicity of Cu and ZnO Nanoparticles: Utility of the Concept of Additivity and a Nested Experimental Design. **Environmental Science and Technology**, v. 50, n. 10, p. 5328–5337, 17 maio 2016.

MAYNARD, A. D. *et al.* Safe handling of nanotechnology. **Nature**; Nature Publishing Group, 16 nov. 2006.

MINGHUI, F. *et al.* Toxic effects of titanium dioxide nanoparticles on reproduction in mammals. **Frontiers in Bioengineering and Biotechnology Frontiers Media S.A**., 2023.

MOUNIER, F. *et al.* Dietary bioaccumulation of persistent organic pollutants in the common sole Solea solea in the context of global change. Part 1: Revisiting parameterisation and calibration of a DEB model to consider inter-individual variability in experimental and natural conditions. **Ecological Modelling**, v. 433, 1 out. 2020.

NOHYNEK, G. J.; DUFOUR, E. K.; ROBERTS, M. S. Nanotechnology, cosmetics and the skin: Is there a health risk? Skin Pharmacology and Physiology. **Anais...**jun. 2008.

NUNES, B. S. *et al.* Use of the genus Artemia in ecotoxicity testing. **Environmental Pollution**, nov. 2006.

OKUMU, M. O. *et al. Artemia salina* as an animal model for the preliminary evaluation of snake venom-induced toxicity. **Toxicon: X**, v. 12, 1 nov. 2021.

OLIVER, A. L. S. *et al.* Bioaccumulation of ionic titanium and titanium dioxide nanoparticles in zebrafish eleutheroembryos. **Nanotoxicology**, v. 9, n. 7, p. 835–842, 3 out. 2015.

PINHEIRO, S. K. DE P. *et al.* Assessing toxicity mechanism of silver nanoparticles by using brine shrimp (*Artemia salina*) as model. **Chemosphere**, v. 347, 1 jan. 2024.

RACOVITA, A. D. Titanium Dioxide: Structure, Impact, and Toxicity**. International Journal of Environmental Research and Public Health;** MDPI, 1 maio 2022.

RAJAKARUNA, T. P. B. *et al.* Nonhazardous Process for Extracting Pure Titanium Dioxide Nanorods from Geogenic Ilmenite. **ACS Omega**, v. 5, n. 26, p. 16176–16182, 7 jul. 2020.

SERVIN, A. D. *et al.* Synchrotron micro-XRF and micro-XANES confirmation of the uptake and translocation of TiO_2 nanoparticles in cucumber (*Cucumis sativus*) plants. **Environmental Science and Technology**, v. 46, n. 14, p. 7637–7643, 17 jul. 2012.

SMIJS, T. G.; PAVEL, S. Titanium dioxide and zinc oxide nanoparticles in sunscreens: Focus on their safety and effectiveness. **Nanotechnology, Science and Applications Dove Medical Press Ltd**, 2011.

SORGELOOS, P.; REMICHE-VAN DER WIELEN, C.; PERSOONE, G. The Use of Artemia Nauplii for Toxicity Tests-A Critical Analysis. **Ecotoxicology And Environmental Safety**. [s.l.] Harwich and Scott, 1978.

TANG, T.; ZHANG, Z.; ZHU, X. Toxic effects of TiO2 NPs on Zebrafish. International **Journal of Environmental Research and Public Health**, v. 16, n. 4, 2 fev. 2019.

WANG, X. *et al.* Nano-TiO_2 Adsorbed Decabromodiphenyl Ethane and Changed Its Bioavailability, Biotransformation and Biotoxicity in Zebrafish Embryos/Larvae. **Frontiers in Environmental Science**, v. 10, 14 mar. 2022.

WANG, X. *et al.* Nano-TiO_2 Adsorbed Decabromodiphenyl Ethane and Changed Its Bioavailability, Biotransformation and Biotoxicity in Zebrafish Embryos/Larvae. **Frontiers in Environmental Science**, v. 10, 14 mar. 2022.

ZHANG, P.; MA, Y.; ZHANG, Z.; HE, X.; LI, Y.; ZHANG, J.; ZHENG, L.; ZHAO, Y. Species-specific toxicity of ceria nanoparticles to Lactuca plants. **Nanotoxicology**, v. 9, n. 1, p. 1–8, 2015.

4 CAPÍTULO I – Interação entre *Lactuca sativa* e TiO_2

Este capítulo abordará a compreensão dos aspectos da interação entre TiO_2 e alface. Está dividido em dois artigos; o primeiro foi publicado no periódico *Bulletin of Environmental Contamination and Toxicology* (BECT). O texto completo é apresentado a seguir.

4.1 PAPER 1 – Effect of TiO_2 microparticles in lettuce (*Lactuca sativa* L.) seeds and seedlings

Published: Bulletin of Environmental Contamination and Toxicology (2023).

Bulletin of Environmental Contamination and Toxicology (2023) 110:116
https://doi.org/10.1007/s00128-023-03752-2

Effect of TiO_2 Microparticles in Lettuce (*Lactuca sativa* L.) Seeds and Seedlings

Ana Kamila Medeiros Lima[1] · Alexya Vitória Felix Carvalho[1] · Sergimar Kennedy de Paiva Pinheiro[1] · Yan Torres[2] · Thaiz Batista Azevedo Rangel Miguel[3] · Saulo Fernandes Pireda[4] · Pierre Basilio Almeida Fechine[5] · Lais Gomes Fregolente[6] · Emilio de Castro Miguel[1]

Received: 7 December 2022 / Accepted: 23 May 2023 / Published online: 15 June 2023

ABSTRACT

The particle reduction technology is used in several segments, including sunscreens and new techniques and product improvement. One of the main particles used in the sunscreens formulation is titanium dioxide (TiO_2). This formulation allows better characteristics of these products. Perspectives like the particles incorporate by other biological systems beyond humans and their effects should be observed. The aim of this work was to evaluate the titanium dioxide microparticles phytotoxicity on *Lactuca sativa* L. plants through tests of germination, growth and weight analysis using microscopy techniques: optical microscopy (OM) and scanning electron microscopy (SEM). Some of the results showed cellular and morphological damage, mainly in the roots, confirmed by SEM. Additionally, anatomical damages were observed on the three main organs (root, hypocotyl and leaves) evidenced by the OM. Perspectives to confirm new hypotheses and improve knowledge of the interaction of nanomaterials with biological systems are necessary for a better problem understanding.

Keywords: Titanium dioxide. Phytotoxicity. Microscopy. Plant morphology. Plant anatomy.

4.1.1 Introduction

Commercial and industrial use of small diameter particles has grown rapidly in recent years and applied in several segments (Weir *et al* 2012;) such as cosmetics (Hanigan *et al* 2018), pharmacological (Namdeo *et al* 2008), agriculture (Rodríguez-González *et al.* 2019) among others. Titanium dioxide (TiO_2) exists as rutile, anatase and brookite crystalline polymorphic forms (Sadrieh *et al.* 2010). The rutile phase is more stable and has lower photocatalytic activity than anatase (Barbosa *et al.* 2018). The TiO_2 has been used as an inorganic filter in sunscreens due to protection effect against UV radiation absorbing, scattering and reflecting (Lu *et al.* 2015).

According to (Haynes *et al.* 2017), studies investigating the photocatalytic effects caused by nano titanium dioxide in aquatic organisms are scarce. Among the most diverse applications is the use of microparticles (MPs) and nanoparticles (NPs) in sunscreens (Flor *et al.* 2008; Sendra *et al.* 2017).

The concern about the use of titanium dioxide is a result of the combination of different properties (molecular size, proteinase complexes formation and free radicals' generation), since TiO_2 and zinc oxid (ZnO) are known as photocatalysts are used in the generation of electric energy in photovoltaic cells (Lu *et al.* 2018). The penetration of these particles in human skin is possible through the formation of complexes that have different biochemical properties from non-complexed or larger nanoparticles (Newman *et al.* 2009). However, according to a study by Newman *et al.* (2009), there is still no need for bigger concerns about the toxicity of sunscreens containing TiO_2, as the penetration of these nanoparticles through the stratum corneum of the skin was not significant enough to cause damage to cells and DNA (Balogh *et al.* 2011). In mammalian cells according to in vitro experiments performed in Nohynek *et al.*, (2008) there was no concern about titanium penetration through the skin, either. However, the understanding of the interaction at the cellular and molecular level of these compounds in biological systems is insufficient (Maynard *et al.* 2006).

Because of the need for more toxicity studies in other taxa besides humans, lettuce (*Lactuca sativa*) was chosen. The genus *Lactuca* L. (*Asteraceae*) comprises approximately 100 species, in which the edible lettuce genotypes were divided into six groups of lettuce (curly, lisa, americana, mimosa, roman and red) predominant in the countries cultivation that meet the demand of the consumer market (Sala and Costa 2012).

This plant was chosen as a study model due to its wide distribution because it is the

most important leafy vegetable in the world, for its high consumption and for the ease of in vitro cultivation (Sala and Costa 2012). Furthermore, *L. sativa* is a well-established model of ecotoxicity in the literature with experimental details on plant reaction, growth, and exposure conditions (Larue *et al.* 2014).

The aim of this work was to evaluate the acute toxicity of titanium dioxide (TiO_2) microparticles in *Lactuca sativa* seedlings germination, describing the effect of interactions between *L. sativa* plants and TiO_2 microparticles. Also, describe changes in lettuce anatomy after interaction with the particle based on optical and scanning electron microscopy techniques. Furthermore, investigate the incorporation of TiO_2 into the plant by observing structural changes.

4.1.2 Material and methods

For the experimental design of this process, the methodology of Pinheiro et al (2020) was utilized to standardize parameters such as the choice for concentrations, the organism sample and microscopical analysis.

The titanium dioxide particles were kindly provided by the Advanced Materials Chemistry Group (GQMat) coordinated by Dr. Pierre Fechine - Department of Analytical Chemistry and Physical Chemistry, Federal University of Ceará – UFC. This particle was characterized in a previous study (Barbosa *et al.* 2018). The particle used underwent a sonochemical process for size reduction and has an average size of 104.4 ± 2.29 nm. The rutile form were used in this study with its zeta potential of −17.36 ± 0.11, its hydrodynamic size value of 297.46 ± 3.66 nm.

The experiment was carried out with seeds of L. sativa, 'Crespa Grand Rapids' of the brand ISLA PAK© acquired in Fortaleza, Ceará, Brazil. The assays were carried out in Petri dishes measuring 90x15 mm, between Germitest paper with a weight of 65 g/m2 and neutral pH, at a temperature of 25 ºC. Ten seeds were placed in each plate for each treatment according to the established concentrations.

The seeds were exposed for 2 hours to different concentrations of titanium dioxide microparticles: 12.5; 25; 50 and 100 ppm and 50 seeds/concentration were used totaling 50 seeds/concentration. The negative control was performed with distilled water and positive control with 0.2 M potassium dichromate ($K_2Cr_2O_7$) solution. Experiment was carried out for seven days, and the plates were rehumidified daily with 1.5 ml of distilled water. The growth was also measured, using a digital caliper. The wet weight and dry weight of the plants germinated on the seventh (last) day of the test.

Other exposure tests were carried out, this time after germination, which took place on the third day of sowing, where, once again, the newly germinated seedlings were exposed for 2 hours, at the same concentrations (12.5 ppm, 25 ppm, 50 ppm and 100 ppm) in addition to the two controls, positive (potassium dichromate) and negative (distilled water). After exposure, the seedlings were relocated in new clean and sterilized petri dishes with germitest paper and continued to be rewetted and measured daily until the seventh day of assay.

After the collection and fixation of the samples, processing for visualization on optical microscopy was carried out. First step, the material was washed three times in sodium cacodylate 0,05M. Second, dehydration was done by increasing the series of ethanol, 50%, 70%, 80%, 90% and three series of 100% ethanol, each interval 40 minutes apart. After dehydration, the samples were placed in historesin. After this step, the samples were assembled into blocks and cut using the microtome (Leica RM2255 Rotating Microtome).

The final stage in preparing the material for observation under optical microscopy was the assembly of the slides. To stain the slides, an aqueous solution of Toluidine blue (TB) 0.025% pH = 4.0 was used for 1 minute at room temperature. This procedure was followed by three washes in distilled water (O'Brien and Feder 2005). After drying, the slides were mounted with an acrylic resin-composed varnish. The visualization of the samples and the respective documentation was finalized in a photomicroscope (Zeiss) equipped with an Olympus UC30 camera, and the basic software for the acquisition of Cell^B images.

For the preparation to scanning electron microscopy (SEM), the material collected on the last day of the experiment was fixed in an aqueous solution containing 2.5% glutaraldehyde, 4% formaldehyde, 0.05 M sodium cacodylate buffer, pH 7.2, in room temperature for 24 hours. After this step, the material was washed in 0.05M sodium cacodylate buffer, three times, each wash lasting 45 minutes. Subsequently, the samples were dehydrated, in an increasing ketone series of 50%, 70%, 90%, 100%, for 40 minutes in each step. After dehydration, the material was critical point dryed (K850 Critical Point Dryer).

The dried samples were fixed in aluminum stubs using double sided carbon tape and then covered by sputtering with a 20 nm layer of gold, using the Quorum Q150T ES instrument. Sample observation and image capture were performed using a scanning electron microscope (SEM) with 20kV beam voltage acceleration (Quanta FEG 450 – FEI).

The database containing the measure of the 300 seeds (50 for each treatment) was organized in a spreadsheet in Microsoft Excel. The growth, weight and germination graphs were generated in the Graphpad Prism, 8th version was used. In addition, the R program was used to perform the comparisons between the treatments through a non-parametric analysis

(Kruskall-Wallis) and post-hoc analysis (Dunn's test). Furthermore, the software was also applied for checking outliers and the other graphs of this work.

4.1.3 Results and discussion

The results will be presented in topics, because two different experiments were carried out to visualize the toxic effects caused by titanium in different statistical, morphological and anatomical aspects.

The total plant growth on the 7th day was compared between the two exposure conditions (before and after germination) of the present work. On the first one, exposure happened on the first day of the assay. With the second one, exposure happened on the third day. When exposure was made before germination there were no significant differences between treatments, and neither between treatments nor distilled water (negative control). The significant differences obtained were only between the treatments and dichromate (positive control?) ($\chi 2$ Kruskal -Wallis = 21.4, d.f. = 5, p-value < 0.001; Table with Dunn's test Annex). When going to the exposure condition after germination on 3rd day there were no significant differences between treatments (χ_2 Kruskal -Wallis = 2.4, d.f. = 5, p-value = 0.80). We also compared whether there was a difference in day-to-day growth during the 7 days between the first and second exposure conditions. In this context, all treatments showed significant differences in growth between the two conditions, except for 25 ppm (p-value = 0.08).

On the first day of sowing, no seeds germinated. On the second day, more than 90% of the seeds germinated; on the third day it increased a little more and from the fourth day onwards, this number remained stable. Thus, it is safe to assume that titanium dioxide did not significantly affect the germination process itself. Since aqueous solutions of different concentrations succeed to break seed dormancy and start the life cycle of individual seeds.

All the treatments and controls obtained similar results related to growth. The observed non-inhibitory effect of TiO_2 in the germination stage of lettuce plants is corroborated by Andersen *et al.* (2016) which found that synthetic nanomaterials, such as titanium dioxide, do not cause acute generalized toxicity during germination and early growth in an essay with 10 species, where lettuce was one of them. Tests such as chlorophyll content in plant, germination and elongation performed by Iannone *et al.* (2016) concluded that heavy metals such as iron oxide did not affect the germination rate as well. In addition, it is worth mentioning that seed germination occurred within the normal expected period of up to two days of germination according to Grasso *et al.* (2018) in his study using two lots of 'Mirella' F1 watermelon dried seeds.

However, the Kruskal-Wallis test was performed, an analogous test used for non-normal data but with significant differences found in the test (Kruskal -*Wallis chi- squared* = 22.296, d f = 5, p - value = 0.00046). Then, an ANOVA test was performed to compare the mean growth between treatments, and no significant difference was found ($F_{5, 187} = 0.43$, p = 0.82) between treatments, comparing both with controls and with the other titanium concentrations (all possible pairs). This is shown in Figure 1 below. Where it is possible to observe a compilation of graphs on the average size of the groups of according to each treatment during the experiment.

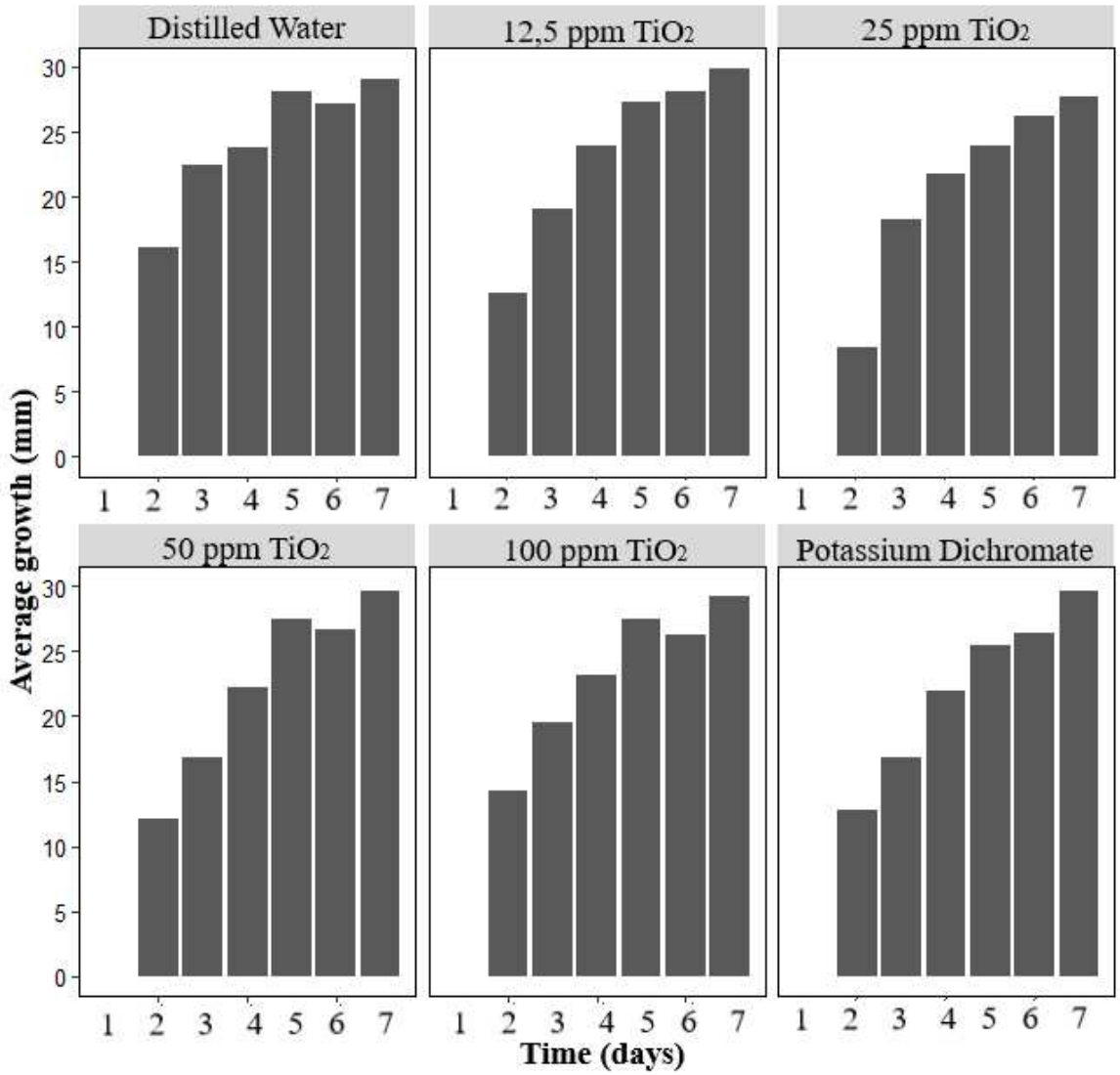

Fig. 1 - Graphs of the average daily growth (mm) of *Lactuca sativa* seeds during the seven days of experiment according to the treatment used in pre-germination with two controls: the negative, distilled water (H2Od) and the positive, potassium dichromate ($K2Cr_2O_7$)) and different concentrations of TiO_2 MP's (12.5 ppm, 25 ppm, 50 ppm and 100 ppm). Note that, in each representation, the highest y-axis value varies according to the average growth in each treatment.

The seedling size did not vary significantly when compared on the same days, indicating that TiO_2 does not change the plant's growth pattern. About the weight, an increase in fresh weight was observed compared to the negative control. The figure shows results that

corroborates with the presented by Rastogi *et al.* (2017). Which cite one of the influences that titanium can bring to the plant is the increase in fresh weight.

Note that the groups of concentrations 12.5 and 25 ppm are very close to each other, as well as the groups of 50 and 100 ppm. According to Clemente (2012) there are several guidelines for toxicological tests, but this is not yet well defined for the nanoecotoxicological tests. Only some gorvenamental bodies, such as the OECD (*Organization for Economic Co-operation and Development*) suggests that a general LC50 is found up to a concentration of 100 ppm.

Although there was no difference of dry weight between the groups, Movafeghi *et al.* (2018) who worked with the species aquatic plant *Spirodela polyrrhiza* observed a decrease in dry weight as one of the parameters affected by titanium NPs. The lowest dry weight among the titanium treatments is that of group of 50 ppm, corroborating the suggestion by the OECD that the LC50 would be found until the concentration of 100 ppm (Clemente, 2012).

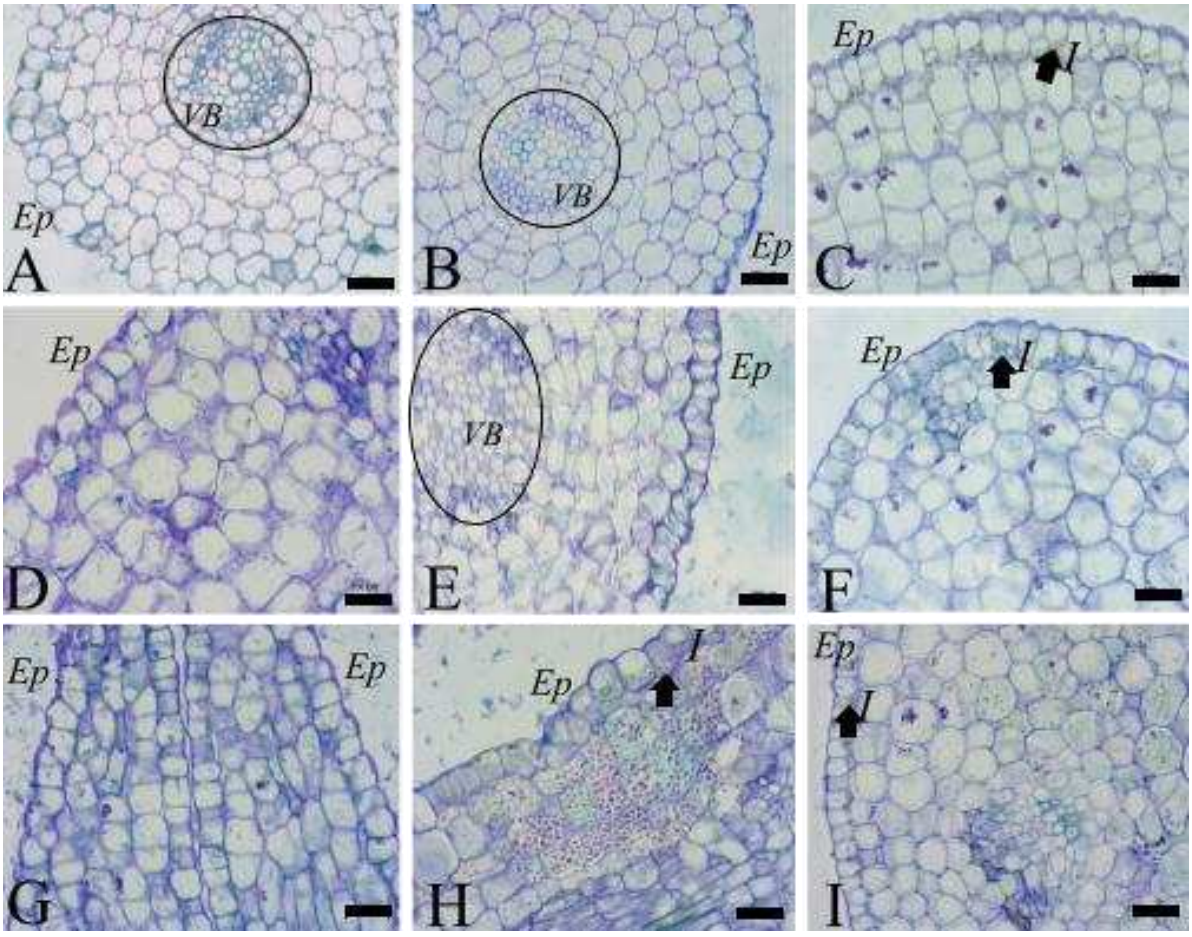

Fig. 2 – Optical microscopy of the root (A - C), hypocotyl (D - F) and leaf (G - H) of *Lactuca sativa* 3 days after germination. A: Root without treatment (distilled water). B: Root 50 ppm TiO_2. C: Root submitted to Potassium dichromate with thickening in epidermis (Ep) and presence of inclusions. D: Untreated (distilled water) hypocotyl with thickened epidermis. E: Hypocotyl at 50 ppm TiO_2 with disruption of the vascular bundle. F: hypocotyl in dichromate of potassium and presence of inclusions (I). G: Leaf without treatment (distilled water). H: Sheet at 50 ppm TiO_2 and high number of inclusions. I: Potassium dichromate leaf with presence of inclusions. Ep: Epidermis; VB: Vascular bundle; I: Inclusions. Scale bars: 200µm.

The damages caused by TiO_2, can be seen in figures **2A**, **2D** and **2G.** Since in them is possible compare the differences between the control sample and treatments. On image **2A**, it is possible to observe a regular epidermis (EP) cell layers through the cortex until the vascular bundle (VB), both structures well-defined. In figures **2D** and **2G** other organs of the plant (hypocotyl and leaf) are shown without any titanium treatment. Figures **2C**, **2F** and **2I** show from another perspective how lettuce anatomy is affected by the potassium dichromate, which is toxic to the plant, and offers a comparison parameter.

By analyzing cellular differences, cell wall thickening was also found in the images of Manesh *et al.* (2018) where radish plants (*Raphanus sativus)* also underwent exposure to titanium.

At this point, it is possible to observe that there is early thickening of the cell wall of the epidermal cells and inclusions that appears not only in the root epidermis, but also in the leaf epidermis and cortex (Figure **2H**). Irregularity of cell morphology was found in the cortical meristem (figure **2E**) where defective cells with cytoplasm retraction were observed. These irregularities can be pointed out as a sign of the stress suffered by the plant due to the treatment to which it was submitted.

In the work carried out with lettuce plants by Begum *et al.* (2011) cytoplasmic alterations were also considered as cellular damage prior to cell death with membrane disintegration and release of its constituents.

In the figure **2E**, in addition, there was a disruption of the vascular bundle that did not occurred in the other treatments, not even in the positive control with potassium dichromate. This observation indicates 50 ppm as a concentration that causes more anatomical damage to the plant than the highest concentration tested (100 ppm), since in this treatment not major damage was found.

The presence of inclusions in both treatments (titanium and dichromate) was observed. Their number varies according to the increase concentration of treatment. All images that have inclusions (I) in bigger numbers in the cells and throughout the sample, **2H** figure for example, are from the 50 ppm group, is the one that presents the most expressive difference in relation to the other concentrations and controls.

Now, from scanning electron microscopy perspective, the most visible differences in the the root between exposed and non-exposed plants were in the root width, root hair density and root size (figures **3B** and **3E**).

Begum and Fugetsu (2012) pointed out several toxicity-related damage to root cells in the outermost layers, such as damaged cell walls, cracks, tissue loss and detachment of cell

layers. In tests performed by Begum and Fugetsu (2012) using carbon nanotubes, corrupted epidermis and root cap were observed, corroborating the results presented here.

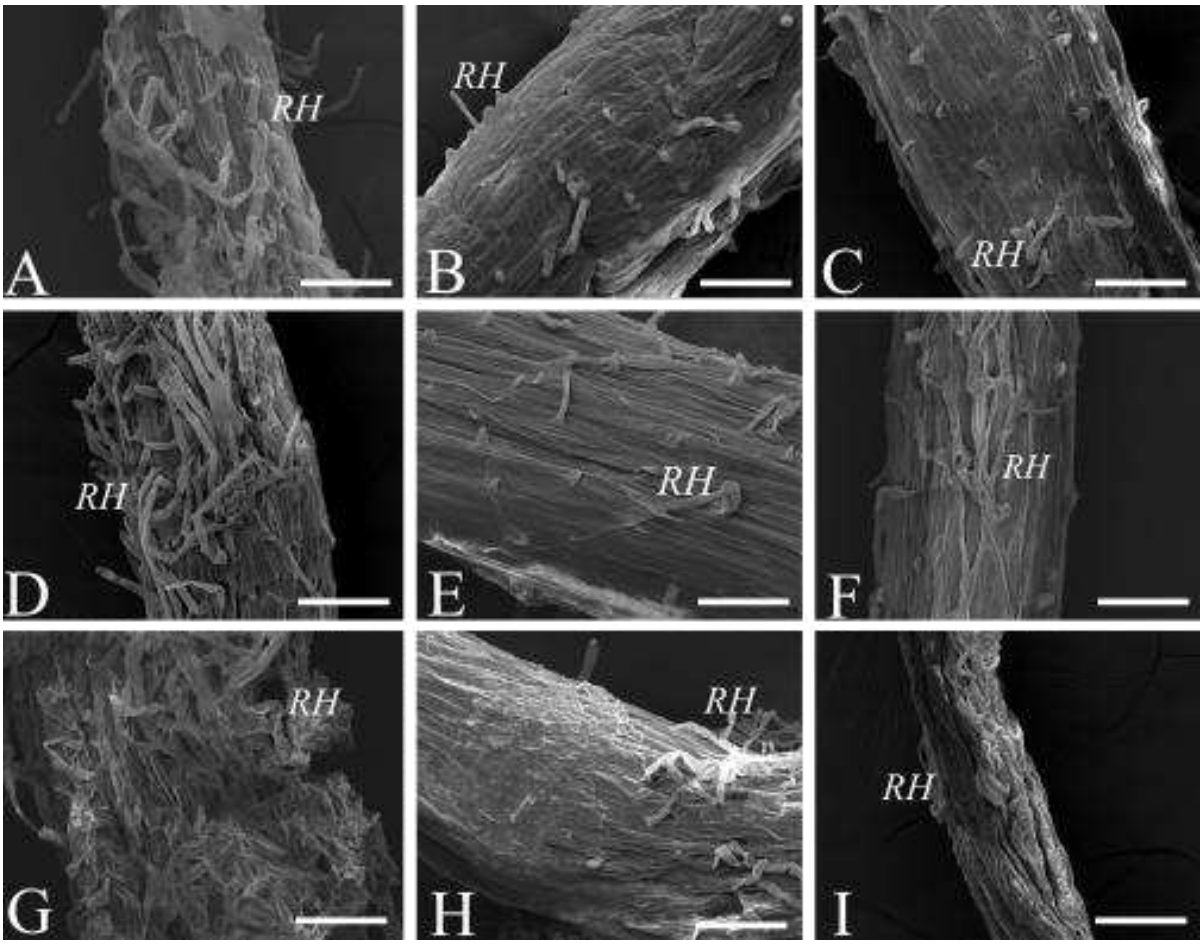

Fig. 3 - Scanning electron microscopy (SEM) of the zona pilifera of *Lactuca sativa* 3 days after germination (A, B, C). 7 days after germination and contact with titanium (D, E and F) and at 7 days where exposure to titanium were post germination (G, H, I) in treatments many different. A, D, G: No treatment (water). High density of root hairs. B, E, H: 50 ppm TiO_2. Small amount and short length of root hairs. C, F, I: Potassium Dichromate. Small amount, absence of hair in some regions. RH: Root hair. Scale bars: 100µm.

In Figure 4, changes in cell morphology were observed in the cortical region of the root. The damage occurs gradually starting from a concentration of 12.5 ppm reaching its apex of disorder and deformation in the group of 50 ppm (**4B**) with cells showing irregular morphology and disruption of the vascular bundle. Thus, the thickening of the epidermis is an indication of stress suffered by the plant. A result observed by Begum *et al.* (2011) in cabbage root treated with graphene (carbon nanomaterial), in which the excess of this nanomaterial resulted in a swelling of the epidermis cells. Balaji *et al.* (2007) observed the shrinkage of the epidermis in barley leaves as one of the anatomical changes undergone by the plant in response to heavy metal toxicity.

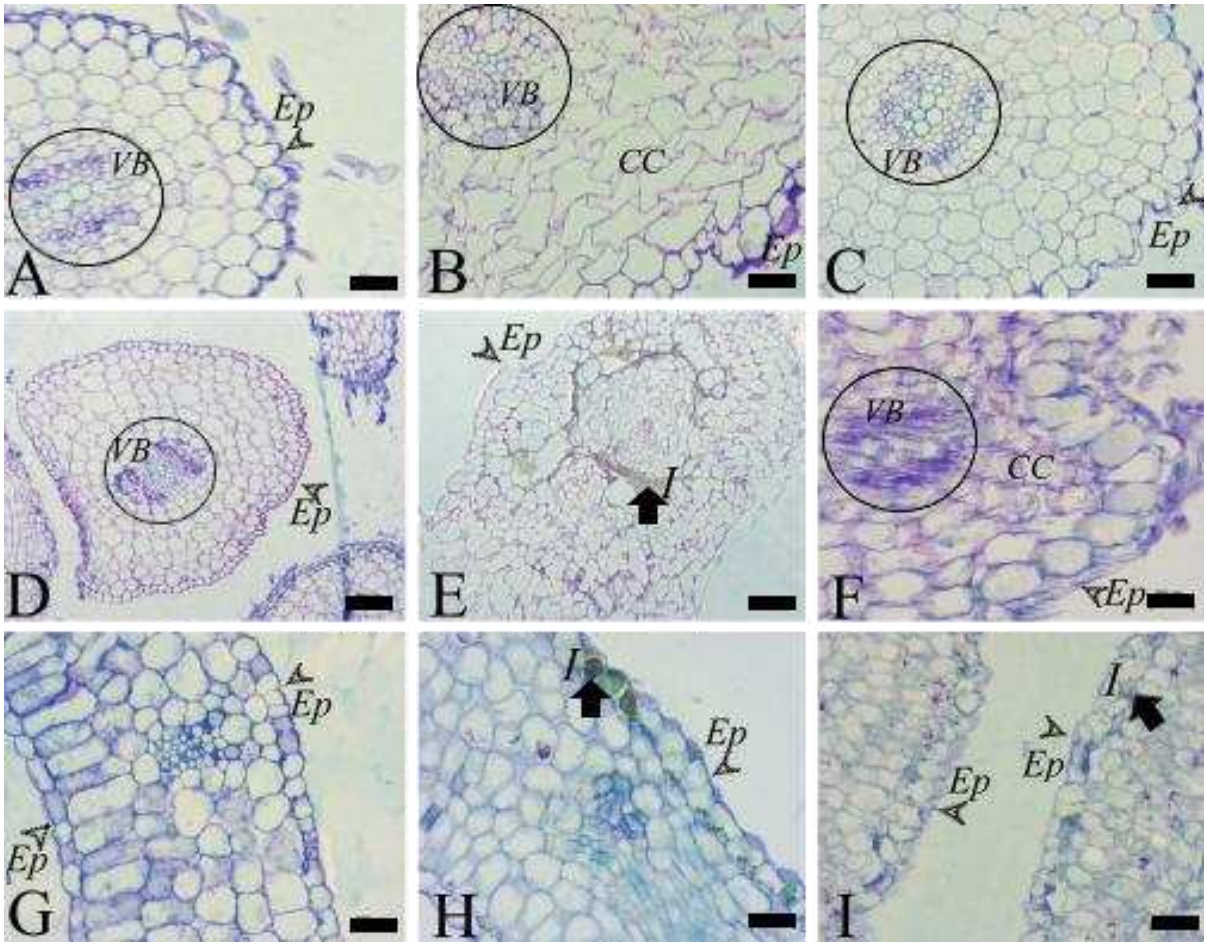

Fig. 4- Optical microscopy of the root, hypocotyl and leaf of *Lactuca sativa* 7 days after germination. A: Root without treatment (water). B: Root 50 ppm TiO_2. C: Root submitted to potassium dichromate. D: Untreated (water) hypocotyl with regular epidermis. E: Hypocotyl submitted to 50 ppm of TiO_2 showed disruption of the vascular bundle with the presence of inclusions and cortex cells with affected morphology. F: hypocotyl in dichromate of potassium with disruption of the vascular bundle, cortex cells with affected morphology and desquamation of the epidermis. G: Leaf without treatment (water). H: Leaf at 50 ppm TiO_2 with presence of inclusions in epidemic cells. I: Leaf submitted to potassium dichromate. note the presence of inclusions. Ep: Epidermis; VB: Vascular bundle; I: Inclusions; CC: Cortex cells. Scale bars: 200µm.

Likewise, the inclusions gradually increased according to the concentrations and reached its apex in the treatment of 50 ppm (figure **4E** and **4H**). This was the most apparent and expressive damage presented until this moment of that given concentration. Inclusions appears throughout practically the entire mesophyll. Therefore, proving that the 50 ppm group is the most harmful in the assay. Beyond that some images show this thickening of the epidermis (**4B** and **4H**) that is not present in the control sample that did not undergo any type of treatment.

According to Bellani *et al.* (2020) the particles of titanium dioxide were observed in the form of aggregates in the vacuole, cytoplasm and in the space between the cell wall and the plasma membrane. In the same way, these inclusions were also found in the tests of radish seeds (*Raphanus sativus*) (Manesh *et al.* 2018). According to Cox *et al.* (2017) and Ralyia *et al.* (2015), once the titanium particles are absorbed by the root or leaf cells they are translocated by the plant through the vascular system. Also, Chichiriccò and Poma (2015) observed that NPs can accumulate in the rhizoderm of plants and penetrate the cell wall and even be

translocated. In the Santos Filho *et. al*, (2019) work, inclusions were also found and described as oily bodies and with peripheral disposition.

During the study Santos Filho *et. al* (2019) it was observed that the titanium particles are not homogeneous, as they presented different dimensions and sizes, which can cause damage to cells with the formation of inclusions. Probably, as the present results (fig **4E** and **4H**). In addition, the translocation of particles to other plant organs such as stem and root was evidenced by Chichiriccò and Poma (2015) through the leaf epidermis and stomata.

The increase in fresh weight was evidenced in comparison to the negative control. Moreover characteristics such as: irregularities in the epidermal cells of the cell and change in the morphology of the cortical cell wall were observed. Again, the concentration of 50 ppm presented these parameters in a more accentuated way.

Regarding the root hypocotyl axis, the images show several stress indicators from a more superficial level in the plant, such as irregularities in the epidermis (figure **5B**) and increase in intercellular space, that is likely to come from a different arrangement between cells. Another noteworthy point was the rupture of cell wall. This was presented by some cells that occur along the entire length of the cut.

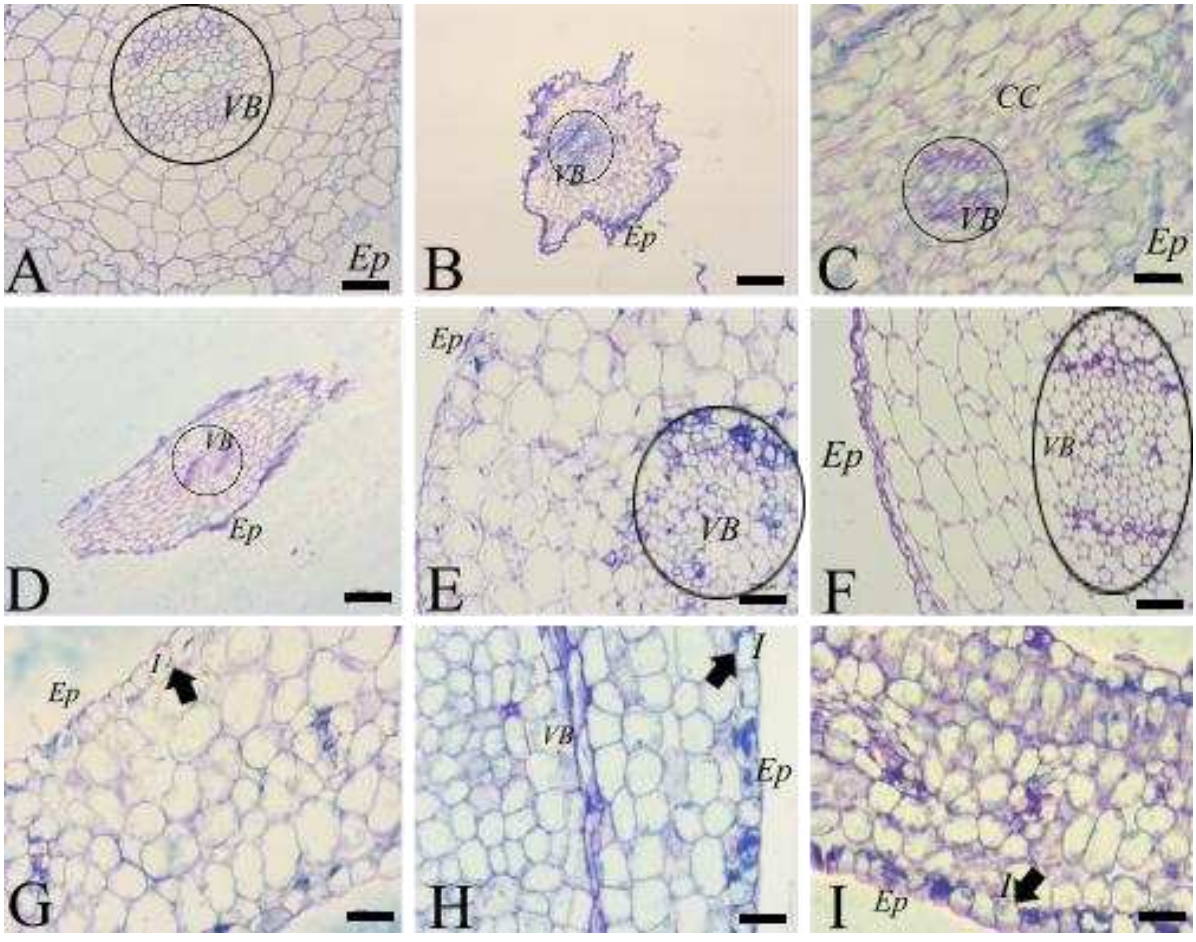

Fig. 5 – Optical microscopy of the root, hypocotyl and leaf of *Lactuca sativa* 7 days after germination and 4 days after exposure to different treatmens. A: Root without treatment (water). B: Root submitted to 50 ppm TiO_2 with affected (irregular) cortex cells and patchy epidermis. C: Root submitted to Potassium dichromate with affected cortex cells and patchy epidermis. D: Untreated (water) hypocotyl. E: Hypocotyl at 50 ppm TiO_2 with disruption of the vascular bundle. F: hypocotyl in dichromate of potassium and with disruption of the vascular bundle. G: Leaf without treatment (water). H: Leaf submitted to 50 ppm TiO_2 and presence of inclusions. I: Leaf submitted to Potassium dichromate. Presence of inclusions. Ep: Epidermis; VB: Vascular bundle; I: Inclusions; CC: Cortex cells. Scale bars: 200μm.

The previously mentioned piliferous zones (figure 3) shows a well-defined characteristics about root hairs. Which is the absence of hair in certain regions (fig. **3H**). The other small amount, that appeared, were atrophied. There were also regions where a complete absence of hair, clearly showing that there is a great impact of treatments on the morphology of this area (fig. **3H** and **3I**).

One of the toxicity evidences caused by carbon nanotubes, according to Begum and Fugetsu (2012), is the small amount and length of root hairs (fig. **3H**) and in some cases the absence of them.

The damage to root hairs was also found by Schwab *et al.* (2016) where these changes occurred at different concentrations. An explanation given by García-Sánchez *et al.* (2015) for this type of effect is caused by transcriptional repression of root development genes that predicted an altered root phenotype in plants that have been exposed to NPs (including carbon dioxide titanium).

Similar results observed in studies carried out with radish seeds (Chichiriccò and Poma 2015, Manesh *et al.* 2018) showed that exposure to NPs during root elongation is associated with abnormal cell emergence.

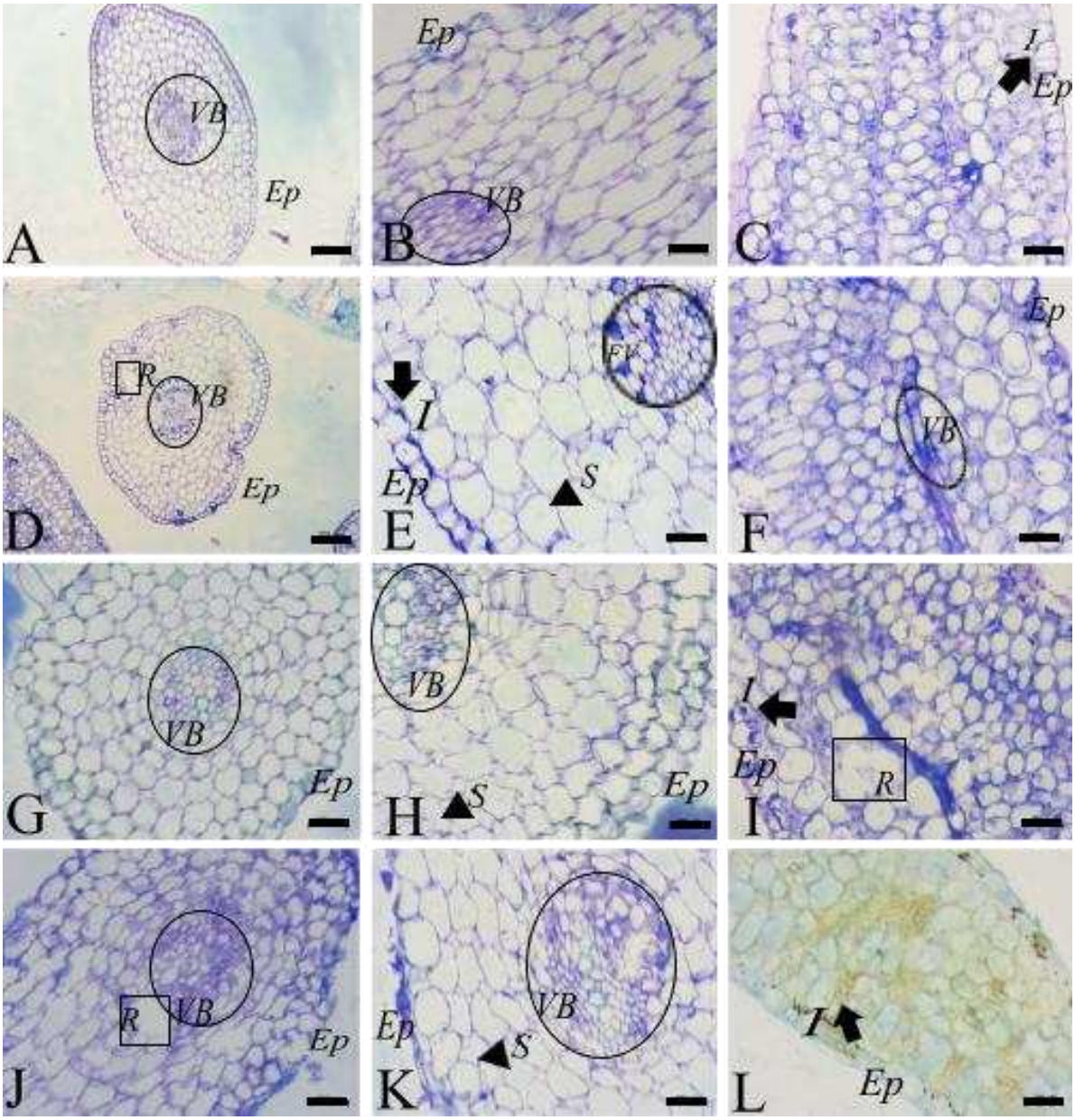

Fig. 6 – Optical microscopy of *Lactuca sativa* root 7 days after germination, in the treatment of 50 ppm of TiO_2 in different exposure times. A: Root without treatment and no damages, 1h. B: Hypocotyl with cell wall rupture, 1h. C: Leaf, 1h. D: Root with cell rupture 4h. E: Hypocotyl with some inclusions and higher intercell space 4h. F: Leaf, 4h G: Root, 8h. H: Hypocotyl with some cell disorder and higher intercell space, 8h. I: Leaf with inclusion in epidermis and cell rupture, 8h. J: Root with cell wall rupture, 16h. K: Hypocotyl, with cell wall disorder and higher intercell space; 16h. L: Leaf with many inclusions, 16h. Ep: Epidermis; I: presence of inclusions (NPs); VB: disruption of the vascular bundle. S: Intercell space. R: cell rupture. Scale bars: 200µm.

As expected, and following a pattern that was drawn throughout these analyses, several of the indicators used in this work were present in the images such as cell wall disruption, increase in intercellular space and change in morphology of cortical cells, parameters that evolved over time of exposure. In samples with 16 hours of contact with titanium dioxide, it is possible to observe the disruption of the vascular bundle, as well as the large numbers of inclusions on leaf (fig. **6L**).

Studies carried out by Raliya *et al.* (2015) using TiO_2 and ZnO showed that these particles were able to reach the fruits of tomato plants analyzed independently of the exposure

method. The two possible absorption pathways indicate the bioaccumulation of NTFS (N-TiO_2 doped with nitrogen and Fe_3 O_4 SiO_2) and consequent entry into the food chain (Zhang *et al.* 2019). In studies carried out by Tombuloglu *et al.* (2018) it was shown that barley can capture and translocate NPs, from the root to the aerial organs. Furthermore, Chichiriccò and Poma, (2015) reported that cuticular and stomatal uptake of NPs and translocation to the vascular system can be via apoplastic and symplastic pathways. This fact may explain the finding of inclusions in cortical and vascular bundle regions.

4.1.4 Conclusions

Although problems related to germination by TiO_2 were not found, damage was found at radicle, hypocotyl and primary leaf of *Lactuca sativa*. They were both external and superficial as evidenced using electron microscopy scans, such as internals brought on using light microscopy. Related to weight gain, there were no significant changes. The tests showed that *Lactuca sativa* seedlings can incorporate TiO_2 NPs and transport these particles due to the observation of inclusions in vascular bundle cells.

Perspectives for confirming new hypotheses and improving knowledge regarding the question of the interaction of nanomaterials with biological systems are promising. As stated in this manuscript, it is necessary to carry out tests that measure ROS, biochemical tests to measure oxidative stress and use of microscopy transmission electronics for better understanding of TiO_2 translocation dynamics used in sunscreens within the *Lactuca sativa* organism.

ACKNOWLEDGMENTS

TBARM acknowledges funding from CNPq (grant 350023/ 2020-4) and Analytical Center-UFC/CT-INFRA-FINEP/Pro-Equipamentos-CAPES/CNPq-SisNano-MCTI 2019 (Grant 442577/ 2019-2). Capes, INCT and FUNCAP. This work is part of the PhD research of AKML and SKPP.

AUTHOR CONTRIBUTION

All authors contributed to the study conception and design**.** Developed research (Emilio de Castro Miguel). Write the manuscript (Ana Kamila Medeiros Lima). Review of the manuscript (Thaiz Batista Azevedo Rangel Miguel and Saulo Pireda). Synthesized the nanoparticles (Pierre Basílio Almeida Fechine). Performed the experiments (Ana Kamila Medeiros Lima, Alexya Vitória Félix Carvalho and Sergimar Kennedy de Paiva Pinheiro). Statistical analysis (Yan Torres). All authors read and approved the final manuscript.

CONFLICTS OF INTEREST

The authors declare no conflict of interest.

REFERENCES

Andersen CP, King G, Plocher M, Storm M, Pokhrel LR, JohnsonMG, Rygiewicz PT (2016) Germination and early plant development of ten plant species exposed to titanium dioxide and cerium oxide nanoparticles. Environ. Toxicol. Chem. 35: 2223–2229. https:// doi.org/10.1002/etc.3374

Balaji B MS, Fengxiang X H, Diehl SV, Monts DL; Su Y (2007) Effects of Zn and Cd accumulation on structural and physiological characteristics of barley plants. Braz. J. Plant Physiol. 19(1): 15–22. https:// doi.org/ 10.1590/S1677-04202007000100002

Balogh TS, Velasco MVR, Pedriali CA, Kaneko TM, Baby AR (2011) Proteção à radiação ultravioleta: Recursos disponíveis na atualidade em fotoproteção. Anais Brasileiros de Dermatologia 86(4): 732–742. https://doi.org/10.1590/S0365-05962011000400016

Barbosa JS, Neto DMA, Freire RM, Rocha JS, Fechine LMUD, Denardin JC et al (2018) Ultrafast sonochemistry-based approach to coat TiO2 commercial particles for sunscreen formulation. Ultrason Sonochem 48: 340–348. https://doi.org/10.1016/j.ultsonch.2018.06.015

Begum P, Ikhtiari R, Fugetsu B. (2011) Graphene phytotoxicity in the seedling stage of cabbage, tomato, red spinach, and lettuce. Carbon, 49: 3907–3919. https://doi.org/10.1016/j.carbon.2011.05.029

Begum P, Fugetsu B. (2012) Phytotoxicity of multi-walled carbon nanotubes on red spinach (Amaranthus tricolor L) and the role of ascorbic acid as an antioxidant. J. Hazard. Mater, 243: 212–222. https://doi.org/10.1016/j.jhazmat.2012.10.025

Cox A, Venkatachalam P, Sahi S, Sharma N (2017) Reprint of: Silver and titanium dioxide nanoparticle toxicity in plants: A review of current research. P. Physiol. Biochem., 110: 33–49. https://doi.org/10.1016/j.plaphy.2016.05.022

Chichiriccò G, Poma A. (2015) Penetration and toxicity of nanomaterials in higher plants. Nanomaterials, 5: 851–873. https://doi.org/10.3390/nano5020851

Clemente, Z. (2012) Archive of SID Organisms of Aquatic Ecosystems Archive of SID. 6: 33–50.
De Paiva Pinheiro SK, De Medeiros Chaves M, Rangel Miguel TB A, De Freitas Barros FC, Farias CP, Ferreira OP, De Castro Miguel E (2020) Toxic effects of silver nanoparticles on the germination and root development of lettuce (Lactuca sativa). Aust. J. Bot. 68(2): 127–136. https://doi.org/10.1071/BT19170

Flor J, Davolos MR, Correa MA (2008) Protetores solares. Revista Brasileira de Medicina 65: 6–11.
García-Sánchez S, Bernales I, Cristobal S, (2015) Early response to nanoparticles in the Arabidopsis transcriptome compromises plant defence and root-hair development through salicylic acid signalling. BMC Genomics, 16 https://doi.org/10.1186/s12864-015-1530-4

Grasso R, Gulino M, Giuffrida F, Agnello M, Musumeci F, Scordino A. (2018) Non-destructive evaluation of watermelon seeds germination by using Delayed Luminescence. J. Photochem. and Photobiol. B: Biology, 187: 126–130. https://doi.org/10.1016/j.jphotobiol.2018.08.012

Hanigan D, Truong L, Schoepf J, Nosaka T, Mulchandani A, Tanguay RL, Westerhoff P (2018). Trade-offs in ecosystem impacts from nanomaterial versus organic chemical ultraviolet filters in

sunscreens. Water Res., 139: 281–290. https://doi.org/10.1016/j.watres.2018.03.062

Haynes V N, Ward J E, Russell B J, Agrios A G (2017). Photocatalytic effects of titanium dioxide nanoparticles on aquatic organisms—Current knowledge and suggestions for future research. Aquat. Toxicol., 185: 138–148. https://doi.org/10.1016/j.aquatox.2017.02.012
Iannone M F, Groppa M D, Sousa M E, Fernández Van Raap M B, Benavides M P. (2016) Impact of magnetite iron oxide nanoparticles on wheat (Triticum aestivum L.) development: Evaluation of oxidative damage. EEB. 131: 77-88 https://doi.org/10.1016/j.envexpbot.2016.07.004

Larue C, Castillo-Michel H, Sobanska S, Cécillon L, Bureau S, Barthès V, *et al.* (2014). Foliar exposure of the crop Lactuca sativa to silver nanoparticles: Evidence for internalization and changes in Ag speciation. J. Hazard. Mater., 264: 98–106. https://doi.org/10.1016/j.jhazmat.2013.10.053

Lu P J, Fang S W, Cheng W L, Huang S C, Huang M C, Cheng H F (2018). Characterization of titanium dioxide and zinc oxide nanoparticles in sunscreen powder by comparing different measurement methods. JFDA 26(3): 1192–1200. https://doi.org/10.1016/j.jfda.2018.01.010

Lu Pei Jia, Huang S C, Chen Y P, Chiueh L C, Shih D Y C (2015). Analysis of titanium dioxide and zinc oxide nanoparticles in cosmetics. JFDA, 23(3): 587–594.
https://doi.org/10.1016/j.jfda.2015.02.009

Manesh R R, Grassi G, Bergami E, Marques-Santos L F, Faleri C, Liberatori G, Corsi I (2018) Co-exposure to titanium dioxide nanoparticles does not affect cadmium toxicity in radish seeds (Raphanus sativus). Ecotoxicol. Environ. Saf., 148: 359–366. https://doi.org/10.1016/j.ecoenv.2017.10.051

Maynard A D, Aitken R J, Butz T, Colvin V, Donaldson K, Oberdörster G, *et al.* (2006). Safe handling of nanotechnology. Nature, 444(7117): 267–269. https://doi.org/10.1038/444267a

Movafeghi A, Khataee A, Abedi M, Tarrahi R, Dadpour M, Vafaei F. (2018) Effects of TiO2 nanoparticles on the aquatic plant Spirodela polyrrhiza: Evaluation of growth parameters, pigment contents and antioxidant enzyme activities. J. Environ. Sci., 64: 130–138.
https://doi.org/10.1016/j.jes.2016.12.020

Namdeo M, Saxena S, Tankhiwale R, Bajpai M, Mohan, Y M, Bajpai S K (2008). Magnetic nanoparticles for drug delivery applications. J. Nanosci. Nanotechnol, 8(7): 3247–3271.
https://doi.org/10.1166/jnn.2008.399

Newman M D, Stotland M, Ellis J I (2009). The safety of nanosized particles in titanium dioxide- and zinc oxide-based sunscreens. JAAD, 61(4): 685–692. https://doi.org/10.1016/j.jaad.2009.02.051

Nohynek G J, Dufour E K, Roberts M S (2008). Nanotechnology, cosmetics and the skin: Is there a health risk? Skin Pharmacol. Physiol., 21(3): 136–149. https://doi.org/10.1159/000131078

Raliya R, Nair R, Chavalmane S, Wang W N, Biswas P, (2015) Mechanistic evaluation of translocation and physiological impact of titanium dioxide and zinc oxide nanoparticles on the tomato (Solanum lycopersicum L.) plant. Metallomics, 12: 1584–1594. https://doi.org/10.1039/c5mt00168d
Rastogi, A.; Zivcak, M.; Sytar, O.; Kalaji, H. M.; He, X.; Mbarki, S.; Brestic, M. (2017) Impact of metal and metal oxide nanoparticles on plant: A critical review. Front. Chem., 5: 1–16.
https://doi.org/10.3389/fchem.2017.00078

Rodríguez-González V, Terashima C, Fujishima A (2019). Applications of photocatalytic titanium dioxide-based nanomaterials in sustainable agriculture. J. Photochem. Photobiol. C: Photochemistry Reviews, *40*: 49–67. https://doi.org/10.1016/j.jphotochemrev.2019.06.001

Sadrieh N, Wokovich A M, Gopee N V, Zheng J, Haines D, Parmiter D, *et al.* (2010). Lack of

significant dermal penetration of titanium dioxide from sunscreen formulations containing nano- and submicron-size TiO2 particles. ToxSci, 115(1): 156–166. https://doi.org/10.1093/toxsci/kfq041
Sala F C, Costa C P da (2012). Retrospectiva e tendência da alfacicultura brasileira. Hortic Bras., 30(2): 187–194. https://doi.org/10.1590/s0102-05362012000200002

Santos Filho R, Vicari T, Santos S A, Felisbino K, Mattoso N, Sant'anna-Santos B F, Cestari M M, Leme D M (2019) Genotoxicity of titanium dioxide nanoparticles and triggering of defense mechanisms in Allium cepa. Genet. Mol. Biol, 42: 425–435. https://doi.org/10.1590/1678-4685-GMB-2018-0205

Sendra M, Sánchez-Quiles D, Blasco J, Moreno-Garrido I, Lubián L M, Pérez-García S, Tovar-Sánchez A. (2017). Effects of TiO2 nanoparticles and sunscreens on coastal marine microalgae: Ultraviolet radiation is key variable for toxicity assessment. Environ. Int, 98: 62–68. https://doi.org/10.1016/j.envint.2016.09.024

Schwab F, Zhai, G, Kern M, Turner A, Schnoor J L, Wiesner M R (2016) Barriers, pathways and processes for uptake, translocation and accumulation of nanomaterials in plants - Critical review. Nanotoxicology, 10: 257–278. https://doi.org/10.3109/17435390.2015.1048326
O'Brien T P, Feder N M E M (2005). Polyehromatic Staining of Plant Cell Walls by Toluidine Blue O, 1–8. https://doi.org/10.1007/BF01248568

Tombuloglu, H.; Tombuloglu, G.; Slimani, Y.; Ercan, I.; Sozeri, H.; Baykal, A. (2018) Impact of manganese ferrite (MnFe2O4) nanoparticles on growth and magnetic character of barley (Hordeum vulgare L.). Environ. Pollut., 243: 872–881. https://doi.org/10.1016/j.envpol.2018.08.096.
Weir A, Westerhoff P, Fabricius L, von Goetz N, (2012). Titanium Dioxide Nanoparticles in Food and Personal Care Products NIH Public, Sci Technol E. 46(4): 2242–2250. https://doi.org/10.1021/es204168d

Zhang W, Yu Z, Rao P, Lo I M C (2019) Uptake and toxicity studies of magnetic TiO2-Based nanophotocatalyst in Arabidopsis thaliana. Chemosphere, 224: 658–667. https://doi.org/10.1016/j.chemosphere.2019.02.161>.

4.2 MANUSCRIPT 2 – Ultrastructural effects of titanium dioxide (tio2) microparticles *on Lactuca sativa* l. Seedlings

Ana Kamila Medeiros Lima[1]; João Vinicius Sousa Fernandes[1]; Jorge Henrique Andrade Vieira[1]; Fernanda Gomes Trindade[2]; Maura da Cunha[2], Thaiz Batista Azevedo Rangel Miguel[1], Antje Biesemeier[3]; Tom Wirtz[3]; Emilio de Castro Miguel[1*]

[1] Biomaterials Laboratory, Department of Metallurgical Engineering and Materials and Analytical Center, Federal University of Ceará (UFC), Fortaleza, CE, Brazil.

[2] Cell and Tissue Biology Laboratory, State University of Norte Fluminense Darcy Ribeiro (UENF), Campos dos Goytacazes, Brazil.

[3]Luxembourg Institute of Science and Technology (LIST), Materials Research and Technology (MRT), Advanced Instrumentation for Ion Nano-Analytics (AINA), Esch-sur-Alzette, Luxembourg.

***Corresponding author**

Emilio de Castro Miguel

Federal University of Ceara

Pici Campus

Department of Metallurgical Engineering and Materials (DEMM)

Biomaterials Laboratory (BIOMAT)

zip code: 60455-900

Fortaleza - Ceará - Brazil

+85 33669256

emiliomiguel@ufc.br

GRAPHICAL ABSTRACT

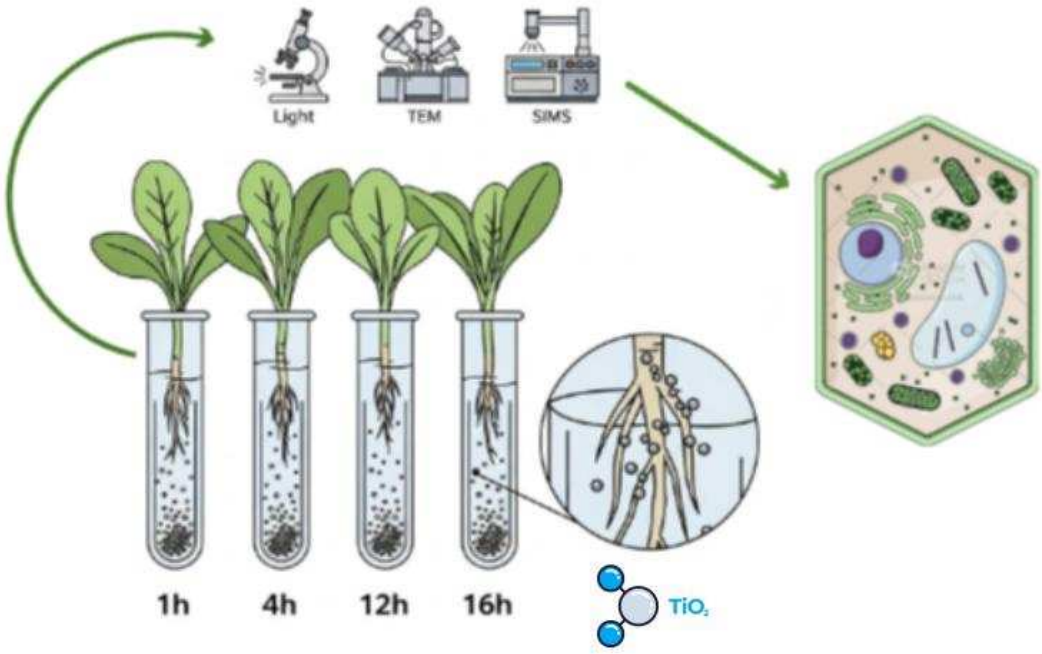

ABSTRACT

Titanium dioxide (TiO_2) is a chemically stable and insoluble compound widely used in cosmetics, food, and agriculture. It is among the most produced nanomaterials globally, with an estimated production of 2.5 million metric tons by 2025. Although long considered inert, increasing evidence indicates that TiO_2 can induce cellular and physiological damage in plants, even at environmentally relevant concentrations. This study aimed to investigate the ultrastructural and metabolic effects of TiO_2MPs exposure in *Lactuca sativa*, a model species for phytotoxicity assessments. Rutile-form TiO_2 nanoparticles (ζ-potential: −17.36 ± 0.11 mV; hydrodynamic size: 297.46 ± 3.66 nm) were prepared at 50 mg/L and sonicated for 15 minutes prior to exposure. Seven-day-old seedlings were then exposed to the suspension for 1 h, 4 h, 12 h, and 16 h. Light microscopy, transmission electron microscopy (TEM), and secondary ion mass spectrometry (SIMS) were used for analyses. The results revealed structural disorganization at the tissue level, ultrastructural alterations such as cell wall deformities and organelle extrusion, and metabolic changes including the accumulation of phenolic compounds. These effects intensified with longer exposure times, even in the absence of confirmed Ti uptake—likely due to the larger particle size—demonstrating that contact alone with TiO_2 microparticles can exert significant toxic effects on *L. sativa*.

Keywords: titanium dioxide; phytotoxicity; *Lactuca sativa*; plant cell ultrastructure; secondary ion mass spectrometry.

4.2.1 Introduction

Titanium dioxide nanoparticles (TiO_2NPs) have attracted considerable attention due to their extensive applications (cosmetics, food, agriculture and industry); however, their multifaceted influence on plant physiology and the broader environment remains a complex subject (Trela-Makowej *et al.* 2024). Metal-based nanoparticles such as titanium dioxide (TiO_2), silver (Ag) and zinc oxide (ZnO) pose significant challenges to environmental safety due to their unique properties and widespread applications. These NPs can have toxic effects on various organisms, including bacteria, earthworms, algae, fish, and plants, leading to disruptions in ecosystems and food chains (Corsi; Desimone; Cazenave, 2022; Polischuk *et al.*, 2022).

Zahra *et al.* (2020) highlighted the potential exposure pathways of TiO_2NPs originating from industrial applications to wastewater treatment systems and their subsequent impacts on the agro-environment. Their study underscores the importance of elucidating these pathways, particularly in the context of wastewater treatment, agricultural practices, and environmental safety. It also has complex, two-way interactions with plants and soil microorganisms, with effects that are modulated by a variety of factors including nanoparticle concentration, size, and reactivity (Trela-Makowej *et al.* 2024).

The review by Khan *et al.* (2021) indicates that research on the phytotoxicity of TiO_2 NPs in plants is still limited compared to other organisms. Their work highlights that higher concentrations of TiO_2 NPs (>40 ppm) can hinder seed germination, growth, and vigor in species such as *Foeniculum vulgare* (fennel), drawing attention to the potential phytotoxicity of metal-based nanoparticles including ZnONPs, TiO_2NPs, and AgNPs. These findings underscore the need for comprehensive assessments of their environmental risks. Complementing this, Chahardoli, Karimi, and Sharifan (2025) demonstrated that sub-chronic exposure of *Dracocephalum kotschyi* to TiO_2 nanoparticles (average diameter 20 nm) had dose-dependent effects: 50 ppm promoted plant biomass and height, suggesting potential benefits for agricultural productivity, whereas 100 ppm negatively affected photosynthetic pigments and root biomass, highlighting the narrow threshold between beneficial and detrimental impacts. Such studies emphasize the importance of carefully evaluating the consequences of TiO_2 exposure on plant physiology to inform safe and sustainable agro-environmental applications.

Sharma *et al.* (2025) discuss whether titanium should be regarded as a promising metal for the future or as a potential environmental contaminant. Although titanium (Ti) may offer positive effects depending on exposure time or concentration, the review also addresses

Ti contamination's potential advantages or disadvantages in comparison to other materials, although there is a clear focus on negative impacts. Ti is considered a non-essential element for plant, animal, and human nutrition and is not toxic at low levels of uptake.

Extending this knowledge, the trophic transfer and toxicity of TiO_2 NPs in microcosms mimicking terrestrial and aquatic ecosystems were evaluated by (Vijayaraj *et al.*, 2018) and there was a significant translocation of Ti to *M. truncatula* leaves in the terrestrial ecosystem, highlighting the uptake of TiO_2 NPs by plants. In the terrestrial ecosystem, the study observed significant reductions in plant height (-17%), number of leaves (-29%), and aboveground biomass (-53%) due to exposure to TiO_2 NPs, indicating phytotoxic effects. Additionally, TiO_2 NPs exposure at 50-400 mg/L deteriorated the lettuce nutritional quality in a dose-dependent fashion. Nutrient element content reduction induced by 50-200 mg/L TiO_2 NPs exposure was attributable to the biomass dilution effect (Hu *et al.*, 2020).

A recent review of five major metal nanoparticles used in the medical field (silver, gold, iron oxide, zinc oxide, and titanium dioxide) emphasizes that, despite their benefits in antimicrobial activity, anti-cancer properties, and applications in disease diagnostics, these elements might play both beneficial and toxic roles in various physiological processes. Their effects depend largely on particle size, surface coating, and the administered dose (Krishna *et al.*, 2024). They are essential, although excessively they might become dangerous for growth and development of plants. Uptake and accumulation of metals and metalloids at high concentrations cause direct morphological, structural and ultrastructural changes that affect physiological and biochemical reactions. Even though, some anatomical alterations of plant tissues can be considered as strategies that have been developed to overcome these harmful conditions (Yadav *et al.*, 2021).

TiO_2 NPs of 25 nm induced significant morphological and mechanical alterations in tomato root tissues when incorporated into the growth medium. Their small size facilitated internalization and accumulation within cell walls and intercellular spaces, leading to reduced cell area in the epidermis and vascular bundles, while the parenchyma area increased notably. These effects highlight how nanoscale TiO_2 can alter plant tissue structure at the cellular level (Nicolás-Álvarez *et al.*, 2021).

However, Farahi *et al.* (2023) investigated the effects of TiO_2NPs on photosynthetic pigments and several biochemical activities and antioxidant enzymes of the *Vitex* plant on different concentrations (0, 200, 400, 600 and 800 ppm). At 600 ppm, most physiological parameters improved; therefore, this concentration can be considered the most effective treatment, as it increased dry mass, photosynthetic pigments, and antioxidant enzyme activities.

Although the author highlights the particle should be used with caution because the effect depends on the shape, dose, type of particle and the species.

Current scientific findings regarding the toxic effects of nanoTiO_2 at environmentally relevant exposure concentrations call for a critical reappraisal of existing environmental policy criteria and the regulatory framework for minimizing the cradle to grave release and impacts of nanoTiO_2 during production and use (Luo *et al.*, 2020). Careful handling is necessary when dispersing TiO_2 catalytic slurries into the environment to prevent long-term impacts on ecosystems (Racovita, 2022).

Vishnu *et al.*, (2019) underscores the importance of further research to elucidate the specific pathways through which nanoparticles induce cellular damage and impact plant physiological processes, ultimately influencing plant health and ecosystem dynamics. Titanium dioxide also can modify the cell wall to increase fluidity, thereby aiding in cell expansion. TiO_2 NPs also have been suggested to trigger the accumulation of carotene pigment in water-deficit plants (Mustafa *et al.* 2021) and enhanced the uptake of K and P under both well-watered and water-deficit conditions (Aghdam *et al.* 2016).

While these studies highlight the multiple mechanisms by which TiO_2 nanoparticles can interfere with plant physiology, ranging from cell wall modification to altered nutrient uptake and pigment accumulation, it is equally important to consider suitable model species to evaluate such effects under controlled conditions.

Lactuca sativa, commonly known as lettuce, serves as a valuable toxicity model in various studies assessing the impact of different chemical compounds on plant growth and development (Egler *et al.*, 2024; Pino *et al.*, 2016). Research has shown that *L. sativa* is sensitive to substances like glyphosate, pharmaceutical products, metal nano and microparticles and emerging contaminants from personal care products, exhibiting phytotoxic and cytogenotoxic effects such as reduced root and shoot growth, altered cell cycle, chromosomal anomalies, morphological and anatomical changes (Chan-Keb *et al.*, 2022; Lima *et al.*, 2023; Vieira; Marcon; Droste, 2024).

Due to the presentation of the possible effects that the interaction with titanium dioxide can cause in the most diverse plants, this work aims to deepen the explanation of these damages at ultrastructural levels using the *Lactuca sativa* seedlings as a model.

4.2.2 Material and methods

The titanium dioxide microparticles (TiO_2MPs) have this nomenclature in this paper according to new scientific findings of European Comission (EC) and the regulatory

experience, adopted an updated definition of nanomaterial. Natural, incidental or manufactured material consisting of solid particles present, either on their own or as identifiable constituent particles in aggregates or agglomerates and one or more external dimensions of the particle are in the size range 1 nm to 100 nm (European Comission, 2022).

The titanium dioxide microparticles (TiO_2MPs) were kindly provided by the Advanced Materials Chemistry Group (GQMat) coordinated by Dr. Pierre Fechine - Department of Analytical Chemistry and Physical Chemistry, Federal University of Ceará – UFC. This particle was characterized in a previous study (Barbosa *et al.* 2018). The particle used underwent a sonochemical process for size reduction and has an average size of 104.4 ± 2.29 nm. The rutile form was used in this study with its zeta potential of −17.36 ± 0.11, its hydrodynamic size value of 297.46 ± 3.66 nm. The solution of 50 mg/L was prepared and sonicated for 15 minutes for the exposure test.

The investigation of the TiO_2MPs toxicity took place at different exposure times. Initially, 50 seeds were germinated in petri dishes and germitest paper and distilled water. After the 7th day of sowing, the seedlings were subjected to interaction with TiO_2MPs at the 50 mg/L concentration which proved to be most toxic to *Lactuca sativa* in a previous study (Lima *et al.*, 2023), using the following exposure periods: 1h, 4h, 12h and 16h.

Seven days after sowing, uniform seedlings were selected and individually transferred to micro tubes containing 0.5 mL of 50 mg/L TiO_2MPs aqueous dispersion. The dispersion was applied in a way that only the roots were in contact with the suspension, avoiding exposure of the aerial parts. During the exposure periods, the plants were kept on a laboratory bench at a controlled temperature of 22 °C under continuous light conditions.

After exposure, radicle, hypocotyl and leaf samples were immediately fixed for each exposure time for future analysis using Light Microscopy (LM) and Transmission Electron Microscopy (TEM) in an aqueous solution containing 2.5% glutaraldehyde, 4% formaldehyde, diluted in 0.5 M sodium cacodylate buffer, pH 7.2, at room temperature (modified Karnovsky), for 24 hours.

Light Microscopy (LM)

After the collection and fixation of the samples, fragments were washed three times in sodium cacodylate 0,05M. Subsequently, dehydration was done by increasing the series of ethanol, 50%, 70%, 80%, 90% and three series of 100% ethanol, each interval 40 minutes. After dehydration, the samples were embeded in historesin (Leica). After this step, the samples were assembled into blocks, polymerized and cutted (5µm) using a rotative microtome (Leica

RM2255 Rotating Microtome).

The final stage in preparing the material for observation under light microscopy was the assembly of the slides. To stain the slides, an aqueous solution of Toluidine blue (TB) 0.025% pH 4.0 was used for 1 minute at room temperature. This procedure was followed by three washes in distilled water (O'Brien and Feder, 1964). After drying, the slides were mounted with Entellan. The visualization of the samples and the respective documentation was finalized in a Zeiss Primo Star equipped with a digital camera, and the Zen Lite software for the acquisition of images.

Transmission Electron Microscopy (TEM)

Samples were fixed and washed following the same procedure used for optical microscopy. Post-fixation was carried out with 1% osmium tetroxide (OsO_4) at pH 7.02 for two hours. Subsequently, the samples were washed three times for 40 minutes each in 0.05 M cacodylate buffer. Dehydration was performed in a graded acetone series (50%, 70%, 90%, and three changes of 100%), with each step lasting 40 minutes.

After dehydration, the samples were infiltrated in epoxy resin (Embed 812). After this process, the blocks were assembled and polymerized for 48 hours at 60°C. The ultrathin sections (60nm) were made with ultramicrotome Leica UC7 and the observation in the Jeol TEM 1011 Plus at 120kv.

Secondary Ion Mass Spectrometry (SIMS)

Samples previously prepared for TEM and embedded in Embed 812 resin were sectioned using an ultramicrotome at a thickness of approximately 300 nm and mounted onto silicon wafers (Ted Pella) for analysis. The measurements were performed using the RAITH IONMASTER, a focused ion beam (FIB) platform equipped with a liquid metal alloy ion source (LMAIS) from RAITH, operating at landing energies below 35 keV. This system enables high-resolution imaging and chemical analysis of biological samples. Compositional information, such as the identification and subcellular localization of metal nanoparticles embedded in biological matrices, was obtained using the integrated compact magnetic sector secondary ion mass spectrometry (SIMS) system, which offers lateral resolution below 15 nm. The delay-line microchannel plate detector enables parallel mass detection for each scanned pixel across the selected mass range, providing hyperspectral SIMS imaging in both positive and negative polarities as described by Ost *et al.* (2024). In this study, measurements were performed in

positive mode with a magnetic field of 250 mT, where peaks corresponding to titanium (Ti; m/z 46–50, with a main peak at m/z 48) and titanium oxide species (TiO; m/z 63–67, with a main peak at m/z 65) were detected. Here, m/z refers to the mass-to-charge ratio.

4.2.3 Results and discussion

For each experimental condition, a control was included, and TEM images were obtained from the same regions analyzed by LM, ensuring consistency between techniques and reliability of the results. This approach allowed a direct correlation between tissue-level observations and ultrastructural alterations, providing a more comprehensive interpretation of the effects observed under the different treatments.

The milder exposure for 1 hour shows that the tissue structure of the three organs analyzed (radicle, hypocotyl, and leaf) was preserved when compared to the controls. At 4 hours, in control (1A and 1B), the epidermis, cortex cells (1E), and vascular bundles were also preserved. In contrast, it was not possible to clearly define the delimitation of the endodermis and pericycle, and a disruption of the cortical tissue structure was observed (1C and 1D), both in the radicle and in the hypocotyl, indicating the onset of toxicity spreading through the plant. This result is consistent with Yadav *et al*. (2021), who reported that exposure to various metals, such as aluminum, cadmium, and copper, caused alterations in root architecture and tissue disruption in different species, including *Arabidopsis thaliana*, *Phaseolus vulgaris*, and *Mentha aquatica* L.

The TEM microscopy emphasizes the cellular traces of titanium-induced toxicity, when compared to the control (1B), evidenced by the appearance of peroxisomes and vesicle ruptures in the cortical region of the hypocotyl (1F) as observed through both light and transmission electron microscopy. These organelles play a fundamental role in cellular defense against toxic effects, particularly under oxidative stress conditions such as salinity (Baranova *et al.*, 2018), supporting the hypothesis that their presence and disruption are associated with the toxic response to TiO_2, an abiotic factor, even at early exposure stages. Additional ultrastructural alterations such as plastid rupture (1I), altered morphology of the Golgi apparatus and secretion activity (1J), cytoplasmic rupture (1K), and changes in cell shape, thickening of the cell wall, and rupture of a large vesicle (1L) reinforce the toxic effect of this nanoparticle. These findings collectively suggest that TiO_2 induces early but significant structural disturbances, especially in organelles involved in stress signaling and intracellular trafficking.

After 4 hours of exposure to TiO_2, the leaf cells of *L. sativa* (1G and 1H) exhibited a severely compromised ultrastructure, with an almost complete loss of cytoplasmic and

organellar integrity. Only the cell wall and possible remnants of the nucleus and vacuole were distinguishable. Although the nuclear envelope was not clearly defined (1H), the density pattern and intracellular position strongly suggest a collapsed nucleus undergoing condensation, characteristic of the final stages of programmed cell death (PCD). These alterations—organelle condensation, fragmentation, and degradation—are consistent with toxic stress-induced PCD. According to van Doorn *et al*. (2011), vacuolar cell death is typically associated with plant development, while necrosis is more common under abiotic stress, supporting the interpretation that TiO_2 exposure triggered a stress-related cell death pathway.

The morphological alterations observed under light microscopy (1C and 1D), together with irregularities in the hypocotyl cell wall (1L), likely represent structural adaptations to toxic stress. These changes are comparable to those reported in *Medicago sativa* (Fabaceae) following long-term cadmium exposure. In *M. sativa*, the accumulation of xylogalacturonan and modulation of cell wall proteins contributed to tolerance by modifying the wall's capacity to sequester cadmium (Gutsch *et al.*, 2019). Likewise, the irregular cell wall contours and altered morphology in our study suggest remodeling of the cell wall architecture, possibly as a mechanism to limit metal uptake and mitigate cellular damage.

In this study, titanium particles primarily contacted the radicle, which served as the main site of exposure. As a result, several structural alterations were observed, including irregular contours (1G and 1H), cell wall thickening (1L), and the presence of vesicles between the plasma membrane and the cell wall suggesting apoplast way. At the cellular level, heavy metals typically interact with the plant cell wall through physical adsorption or chemical bonding. Cell wall components such as pectin and cellulose exhibit high affinity for metal ions, promoting their binding and the formation of complexes or precipitates (Li *et al.*, 2024).

Although titanium dioxide is a chemically stable and insoluble compound that does not ionize under physiological or environmental conditions (French *et al.*, 2009), the cellular alterations observed suggest that contact with TiO_2 may have triggered remodeling of the cell wall, possibly via polysaccharide modification or vesicle-mediated transport. Cell wall-associated proteins, such as expansins, extensins, PMEs, and XTHs, regulate the balance between wall loosening and reinforcement, playing a central role in stress responses (Tenhaken, 2015; Cosgrove, 2016). Recent reviews suggest that similar mechanisms may also be activated under abiotic stress induced by nanoparticles (Dutta *et al*., 2022; Khan *et al.,* 2017; Singh *et al.,* 2015;).

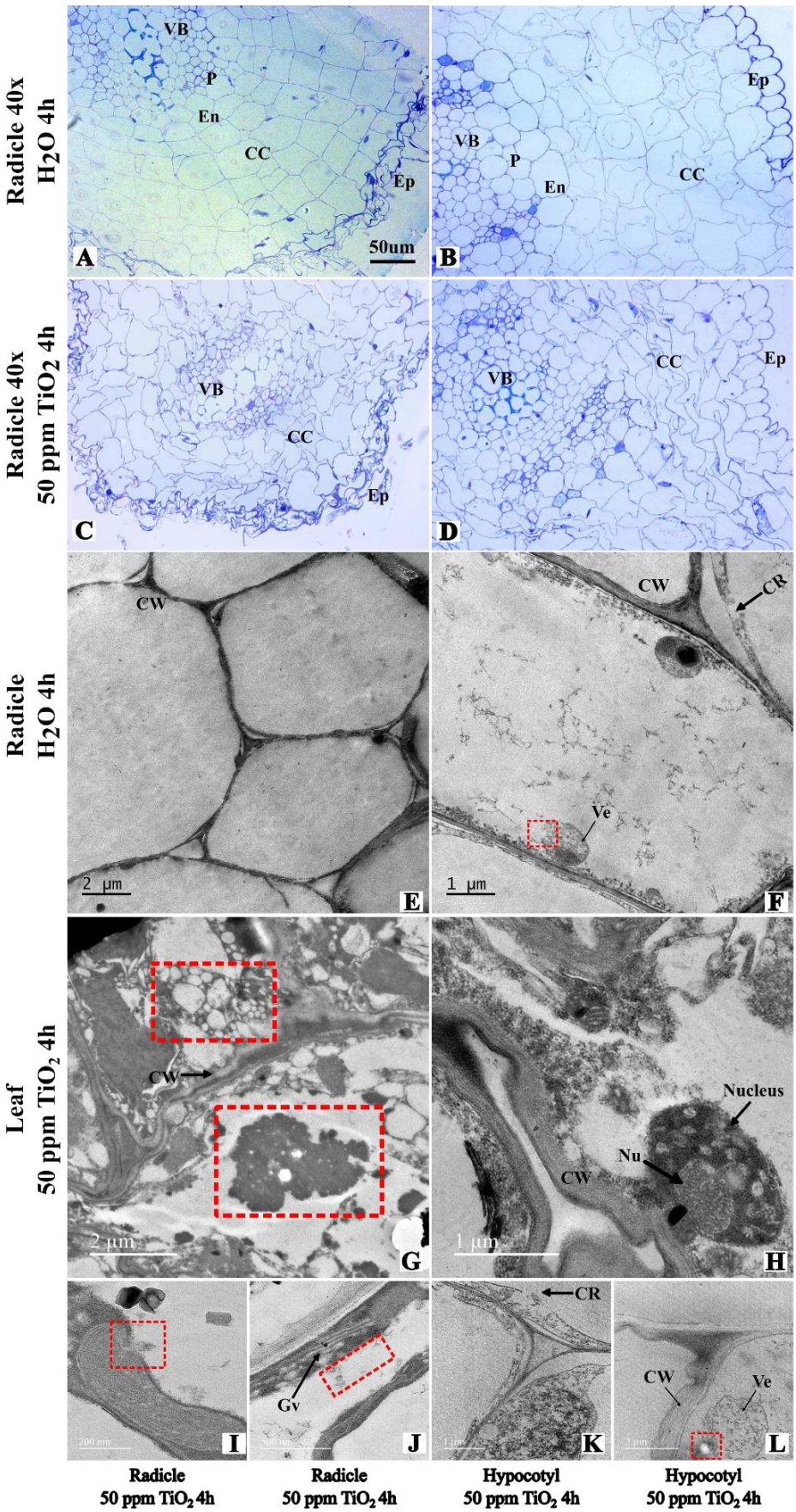
Radicle 40x H2O 4h
Hypocotyl 40x H2O 4h
Radicle 40x 50 ppm TiO2 4h
Hypocotyl 40x 50 ppm TiO2 4h
Radicle H2O 4h
Hypocotyl 50 ppm TiO2 4h
Leaf 50 ppm TiO2 4h
Leaf 50 ppm TiO2 4h
VB
P
En
CC
Ep
50um
A
B
C
D
CW
CR
Ve
2 µm
1 µm
E
F
Nucleus
Nu
G
H
Gv
I
J
K
L
Radicle 50 ppm TiO2 4h
Radicle 50 ppm TiO2 4h
Hypocotyl 50 ppm TiO2 4h
Hypocotyl 50 ppm TiO2 4h

Figure 1. Light and transmission electron micrographs of radicle, hypocotyl, and leaf tissues of *Lactuca sativa* seedlings 7 days after germination, exposed to 50 ppm TiO_2 for 4 hours. (A, B, E) Control sections (H_2O) of radicle (A, E) and hypocotyl (B) show preserved tissue organization and normal ultrastructure. (C, D, F) Corresponding regions in seedlings exposed to TiO_2 show marked structural alterations. Disorganization of the pericycle and endodermis is evident in both radicle (C) and hypocotyl (D), compared to their respective controls. In (F), the presence of peroxisomes (P) and vesicle rupture (highlighted in red) are observed—features absent in the control (E). Leaf cells from exposed seedlings (G, H) display extensive cytoplasmic degradation, where only the cell wall (CW), remnants of the nucleus (N), and vacuole (V) are distinguishable. Organelle fragmentation and cytoplasmic condensation, typical of programmed cell death, are marked in red. (I) Shows plastid rupture; (J) indicates altered Golgi apparatus morphology and secretion activity; (K) highlights cytoplasmic rupture (CR); (L) displays altered cell shape, thickening of the cell wall, and rupture of a large vesicle (red highlight). Ep – epidermis; CC – cortex cells; VB – vascular bundle; En – endodermis; P – pericycle; CW – cell wall; P – peroxisome; Gv – Golgi vesicle; Ve – vesicle; Nu – nucleolus; CR – cytoplasmic rupture.

Wakabayashi *et al.* (2023) showed that lead (Pb) exposure in rice coleoptiles reduced growth by decreasing wall extensibility and increasing wall thickness through polysaccharide accumulation, without enhancing phenolic cross-linking. These structural changes led to mechanical stiffening of the wall and growth inhibition. A comparable response may be occurring in lettuce roots under TiO_2 exposure, where damage thickening and remodeling, even without Ti translocation, could contribute to the ultrastructural damages observed.

The vascular bundle also shows disorganization (1D) when compared to the control and samples from previous exposure times. Caspary strip in the endodermis can prevent nanoparticles from entering the vascular bundle, however, with disorganization of the endodermis where these striations may not have been formed or are disconnected, the vascular bundle is susceptible to the entry of NPs (Huang *et al.*, 2022; Muccifora *et al.*, 2021).

Advancing in the characterization of the toxic effects, greater intensity was observed after 12 hours of exposure (Fig. 2). In the root, severe damage occurred, such as cell disruption in the vascular bundle (2D), close to xylem cells, along with partial disorganization of the pericycle and endodermis, although the epidermis remained preserved (2D).

In the leaves, the palisade parenchyma appeared disorganized (2F), with its cells intermingled with those of the spongy parenchyma. Similar anatomical alterations, including changes in mesophyll cells, epidermis thickness, and vascular bundles, have also been reported in *Betula pendula* and *Acer platanoides* exposed to volatile organic compounds near industrial emissions (Tyulkova, 2020). Despite involving different plant species and distinct toxic agents, both cases reveal comparable damage patterns, suggesting a common plant response to toxic environments.

Complementing these observations, an increase in electron-dense, blue-stained spots was detected inside the cells (2F) compared to the control (2C), representing another sign

of the toxicity endured. These areas, visualized by light microscopy, may correspond to electron-dense aggregates in the cytoplasm observed under TEM (3H), reinforcing the occurrence of cellular disorganization and injury. Unlike *Chenopodium quinoa* under hydric stress, which did not exhibit such dense deposits and showed recovery without impairing photosynthesis (Manaa et al., 2021), *Lactuca sativa* exposed to TiO_2 nanoparticles demonstrated persistent structural damage. This difference indicates that photosynthesis in lettuce may be more severely compromised, especially given the absence of recovery indicators after exposure—contrasting with the tolerance observed in *C. quinoa*.

This interpretation is further supported by the findings of Tripathi *et al.* (2024), where plant exposure to silver nanoparticles also led to increased ROS production, resulting in cytoplasmic retraction, inactivation of photosystems I and II, and consequent damage to chloroplasts and mitochondria. Similarly, the electron-dense aggregates observed in lettuce cells may reflect oxidative stress-induced degradation, suggesting that photosynthetic impairment and redox imbalance are key elements of TiO_2 nanoparticle toxicity in plant cells. Also, its role in enzyme activity and its capacity to regulate oxidative stress and antioxidant metabolism in plants further underlines its complex interaction with plant physiology (Trela-Makowej *et al.* 2024).

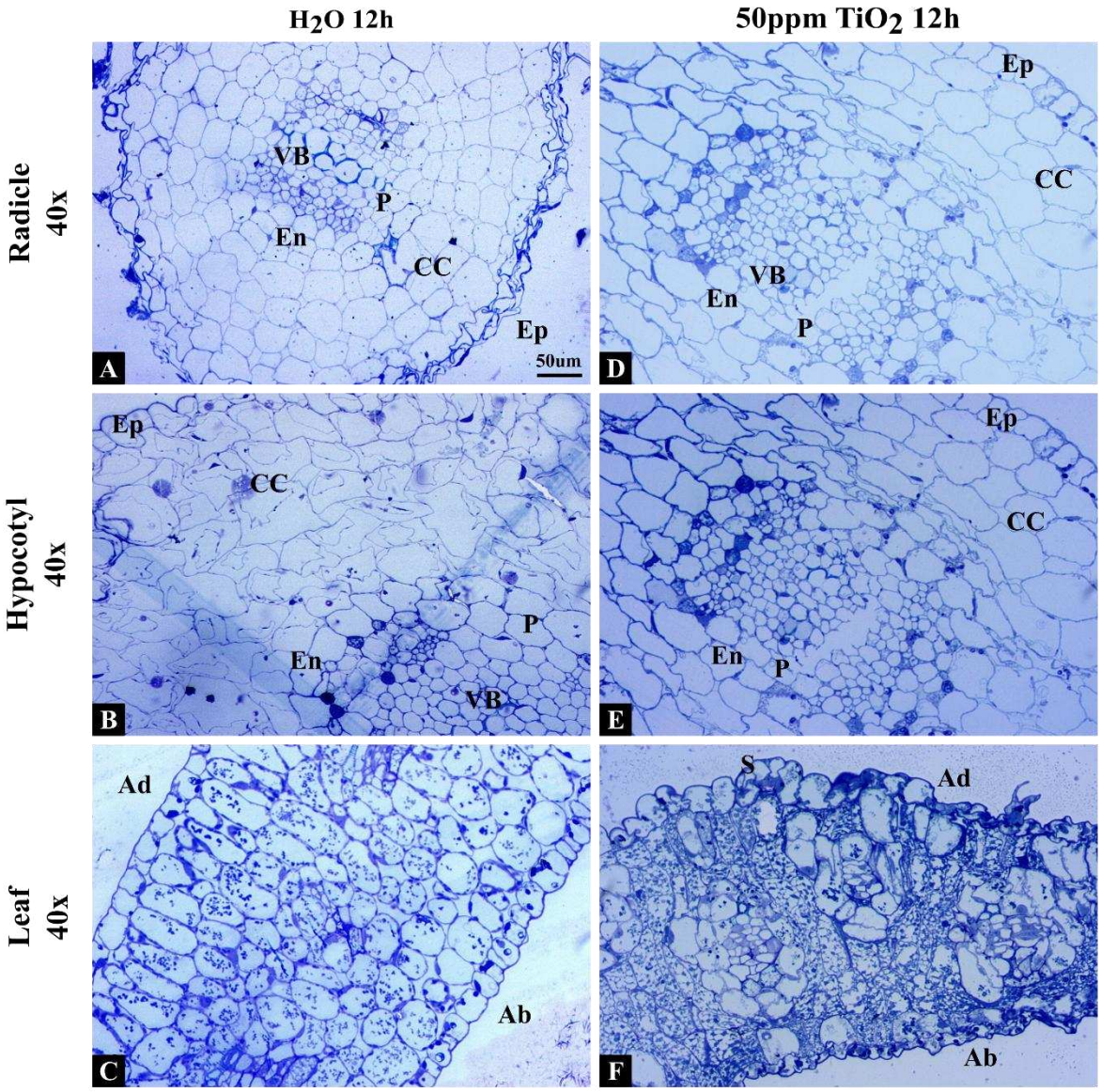

Figure 2. Optical micrographs of radicle, hypocotyl, and leaf sections of *Lactuca sativa* seedlings 7 days after germination, exposed to 50 ppm TiO_2 for 12 hours, and respective controls. (A–C) Control sections (H_2O) of the radicle (A), hypocotyl (B), and leaf (C) showing preserved tissue organization. (D–F) Corresponding tissues exposed to 50 ppm TiO_2 for 12 hours. In the radicle (D), pericycle cells are affected but still distinguishable compared to the control. In the hypocotyl (E), cell rupture is evident in the vascular bundle. In the leaf (F), cells of both the palisade and spongy parenchyma appear deformed. The letters indicate the main tissue components where toxic effects may be observed. Ep – epidermis; CC – cortex cells; VB – vascular bundle; En – endodermis; P – pericycle; Ad – adaxial surface; Ab – abaxial surface; S – stoma. **Scale bar:** 50 µm.

Detailed TEM analysis revealed a sinuous cell wall in the radicle (3B) compared to the preserved ultrastructure of the 12-hour non-exposed seedling (3A). Similar effects were reported by Minkina et al. (2020), who observed reduced stele diameter and disorganized initial root cells in *H. sativum* exposed to copper-contaminated soil, corroborating the damage observed here as toxicity-induced.

In the same region, vesicles were detected between the cell wall and the intercellular space (3B), suggesting a possible excretion process. Electron-dense bodies adhered to the inner

cell wall (3B, 3C, 3D) indicate phenolic compound accumulation. In some cases, vesicles were attached to the cell wall and surrounded by electron-dense filaments (3B, 3C), likely composed of phenolic material. Additionally, mitochondria (Mt) and plastids (P) appeared to contribute to filament formation (3C), suggesting a role of these organelles in phenolic metabolism and stress responses. Notably, Jung, Choi, and Mun (2019) demonstrated through electron microscopy that vesicles are often linked to autophagy, a process crucial for cell survival and maintenance, supporting the interpretation of the vesicles observed here.

This interpretation is further reinforced by Rao and Zheng (2025), who reported that nanoparticle-induced stress modulates phenylpropanoid metabolism, enhancing polyphenol production with antioxidant functions. Similarly, Shelke et al. (2023) emphasized the protective role of these compounds in mitigating oxidative stress. Consistently, the presence of numerous vesicles (3E, 3F) and vacuolar rupture in the hypocotyl (3F) may reflect intensified intracellular trafficking and stress signaling, contributing to structural remodeling under abiotic stress conditions.

In the leaves, ultrastructural damage was also evident. TEM revealed compromised chloroplasts and nuclei (3H), likely impairing gene expression regulation, along with a large electron-dense mass (3I) and myelin-like figures (3G), which may represent defense mechanisms. Comparable effects were described by Tripathi et al. (2024), where exposure to silver nanoparticles caused metabolic alterations and nuclear damage, impairing protein synthesis linked to photosynthesis, glycolysis, antioxidant defense, respiration, and pathogen resistance.

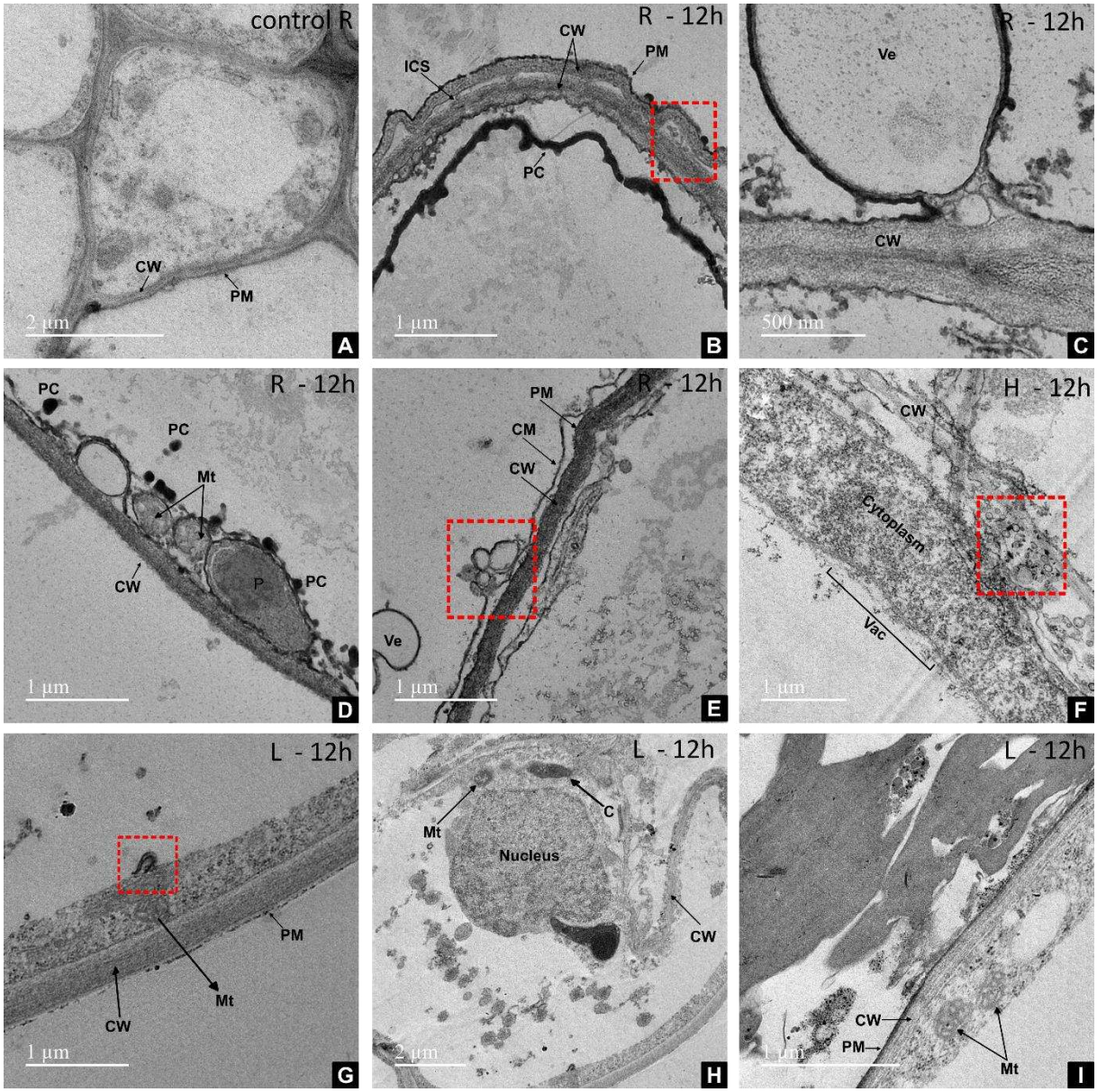

Figure 3. Transmission electron micrographs of *Lactuca sativa* radicle, hypocotyl, and leaf cells after 12-hour exposure to 50 mg/L TiO_2. A: Control radicle cell (H_2O), presenting typical ultrastructure with organelles well defined and integrity of cell wall. B: Treated radicle cell showing cell wall thickening, vesicles in the intercellular space (red square), and an electron-dense filament (PC) suggestive of phenolic compound accumulation. C: Radicle cell with a vesicle attached to the cell wall and surrounded by an electron-dense filament, likely composed of phenolic material. D: Radicle cell containing phenolic granules, with mitochondria (Mt) and a plastid (P) seemingly being incorporated into the formation of the electron-dense phenolic filament. E: Radicle cell showing vesicles budding inward from the plasma membrane (PM) into the cytoplasm. F: Hypocotyl cell displaying vesicles between the plasma membrane and cytoplasm, with a high density of ribosomes. G: Leaf cells show dense cytoplasm, the presence of mitochondria, and a myelin-like figure (highlighted in red). H: Leaf cell with a nucleus (Nu) exhibiting signs of damage, a vacuole (Vac) containing electron-dense aggregates, and structurally compromised chloroplasts (C). I: Leaf cells lack visible vacuolar delimitation, containing a large electron-dense mass. P – plastid; CW – cell wall; Ve – vesicle; Nu – nucleolus; Mt – mitochondria; PC – phenolic compounds; PM – plasma membrane; Vac – vacuole; C – chloroplast.

Comparing both light and TEM microscopy in figure 4, the radicle (4D) presents the smallest injury compared to the other two organs (4E and 4F). The hypocotyl maintains the pattern of cortical cell disorganization, as evidenced by light microscopy (4E) and further

detailed by transmission electron microscopy (4G and 4H). Furthermore, it is possible to observe the disruption of the plasma membrane. In (Khan *et al.*, 2021a), studies carried out with ZnO particles (500 mg/L) in rice seeds showed that the cell wall and plasma membrane of mesophyll cells became wrinkled as one of the most significant ultrastructural changes, agreeing with present results. In addition to the increased spacing observed between the membranes of affected thylakoids, nuclei, and other membranous organelles, the fact that ZnO and TiO_2 are commonly combined in sunscreen formulations further supports the evidence of their toxic effects, both individually and in combination.

The leaf (4F, 4I, and 4J) was the organ that presented the most extensive lesions among those analyzed, including accumulation of lipid inclusions (4I), extrusion of organelles, and chloroplast damage (4J). This finding is particularly concerning because the leaf constitutes an edible part of the species. Although titanium dioxide (TiO_2) has often been considered safe due to its low oral absorption, recent animal studies have indicated dose-dependent toxic effects, including liver damage, kidney injury, inflammatory responses, and tissue deposition in the spleen (Brand *et al.,* 2020; Javaheri *et al.,* 2023).

Meanwhile, the non-exposed seedlings (4C and 4K) appear uniform with typical cytoplasm structure, with an intact vacuole, well-defined organelles, and healthy chloroplasts (4L), which are not found in samples exposed to titanium. According to Chahardoli *et al.*, (2022); Vishnu *et al.*, (2019), the alteration of the chloroplast substructure is one of the toxic effects caused by titanium, and at high levels, the photosynthetic capacity can be altered due to the interruption of enzymes such as ribulose-1,5-bisphosphate carboxylase/oxygenase (Rubisco).

It is difficult to determine the adaxial and abaxial surfaces of the leaves (4F), as the tissues that are the reference for this identification (palisade and lacunous parenchyma) appear completely disorganized due to high-grade damage. In TEM images, it is possible to point out that the electron-dense regions that fill the leaf (4I and 4J) are a mixture of lipid body accumulation and organelle extravasation, which occupy almost the entire intracellular space. According to Ruffini Castiglione *et al.* (2016), when programmed cell death occurs, the number of non-distinguishable electron-dense bodies increases, as in (4I) and (4J), along with the appearance of non-recognizable organelles and may be related to severe toxic stress damage preceding cell death.

The phytotoxicity of *L. sativa* was also evaluated in association with nonylphenol, an endocrine-disrupting chemical (EDC), and according to De Bruin *et al.* (2017), findings such as lipid accumulation, organelle extravasation, and vacuole fragmentation indicated how

nonylphenol affected *Lactuca sativa* plants. Their results corroborate the data found in the present experiment. In addition, there is an increase in the electron density of the cytoplasmic matrix, which also indicates metabolic stress.

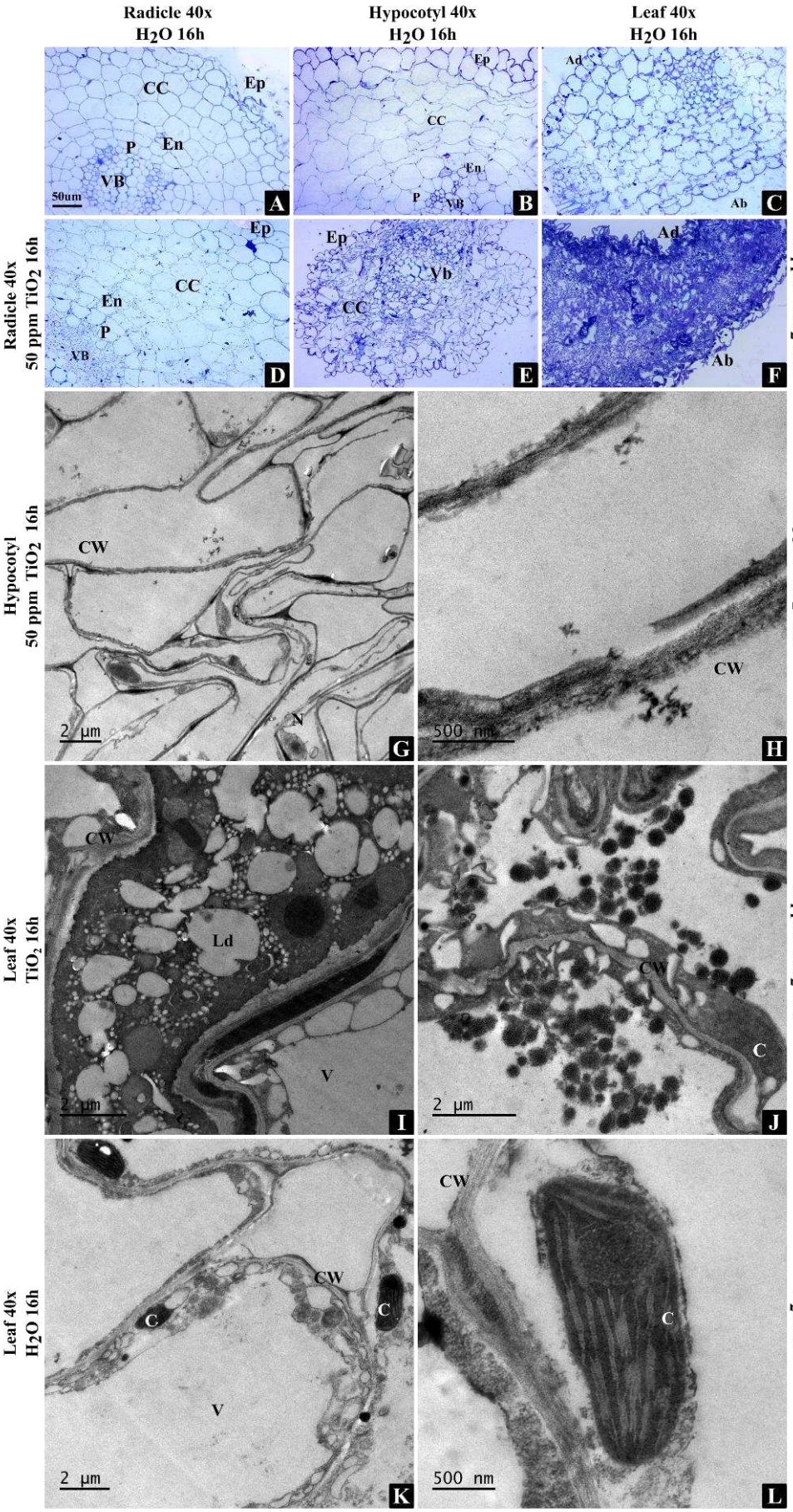
Radicle 40x
H2O 16h
Hypocotyl 40x
H2O 16h
Leaf 40x
H2O 16h
CC
Ep
P
En
VB
50um
A
Ep
CC
En
P
VB
B
Ad
Ab
C
Radicle 40x
50 ppm TiO2 16h
En
CC
P
VB
Ep
D
Ep
Vb
CC
E
Leaf 40x
50 ppm TiO2 16h
Ad
Ab
F
Hypocotyl
50 ppm TiO2 16h
CW
2 µm
N
G
Hypocotyl
50 ppm TiO2 16h
CW
500 nm
H
Leaf 40x
TiO2 16h
CW
Ld
V
2 µm
I
Leaf 40x
50 ppm TiO2 16h
CW
C
2 µm
J
Leaf 40x
H2O 16h
CW
C
C
V
2 µm
K
CW
C
500 nm
L

Figure 4. Optical and transmission electron micrographs of radicle, hypocotyl, and leaf tissues of *Lactuca sativa* seedlings 7 days after germination, exposed to 50 ppm TiO_2 for 16 hours, and respective controls (H_2O). (A–C, K–L) Control sections of the radicle (A), hypocotyl (B), and leaf (C, K, L) showing preserved cellular architecture. (D–F, I–J) Corresponding tissues exposed to TiO_2 for 16 hours: radicle (D), hypocotyl (E, G, H), and leaf (F, I, J). Significant structural damage is evident in the hypocotyl and leaf tissues (E and F) compared to controls (B and C), with further confirmation under electron microscopy. In the hypocotyl, TEM reveals extensive tissue degradation (G) and disruption of the cell wall (H). In the leaf, titanium exposure leads to the accumulation of lipid inclusions (I), extrusion of organelles, and chloroplast damage (J), in contrast with the preserved structures seen in control images (K, L). Ep – epidermis; CC – cortex cells; VB – vascular bundle; En – endodermis; P – pericycle; CW – cell wall; PM – plasma membrane; P – peroxisome; V – vacuole; Ld – lipid accumulation; C – chloroplast.

Figure 5 provides a detailed view of what happened to the tissues structure at 16 hours of exposure. The ultrastructural disorganization of the tissues is evident (5A, 5D and 5F) especially when compared to the same type of section from a control cell. Ultrastructural analysis revealed progressive damage across the radicle, hypocotyl, and leaf tissues of *Lactuca sativa*. In the radicle (5A–5C), cells exhibited moderate alterations, such as disorganization of the cell wall and rupture of the plasma membrane (5A), the presence of a slightly electron-dense body adhered to the inner cell wall (5B), and vesicles of different sizes within the cytoplasm, apparently in transit (5C), suggesting active vesicular trafficking or exocytosis potentially related to a detoxification mechanism.

The hypocotyl (5D–5F) showed more pronounced damage, with multiple structurally compromised cells, including ruptured vacuolar membrane (tonoplast) and cytoplasm (5D, red square), dense cytoplasm containing a myelin-like figure (5E), and small electron-dense inclusions near the cell wall (5F), all indicative of advanced cellular stress and possibly the onset of programmed cell death (PCD). In the leaf tissue (5G–5I), the injuries were even more severe. The ultrastructure was largely destroyed, with nuclei showing signs of degeneration (5G), presence of small electron-dense aggregates within the nucleus and cytoplasm (5H), and a large amorphous electron-dense mass with no identifiable organelles (5I), consistent with cytoplasmic collapse.

Supporting the present findings, previous studies on *Hordeum sativum* (Poaceae) exposed to copper toxicity revealed significant ultrastructural alterations when compared to control plants. These included disruptions in the cell wall and cytoplasmic membranes of root cells, deposition of electron-dense material, and structural changes in organelles such as the endoplasmic reticulum, mitochondria, chloroplasts, and peroxisomes in stem and leaf tissues (Minkina *et al.*, 2020).

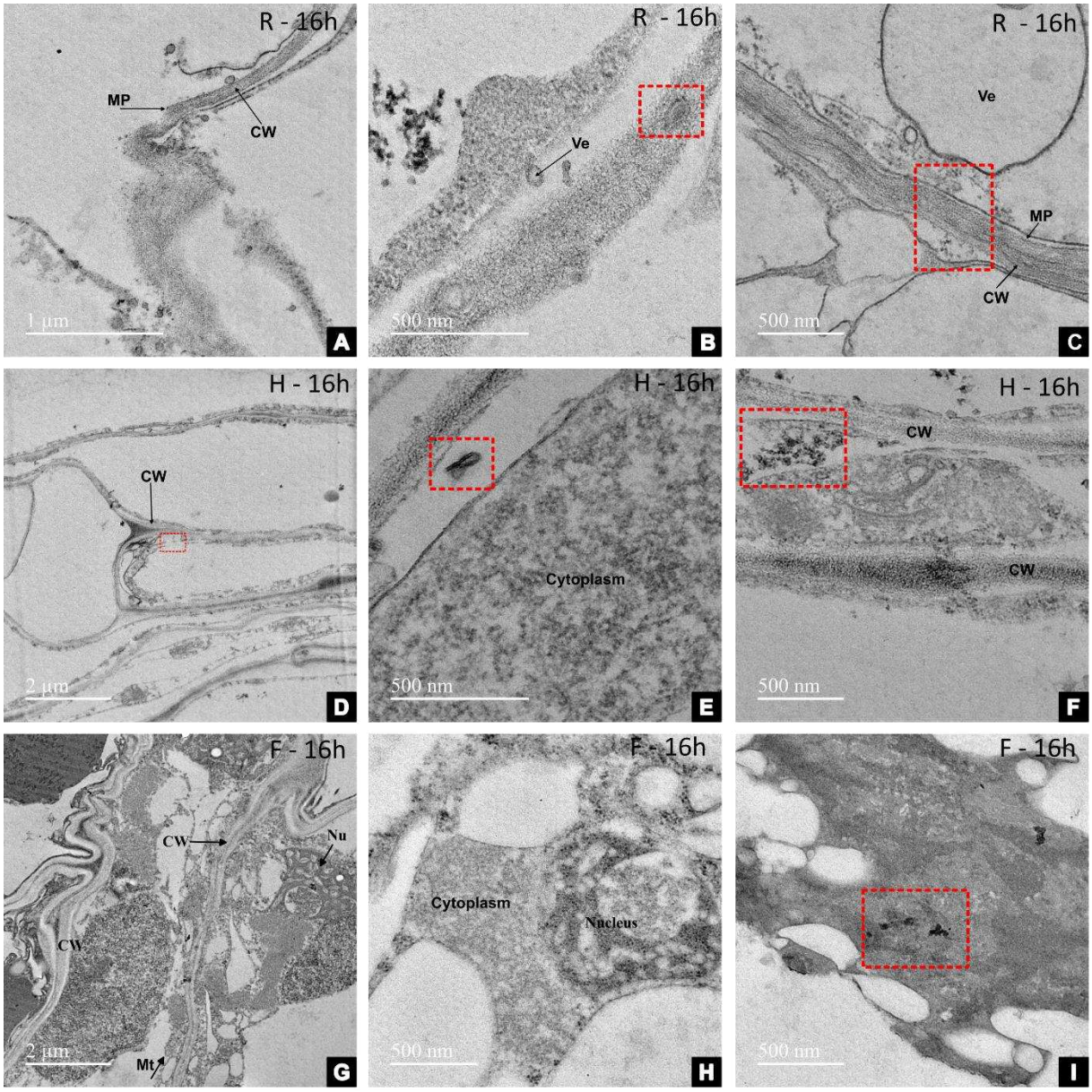

Figure 5. Transmission electron and SIMS micrographs of *Lactuca sativa* radicle, hypocotyl, and leaf cells after 16-hour exposure to 50 mg/L TiO_2. A: Radicle cell showing a disorganized cell wall (CW) and ruptured plasma membrane (PM). B: Radicle cell with a slightly electron-dense body adhered to the inner side of the cell wall. C: Radicle cell containing vesicles (Ve) of different sizes, apparently in transit through the cytoplasm. D: Hypocotyl section displaying multiple structurally damaged cells, with vacuole and cytoplasm rupture highlighted (red square). E: Hypocotyl cell showing dense cytoplasm and the presence of a myelin-like figure. F: Hypocotyl cell exhibiting small electron-dense inclusions near the cell wall. G: Leaf tissue severely damaged, with organelles no longer distinguishable and a nucleus (Nu) showing signs of degeneration. H: Leaf cell with nucleus and cytoplasm containing small electron-dense inclusions. I: Leaf cell presenting a large, amorphous electron-dense body without identifiable organelles. CW – cell wall; PM – plasma membrane; Ve – vesicle; Nu – nucleus.

Muccifora et al. (2021) reported that exposure to TiO_2 nanoparticles induced cytoplasmic and mitochondrial damage, plasmolysis, cell wall ruptures, and even the transfer of organelles and nanoparticles between *Pisum sativum* cells. These alterations were observed mainly in cortex cells located near the rhizoderm, where nanoparticles tended to accumulate. The authors also highlighted that particle size played a decisive role, as only the smallest

nanoparticles (15–300 nm) were able to cross the cell wall. This evidence supports the findings of the present study, in which TiO_2 microparticles, although unable to penetrate the cell wall, still induced significant cellular damage.

Although the toxic effects of titanium on *Lactuca sativa* leaves have been previously reported, the present study demonstrates that their severity is strongly time dependent. The alterations first appeared in a subtle form and progressively intensified with longer exposure, reaching a maximum at the later intervals. In particular, Figures 4 and 5 show that at 16 hours the damage was more pronounced than that observed at 12 hours.

The nanoparticles toxicity caused by exposing plants were highlighted in (Vishnu *et al.*, 2019) and several damages were pointed such as disruption in the cell wall, cell membrane, chloroplast structure, thylakoids, abnormal size of plastoglobules and starch granules, destructive changes in peroxisomes, swollen mitochondrial cristae, abnormal nucleus, and alterations in mesophyll cells supporting the present data relating to toxicity induced by titanium. Even though in the current work it was not possible to determine if TiO_2 absorption occurred, Vishnu *et al.* (2019) explained that electron-dense materials were found to be deposited near cell walls, indicating a potential mechanism of interaction between nanoparticles and plant cells. Moreover, such electron-dense inclusions may also represent degenerative protein aggregates and autophagic bodies, reflecting cellular stress responses and degradation processes.

During the TEM analysis, a diffraction test was performed to indicate whether there was a pattern that could suggest the presence of titanium in the samples. Although it was not possible to detect the absorption and translocation of TiO_2 MPs, data presented in (Wang *et al.*, 2023) indicate that particles above 100 nm can still be absorbed by the plant. The absorption range of titanium particles is 36–140 nm according to (Larue *et al.*, 2012).

Complementing these findings, SIMS analysis of radicle cells (Fig. 6) at 16 hours of exposure revealed sodium accumulation in the cell wall (6G) and a potassium gradient concentrated in the same region (6H). Notably, the distribution of these ions differed in areas where titanium was absent (6A, 6B). No titanium signal was detected in the majority of tissues (6C–6F), although small titanium peaks within cells were observed (6I–K) and confirmed by the graph (6L), which highlights the peak in the pink square. Ondrasek *et al*., (2019) demonstrated the ionic distribution (Na and K) was also affected by zinc and cadmium 24-hour exposure in *Raphanus sativus* L and alterations in the spatial distribution of these ions can therefore serve as sensitive indicators of cellular toxicity and stress responses. Along with our results it highlights their central role in maintaining ionic balance and osmotic stability.

These results suggest limited nanoparticle uptake but clear evidence of ionic imbalance, likely contributing to the observed structural disintegration. Such alterations reinforce the hypothesis that nano-TiO_2 modulates ion distribution and homeostasis in plant tissues, thereby driving physiological stress responses. Consistently, Trela-Makowej *et al.* (2024) and Hu *et al*. (2020) reported that nano-TiO_2 exposure significantly alters the uptake and internal concentrations of essential nutrients (K, Ca, Mg, Fe), depending on dosage and exposure conditions. These ion shifts may underlie both the beneficial and deleterious effects described across different plant species.

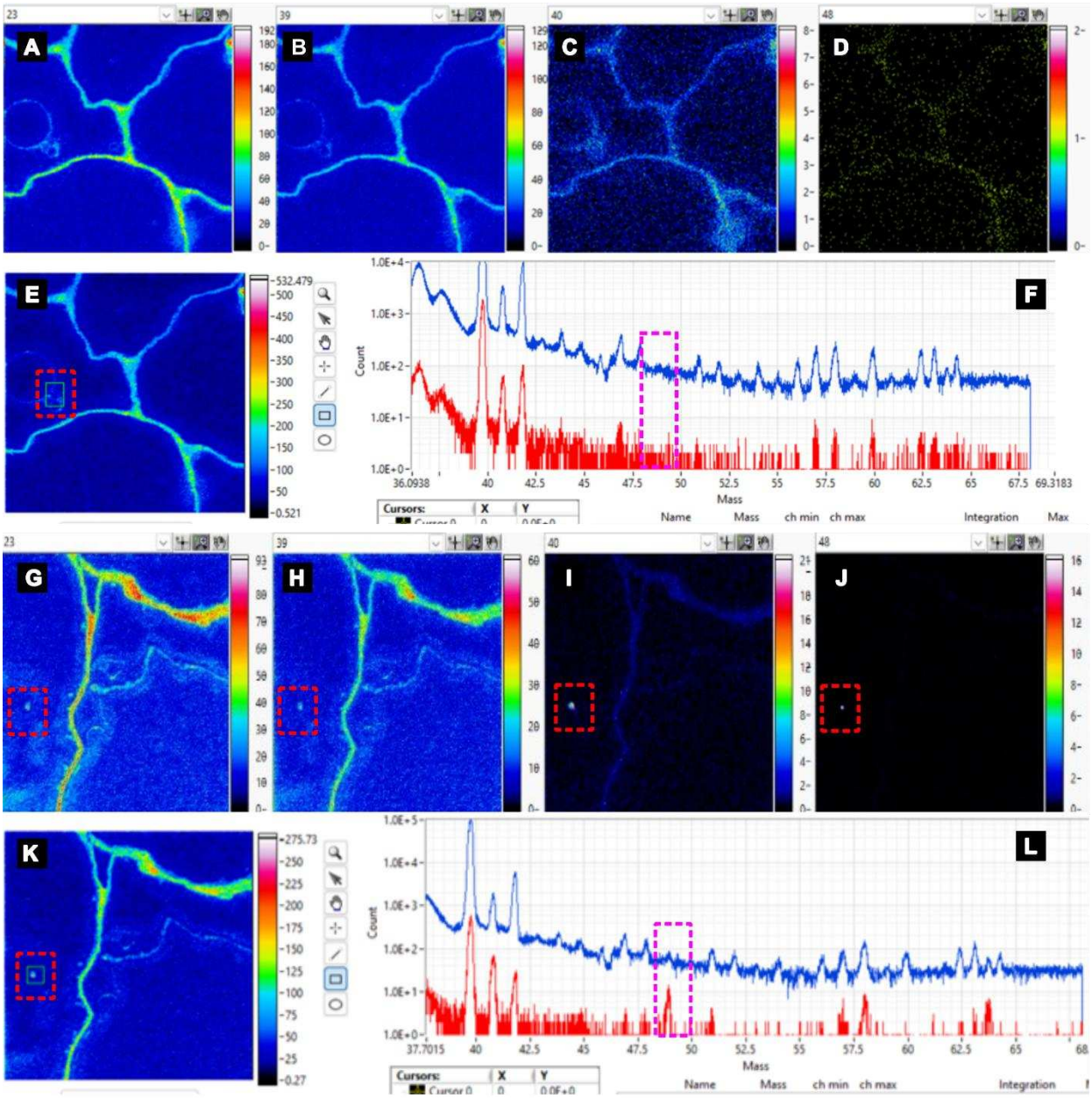

Figure 6. SIMS micrographs of *Lactuca sativa* radicle, hypocotyl, and leaf cells after 16-hour exposure to 50 mg/L TiO_2. A: SIMS image of the radicle showing low sodium (Na^+) concentration in the cell wall region (green

gradient). B: SIMS image of the radicle revealing low potassium (K^+) concentration (gradient blue to green) concentrated in the cell wall region. C, D: SIMS images showing no sign of titanium (Ti) inside the cell (40 and 48 are the possible titanium peak detection). E, F: SIMS image and graph showing no titanium peak (Ti – pink square) inside the cell. G: SIMS image of the radicle showing high sodium (Na^+) concentration in the cell wall region (gradient orange to red) and the likely titanium particle (red square). H: SIMS image of the radicle revealing a potassium (K^+) gradient (green to red) concentrated in the cell wall region and the likely titanium particle (red square). I, J: SIMS images of the radicle detecting a small titanium (Ti) (red square) K, L: SIMS image and graph showing a small titanium peak (Ti – pink square) inside the cell.

The small titanium peak observed (6L) does not confirm efficient microparticle uptake, most likely due to the larger size of TiO_2 and the short exposure time. Considering its low solubility and tendency to precipitate, the amount of particles available for cellular penetration was possibly insufficient. Nevertheless, mere contact with the radicle of *L. sativa* was enough to trigger toxic effects. These findings highlight that TiO_2 cannot be considered free of toxic potential, and that environmental variables such as concentration and bioavailability should be considered, as they may enhance its phytotoxicity.

4.2.4 Conclusions

This study confirmed that titanium dioxide microparticles (TiO_2MPs) exert toxic effects on *Lactuca sativa* seedlings following root exposure. Structural alterations included the loss of endodermis and pericycle definition, irregularities in the cell wall, vascular bundle disruption, and the presence of peroxisomes in the cortical region of the hypocotyl. In leaves, the palisade parenchyma appeared highly disorganized, and electron-dense regions were detected, potentially linked to photosynthetic impairment. Ultrastructural analyses further revealed severe plasma membrane rupture, organelle leakage, lipid body accumulation, and degenerated autophagic structures, indicating irreversible cellular damage. Nuclear disintegration likely triggered the release of hydrolytic enzymes, accelerating cell autolysis.

Crucially, the observed toxicity occurred even without confirmed internalization of TiO_2 by plant cells, demonstrating that prolonged exposure and direct surface contact alone are sufficient to induce structural degeneration, metabolic disturbances, and ionic imbalance. These findings highlight that TiO_2 toxicity in plants is governed not only by uptake capacity but also by the dynamics of contact, underscoring the need for careful assessment of its environmental risks.

ACKNOWLEDGMENTS

ECM acknowledges funding from Universal 2023 (Grant number 406371/2023-7) and Produtividade em Pesquisa (Grant number 312014/2025-2) and Analytical Center-UFC/CT-INFRA-FINEP/Pro-Equipamentos-CAPES/CNPq-SisNano-MCTI 2019 (Grant 442577/ 2019-2). Capes, INCT and FUNCAP. This work is part of the PhD research of AKML. CNPEM and LIST and GQMat.

AUTHOR CONTRIBUTION

All authors contributed to the study conception and design**.** Developed research (ECM and AKML). Write the manuscript (AKML). Review of the manuscript (FGT, MC, TBARM). Performed the experiments (AKML, JVSF and JHAV). TEM analysis (AKML and FGT). SIMS analysis (AB and TW) All authors read and approved of the final manuscript.

CONFLICTS OF INTEREST

The authors declare no conflict of interest.

REFERENCES

AGHDAM, Mohammad Taieb Baiazidi; MOHAMMADI, Hamid; GHORBANPOUR, Mansour. Effects of nanoparticulate anatase titanium dioxide on physiological and biochemical performance of *Linum usitatissimum* (Linaceae) under well-watered and drought stress conditions. **Brazilian Journal of Botany**, v. 39, p. 139–146, 2016.

BARANOVA, Ekaterina N. et al. Targeted protection of mitochondria of mesophyll cells in transgenic CYP11A1 CDNA expressing tobacco plant leaves after NaCl-induced stress damage. **Proceedings of the Latvian Academy of Sciences**, p. 334–340, 2018.

BARBOSA, J. S.; NETO, D. M. A.; FREIRE, R. M.; ROCHA, J. S.; FECHINE, L. M. U. D.; DENARDIN, J. C. et al. Ultrafast sonochemistry-based approach to coat TiO_2 commercial particles for sunscreen formulation. **Ultrasonics Sonochemistry**, v. 48, p. 340–348, 2018.

BRAND, W.; PETERS, R. J. B.; BRAAKHUIS, H. M.; MAŚLANKIEWICZ, L.; OOMEN, A. G. Possible effects of titanium dioxide particles on human liver, intestinal tissue, spleen and kidney after oral exposure. **Nanotoxicology**, v. 14, n. 7, p. 985–1007, 2020.

CASTIGLIONE, Monica Ruffini et al. Root responses to different types of TiO_2 nanoparticles and bulk counterpart in plant model system *Vicia faba* L. **Environmental and Experimental Botany**, v. 130, p. 11–21, 2016.

CHAHARDOLI, Azam; KARIMI, Naser; SHARIFAN, Hamidreza. Elucidating the phytotoxic endpoints of sub-chronic exposure to titanium dioxide nanoparticles in endemic Persian *Dracocephalum* species. **Chemosphere**, v. 370, p. 143853, 2025.

CHAN-KEB, C. A. et al. Acute phytotoxicity of four common pharmaceuticals on the germination and growth of *Lactuca sativa* L. **Applied Ecology and Environmental Research**, v. 20, n. 5, p. 3737–3746, 2022.

COSGROVE, D. J. Catalysts of plant cell wall loosening. **F1000Research**, v. 5, p. 119, 2016.

CORSI, Ilaria; DESIMONE, Martin Federico; CAZENAVE, Jimena. Building the bridge from aquatic nanotoxicology to safety by design silver nanoparticles. **Frontiers in Bioengineering and Biotechnology**, 2022.

DE BRUIN, Willeke et al. Ultrastructural and developmental evidence of phytotoxicity on cos lettuce (*Lactuca sativa*) associated with nonylphenol exposure. **Chemosphere**, v. 169, p. 428–436, 2017.

DUTTA, P. et al. Nanoparticles: the plant saviour under abiotic stresses. **Nanomaterials**, v. 12, n. 21, p. 3915, 2022.

EGLER, S. G. et al. Phytotoxicity of single and mixed rare earth element (La, Nd and Sm) exposures on *Lactuca sativa* seed germination and growth. **Ecotoxicology**, v. 33, n. 10, p. 1193–1209, 2024.

EUROPEAN COMMISSION. Commission recommendation of 10.06.2022 on the definition of nanomaterial. Brussels, 2022.

FARAHI, Seyed Mostafa Moshirian et al. The effects of titanium dioxide (TiO_2) nanoparticles on physiological, biochemical, and antioxidant properties of *Vitex agnus-castus* L. **Heliyon**, v. 9, n. 11, 2023.

FRENCH, Rebecca A. et al. Influence of ionic strength, pH, and cation valence on aggregation kinetics of titanium dioxide nanoparticles. **Environmental Science & Technology**, v. 43, n. 5, p. 1354–1359, 2009.

GUTSCH, A. et al. Does long-term cadmium exposure influence the composition of pectic polysaccharides in the cell wall of *Medicago sativa* stems? **BMC Plant Biology**, v. 19, n. 1, p. 271, 2019.

HU, J. et al. Potential application of titanium dioxide nanoparticles to improve the nutritional quality of coriander (*Coriandrum sativum* L.). **Journal of Hazardous Materials**, v. 389, p. 121837, 2020.

HU, J. et al. TiO_2 nanoparticle exposure on lettuce (*Lactuca sativa* L.): dose-dependent deterioration of nutritional quality. **Environmental Science: Nano**, v. 7, n. 2, p. 501–513, 2020.

HUANG, Danyu et al. Uptake, translocation, and transformation of silver nanoparticles in plants. **Environmental Science: Nano**, v. 9, n. 1, p. 12–39, 2022.

JAVAHERI, R.; RAJI, A. R.; MOGHADDAM JAFARI, A.; NOURANI, H. Effects of oral exposure to titanium dioxide nanoparticles on the liver, small intestine, and kidney of rats assessed by light microscopy and transmission electron microscopy. 2023.

JUNG, Minkyo; CHOI, Hyosun; MUN, Ji Young. The autophagy research in electron microscopy. **Applied Microscopy**, v. 49, n. 1, p. 11, 2019.

KHAN, Ali Raza et al. Ethylene participates in zinc oxide nanoparticles induced biochemical, molecular and ultrastructural changes in rice seedlings. **Ecotoxicology and Environmental Safety**, v. 226, p. 112844, 2021.

KHAN, M. N.; MOBIN, M.; ABBAS, Z. K.; ALMUTAIRI, K. A. Role of nanomaterials in plants under challenging environments. **Plant Physiology and Biochemistry**, v. 110, p. 194–209, 2017.

KHAN, Maryam et al. The potential exposure and hazards of metal-based nanoparticles on plants and environment. **Environmental Advances**, 2021.

KRISHNA, R. et al. Toxicological effects of metal nanoparticles employed in biomedicine. **Macromolecular Symposia**, v. 413, n. 1, 2024.

LARUE, Camille et al. Comparative uptake and impact of TiO_2 nanoparticles in wheat and rapeseed. **Journal of Toxicology and Environmental Health, Part A**, v. 75, n. 13–15, p. 722–734, 2012.

LI, Su et al. Auxin acts upstream of nitric oxide to regulate cell wall xyloglucan in *Arabidopsis thaliana*. **Planta**, v. 259, n. 3, p. 52, 2024.

LIMA, Ana Kamila Medeiros et al. Effect of TiO_2 microparticles in lettuce (*Lactuca sativa* L.) seeds and seedlings. **Bulletin of Environmental Contamination and Toxicology**, v. 110, n. 6, 2023.

LUO, Zhen et al. Rethinking nano-TiO_2 safety. **Small**, v. 16, n. 36, p. 2002019, 2020.

MANAA, Arafet et al. Photosynthetic performance of quinoa (*Chenopodium quinoa* Willd.). **Biochimica et Biophysica Acta – Bioenergetics**, v. 1862, n. 5, p. 148383, 2021.

MINKINA, Tatiana et al. Anatomical and ultrastructural responses of *Hordeum sativum*. **Environmental Geochemistry and Health**, v. 42, n. 1, p. 45–58, 2020.

MUCCIFORA, Simonetta et al. Synchrotron radiation spectroscopy and TEM evaluation of TiO_2 NPs in *Pisum sativum* L. **Nanomaterials**, v. 11, n. 4, p. 921, 2021.

MUSTAFA, Hina et al. Biosynthesis and characterization of TiO_2 nanoparticles in wheat. **Ecotoxicology and Environmental Safety**, v. 223, p. 112519, 2021.

NICOLÁS-ÁLVAREZ, Dulce Estefanía et al. Effects of TiO_2 nanoparticles in tomato roots. **Nanomaterials**, v. 11, n. 5, p. 1127, 2021.

O'BRIEN, T. P.; FEDER, N.; MCCULLY, M. E. Polychromatic staining of plant cell walls by toluidine blue O. **Protoplasma**, v. 59, n. 2, p. 368–373, 1964.

ONDRASEK, Gabrijel et al. Zinc and cadmium mapping in radish tissues. **International Journal of Environmental Research and Public Health**, v. 16, n. 3, p. 373, 2019.

OST, Alexander D. et al. The Ionmaster magSIMS. 2024.

PINO, M. R. et al. Phytotoxicity of pharmaceuticals on *Lactuca sativa*. **Environmental Science and Pollution Research International**, v. 23, n. 22, p. 22530–22541, 2016.

POLISCHUK, S. D. et al. Reasons for different environmental effects of technogenic nanoparticles. 2022.

RAO, M. J.; ZHENG, B. Polyphenols in abiotic stress tolerance. **Antioxidants**, v. 14, n. 1, p. 74, 2025.

RACOVITA, Anca Diana. Titanium dioxide: structure, impact, and toxicity. **International Journal of Environmental Research and Public Health**, 2022.

SHELKE, D. B. et al. Mycogenic nanoparticles in crops. **Biocatalysis and Agricultural Biotechnology**, v. 52, p. 102805, 2023.

SINGH, A. et al. Plant–nanoparticle interaction. **Environmental Chemistry Letters**, v. 13, p. 429–441, 2015.

TENHAKEN, R. Cell wall remodeling under abiotic stress. **Frontiers in Plant Science**, v. 5, p. 771, 2015.

TRELA-MAKOWEJ, Agnieszka; ORZECHOWSKA, Aleksandra; SZYMAŃSKA, Renata. Hormetic effect of TiO_2 nanoparticles on plants. **Science of the Total Environment**, v. 910, p. 168669, 2024.

TRIPATHI, Sneha et al. Interaction of silver nanoparticles with plants. **Plant Nano Biology**, p. 100082, 2024.

VAN DOORN, Wouter G. et al. Morphological classification of plant cell deaths. **Cell Death & Differentiation**, v. 18, n. 8, p. 1241–1246, 2011.

VIEIRA, C.; MARCON, C.; DROSTE, A. Phytotoxic and cytogenotoxic assessment of glyphosate on *Lactuca sativa* L. **Brazilian Journal of Biology**, v. 84, 2024.

VIJAYARAJ, Vinita et al. Transfer and ecotoxicity of TiO_2 nanoparticles. **Environmental Science and Technology**, v. 52, n. 21, p. 12757–12764, 2018.

VISHNU, D. et al. Structural and ultrastructural changes in nanoparticle exposed plants. 2019.

WAKABAYASHI, K. et al. Cell wall modification under lead stress. **Life**, v. 13, n. 2, 2023.

WANG, Xueran et al. Nanoparticles in plants. **Materials**, v. 16, n. 8, p. 3097, 2023.

TYULKOVA, E. G. Anatomical structure of wood plant leaf under VOC exposure. **Ecology and Noospherology**, v. 31, n. 1, p. 52–58, 2020.

YADAV, Vaishali et al. Structural modifications of plant organs by metals. **Plant Physiology and Biochemistry**, 2021.

ZAHRA, Zahra et al. Exposure route of TiO_2 nanoparticles and agro-environment impacts. **Nanomaterials**, 2020.

5 CAPÍTULO II - Interação entre *Artemia* salina e TiO_2

Este capítulo aborda a compreensão dos aspectos da interação entre TiO_2 e *Artemia salina*. Ele é composto de um artigo publicado no periódico *Microscopy Research Technique*, cujo texto completo é apresentado a seguir.

5.1 PAPER 3 – Acute toxicity of titanium dioxide microparticles in *Artemia sp.* nauplii instar I and II.

Received: 2 September 2022 | Revised: 4 January 2023 | Accepted: 2 March 2023
DOI: 10.1002/jemt.24312

RESEARCH ARTICLE

MICROSCOPY RESEARCH TECHNIQUE WILEY

Acute toxicity of titanium dioxide microparticles in *Artemia* sp. nauplii instar I and II

Sergimar Kennedy de Paiva Pinheiro[1] | Ana Kamila Medeiros Lima[1] | Thaiz Batista Azevedo Rangel Miguel[2] | Saulo Pireda[3] | Pierre Basílio Almeida Fechine[4] | Antonio Gomes Souza Filho[5] | Emilio de Castro Miguel[1]

[1]Biomaterials Laboratory, Department of Metallurgical Engineering and Materials and Analytical Center, Federal University of Ceará, Fortaleza, Ceara, Brazil

[2]Biotechnology Laboratory, Food Engineering Department, Federal University of Ceará, Campus do Pici Fortaleza, Fortaleza, Ceara, Brazil

[3]Cell and Tissue Biology Laboratory, North Fluminense State University – UENF, Campos dos Goytacazes, Rio de Janeiro, Brazil

[4]Group of Chemistry of Advanced Materials, Department of Analytical Chemistry and Physical-Chemistry, Federal University of Ceará, Fortaleza, Ceara, Brazil

[5]Departamento de Física, Centro de Ciências, Universidade Federal do Ceará, Fortaleza, Ceara, 60455-900, Brazil

Correspondence
Emilio de Castro Miguel, Biomaterials Laboratory (BIOMAT), Department of Metallurgical Engineering and Materials (DEMM), Federal University of Ceará, Campus do Pici, 60455-900, Fortaleza, Ceará, Brazil.
Email: emiliomiguel@ufc.br

Funding Information
Conselho Nacional de Desenvolvimento Científico e Tecnológico, Grant/Award Number: 350023/2020-4; Coordenação de Aperfeiçoamento de Pessoal de Nível Superior, Grant/Award Number: 4425 77/2019-2; Fundação Cearense de Apoio ao Desenvolvimento Científico e Tecnológico

Review Editor: Paolo Bianchini

Abstract

In this study, the toxicity effects of titanium dioxide ($MTiO_2$) microparticles on *Artemia* sp. nauplii instar I and II between 24 and 48 h was evaluated. The $MTiO_2$ were characterized using different microscopy techniques. $MTiO_2$ rutile was used in toxicity tests at concentration of 12.5, 25, 50, and 100 ppm. No toxicity was observed in *Artemia* sp. nauplii instar I at the time of 24 and 48 h. However, *Artemia* sp. nauplii instar II toxicity was observed within 48 h of exposure. $MTiO_2$ at concentrations of 25, 50 and 100 ppm was lethal for *Artemia* sp. with a significant difference ($p \leq .05$) in relation to the control artificial sea water with LC_{50} value at 50 ppm. Analysis of optical and scanning electron microscopy revealed tissue damage and morphological changes in *Artemia* sp. nauplii instar II. By using confocal laser scanning microscopy, cell damage was observed due to the toxicity of $MTiO_2$ at a concentration of 20, 50, and 100 ppm. The high mortality rate is related to the filtration of $MTiO_2$ by *Artemia* sp. nauplii instar II due to the complete development of the digestive tract.

KEYWORDS
Artemia sp., confocal laser scanning microscopy, electron microscopy, $MTiO_2$, toxicity

Research Highlights

- No mortality was observed in *Artemia* sp. nauplii instar I exposed to titanium dioxide ($MTiO_2$) at 24 and 48 h.
- A high percentage of mortality was observed in *Artemia* sp. nauplii instar II exposed to $MTiO_2$ at concentrations of 50 and 100 ppm.
- Cell damage and morphological changes was observed by confocal laser scanning microscope and scanning electron microscope in *Artemia* sp. nauplii instar II.

5.1.1 Introduction

Metallic particles are present in several science and industry areas and are used in

the environmental protection and building engineering, medicine, agriculture and the food and cosmetic industry (Sirotkin *et al.*, 2021). Among the metal particles, titanium dioxide (TiO_2) has desirable properties in the production of new materials because they have low combustion, odorless, high resistance to corrosive agents, high density and very high refractive index (Shi *et al.*, 2013). TiO_2 exists as rutile, anatase and brookite bulk crystalline polymorphic forms (Sadrieh *et al.*, 2010). The rutile phase is more stable and has lower photocatalytic activity than anatase (Barbosa *et al.*, 2018). This oxide has been used as an inorganic filter in sunscreens due to protection effect against UV radiation absorbing, scattering and reflecting (Lu *et al.*, 2015).

Titanium dioxide are the most relevant nanomaterial in terms of world production volumes with reaches about 10 tons per year (Bundschuh *et al.*, 2018), and used worldwide in several areas in the manufacture of products such as sunscreen, cosmetics, paints, food additives, medicines and construction (Ozkan *et al.*, 2016). The daily use of these products results in the release of TiO_2 particles (in the micro and nano scale) into the environment, negatively affecting aquatic organisms (Nowack & Bucheli, 2007), through the food chain (Farré *et al.*, 2009). Most of the studies currently are related to the toxicity of TiO_2 on a nanometric scale and few research related to the toxicity of TiO_2 microparticles has been done.

The toxicity of TiO_2 is related to their photocatalytic properties. Under UV-A radiation they become reactive, oxidizing molecules and organic substrates causing cellular damage (Fu *et al.*, 2014). In ecotoxicological tests using aquatic organisms, it was observed that titanium oxide nanoparticles (TiO_2NPs) were toxic to algae and microcrustaceans (Clément *et al.*, 2013). With *Daphnia magna*, it was observed that TiO_2 caused mortality above 50% in individuals and the toxicity was proportional to the increase of particles concentration (Hund-Rinke &Simon, 2006). In addition to *D. magna*, *A. salina* are used in toxicity tests as noted by Rekulapally *et al.* (2019) using different types of particles. These toxic effects were generated through the accumulation of NPs in aquatic environments (Kachenton *et al.*, 2019), directly affecting zooplankton (Farré *et al.*, 2009). Thus, our hypothesis is that titanium dioxide ($MTiO_2$) enters the environment causing toxic effects for biota. To assess possible toxicity of $MTiO_2$, we used *Artemia sp.* as study model.

The genus *Artemia* is worldwide distributed and extensively used to toxicological test (Nunes *et al.*, 2006), being the taxon with the highest biomass and primary consumer in the food chain. (Sorgeloos *et al.*, 1978). The life cycle of brine shrimp begins with the breaking of the cyst dormancy, small spheres with great physical and chemical resistance. Dormancy breaks when the spheres come into contact with saline water (Morgana *et al.*, 2018).

The use of this species as a model in toxicity tests is related to easy handling, high

adaptation to laboratory conditions, low maintenance cost, short life cycle and high reproduction rate (Manfra *et al.*, 2014). In addition, the reliability and validity of ecotoxicological tests using A. salina has been confirmed by several tests using different stressors like chemical compounds (Manfra *et al.*, 2014) and pharmaceutical (Nunes *et al.*, 2006)Using NPs, several studies point to acute toxicity in *A. salina*, among them are AgNPs (An *et al.*, 2019; Lacave *et al.*, 2017), ZnO NPs (Ates, Daniels, Arslan, & Farah, 2013; Khoshnood *et al.*, 2017; Sarkheil *et al.*, 2018), MO-NPs (Gambardella *et al.*, 2014) and TiO_2NPs (Ozkan *et al.*, 2016). All these studies show the toxicity of NPs, however, different results can be observed due to different experimental conditions and characteristics of NPs (Sarkheil *et al.*, 2018; Shokry *et al.*, 2021) justifying ecotoxicological tests.

The aim of this work was to evaluate the acute toxicity of $MTiO_2$ with emphasis on morphological changes, cell damage and number of dead individuals. In our study, it was used $MTiO_2$ in the rutile crystalline phase for acute toxicity tests in *Artemia sp.* nauplii instar I and instar II.

5.1.2 Materials and methods

Synthesis and characterization of $MTiO_2$

$MTiO_2$ (ViaFarma) was used as received without any purification. The characterization of was carried out by Barbosa *et al.* (2018) using techniques such as x-ray powder diffraction (XRPD), Fourier trans- form infrared spectroscopy (FT-IR), dynamic light scattering (DLS), energy dispersive spectroscopy (EDS), scanning electron microscopy (SEM), and transmission electron microscopy (TEM).

Test organism

Artemia sp. cysts were purchased from aquaculture store in Fortaleza, Ceará - Brazil. Dehydrated cysts were kept at 4◦C and used in all experiments. Nauplii instar I and instar II (24 and 48 h post hatching)

were obtained as described by (Garaventa *et al.*, 2010). Briefly, 500 mg of cysts incubated for 24 h at 28◦C under 16 h light, 8 h dark conditions and continuous aeration of the cyst suspension in artificial sea water (ASW) (30% salinity). The hatched nauplii were separated from non-hatched cysts based on their positive phototaxis and then transferred by a Pasteur pipette into beakers containing the ASW.

Titanium dioxide LC50

The present study performed an acute toxicity test by determining of the lethal concentration that kills 50% of individuals (LC50) in *Artemia sp.* nauplii instar I and II exposed to $MTiO_2$ at a concentration of 12.5, 25, 50, and 100 ppm in 24 and 48 h. After exposure, a correlation graph between $MTiO_2$ concentration and percentage dead nauplii was plotted. In addition, LC50 was plotted with confidence limits for $K_2Cr_2O_7$ validating the experiment (Supplementary material).

Acute toxicity test of $MTiO_2$

Acute exposure was conducted on *Artemia sp.* nauplii instar I and II for 24 and 48 h exposure according to (Johari *et al.*, 2019) and Organization for Economic Cooperation and Development, testing guidelines (OECD, 2004). Briefly, four different test concentrations (12.5, 25, 50, and 100 ppm) of $MTiO_2$ were administered in nauplii within 24 and 48 h. Negative control group was exposed to ASW and positive con- trol was exposed to potassium dichromate ($K_2Cr_2O_7$) 0.5 M. The experiment was carried out on 24-well polystyrene microplates with 2 mL. Each concentration carried out by three replicate and each replication contained 10 newly hatched nauplii. The room temperature was set to 24◦C and photoperiod of 12 h dark/12 h light. After that, the numbers of dead larvae were counted under a stereomicroscope Stemi 508 with attached camera ZEISS (Axiocam 208/202 mono). The test considered valid only when survival rate in the control group was ≥90% (OECD, 2004).

Optical Microscopy

For analysis of $MTiO_2$ accumulation, *Artemia sp.* nauplli instar II were collected at 24 and 48 h of experiment and washed in ASW. We do not use nauplii instar I, because at this stage the mouth and anus of

A. salina are not developed (Ocaranza-Joya *et al.*, 2019), preventing the accumulation of $MTiO_2$ by the animal. The nauplii were mounted on a glass slide and images were obtained using optical microscopy Primo Star with Axiocam Color camera coupled. Subsequent microscopy analyzes such as confocal laser scanning microscopy (CLSM - LM 710 Zeiss) and scanning electron microscopy (SEM—Quanta FEG 450) (FEI) were performed only with *Artemia sp.* nauplii instar II within the 48-h exposure, because at this stage there was a higher mortality rate.

Confocal laser scanning microscopy

To assess possible cellular damage caused by $MTiO_2$, acridine orange was used in *Artemia sp.* nauplii instar II, exposed to different concentrations of $MTiO_2$, in addition to the ASW and $K_2Cr_2O_7$ controls. Briefly, *Artemia sp.* was transferred to 24-well polystyrene microplates of 2 mL and then 500 µL of acridine orange at a concentration of 5 µg/mL was added to each well for 20 min at room temperature. After 20 min, *Artemia sp.* were washed in phosphate buffer solution, pH 7.2. Stained samples were observed under CLSM with 488 nm excitation and 532–580 nm emission.

Scanning electron microscopy

Samples of *Artemia sp.* nauplii instar II were collected at 24 and 48 h and fixed in solution of glutaraldehyde 2.5%, formaldehyde 4.0% in cacodylate buffer 0.05 mol L^{-1}, pH 7.2 at room temperature for 24 h. Subsequently, the material was rinsed in the sodium cacodylate buffer 0.05 M three times for 45 min each wash. After the washes, the samples were increasing series dehydrated with acetone for 45 min each step. After dehydration, the material was critical point dried (EMS 850). Dried samples were placed in stubs and sputtered with 20 nm gold in metallization equipment QUO- RUM 150T ES. Observation and documentation were performed in scanning electron microscope (Quanta FEG 450 FEI), with 20 kV beam acceleration.

Statistical analysis

For the statistical analyses, the data were recorded daily as the mean and standard deviation. The normality of the data and the averages significance was performed through the R environment, using the psych package. The normality of the data was assessed using the Shapiro–Wilk test as a function of $n < 30$, through the Shapiro.test function. The t test was used to verify the significance of differences between the means of each treatment (12.5, 25, 50, 100 ppm) and $K_2Cr_2O_7$ as a function of the control treatment (ASW), through the t test function. The nonlinear regression analyzes were performed using the Sigma Plot 11.0 software package.

5.1.3 Results

LC50 of titanium dioxide

No mortality was observed for nauplii instar I exposed to $MTiO_2$ between 24 and 48 h. No correlation between exposure time and increase in $MTiO_2$ concentration (Table 1). Same result was observed for nauplii instar II with 24 h exposure a $MTiO_2$ (Table 2). However, a correlation between $MTiO_2$ concentration and percentage of mortality was observed, revealing a dose-dependent effect at 48 h experiment for *Artemia sp.* nauplii instar II (Figure 1). The polynomial nonlinear regression ($p \leq .05$) demonstrates a strong relationship ($R2 = 0.94$) between concentration of the $MTiO_2$ and number of dead nauplii (Figure 1). In addition, the LC50 of $MTiO_2$ was 50 ppm for nauplii instar II in 48 h exposure (Figure 1).

Acute toxicity test of $MTiO_2$

Artemia sp. nauplii instar I submitted to concentration of 12.5, 25, 50, and 100 ppm of $MTiO_2$ no mortality rate was observed in 24 and 48 h experiment, not being observed significant difference ($p \leq .05$) in relation to the control (ASW) (Table 1). K_2Cr2O_7 was lethal for all nauplii instar I in 24 and 48 h of experiment (Table 1). Similar result was observed in *Artemia sp.* nauplii instar II within the 24 h exposure interval.

Artemia sp. nauplii instar II within the 48-h exposure, a toxic effect was observed for TiO_2 at the concentration of 25, 50, and 100 ppm (Table 2). *Artemia sp.* nauplii instar II submitted to concentration of 25, 50, and 100 ppm of $MTiO_2$ exhibited mortality of 30%, 50%, and 30% respectively (Table 2). The negative control (ASW) and positive control (K_2Cr2O_7) presented 0% and 100% mortality (Table 2).

TABLE 1 Acute toxicity of $MTiO_2$ in *Artemia* sp. nauplii instar I and percentage of individuals dead within 24 and 48 h.

A. Salina—nauplii instar I						
24 h of exposure				48 h of exposure		
Treatments	Mean ± SD of living individuals	*p* value	% Mortality	Mean ± SD of living individuals	*p* value	% Mortality
ASW	10.0 ± 0.0	–	0	10.0 ± 0.0	–	0
$K_2Cr_2O_7$	0.0 ± 0.0*	$p \leq 0.01$*	100	0.0 ± 0.0*	$p \leq .01$*	100
12.5 ppm	10.0 ± 0.0	p = NA	0	10.0 ± 0.0	p = NA	0
25 ppm	10.0 ± 0.0	p = NA	0	10.0 ± 0.0	p = NA	0
50 ppm	10.0 ± 0.0	p = NA	0	10.0 ± 0.0	p = NA	0
100 ppm	10.0 ± 0.0	p = NA	0	10.0 ± 0.0	p = NA	0

Note: At this stage of development, no toxicity of $MTiO_2$ was observed at 12.0, 25, 50, and 100 ppm concentrations. Mean ± standard deviation (σ) obtained from the triplicate in each treatment. Significant difference between ASW and *Artemia* sp. exposed to $MTiO_2$ are symbolized by an asterisk * (*t*test, $p < .05$).

TABLE 2 Acute toxicity of $MTiO_2$ in *Artemia* sp. nauplii instar II and percentage of individuals killed within 24 h and 48 h.

A. Salina—nauplii instar II						
24 h of exposure				48 h of exposure		
Treatments	Mean ± SD of living individuals	*p* value	% Mortality	Mean ± SD of living individuals	*p* value	% Mortality
ASW	10.0 ± 0.0	–	0	9.33 ± 1.15	–	6.67
$K_2Cr_2O_7$	0.0 ± 0.0*	$p \leq .01$*	100	0.0 ± 0.0*	$p \leq .01$*	100
12.5 ppm	9.67 ± 0.58	$p = 0.4226$	3.33	8.0 ± 0.0	$p = .1835$	20
25 ppm	10.0 ± 0.0	p = NA	0	7.0 ± 1.73*	$p = .0198$*	30
50 ppm	10.0 ± 0.0	p = NA	0	5.0 ± 0.0*	$p = .0228$*	50
100 ppm	10.0 ± 0.0	p = NA	0	7.0 ± 1.0*	$p = .0474$*	30

Note: At 24 h of exposure to $MTiO_2$, no toxicity was observed in nauplii instar II. However, in 48 h of exposure the toxicity was directly proportional to the concentration of $MTiO_2$. Mean ± standard deviation (σ) for all concentrations. Significant difference between ASW and *Artemia salina* exposed to $MTiO_2$ are symbolized by an asterisk * (*t* test, $p < .05$).

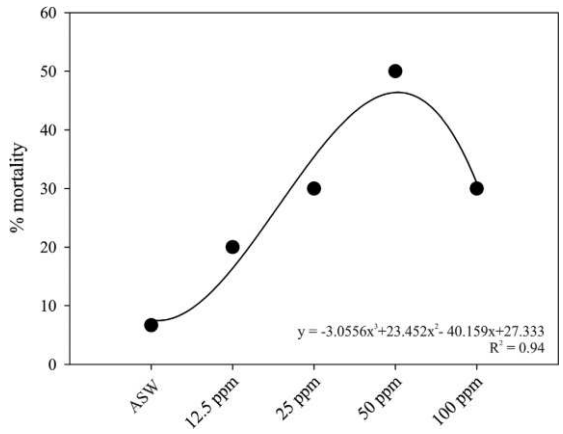

FIGURE 1 Polynomial nonlinear regression demonstrating the dose-dependent effect with gradual increase shows relationship between $MTiO_2$ concentrations ranged from 0 to 100 ppm and percentage of mortality (%) for *Artemia* sp. nauplii instar II, in the 48-h exposure time.

$MTiO_2$ accumulation

The accumulation of $MTiO_2$ in *Artemia sp.* was observed by optical microscopy at the time of 24 and 48 h. The control group showed no morphological damage (Figure 2a). With 24 h exposure was observed $MTiO_2$ accumulation in the gut of the nauplii instar II, no apparent damage, presenting similar morphology to the control. Low $MTiO_2$ accumulation was observed in the gut of animals exposed to 12.5 and 25 ppm (Figure 2b, c). At higher concentrations (50 and 100 ppm) $MTiO_2$ was observed in the animal's gut (Figure 2d, e) and swelling in the cephalothorax (Figure 2e). Individuals exposed to positive control ($K_2Cr_2O_7$) showed underdeveloped body (Figure 2f).

The $MTiO_2$ aggregation in A. salina is directly associated with the consumption of microparticles and may present a large accumulation gut even in low concentrations (12.5 and 25 ppm). In *Artemia sp.* nauplii instar II within 48 h of exposure, the control (ASW) showed no damage in its morphology with appendages and translucent gut (Figure 3a). At the minimum concentration used (12.5 ppm), $MTiO_2$ were observed only in the gut region (Figure 3b). A

similar result was observed at 25 and 50 ppm (Figure 3c, d). However, at the maximum concentration tested (100 ppm), $MTiO_2$ dispersed throughout the animal's body were observed causing morphological alteration with tissue degradation (Figure 3e). Individuals exposed to $K_2Cr_2O_7$ was observed incomplete development with abnormalities in the appendages and abdomen (Figure 3f). The images corroborate the statistical data, which point to toxicity of $MTiO_2$ in high concentrations, time of exposure and stage of life of the *Artemia sp.*

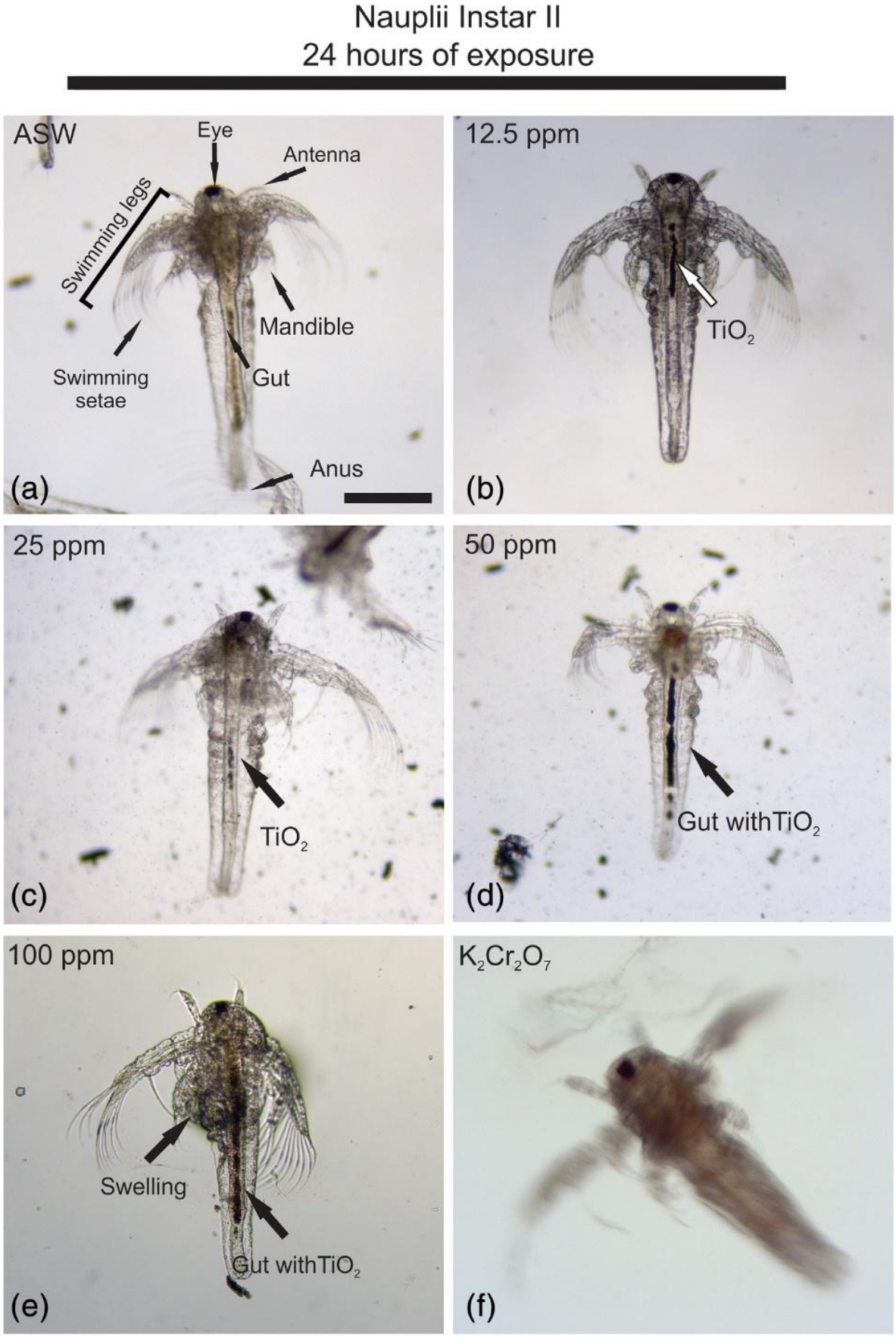

FIGRURE 2. Optical microscopy of *Artemia sp.* nauplii instar II, submitted to different concentrations of $MTiO_2$ within 24 h of exposure. (a) *Artemia sp.* in ASW; *Artemia sp.* nauplii exposed to a 12.5 ppm of $MTiO_2$ concentration: *Artemia sp.* nauplii exposed to a concentration of 25 ppm; (d) Nauplii submitted to 50 ppm of MTiO2

concentration with accumulation of $MTiO_2$ in the gut; (e) nauplii submitted to concentration of 100 ppm $MTiO_2$ with swelling in the cephalothorax; (f) nauplii instar II in $K_2Cr_2O_7$ (Positive control).

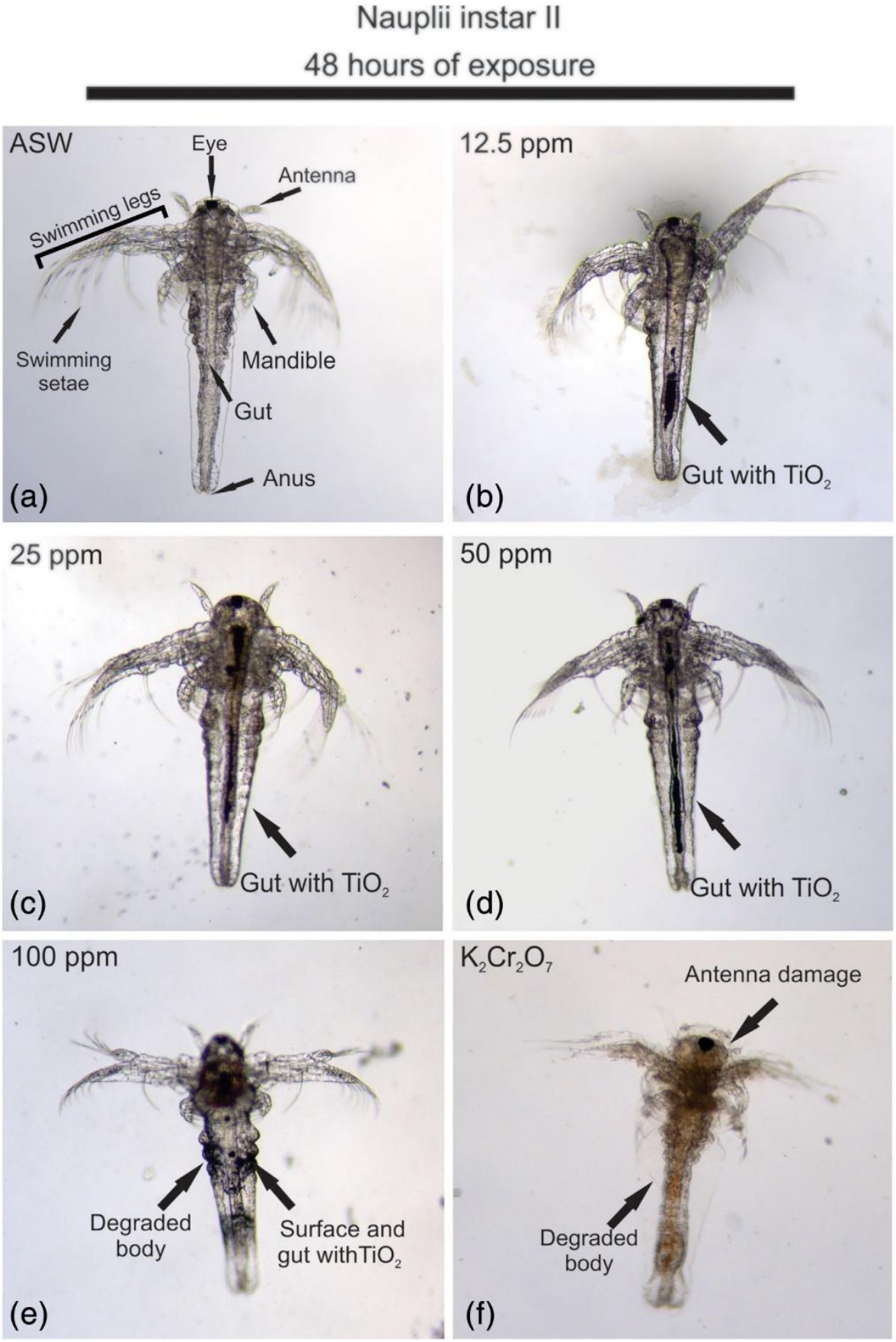

FIGURE 3. Optical microscopy of *Artemia sp.* nauplii instar II, submitted to different concentrations of $MTiO_2$ within 48 h of exposure. (a) *Artemia sp.* nauplii in artificial sea water; (b) $MTiO_2$ accumulation in the gut of the *Artemia sp.* At a concentration of 12.5 ppm, no damage was observed to the animal's body; (c) Gut with accumulation of $MTiO_2$; (d) Gut with aggregation of $MTiO_2$; (e) $MTiO_2$ dispersed throughout the animal's body. Due to the toxic effect of $MTiO_2$ the animal's body begins to degrade; (f) *Artemia sp.* nauplii in $K_2Cr_2O_7$. Bars: 200 µm.

Cell damage analysis

To assess cell damage, *Artemia sp.* nauplii instar II was submitted to different concentrations of $MTiO_2$ with acridine orange in the interval of 48 h. In a ASW *Artemia sp.* showed low fluorescence emission because the cells were not damaged (Figure 4a). In addition, image of the ASW without acridine orange was performed, which presented an emission pattern similar to the ASW with acridine orange (Supplementary material). In low concentration of $MTiO_2$ (12.5 ppm) the result was similar to ASW (Figure 4b). At 25 ppm concentration, many fluorescent spots were observed in the abdomen of *Artemia sp.* (Figure 4c), due to cell damage. In moderate concentration of $MTiO_2$ there was an increase in fluorescence emission related to cell damage, observed in *Artemia sp.* exposed to a 50 ppm concentration (Figure 4d). In high concentrations of $MTiO_2$ (100 ppm) fluorescence emission was observed throughout the animal's body (Figure 4e), indicating cell damage. Positive control showed strong emission due to cell damage caused by $K_2Cr_2O_7$ (Figure 4f).

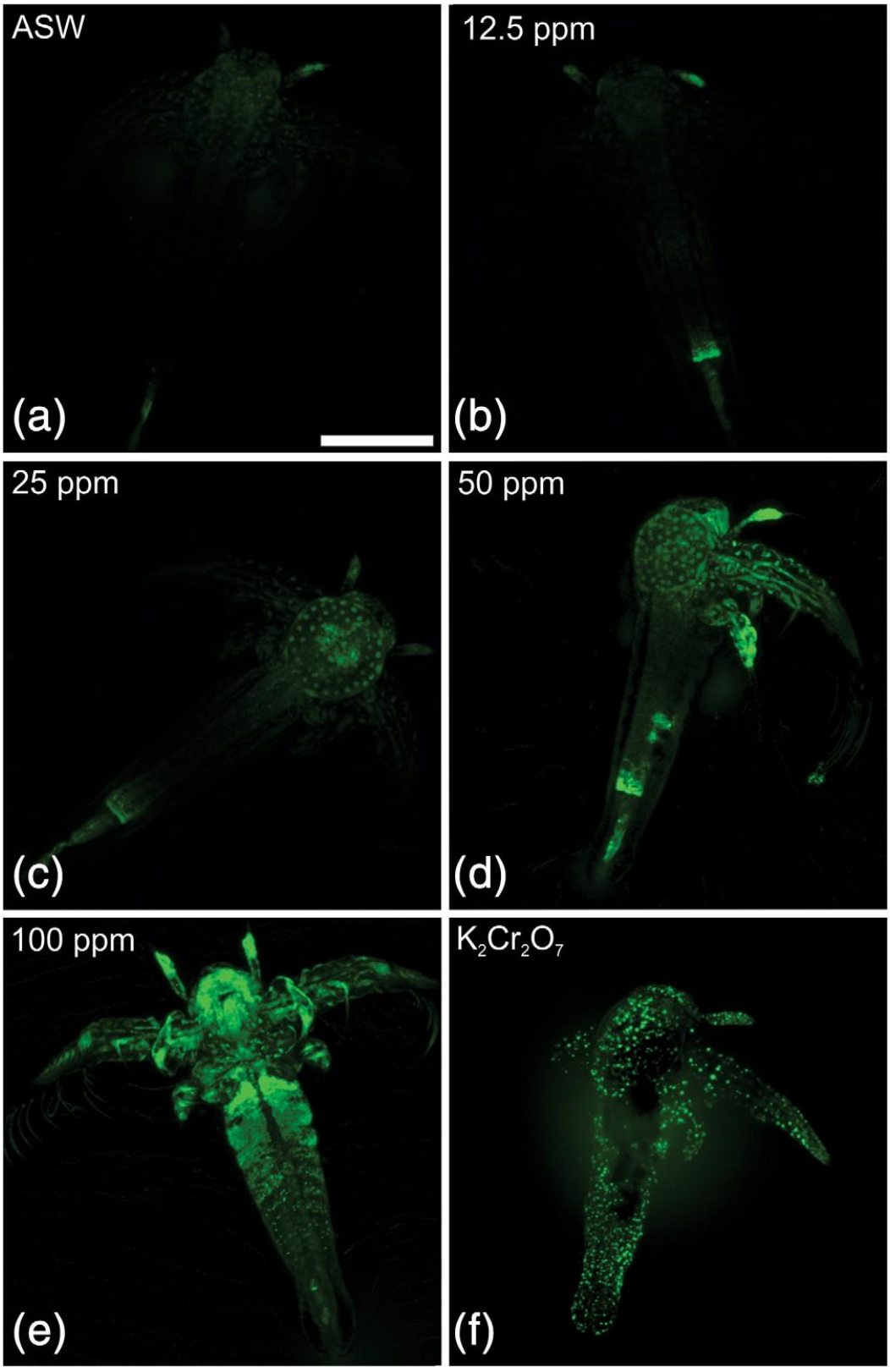

FIGURE4. Confocal laser scanning microscopy in *Artemia sp.* nauplii instar II, submitted to different concentrations of MTiO2 with acridine orange stained within 48 h of exposure. (a) Artificial sea water presented low emission is related to damage to the animal's body; (b) *Artemia sp.* submitted to the concentration of 12.5 ppm of $MTiO_2$; (c) *Artemia sp.* submitted to a concentration of 25 ppm of MTiO2; (d) At a concentration of 50 ppm $MTiO_2$, a higher fluorescence emission was observed due to cell damage; (e) At the maximum tested concentration (100 ppm), fluorescence emission was observed throughout the animal's body, due to the accumulation and damage caused by $MTiO_2$; (f) *Artemia sp.* submitted to K Cr O presented strong emission due to cell damage caused by the reagent. Bars: 200 µm.

Morphological changes

Morphological changes in *Artemia sp.* nauplii instar II were observed under scanning electron microscopy and morphological changes were observed in high concentrations of $MTiO_2$. Overview of *Artemia sp.* in ASW (Figure 5a), with normal development of the swimming legs (Figure 5b) and posterior region (Figure 5c). *Artemia sp.* submitted to $MTiO_2$ at a concentration of 12.5 ppm (Figure 5d) no damage to the swimming legs (Figure 5e). Posterior region showed wrinkling cuticle (Figure 5f). At the 25 ppm slight body wrinkling was observed (Figure 5g), no damage on swimming legs (Figure 5h) and posterior region with wrinkling cuticle (Figure 5i).

At the concentration 50 ppm, wrinkling was observed on the surface of the body of *Artemia sp.* (Figure 5j) and cavities were observed in the abdomen. No damage was observed in the swimming legs (Figure 5k), however posterior region showed wrinkling cuticle (Figure 5l). At the maximum concentration tested (100 ppm), *Artemia sp.* showed the damage body with remarkable surface wrinkling and absence swimming setae (Figure 5m). Significant damage was also observed on the swimming legs (Figure 5n). The posterior region showed abnormalities with cuticle rupture (Figure 5o). The positive control ($K_2Cr_2O_7$) cuticle wrinkling was not observed on the animal's body (Figure 5p). however, absence of swimming setae was observed in swimming legs (Figure 5q). The posterior region showed morphological alteration such as deformations on the surface of the animal's body (Figure 5r).

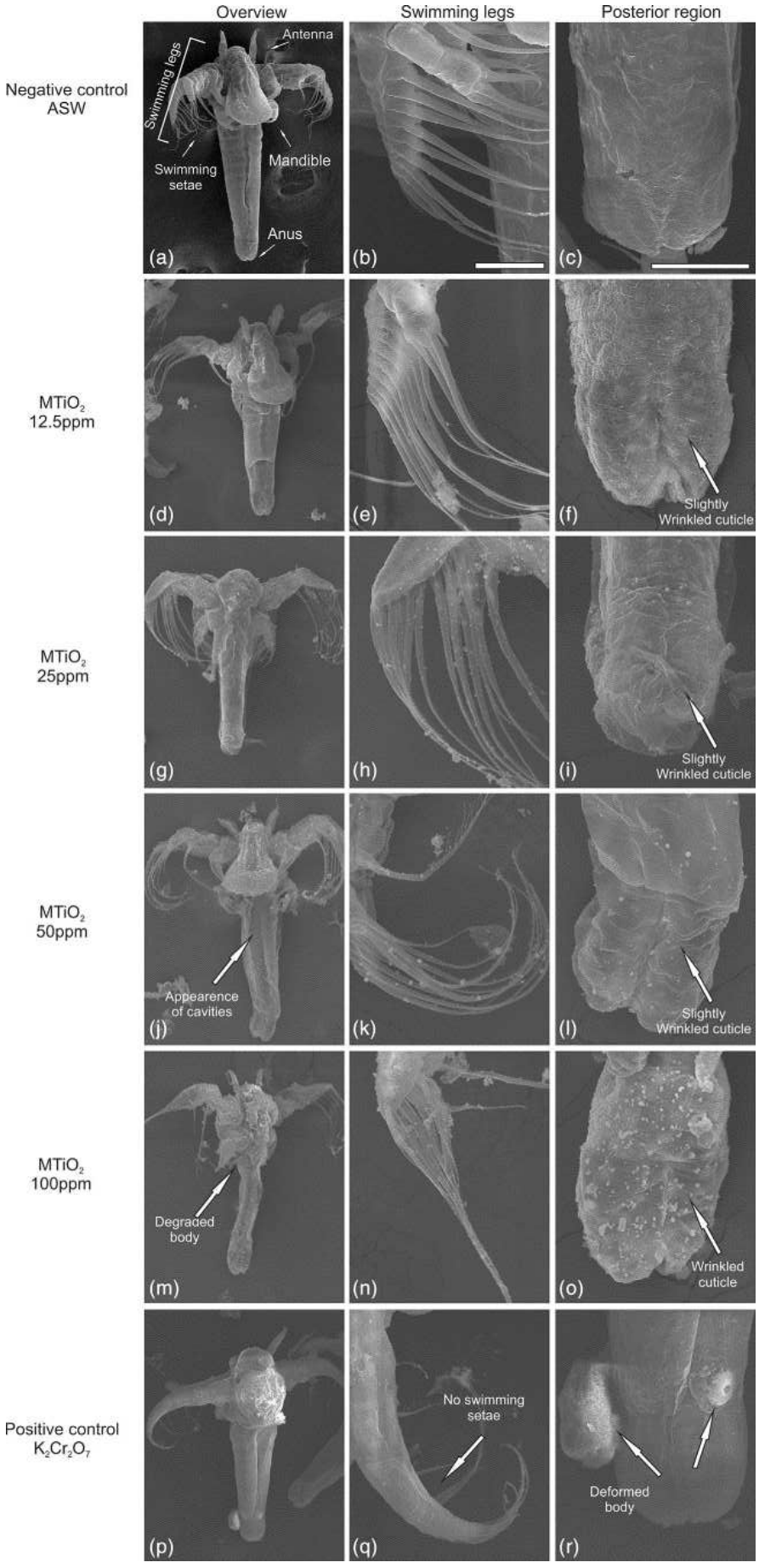
Overview
Swimming legs
Posterior region
Negative control
ASW
Antenna
Swimming legs
Mandible
Swimming setae
Anus
(a)
(b)
(c)
MTiO2
12.5ppm
(d)
(e)
(f)
Slightly Wrinkled cuticle
MTiO2
25ppm
(g)
(h)
(i)
Slightly Wrinkled cuticle
MTiO2
50ppm
Appearence of cavities
(j)
(k)
(l)
Slightly Wrinkled cuticle
MTiO2
100ppm
Degraded body
(m)
(n)
(o)
Wrinkled cuticle
Positive control
K2Cr2O7
No swimming setae
Deformed body
(p)
(q)
(r)

FIGURE 5. Scanning electron microscopy in *Artemia sp.* nauplii instar II, submitted to different concentrations of $MTiO_2$ within 48 h of exposure. (a) Overview of *Artemia sp.* nauplii instar II in ASW; (b) swimming legs; (c) posterior region; (d) overview of *Artemia sp.* submitted to 12.5 ppm concentration, no apparent damage; (e) swimming legs no damage; (f) slightly wrinkled posterior region; (g) overview of *Artemia sp.* submitted to 25 ppm concentration, no apparent damage; (h) swimming legs no damage; (i) slightly wrinkled posterior region; (j) overview of *Artemia sp.* submitted to 50 ppm concentration with cavities in the body; (k) swimming legs no damage; (l) slightly wrinkled posterior region; (m) overview of *Artemia sp.* submitted to 100 ppm concentration. Observe the degraded animal´s body; (n) swimming legs no damage; (o) wrinkled posterior region; (p) overview of *Artemia sp.* nauplii instar II in $K_2Cr_2O_7$; (q) swimming setae with damage; (r) deformed posterior region. Bars: (a, d, g, j, m, and p): 150 µm; (b, e, h, k, n and q): 50 µm; (c, f, i, l, o, and r): 50 µm.

5.1.4 Discussion

The toxicity of $MTiO_2$ is associated with the concentration and exposure time of these particles with *Artemia sp.* No LC50 values were observed for nauplii instar I at 24 and 48 h intervals. The mortality rate is directly proportional to the increase in the concentration of $MTiO_2$ and linear regression graph was observed for nauplii instar II. The value of LC50 were reported to be around 50 ppm within 48 h of exposure, however, in the 24 h interval no LC50 value was observed. Same result observed by Ates, Daniels, Arslan, Farah, and Rivera (2013) in A. salina nauplii exposed to TiO_2NPs at a concentration of 100 mg L^{-1}.

Usually, the LC50 values are related to the exposure time, above 48 h as noted by Ozkan *et al.* (2016) in which the LC50 value for *Artemia sp.* exposed to TiO_2 NPs with size of 44.1 nm was 70.12 and 18.77 mg $^{-1}$ in the 48 and 96h interval respectively. Other authors observed similar results, such as Sarkheil *et al.* (2018) using zinc oxide nanoparticle (ZnONPs) with size of 32.28 nm in *Artemia franciscana* in the 96h interval and Khoshnood *et al.* (2017) using TiO_2NPs with size of 20 nm in the same time interval. Madhav *et al.* (2017) found the LC50 using copper oxide nanoparticles (CuONPs) with a diameter of 114 nm and a concentration of 35.0 mg $^{-1}$ in *A. salina* nauplii instar II at a time of 48 h of exposure. The $MTiO_2$ used in our study showed an average diameter of 114.5 nm showing toxicity in nauplii within 48 h of exposure. The toxicity of TiO_2 in a shorter period of time may be associated with their characteristics such as size, charge, composition and hydrodynamic radius (Boran *et al.*, 2016; Murdock *et al.*, 2008). The different results found in the literature are related to the characteristics of NPs and exposure time (Table 3). In addition, smaller NPs are more toxic for *A. salina*, as they have a large surface area available for interaction with biological organisms (Kvıtek *et al.*, 2008). Also, the increased nanoparticles toxicity is related to the *A. salina* exposure time to the contaminant, as they are filter animals that can ingest and accumulate particles with a diameter of 50 µm (Hund-Rinke & Simon, 2006; Zhu *et al.*, 2017).

TABLE 3. Lethal concentration (LC_{50}) of NPs with different characteristics in *Artemia* sp. nauplii instar II.

Nanoparticle	Particle size (TEM) (nm)*	Concentration (mg L^{-1}) 48 h	96 h	Model organism	Authors
Zn NPs	40-60	ND	100	*A. salina*	Ates, Daniels, Arslan, and Farah (2013)
TiO_2 NPs	44.1	70.12	18.77	*A. salina*	Ozkan et al. (2016)
TiO_2 NPs	20	86.11	30.54	*A. franciscana*	Khoshnood et al. (2017)
CuO NPs	114 nm	35.0	ND	*A. salina*	Madhav et al. (2017)
ZnO NPs	32.28	ND	4.86	*A. franciscana*	Sarkheil et al. (2018)
CAg	ND	902.1	ND	*A. salina*	Demarchi et al. (2020)
PANI/Ag (AMPSA)/GO QDs NC	20	476.0	ND	*A. salina*	Shokry et al., (2021)

Abbreviations: *, transmission electron microscopy; —, no calculated; CAg, carboxymethylchitosan/γ-Fe_2O_3/Ag without reducing agent; CuONPs, copper oxide nanoparticles; PANI/Ag (AMPSA)/GO QDs NC, polyaniline (PANI)/2-acrylamido-2-methylpropanesulfonic acid (AMPSA) capped silver nanoparticles (NPs)/graphene oxide quantum dots nanocomposite; TiO_2NPs, titanium oxide nanoparticles; Zn NPs, zinc nanoparticles; ZnONPs, zinc oxide nanoparticle.

In addition to microparticles, other contaminants also showed toxic effects on *A. salina* as described by several authors. In a study using plant extracts of different species, the LC50 was 1000 µg ml^{-1} in experiment time of 24 and 48 h (Mayorga *et al.*, 2010). Assay evaluating the toxicity of organophosphorous insecticide in *A. salina*, it was observed that the highest toxicity was observed in nauplii instar II (48 h after incubation) with LC50 of 0.16 mg L^{-1} for insecticide chlor pyrifos (Sánchez-Fortún *et al.*, 1996). These results are similar to our study showing toxicity in *Artemia sp.* in the short period of exposure to the contaminant.

No acute toxicity was observed in nauplii instar I. At this stage of life, the animal is less sensitive, due to incomplete mouth development and not actively eating (Sorgeloos *et al.*, 1978). A similar result was observed by (Ocaranza-Joya *et al.*, 2019) in which nauplii instar I was less sensitive to potassium dichromate, due to incomplete development of the mouth and anus.

Artemia sp. nauplii instar II was more sensitive to $MTiO_2$ within 48 h of exposure only at high concentrations of $MTiO_2$ (25, 50, and 100 ppm). This occurs due to the exposure time to the contaminant, because the 24 h interval, no acute toxicity of $MTiO_2$ was observed in *Artemia sp.* nauplii instar II. In study using AgNPs, it was observed that A. salina nauplii instar II was more sensitive to contaminates in the 48 h exposure interval (Lacave *et al.*, 2017). Many authors have described a similar result for acute toxicity only at high concentrations and time of exposure to the contaminant (Ates, Daniels, Arslan, & Farah, 2013; Khoshnood *et al.*, 2017; Sarkheil *et al.*, 2018). However, exposure of *A. salina* nauplii instar II to high concentrations of metal oxide nanoparticles (CeO_2, SnO_2, and Fe_3O_4) did not induce any lethal effect after 48 h of exposure (Gambardella *et al.*, 2014). These adverse toxic effects observed in different studies may be the result of different experimental conditions, as well as the properties of NPs (Sarkheil *et al.*, 2018). In addition, many factors can alter the results of toxicity tests on *Artemia spp.* such as environmental factors (chemical composition of seawater, oxygen, hatching

temperature and duration of the photoperiod), maintenance conditions and origin of the cysts (Libralato, 2014).

The $MTiO_2$ accumulation was observed mainly in the gut, in addition, was also observed $MTiO_2$ dispersed on the surface of the *Artemia sp.* body when exposed to a concentration of 100 ppm. In a study using silver nanoparticles (AgNPs) and silver nanowires (AgNWs), accumulations of these nanomaterials were observed in the gut of *A. salina* (An *et al.*, 2019). Result observed by (Ates, Daniels, Arslan, & Farah, 2013) using TiO_2NPs. In this study, the aggregation of $MTiO_2$ was higher in *A. salina* nauplii instar II due to the complete development of the mouth allowing it to feed actively (Sorgeloos *et al.*, 1978). At this stage of development, *Artemia sp.* feeds on NPs by filtration.

The uptake of NPs through the digestive tract and subsequent aggregation in the animal's gut causes obstruction, leading to mortality (Rekulapally *et al.*, 2019). In a study using anionic carboxylated (PS- COOH) polystyrene nanoparticles (PSNPs) it was observed the accumulation of NPs inside the gut lumen of larvae (48 h). A similar result observed by Pecoraro *et al.* (2021) using silver nanoparticles (AgNPs) and gold nanoparticles (AuNPs) in *A. salina*. This interaction can result in changes in the physiological processes of the larvae with multiple molt events in the short period of exposure (Bergami *et al.*, 2016). In addition, cationic amino (PS-NH2) polystyrene nanoparticles (PSNPs) were absorbed in the sensory antennules and appendages (Bergami *et al.*, 2016) negatively affecting animal survival. As observed in our study, part of the $MTiO_2$ may be retained in the gut of *Artemia sp.,* however, Bergami *et al.* (2016) observed that larvae exposed to PS- NH2 (0, 5, 25, and 50 mg/mL) and transferred to clean natural sea water (NSW) did not show neither aggregate in the gut. The non-formation of aggregates in the gut is related to the elimination of NPs by A. salina as observed by Ozkan *et al.* (2016).

In toxicity study, *A. salina* submitted to TiO_2 NPs and $AgTiO_2$ NPs showed changes in the ocular surface, malformations in the body, loss of the antenna and gut enlargement of (Ozkan *et al.*, 2016). In addition, TiNPs induce gut necrosis of epithelial cells and severe edema, indicated by swelling of the cells with enlarged cytoplasms (Kachenton *et al.*, 2019). All these interactions and NPs accumulation in the animal's intestine lead to oxidative stress with the generation of reactive oxygen species (Ates *et al.*, 2020).

The cell damage observed in *Artemia sp.* was directly proportional to the $MTiO_2$ concentration used. Using CLSM it was possible to observe apoptosis of the cells, characterized by the emission of green fluorescence using acridine orange. The use of acridine orange allows revealing cells in apoptosis because fluorophyll binds to the DNA of cells in apoptosis emitting

green fluorescence at a wavelength of 488–535 nm (Damas-Souza *et al.*, 2019). Acridine orange permeates all living cells and is absorbed when damage occurs in the cytoplasmatic membrane, binding to DNA. Normal living cells have a light emission of fluorophyll, however, early apoptotic cells have a bright green nucleus (Ribble *et al.*, 2005).

At a concentration of $MTiO_2$ 25 and 50 ppm, fluorescence emission was observed, indicating cell damage. At the maximum concentration tested (100 ppm) a high fluorescence emission was observed, due to the marked damage caused by the $MTiO_2$ to the cells. Result observed by Arulvasu *et al.* (2014) using AgNPs in *A. salina* at 12 nM concentration.

Analysis using SEM revealed morphological changes and damage to the body of *Artemia sp.* nauplii instar II. After exposure to different concentrations of $MTiO_2$, the individuals presented cuticle wrinkling. At the 50 ppm concentration, the appearance of cavities in the animal's body was observed. At the maximum concentration tested (100 ppm) damage was observed with rupture in the animal's body, loss of swimming setae and mandible, structures responsible for mobility and feeding respectively. The morphological changes caused by NPs make it difficult to absorb food, change behavior and physiology of *Artemia sp.* affecting the animal's short-term survival (Bergami *et al.*, 2016; Morgana *et al.*, 2018).

Other studies using different NPs showed similar results with our research. In study using graphene oxide in *A. salina*, irreversible damage such as ruptures and holes in the animal's body were observed (Zhu *et al.*, 2017). In another study using α-Fe2O3 nanoparticles, was observed damage to the animal's body (Wang *et al.*, 2017).

These NPs are widely used and inevitably released in aqueous environments, causing ecological and health risks (Wang *et al.*, 2015). As new nanomaterials and products containing particles at the nanoscale are manufactured, many inevitably reach environmental repositories. (Ates, Daniels, Arslan, & Farah, 2013). In addition, TiO_2 particles have been used around the world in a variety of products, including sunscreen, cosmetics, paints, food additives, drugs and building materials (Ozkan *et al.*, 2016) can be disposed of in the environment. Thus, $MTiO_2$ can also be toxic to the environment, particularly to aquatic organisms.

5.1.5 Conclusions

The acute toxicity of $MTiO_2$ was evaluated using nauplii instar I and instar II of *Artemia sp.* in 24 and 48 h assays. $MTiO_2$ toxicity was observed only at concentrations of 25, 50, and 100 ppm in nauplii instar II within 48 h of exposure, with a high mortality rate. The use of microscopy techniques was of fundamental importance to evaluate accumulation, cell

damage and morphological changes. Toxicity in *Artemia sp.* is directly related to the filtration of $MTiO_2$, therefore, in nauplii instar I, $MTiO_2$ did not present toxicity due to incomplete development of the mouth and anus. With this study it was possible to observe the dynamics and interaction of microparticles in *Artemia sp.* and how physicochemical characteristics of microparticles directly affect toxicity in biological systems.

AUTHOR CONTRIBUTIONS

Sergimar Kennedy de Paiva Pinheiro: Writing – original draft; investigation. Ana Kamila Medeiros Lima: Data curation. Thaiz Batista Azevedo Rangel Miguel: Methodology; formal analysis. Saulo Pireda: Data curation; formal analysis. Pierre Basílio Almeida Fechine: Visualization; methodology. Antonio Gomes Souza Filho: Supervision; validation; visualization. Emilio de Castro Miguel: Conceptualization; writing – review and editing; supervision.

ACKNOWLEDGMENTS

TBARM acknowledge funding from CNPq (grant 350023/2020-4) and Central Analítica-UFC/CT-INFRA-FINEP/Pro-Equipamentos-CAPES/ CNPq-SisNano-MCTI 2019 (grant 442577/2019-2). Capes, INCT and FUNCAP. This work is part of PhD research of SKPP and master's degree of AKML.

CONFLICT OF INTEREST STATEMENT

The authors declare no conflict of interest.

DATA AVAILABILITY STATEMENT

The data that support this study are available in Figshare at doi: https://doi.org/10.6084/m9.figshare.21806199.

ORCID - Sergimar Kennedy de Paiva Pinheiro https://orcid.org/0000-0002- 6232-9069

REFERENCES

An, H. J., Sarkheil, M., Park, H. S., Yu, I. J., & Johari, S. A. (2019). Comparative toxicity of silver nanoparticles (AgNPs) and silver nanowires (AgNWs) on saltwater microcrustacean, Artemia salina. Comparative Biochemistry and Physiology Part C: Toxicology and Pharmacology, 218, 62–69. https://doi.org/10.1016/j.cbpc.2019.01.002

Arulvasu, C., Jennifer, S. M., Prabhu, D., & Chandhirasekar, D. (2014). Toxicity effect of silver nanoparticles in brine shrimp Artemia. Scientific World Journal, 2014, 1–10. https://doi.org/10.1155/2014/256919

Ates, M., Danabas, D., Ertit Tastan, B., Unal, I., Cicek Cimen, I. C., Aksu, O., Kutlu, B., & Arslan, Z. (2020). Assessment of oxidative stress on Artemia salina and Daphnia magna after exposure to Zn and ZnO nanoparticles. Bulletin of Environmental Contamination and Toxicology, 104, 206–214. https://doi.org/10.1007/s00128-019-02751-6

Ates, M., Daniels, J., Arslan, Z., & Farah, I. O. (2013). Effects of aqueous suspensions of titanium dioxide nanoparticles on Artemia salina: Assessment of nanoparticle aggregation, accumulation and toxicity. Environmental Monitoring and Assessment, 185, 3339–3348. https:// doi.org/10.1007/s10661-012-2794-7.

Ates, M., Daniels, J., Arslan, Z., Farah, I. O., & Rivera, H. F. (2013). Comparative evolution of impact of Zn and ZnO nanoparticles on brine shrimp (Artemia salina) larvae: Effects of particles size and solubility on toxicity. Environmental Science. Processes & Impacts, 15, 225–233. https:// doi.org/10.1016/j.dcn.2011.01.002.

Barbosa, J. S., Neto, D. M. A., Freire, R. M., Rocha, J. S., Fechine, L. M.

U. D., Denardin, J. C., Valentini, A., de Araújo, T. G., Mazzetto, S. E., & Fechine, P. B. A. (2018). Ultrafast sonochemistry-based approach to coat TiO2 commercial particles for sunscreen formulation. Ultrasonics Sonochemistry, 48, 340–348. https://doi.org/10.1016/j.ultsonch.2018.06.015

Bergami, E., Bocci, E., Vannuccini, M. L., Monopoli, M., Salvati, A., Dawson, K. A., & Corsi, I. (2016). Nano-sized polystyrene affects feeding, behavior and physiology of brine shrimp Artemia franciscana larvae. Ecotoxicology and Environmental Safety, 123, 18–25. https://doi. org/10.1016/j.ecoenv.2015.09.021

Boran, H., Boyle, D., Altinok, I., Patsiou, D., & Henry, T. B. (2016). Aqueous Hg2+ associates with TiO2 nanoparticles according to particle size, changes particle agglomeration, and becomes less bioavailable to zebrafish. Aquatic Toxicology, 174, 242–246. https://doi.org/10.1016/j. aquatox.2016.02.017

Bundschuh, M., Filser, J., Lüderwald, S., McKee, M. S., Metreveli, G., Schaumann, G. E., Schulz, R., & Wagner, S. (2018). Nanoparticles in the environment: Where do we come from, where do we go to? Environmental Sciences Europe, 30, 1–17. https://doi.org/10.1186/s12302-018-0132-6

Clément, L., Hurel, C., & Marmier, N. (2013). Toxicity of TiO2 nanoparticles to cladocerans, algae, rotifers and plants—Effects of size and crystalline structure. Chemosphere, 90, 1083–1090. https://doi.org/10.1016/ j.chemosphere.2012.09.013

Damas-Souza, D. M., Nunes, R., & Carvalho, H. F. (2019). An improved acridine orange staining of DNA/RNA. Acta Histochemica, 121, 450– 454. https://doi.org/10.1016/j.acthis.2019.03.010

Demarchi, C. A., da Silva, L. M., Niedz´wiecka, A., S´lawska-Waniewska, A., Lewin´ska, S., Dal Magro, J., Fossá Calisto, J. F., Martello, R., & Rodrigues, C. A. (2020). Nanoecotoxicology study of the response of magnetic O-carboxymethylchitosan loaded silver nanoparticles on Artemia salina. Environmental Toxicology and Pharmacology, 74, 103298.

Farré, M., Gajda-Schrantz, K., Kantiani, L., & Barcelo´, D. (2009). Ecotoxicity and analysis of nanomaterials in the aquatic environment. Analytical and Bioanalytical Chemistry, 393, 81–95. https://doi.org/10.1007/ s00216-008-2458-1

Fu, P. P., Xia, Q., Hwang, H. M., Ray, P. C., & Yu, H. (2014). Mechanisms of nanotoxicity: Generation of reactive oxygen species. Journal of Food and Drug Analysis, 22, 64–75. https://doi.org/10.1016/j.jfda.2014.01.005

Gambardella, C., Mesari, T., Milivojevi, T., Sep, K., Gallus, L., Carbone, S., Ferrando, S., & Faimali, M. (2014). Effects of selected metal oxide nano- particles on Artemia salina larvae: Evaluation of mortality and behavioural and biochemical responses. Environmental Monitoring and Assessment, 4249–4259, 4249–4259. https://doi.org/10.1007/s10661-014-3695-8

Garaventa, F., Gambardella, C., Di Fino, A., Pittore, M., & Faimali, M. (2010). Swimming speed alteration of *Artemia sp.* and Brachionus plicatilis as a sublethal behavioural endpoint for ecotoxicological surveys. Ecotoxicology, 19, 512–519. https://doi.org/10.1007/s10646-010-0461-8

Hund-Rinke, K., & Simon, M. (2006). Ecotoxic effect of photocatalytic active nanoparticles (TiO2) on algae and daphnids. Environmental Sci- ence and Pollution Research, 13, 225–232. https://doi.org/10.1065/ espr2006.06.311

Johari, S. A., Rasmussen, K., Gulumian, M., Ghazi-Khansari, M., Tetarazako, N., Kashiwada, S., Asghari, S., Park, J. W., & Yu, I. J. (2019). Introducing a new standardized nanomaterial environmental toxicity screening testing procedure, ISO/TS 20787: Aquatic toxicity assessment of manufactured nanomaterials in saltwater lakes using *Artemia sp.* nauplii. Toxicology Mechanisms and Methods, 29, 95–109. https://doi.org/10.1080/15376516.2018.1512695

Kachenton, S., Jiraungkoorskul, W., Kangwanrangsan, N., & Tansatit, T. (2019). Cytotoxicity and histopathological analysis of titanium nanoparticles via Artemia salina. Environmental Science and Pollution Research, 26, 14706–14711. https://doi.org/10.1007/s11356-018- 1856-y.

Khoshnood, R., Jaafarzadeh, N., Sh, J., Farshchi, P., & Taghavi, L. (2017). Acute toxicity of TiO2, CuO and ZnO nanoparticles in brine shrimp, Artemia franciscana. Iranian Journal of Fisheries Sciences, 16, 1287– 1296.

Kvıtek, L., Soukupova, J., Vec, R., Prucek, R., Holecova, M., & Zbor, R. (2008). Effect of surfactants and polymers on stability and antibacter- ial activity of silver nanoparticles (NPs). Journal of Physical Chemistry C, 112, 5825–5834. https://doi.org/10.1021/jp711616v

Lacave, J. M., Fanjul, A´., Bilbao, E., Gutierrez, N., Barrio, I., Arostegui, I., Cajaraville, M. P., & Orbea, A. (2017). Acute toxicity, bioaccumulation and effects of dietary transfer of silver from brine shrimp exposed to PVP/PEI-coated silver nanoparticles to zebrafish. Comparative Biochemistry and Physiology Part C: Toxicology and Pharmacology, 199, 69– 80. https://doi.org/10.1016/j.cbpc.2017.03.008

Libralato, G. (2014). The case of Artemia spp. in nanoecotoxicology. Marine Environmental Research, 101, 38–43. https://doi.org/10.1016/j. marenvres.2014.08.002

Lu, P. J., Huang, S. C., Chen, Y. P., Chiueh, L. C., & Shih, D. Y. C. (2015). Analysis of titanium dioxide and zinc oxide nanoparticles in cosmetics. Journal of Food and Drug Analysis, 23, 587–594. https://doi.org/10. 1016/j.jfda.2015.02.009

Madhav, M. R., David, S. E. M., Kumar, R. S. S., Swathy, J. S., Bhuvaneshwari, M., Mukherjee, A., & Chandrasekaran, N. (2017). Toxicity and accumulation of copper oxide (CuO) nanoparticles in different life stages of Artemia salina. Environmental Toxicology and Pharmacology, 52, 227–238. https://doi.org/10.1016/j.etap.2017.03.013

Manfra, L., Tornambè, A., Savorelli, F., Rotini, A., Canepa, S., Mannozzi, M., & Cicero, A. M. (2014). Ecotoxicity of diethylene glycol and risk assessment for marine environment. Journal of Hazardous Materials, 284, 130–135. https://doi.org/10.1016/j.jhazmat.2014.11.008

Mayorga, P., Pérez, K. R., Cruz, S. M., & Cáceres, A. (2010). Comparaça˜o de bioensaios com os crustáceos Artemia salina e Thamnocephalus platyurus para abordagem de extratos de plantas com toxicidade. Brazilian Journal of Pharmacognosy, 20, 897–903. https://doi.org/10.1590/ S0102-695X2010005000029

Morgana, S., Estévez-Calvar, N., Gambardella, C., Faimali, M., & Garaventa, F. (2018). A short-term swimming speed alteration test with nauplii of Artemia franciscana. Ecotoxicology and Environmental Safety, 147, 558–564. https://doi.org/10.1016/j.ecoenv.2017.09.026

Murdock, R. C., Braydich-Stolle, L., Schrand, A. M., Schlager, J. J., & Hussain, S. M. (2008). Characterization of nanomaterial dispersion in solution prior to in vitro exposure using dynamic light scattering technique. Toxicological Sciences, 101, 239–253. https://doi.org/10.1093/ toxsci/kfm240

Nowack, B., & Bucheli, T. D. (2007). Occurrence, behavior and effects of nanoparticles in the environment. Environmental Pollution, 150, 5–22. https://doi.org/10.1016/j.envpol.2007.06.006

Nunes, B. S., Carvalho, F. D., Guilhermino, L. M., & Van Stappen, G. (2006). Use of the genus Artemia in ecotoxicity testing. Environmental Pollution, 144, 453–462. https://doi.org/10.1016/j.envpol.2005.12.037

Ocaranza-Joya, V. S., Manjarrez-Alcivar, I., Ruizgonzález, L. E., Guerrero- Galván, S. R., & Vega-Villasante, F. (2019). Sensitivity of different stages of Artemia franciscana to potassium dichromate. Pan-American Journal of Aquatic Sciences, 14, 8–12.

OECD. (2004). OECD guideline for testing of chemical, guideline for testing of chemicals, section 2. https://doi.org/10.1787/9789264069947-en

Ozkan, Y., Altinok, I., Ilhan, H., & Sokmen, M. (2016). Determination of TiO2 and AgTiO2 nanoparticles in Artemia salina: Toxicity, morphological changes, uptake and depuration. Bulletin of Environmental Contamination and Toxicology, 96, 36–42. https://doi.org/10.1007/s00128-015-1634-1

Pecoraro, R., Scalisi, E. M., Messina, G., Fragalà, G., Ignoto, S., Salvaggio, A., Zimbone, M., Impellizzeri, G., & Brundo, M. V. (2021). Artemia salina: A microcrustacean to assess engineered nanoparticles toxicity. Microscopy Research and Technique, 84, 531–536. https://doi.org/10.1002/jemt. 23609

Rekulapally, R., Chavali, L. N. M., Idris, M. M., & Singh, S. (2019). Toxicity of TiO2, SiO2, ZnO, CuO, Au and Ag engineered nanoparticles on hatching and early nauplii of *Artemia sp.* PeerJ, 2019, e6138. https:// doi.org/10.7717/peerj.6138

Ribble, D., Goldstein, N. B., Norris, D. A., & Shellman, Y. G. (2005). A simple technique for quantifying apoptosis in 96-well plates. BMC Biotechnol- ogy, 5, 1–7. https://doi.org/10.1186/1472-6750-5-12

Sadrieh, N., Wokovich, A. M., Gopee, N. V., Zheng, J., Haines, D., Parmiter, D., Siitonen, P. H., Cozart, C. R., Patri, A. K., McNeil, S. E., Howard, P. C., Doub, W. H., & Buhse, L. F. (2010). Lack of significant dermal penetration of titanium dioxide from sunscreen formulations

containing nano- and submicron size TiO_2 particles. Toxicological Sciences, 115, 156–166. https://doi.org/10.1093/toxsci/kfq041

Sánchez-Fortún, S., Sanz, F., & Barahona, M. V. (1996). Acute toxicity of several organophosphorous insecticides and protection by cholinergic antagonists and 2-PAM on Artemia salina larvae. Archives of Environ- mental Contamination and Toxicology, 31, 391–398. https://doi.org/10. 1007/BF00212678

Sarkheil, M., Johari, S. A., An, H. J., Asghari, S., Park, H. S., Sohn, E. K., & Yu, I. J. (2018). Acute toxicity, uptake, and elimination of zinc oxide nanoparticles (ZnO NPs) using saltwater microcrustacean, Artemia franciscana. Environmental Toxicology and Pharmacology, 57, 181–188. https://doi.org/10.1016/j.etap.2017.12.018

Shi, H., Magaye, R., Castranova, V., & Zhao, J. (2013). Titanium dioxide nanoparticles: A review of current toxicological data. Particle and Fibre Toxicology, 10, 1–33. https://doi.org/10.1186/1743-8977-10-15

Shokry, A., Khalil, M., Ibrahim, H., Soliman, M., & Ebrahim, S. (2021). Acute toxicity assessment of polyaniline/Ag nanoparticles/graphene oxide quantum dots on Cypridopsis vidua and Artemia salina. Scientific Reports, 11, 1–9. https://doi.org/10.1038/s41598-021-84903-5

Sirotkin, A. V., Bauer, M., Kadasi, A., Makovicky, P., & Scsukova, S. (2021). The toxic influence of silver and titanium dioxide nanoparticles on cultured ovarian granulosa cells. Reproductive Biology, 21, 100467. https://doi.org/10.1016/j.repbio.2020.100467

Sorgeloos, P., Remiche-Van Der Wielen, C., & Persoone, G. (1978). The use of Artemia nauplii for toxicity tests—A critical analysis. Ecotoxicology and Environmental Safety, 2, 249–255. https://doi.org/10.1016/ S0147-6513(78)80003-7

Wang, C., Jia, H., Zhu, L., Zhang, H., & Wang, Y. (2017). Toxicity of α-Fe_2O_3 nanoparticles to Artemia salina cysts and three stages of larvae. Science of the Total Environment, 598, 847–855. https://doi.org/10.1016/j.scitotenv.2017.04.183

Wang, L. F., Habibul, N., He, D. Q., Li, W. W., Zhang, X., Jiang, H., & Yu, H. Q. (2015). Copper release from copper nanoparticles in the presence of natural organic matter. Water Research, 68, 12–23. https://doi.org/10.1016/j.watres.2014.09.031
Zhu, S., Luo, F., Chen, W., Zhu, B., & Wang, G. (2017). Toxicity evaluation of graphene oxide on cysts and three larval stages of *Artemia salina*. **Science of the Total Environment**, 595, 101–109. https://doi.org/10. 1016/j.scitotenv.2017.03.224

6 CAPÍTULO III – Interação entre *Danio rerio* e TiO_2

Este capítulo abordará a compreensão dos aspectos da interação entre TiO_2 e *Danio rerio*, além da dinâmica das partículas na cadeia alimentar. Está dividido em dois manuscritos: o primeiro aborda a toxicidade aguda do dióxido de titânio em embriões de peixe-zebra. O segundo se concentra nos efeitos tóxicos causados pela ingestão indireta do composto.

6.1 MANUSCRIPT 4 – Chorion-Dependent Toxicity: Acute Effects of Titanium Dioxide Microparticles on *Danio rerio* Embryos

Ana Kamila Medeiros Lima[1]; Luiz Gustavo Vieira Oliveira[1]; Roberta Laiz Bezerra Santos Albano[1]; Alexia Riquet Martins[1]; Jorge Henrique de Andrade Vieira[1]; Emilio de Castro Miguel[1*];

[1] Biomaterials Laboratory, Department of Metallurgical Engineering and Materials and Analytical Center, Federal University of Ceará (UFC), Fortaleza, CE, Brazil.

***Corresponding author**

Emilio de Castro Miguel

Federal University of Ceara

Pici Campus

Department of Metallurgical Engineering and Materials (DEMM)

Biomaterials Laboratory (BIOMAT)

zip code: 60455-900

Fortaleza - Ceará - Brazil

+85 33669256

emiliomiguel@ufc.br

GRAPHICAL ABSTRACT

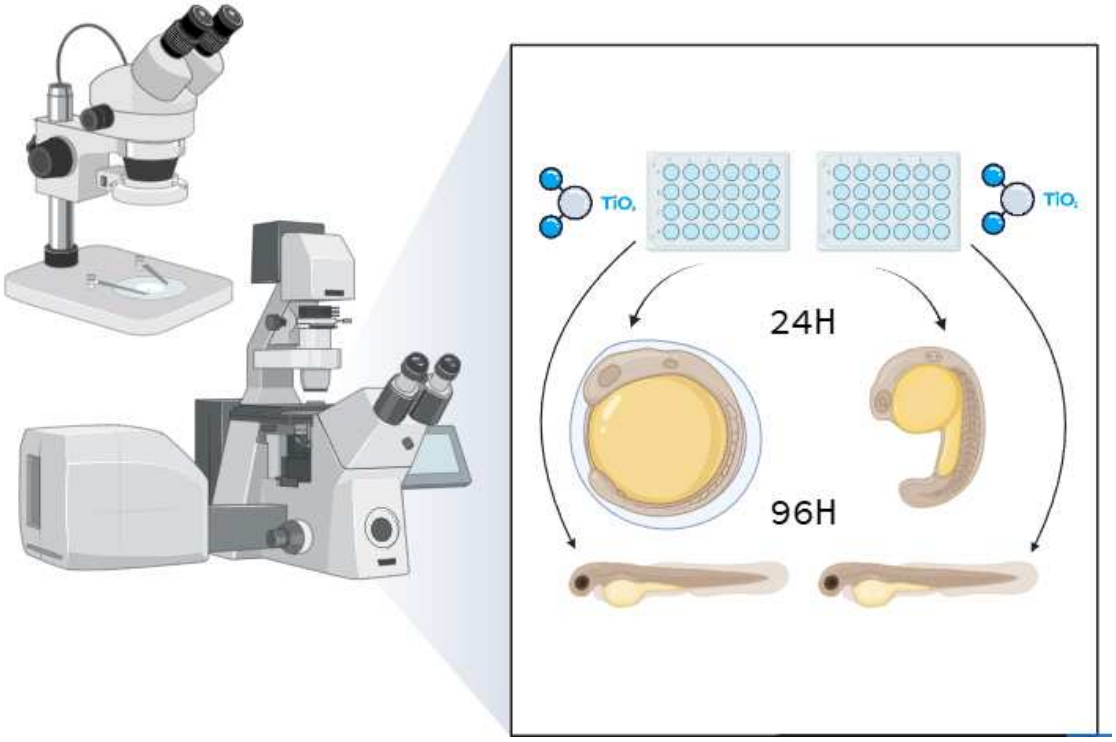

ABSTRACT

Titanium dioxide nanoparticles (TiO_2NPs) are widely used in personal care products and industrial applications and are frequently detected in aquatic environments. This study investigated the acute toxicity of TiO_2NPs in zebrafish (*Danio rerio*) embryos, with a focus on the role of the chorion – an embryonic membrane – as a protective barrier against nanoparticle exposure. Embryos with and without chorion were exposed for 96 hours to TiO_2 at concentrations of 1, 10, and 100 mg/L, following OECD guideline 236. Hatching rate, survival, morphological alterations, and cellular damage were evaluated using stereomicroscopy and confocal laser scanning microscopy (CLSM) with acridine orange staining. FET results showed no significant effect of chorion presence on hatching or survival rates at any tested concentration. However, confocal analysis revealed apoptotic signals in dechorionated embryos even at the lowest concentration, especially in the yolk sac region, while embryos with intact chorion showed cellular damage only at the highest concentration. These findings reinforce the function of the chorion as a partial physical barrier to nanoparticle penetration and highlight the utility of CLSM in detecting sublethal effects not visible under conventional microscopy. The study contributes to a better understanding of the early developmental toxicity of nanomaterials in aquatic vertebrate models.

Keywords: Titanium dioxide nanoparticles; *Danio rerio*; Zebrafish embryos; Confocal microscopy; Nanotoxicology; Chorion barrier.

6.1.1 Introduction

Titanium dioxide nanoparticles (TiO_2NPs) rank among the most widely manufactured nanomaterials (NMs) worldwide among emerging environmental contaminants (HSU *et al.*, 2024). It is estimated that the production of its raw material was estimated at US$ 17.19 billion in 2020, with a projection of 6% annual growth from 2021 to 2028 (Firoozi *et al.*, 2021).

TiO_2NPs are prominent among the emerging pollutants increasingly detected in aquatic environments, owing to their widespread use in personal care products such as cosmetics and sunscreens, as well as in pharmaceuticals, paints, and plastics (Abdel-Latif *et al.*, 2020). TiO_2 is a white pigment found in a wide range of products, including paints, printing inks, plastics, paper, synthetic fibers, rubber, capacitors, pigments, crayons, ceramics, electronic components, food, and cosmetics (Weir *et al.*, 2012; Hanigan *et al.*, 2018; Haider; Jameel; Al-Hussaini, 2019).

The environmental risk of TiO_2NPs, whether alone or in combination with other metal nanoparticles, has been studied. Its toxic potential should be further investigated, especially considering that the presence of TiO_2 can influence the toxicity of other metals, such as cadmium (Cd). Notably, exposure to Cd alone — as well as co-exposure to Cd and TiO_2 — induces toxic effects in zebrafish, including cardiotoxicity and morphological and morphometric alterations (Mamboungou *et al.*, 2022).

Additionally, environmental variables such as salinity, temperature and pH can modulate the effects of chemical compounds across different species (Vasyukova *et al.*, 2021). The toxicity of titanium dioxide has been tested in *Lemna* species, a freshwater angiosperm. Matějová *et al.* (2023) concluded that its effects should not be generalized, as they depend on the preparation methods and stability of the nanoparticles. While Koce (2017) demonstrated greater morphological and biochemical toxicity of CuO compared to TiO_2 in *Lemna minor*. To environmental-friendly approach, TiO_2 NPs were synthesized using *Echinophora cinerea* extract as a green method, with water as the solvent. The nanoparticles were characterized by FTIR, XRD, SEM, and DLS, and key synthesis parameters were optimized. Their acute toxicity was then evaluated in zebrafish (*Danio rerio*) over a 96-hour exposure period and showed toxic

effects both chemically and green synthesized TiO2-NPs, the last one shows toxicity in higher concentrations (Jafari *et al.*, 2022).

Within the context of environmental stressors affecting aquatic biodiversity, not only are organisms directly exposed to contaminants impacted, but also their offspring, through transgenerational effects (Luu *et al.*, 2021). Increased industrial activities have led to the uncontrolled release of metals into the environment, resulting in a global increase in metal pollution. Heavy metals are also consumed from the surface of glasses over a prolonged period of use. Heavy metal pollution is a serious problem that can have wide-ranging and long-lasting impacts on human health and the environment (Nnaji *et al.*, 2023). TiO_2 NPs present in sediments are bioavailable to aquatic plants and fish, indicating that even incidental contamination can have long-term ecological consequences (Asztemborska *et al.*, 2018).

Zebrafish is an important vertebrate model organism and widely used in many standard eco-toxicological tests in OECD, ISO, USEPA (Ceger *et al.*, 2022) guidelines to evaluate the toxicity and endocrine activity of chemicals. Zebrafish provides valuable information concerning the toxic effects of contaminants on vertebrates, including humans (Segner, 2009), as approximately 70% of human genes have at least one clear zebrafish orthologue (Howe et al., 2013). The chorion is an acellular envelope surrounding the oocyte. In fish, this envelope plays a pivotal role during fertilization and protects the developing embryo against environmental and mechanical factors until the moment of hatching (Pérez-Atehortúa *et al.*, 2023).

The fish embryo acute toxicity (FET) test with the zebrafish (*Danio rerio*) was developed to assess the acute fish toxicity of chemicals or environmental samples as a replacement for the Acute Fish Test (AFT) with juvenile fish (Reichstein *et al.*, 2024). Besides the good correlation of FET with the standard acute fish toxicity (AFT) test, the potential of the FET test to predict AFT, which is required by the Registration, Evaluation, Authorization, and Restriction of Chemicals (REACH) regulation is still in discussion. The critical review about applicability of the fish embryo acute toxicity (FET) test (OECD 236) summarizes the main findings and discusses regulatory application of the FET test under REACH. Given some limitations (e.g., neurotoxic mode of action) and/or remaining uncertainties (e.g., deviation of some narcotic substances), it has been found that the FET test alone is currently not sufficient to meet the essential information on AFT as required by the REACH regulation (Sobanska *et al.*, 2018).

Although several studies (Vasyukova *et al.*, 2021; Ortiz-Román; Casiano-Muñiz; Román-Velázquez, 2024; Mishra *et al.*, 2021; Chen; Wang; Liang, 2024) have already demonstrated the potential TiO_2 toxic effects on aquatic organisms, particularly in model species such as zebrafish (*Danio rerio*), significant gaps remain regarding the toxicity of titanium dioxide beyond FET tests. These gaps include understanding the influence of concentration on toxic potential, evaluating the role of chorion as a possible protective barrier, and assessing cellular damage that cannot be adequately detected using conventional techniques such as bright-field microscopy.

Slightly, chorion can protect the embryo from the toxicity of some contaminants with a certain range of molecular weight. Introduced endocrine disruptors can be bioaccumulated by aquatic organisms through food chain, consequently causing wildlife poisoning, following by population degradation and eventually harming the entire aquatic ecosystem (Yang *et al.*, 2020). Polystyrene (PS) NPs in the diameter of 100 nm can be effectively blocked by the chorions of zebrafish embryos. The adsorption of fluorescent and non-fluorescent PS NPs (n-PS) and PS MPs (μ-PS) on the outer surface of chorion changed the mechanical properties of chorion and may lead to a hypoxic microenvironment in the embryos (Duan *et al.*, 2020).

The interaction of titanium-based particles with different biological groups and environmental compartments represents a critical aspect for understanding their potential impacts at the ecosystem level. In this study, the toxicity of titanium dioxide is evaluated in *Danio rerio* embryos, with particular attention to the comparison between chorion-intact and dechorionated individuals regarding the extent of induced damage.

6.1.2 Material and methods

Titanium dioxide

The titanium dioxide microparticles (TiO_2MPs) were kindly provided by the Advanced Materials Chemistry Group (GQMat) coordinated by Dr. Pierre Fechine - Department of Analytical Chemistry and Physical Chemistry, Federal University of Ceará – UFC. This microparticle was characterized in a previous study (Barbosa *et al.* 2018). The particle used underwent a sonochemical process for size reduction and has an average size of 104.4 ± 2.29 nm. The rutile form was used in this study with its zeta potential of −17.36 ± 0.11,

its hydrodynamic size value of 297.46 ± 3.66 nm. The dispersion of 50 mg/L was prepared and sonicated for 15 minutes for the exposure test.

Animals maintainance

The breeding fish (*Danio rerio*) for all experiments were from the vivarium of the Biomaterials Laboratory of the Department of Metallurgical and Materials Engineering at UFC, kept under laboratory conditions (Altamar Rack), with the following parameters: conductivity 650 µS, temperature 28 °C ± 0.2 and pH 7.0±0.2. Conductivity was maintained using Red Sea Salt® and pH controlled with acid and alkaline buffers. These parameters are automatically maintained by the rack and monitored 24/7 via software.

For spawning, individuals were moved to aquariums with physical dividers and kept without direct contact (six males to three females). The following day, the physical barrier was removed from the aquarium and the breeders were kept under lighting. After spawning, the embryos were kept in reconstituted water, prepared in accordance with U.S. Environmental Protection Agency (U.S. EPA68). The procedures used in this study will be previously approved by the Ethics Committee on the Use of Animals (CEUA) of the Federal University of Ceará.

Fish Embryo Acute Toxicity (FET) Test

The *Danio rerio* embryos (3h post-fertilization - hpf) were exposed for 96h to the test conditions, in accordance to OECD's guideline number 236 (OECD, 2013). Preliminary tests were carried out to determine the average lethal concentration range (LC50 $mg.mL^{-1}$) for 50% of organisms exposed. The concentrations of the nanomaterial used (TiO_2MPs - 1, 10 and 100 $mg.mL^{-1}$). Sublethal effects were evaluated by exposing embryos (5.3 hpf) for 96 h to control solutions and nanostructured material solutions. Recosntituted water was used as negative control in each plate. 3,4-dichloroaniline (DCA), an aniline pesticide whose toxicity to fish species at early life stages is well known, was used as a positive control (Vieira *et al.*, 2020).

The exposure was carried out in 24-well polystyrene plates (n=24 organisms/group), with the embryos kept individually in 2 mL of test solution, under a light/dark cycle of 14/10 h at 28.0 ± 0.2 ºC in an incubator in an embryo cultivation chamber (Scienlabor-UV). The embryos and larvae were evaluated every 24 hours using a stereomicroscope (Stemi 508 - Zeiss, Zen Lite software), to determine the occurrence of

malformation and/or mortality. The solutions will be completely changed every 24 hours. At the end of the 96h of exposure, live larvae (n=10 organisms/group) were photographed and measured in total length. LC50 values were computed from the percentage of death.

Statistical differences between groups were obtained through analysis of variance (ANOVA) and Ducan's test for paired and unpaired data. The probability of $p < 0.05$ was considered statistical significance.

Dynamic Light Scattering (DLS)

To analyze the agglomeration of the TiO_2, scattering readings were taken in the medium using DLS equipment, Dynamic Light Scattering (Zetasizer Nano S - Malvern) according to (Chicea *et al.*, 2023). The aliquot tested were 1, 10 and 100 mg/L TiO_2 concentrations, diluted and homogenized. The experiment was conducted testing the concentrations with reconstituted water and ultrapure water as control. The purpose of repeating the concentrations in ultrapure water was to verify whether reconstituted water influences the titanium nanoparticles agglomeration.

Once the concentrations had been diluted and homogenized, 1 ml was placed in a quartz cuvette for analysis in the DLS. The readings were spaced out at increasing hourly intervals, with the first hour being continuous readings (120 total readings) and the following being single readings at 1, 2, 4, 8, 24, 28, 32, 48, 72 and 96 hours after the start of the analysis, gradually monitoring the behavior of the particle in the medium during the same time of FET test duration.

Confocal laser scanning microscopy

To assess possible cellular damage caused by TiO_2MPs, acridine orange was used in *Danio rerio* embryos, exposed to 50 mg/L of TiO_2MPs, in addition to the controls, reconstituted water and 3.4 dichloroaniline, an environmental contaminant. Briefly, the embryos were transferred to 24-well polystyrene microplates of 2 mL and then 500 µL of acridine orange at a concentration of 5 µg/mL was added to each well for 20 min at room temperature. After 20 min, *Danio rerio* were euthanized with tricaine by placed in a solution of MS222 dissolved in water (minimum concentration of 250mg/L). Stained samples were observed under Zeiss CLSM 710 with a laser of 488 nm excitation and 532–580 nm emission.

Statistical analysis

Statistical analysis was performed using a database constructed in Microsoft Excel. Normality was assessed using the Shapiro-Wilk test, and homoscedasticity was evaluated via Levene's test. Due to non-normality, non-parametric tests were applied using RStudio. The Kruskal-Wallis test was employed to assess differences among treatment groups, followed by Dunn's post hoc test to identify pairwise differences where significance was detected. Additionally, the Wilcoxon rank sum test was used to examine the influence of chorion presence on embryonic growth within each treatment.

6.1.3 Results and discussion

The *FET* tests results showed TiO_2MPs samples did not affect the hatching rate or survival of zebrafish (*Danio rerio*) embryos that retained their chorion during the exposure period, which began at 5 hours post-fertilization (hpf), 1 mg/L, 10 mg/L, and 100 mg/L. The embryo survival rate was approximately 95% after four days of exposure. In the negative control group (reconstituted water), the survival rate was 100%, whereas in the positive control group, it was 65%. Similar results were observed for embryo survival in the co-exposure to TiO_2 and CeO_2 reported by Pecoraro *et al.* (2023). Although the highest TiO_2MPs concentration used in their study was 20 mg/L, the effects on embryo survival at this concentration were comparable to those observed at 100 mg/L in the present study, indicating that increased TiO_2MPs concentration did not lead to a corresponding increase in adverse effects on survival.

Similarly, TiO_2MPs nanoparticle samples had no impact on hatching rate or survival of zebrafish embryos whose chorion was removed one day post-fertilization, across the same three concentrations (1 mg/L, 10 mg/L, and 100 mg/L). The survival rate after three days of exposure was close to 100% in both the treatment and negative control groups. In contrast, the survival rate in the positive control group was 78%. This result contrasts to results found in research on perfluorooctanesulfonic acid (PFOS) revealed that dechorionated embryos showed increased mortality and developmental issues, highlighting the chorion's protective role against chemical exposure (Mylroie *et al.*, 2021).

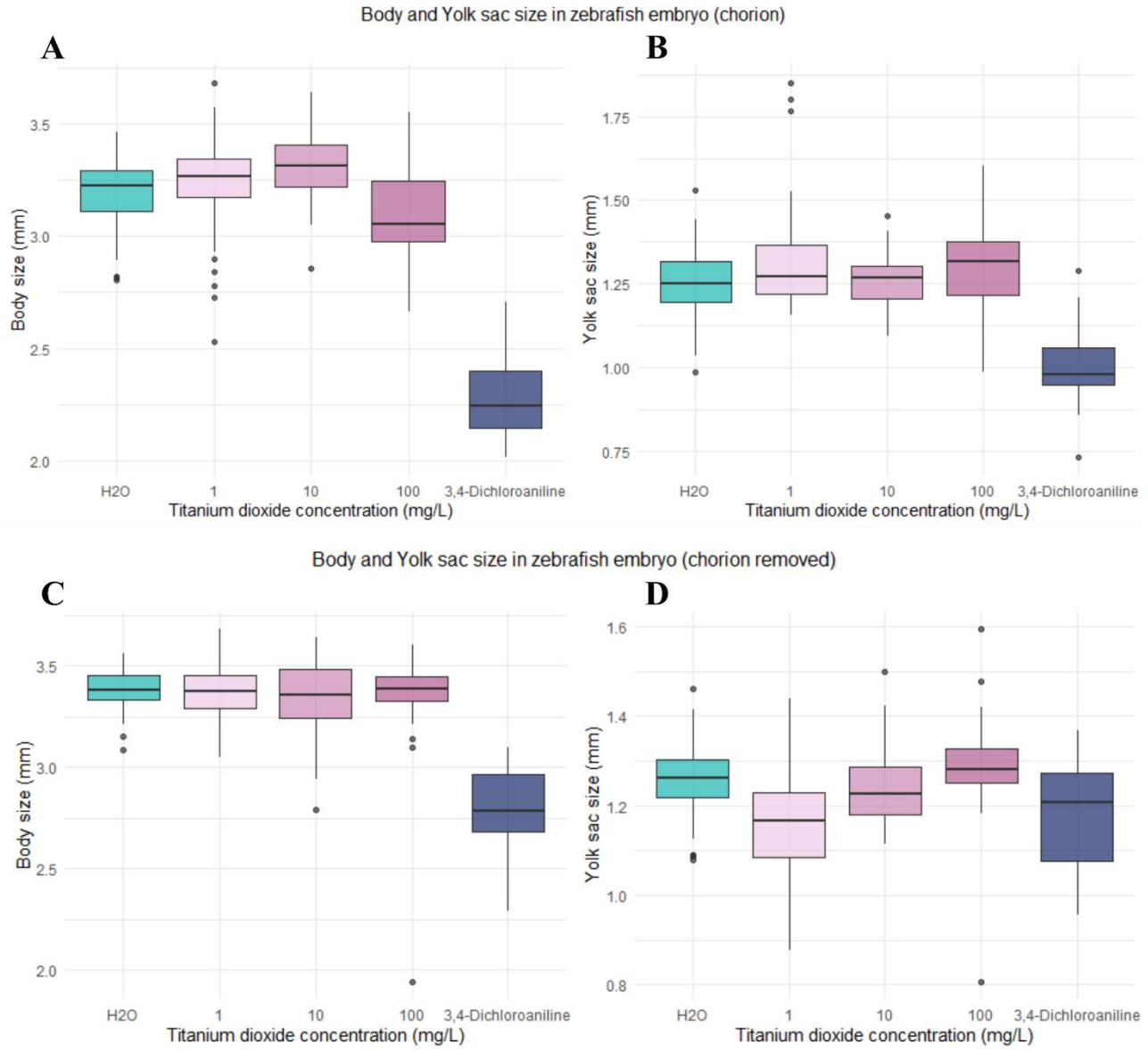

Figure 1. Body size and yolk sac area of zebrafish embryos exposed to different concentrations of TiO_2 under two exposure conditions: with and without chorion.

The body length of the developed embryos with intact chorion (fig. 1A), the 3,4-dichloroaniline treatment (positive control) exhibited statistically significant differences compared to all other groups (1, 10, 100 mg/L TiO_2MPs, and H_2O). The 100 mg/L TiO_2MPs group also differed significantly from both the 1 mg/L and 10 mg/L TiO_2MPs groups, and this difference is attributed to the fact that the 100 mg/L group exhibited the lowest body length values, indicating reduced embryonic growth at this concentration. Meanwhile, the 10 mg/L TiO_2MPs group did not differ significantly from either the 1 mg/L group or the H_2O control (reconstituted water), suggesting a similar growth pattern among these treatments.

In the yolk sac length analysis (fig. 1B), the 3,4-dichloroaniline treatment (positive control) group exhibited statistically significant differences compared to all other groups (1, 10, and 100 mg/L TiO_2, and H_2O; $p < 0.05$). However, no significant differences were observed among the 1, 10, and 100 mg/L TiO_2MPs groups and the control group. Therefore, titanium dioxide exposure did not influence this specific developmental parameter under the tested conditions.

Our results showed that TiO_2MPs (1–100 mg/L) had no significant effect on embryo body size in dechorionated specimens (Fig. 1C) or on yolk sac size in chorion-intact embryos. The lack of a toxic response to the body size parameter may be explained according to Lacave et al. (2016), where insoluble nanoparticles, like SiO_2 NPs, did not show acute effects during early embryo development, largely due to the protective barrier of the chorion. In a study investigating the toxic effects of Bisphenol AF (BPAF), Yang et al. (2020) also demonstrated that dechorionated individuals exhibited increased sensitivity to chemical exposure, with endpoints including delayed hatching and growth, cardiac and yolk sac edema, and underinflation of the swim bladder. Together, these findings reinforce the critical role of the chorion as a modulator of embryonic sensitivity to environmental stressors. However, potential effects on larvae are anticipated, as observations revealed deposition of fluorescent SiO_2 NPs on gill lamellae and excretion through the intestine after hatching. Comparing both results, the insolubility of TiO_2 can be considered a modulator toxicity factor.

The chorion removal condition (fig. 1D) revealed significant variations in yolk sac length. Specifically, the 1 mg/L TiO_2MPs group showed reduced measures and differed significantly from the 10 mg/L, 100 mg/L, and control groups; the 10 mg/L group differed from the 100 mg/L group; and the 100 mg/L group differed from the 3,4-dichloroaniline group. Additionally, H_2O (control group) differed significantly from 3,4-dichloroaniline validating the control groups ($p < 0.05$ for all significant comparisons). This contradicts the expected linear dose-response relationship to TiO_2MPs concentration, in which higher concentrations would typically be associated with more pronounced effects. This non-monotonic behavior may be related to aggregation processes, differences in bioavailability, or distinct toxicity mechanisms at lower doses.

According to Lojk *et al.* (2020), low concentrations of nanoparticles, including TiO_2, do not significantly affect cell viability, cytokine secretion, or NF-κB activation in microglial cells in rats, although they may alter the secretion of cellular stress mediators. Paatero *et al.*, (2017) demonstrated that nanotoxicity profiles are dependent on surface-functionalization controlled penetrance of biological membranes, the embryos were sensitive

to the nanoparticles, especially when the protective chorion membrane was removed, which allowed for better penetration of the particles into the embryos.

The Wilcoxon rank-sum test was employed to compare embryo body size between chorion-present and chorion-removed specimens across treatments (Figure 2). Significant differences were detected in **c**oncentration**s:** 1 mg/L TiO_2 ($p = 1.82 \times 10^{-5}$), 100 mg/L TiO_2MPs ($p = 1.244 \times 10^{-11}$), control group ($p = 3.051 \times 10^{-13}$), and 3,4 dichloroaniline treatment ($p = 3.572 \times 10^{-10}$).

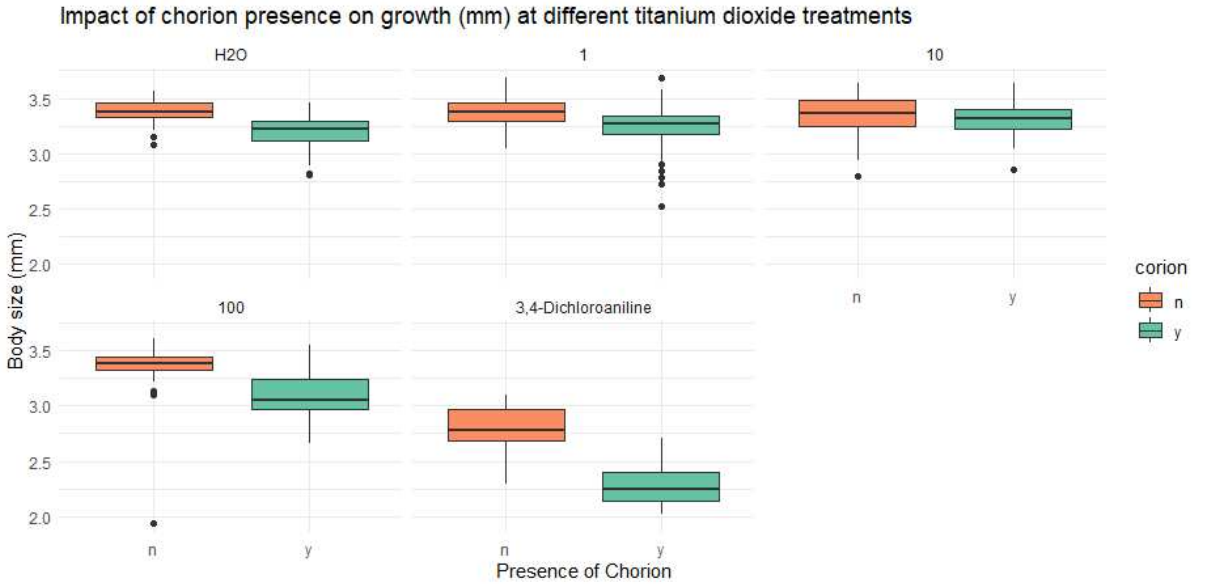

Figure 2. Effect of chorion presence on body size measurements of zebrafish embryos exposed to different concentrations of TiO_2 in an acute toxicity test.

Statistical analysis revealed that the presence or absence of chorion significantly influenced embryo growth in most exposure conditions. Significant differences between the chorion and dechorionated groups were observed at concentrations of 1 mg/L ($p = 1.82\times10^{-5}$), 100 mg/L ($p = 1.244\times10^{-11}$), in the control ($p = 3.051\times10^{-13}$), and in the 3,4 dichloroaniline treatment ($p = 3.572\times10^{-10}$), indicating a strong effect of chorion removal on embryonic development under these conditions. In contrast, at the concentration of 10 mg/L ($p = 0.2337$) the presence of the chorion did not impact notably on embryo growth. Therefore, in addition to treatment concentration, other factors may influence the observed toxic effects. Kim *et al.* (2024) demonstrated that dechorionated zebrafish embryos exhibit greater sensitivity to nanomaterials (NMs) compared to embryos with intact chorions. This heightened sensitivity enhances the accuracy of toxicity assessments, reinforcing the value of dechorionated embryos as a reliable model for evaluating NM toxicity.

Therefore, in higher concentrations particles settled faster. As a metal it is difficult to dissolve, as the days of the experiment progressed, until the chorion was ruptured and the larva had direct contact with the solution, a smaller number of particles would be dissolved in the embryo wells. This may explain that the lowest concentration was the one that remained bioavailable for the longest time for interaction and, therefore, caused more deformation than the others. And, combining this result with the fact that hatching rate and survival did not increase with the concentration continuing similar with 20 mg/L of TiO_2, in (Pecoraro *et al.*, 2023) and the 100 mg/L of TiO_2MPs used in this essay, it supports why the lowest concentration caused more deformation than the highest concentration.

Proper characterization of TiO_2MPs dispersion and aggregation behavior is essential for reliable nanotoxicological assessments. In figure 3, is displayed how each concentration of TiO_2MPs behaves in different dispersants (ultrapure water, control) and reconstituted water (FET medium).

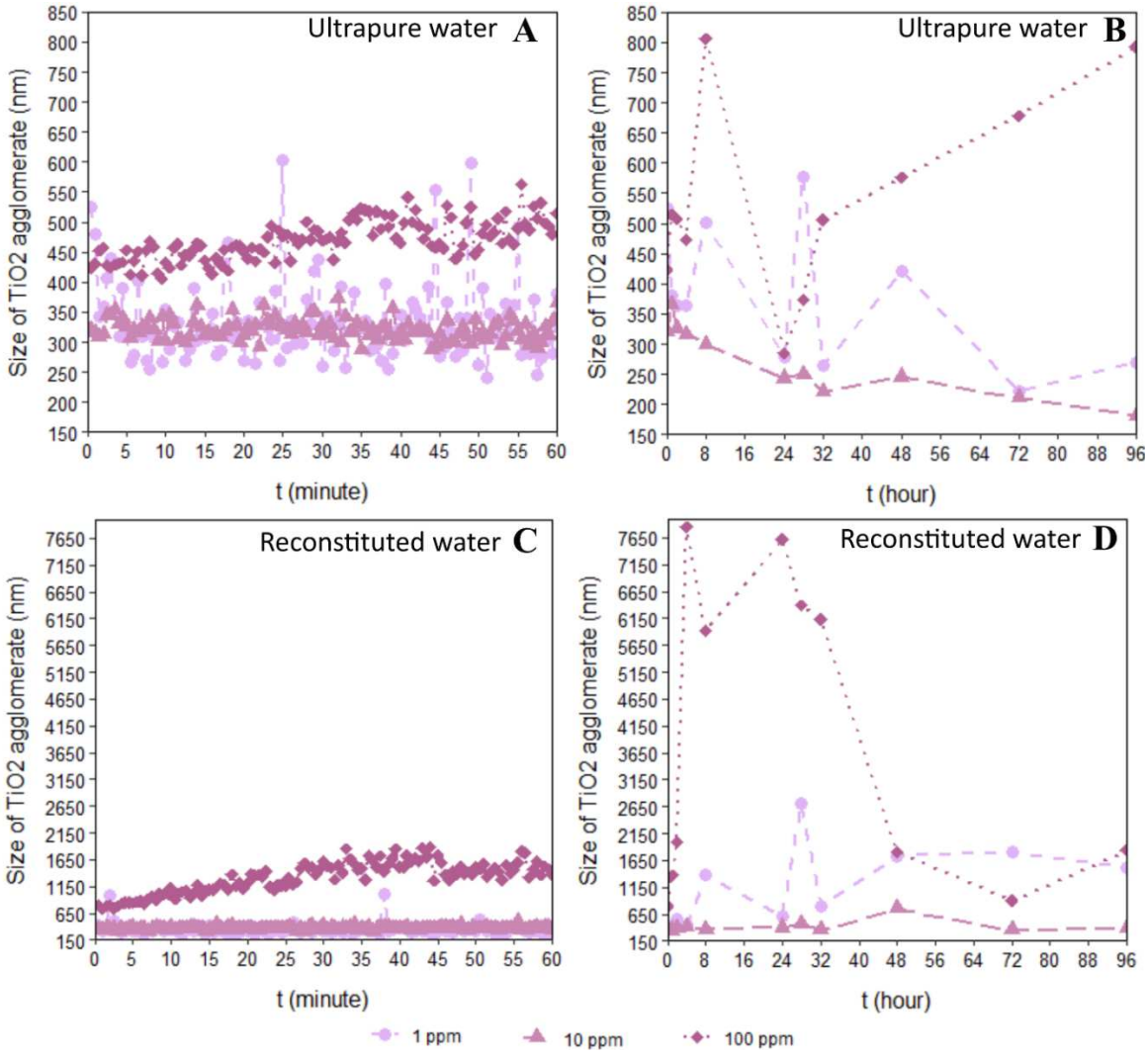

Figure 3. Aggregate sizes of TiO_2 at different concentrations in reconstituted and ultrapure water after 96 hours.

The Dynamic Light Scattering (DLS) results show that the particle behaviors differently depending on the medium. The majority of NM showed tendency to form agglomerates in the different dispersants (Andreani *et al.*, 2020). In the first hour, the size of the agglomerates in reconstituted water (fig. 3A) at higher concentration is more than double the ultrapure water (fig. 3C - DLS control). Additionally, dispersibility does not guarantee the gravitational or colloidal stability of nanoparticles, as exemplified in Sentis *et al.* (2024). Despite the initial appearance of uniform dispersion, the results shown in Figure 3 indicate that particle distribution changes over time.

The DLS measurements went on through the same time duration of FET test, so it could be analyzed titanium dioxide aggregates during the whole experiment. In ultrapure water (fig. 3B), the size of the 1 and 100mg/L of TiO_2MPs agglomerates varied at the first 32 hours. From this time, their size remained increasing until the end of the measurement period. However, the TiO_2MPs behavior in reconstituted water, where the agglomerates sizes decreased by the end of experiment (fig. 3D). However, in fig. 3B, the agglomerate sizes increased through time. The aggregates size grew to 32 hours and then decreased by the end of experiment. Even though the measurements in the graphics show the reduction size of the agglomerates, the values were still bigger than the highest value in the ultrapure water (fig. 3B). Murugadoss *et al.* (2020) demonstrated the increased toxicological responses of TiO_2 nanoparticles have been associated with their agglomeration behavior and bigger aggregates do not appear less biologically active than the smaller ones. Also, it was revealed that the size and stability of agglomerates play a crucial role in how these materials interact with cells (Murugadoss *et al.*, 2021).

At the intermediary concentration of TiO_2MPs (10mg/L) the behavior was different. It was the concentration that had the minor variation between the tested ones. The size of the aggregates had the slightest variation of the experiment. Also, comparing the ultrapure water (fig. 3A and 3B) with the reconstituted water (fig. 3C and 3D), for this concentration, presented the highest dimensions.

The connection between dispersibility, stability and concentration of the particles is a key factor in assessing their toxicity (Sentis *et al.*, 2024). The particle characterization in ecotoxicological studies is crucial and understanding particle dynamics in suspension improves accuracy in estimating actual exposure levels and toxic effects in model organisms.

Structural defects such as yolk deformations, pericardial edemas, kinked notochords, arched tails, and vasculature shattering were analyzed in (Valério *et al.*, 2020) with higher concentrations of TiO_2 nanoparticles correlating to increased occurrences of these defects. These parameters were also included in the current research in figure 4 below.

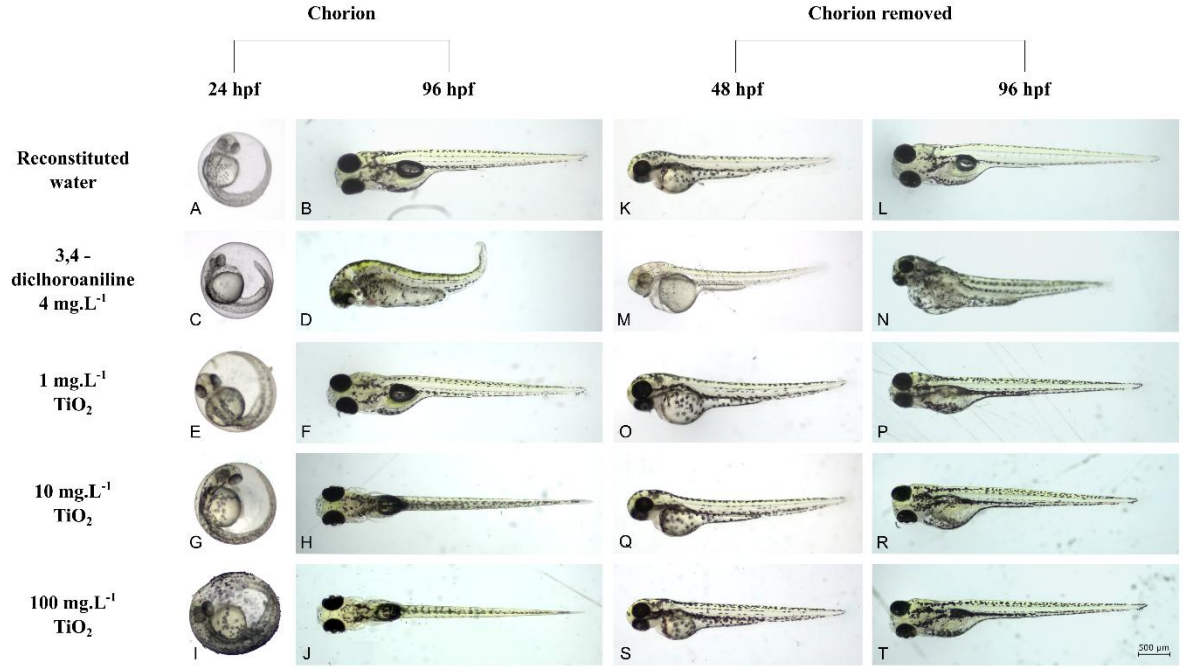

Figure 4. *Danio rerio* embryos at 24 and 96 hours post-fertilization (hpf) from the Fish Embryo Toxicity (FET) test, exposed to different concentrations of TiO_2 and to positive and negative controls, under two exposure conditions: with and without chorion. A and B show the negative control (reconstituted water), with healthy embryos and no morphological alterations. C and D represent the positive control (3.4-dichloroaniline, 4 $mg \cdot L^{-1}$), showing cardiac and yolk sac edema, as well as impaired growth. E and F (1 $mg \cdot L^{-1}$ TiO_2), G and H (10 $mg \cdot L^{-1}$ TiO_2), and I and J (100 $mg \cdot L^{-1}$ TiO_2) show embryos with chorion and no visible morphological alterations, although particle accumulation around the chorion is observed in panel I. K and L depict the negative control without chorion, with healthy embryos and no morphological changes. M and N correspond to the positive control without chorion, showing cardiac and yolk sac edema, impaired growth, and altered pigmentation. O and P (1 $mg \cdot L^{-1}$ TiO_2), Q and R (10 $mg \cdot L^{-1}$ TiO_2), and S and T (100 $mg \cdot L^{-1}$ TiO_2) show embryos without chorion, with no observed morphological alterations. Scale bar: 500 µm.

During the 24-hour assessment at the beginning of the test, embryos with intact chorion had not yet hatched the non-treated group showed no adverse effects (fig. 4A and 4C). The treated groups (fig. 4E, 4G and 4I), also did not show developmental changes in comparison to (fig. 4A and 4C). However, it is possible to notice in the evaluation of the first 24 hours that as the concentration of titanium dioxide increased in the treatments, more particles became adhered to the embryo's chorion (4E, 4G, 4I), which works as a mechanical protection barrier. In a study carried out by (Chokkattu *et al.*, 2022), in addition to acute exposure to titanium in concentrations of 1 µL to 16 µL in a dental gel formulation not offering toxicity, the chorion

was also identified as a protective barrier against TiO_2NPs. This finding supports the present result.

However, silver nanoparticles (AgNPs) induced significant developmental abnormalities, such as yolk sac edema and spinal cord flexures, even in the presence of the chorion. This comparison suggests that while the chorion may offer some protection, the intrinsic toxicity of the nanoparticle material itself is a more dominant factor in determining developmental outcomes (Johnson, 2019).

By the end of the test, in the 96h, the morphology of fry remained preserved in relation to the controls, especially when compared with the 4D image of the positive control, where the animal presents significant cardiac and vitelline edema, in addition to not having reached the expected body length for that stage of development. However, in a toxicological study of metal and metal oxide nanoparticles in zebrafish, TiO_2 were evaluated among other nanoparticles. And the two highlighted points is the fact that the most of studies analyzed were made with adults, and, besides body size, malformations and hatching were not affected, there were swimming and DNA damage (Bai and Tang, 2020).

Although the highest deformation rate (30%) occurred with 3,4-dichloroaniline exposure, a notable 10% was also observed in embryos treated with the lowest concentration of TiO_2MPs (1 mg/L), highlighting the potential developmental impact of the nanoparticle. A study using captopril's influence on *D. rerio* embryonic development induced malformations in embryos at all tested concentrations, ranging from 0.2 to 2000 μg/L. This indicates that even low concentrations, which are considered environmentally relevant, can lead to adverse developmental outcomes in zebrafish embryos (García-Valdespino *et al.*, 2024)**.**

Particle size is a key factor influencing nanomaterial toxicity. In the present study, TiO_2MPs had an average diameter of 104 nm. In contrast, Hu *et al.* (2019) used 5 nm TiO_2 particles complexed with Pb^{2+}, demonstrating their ability to permeate the chorion and induce toxicity. These findings highlight that bioavailability—along with concentration and solubility in the surrounding medium— is critical in ecotoxicological interactions. Although the larger particle size used in this study likely hindered TiO_2 from crossing the chorion, developmental deformations were still observed at the lowest concentration, suggesting that even limited bioavailability may be sufficient to elicit toxic effects. Likewise, Hansjosten *et al.* (2022) reported that titania and ceria nanoparticles (5–50 nm), despite their smaller primary sizes, were fully agglomerated, which likely reduced their bioavailability due to sedimentation and limited diffusion to the chorion. These results support the hypothesis that the chorion acts as a physical barrier against poorly soluble nanomaterials, offering protection to embryos until hatching.

In the analysis of chorion removed condition (figure 4K – 4T), the morphological results demonstrated that TiO_2MPs did not exhibit toxicity to *Danio rerio* under the parameters evaluated. Survival rate and malformation incidence, of zebrafish embryos and larvae were very similar between the reconstituted water and the three tested TiO_2 concentrations in both experimental conditions. In contrast, the figure 3M and 3N, the 3.4 dichloroaniline caused heart edema, color pattern change and body deformation which was not found in any of TiO_2 treatments (4O - 4T). The study using 50-nm fluorescein 5 (6)-isothiocyanate-incorporated silica nanoparticles (FITC-SiO_2 NPs) indicates that dechorionated embryos are more susceptible to the toxic effects of NMs, because of the lower lethal concentration (LC50) values (Kim *et al.*, 2024). The lack of toxicity of TiO_2 nanoparticles at lower concentrations underscores the importance of comprehensive toxicity assessments for different nanoparticle types to understand their potential ecological impacts and guide risk assessment strategies in aquatic environments (Aruoja *et al.*, 2015).

Although the deformation observed was slight, a study conducted by Wang *et al.* (2022) demonstrated that co-exposure to titanium dioxide nanoparticles ($nTiO_2$) and decabromodiphenyl ethane (DBDPE) significantly increased the uptake of DBDPE by zebrafish embryos, altering the metabolite profile compared to exposure to DBDPE alone.

comparing the findings of the present study with those reported by Zavitri *et al.* (2023), who investigated the toxicity of zinc oxide nanoparticles (ZnO NPs) synthesized using papaya extract in zebrafish embryos, distinct differences in toxicological responses are evident. In the first study, ZnO NPs caused high embryonic mortality, with complete lethality observed at 100 mg/L (aqueous extract) and 20 mg/L (methanolic extract). In contrast, exposure to TiO_2MPs nanoparticles in the present study did not significantly affect hatching or embryonic survival, even at higher concentrations. These differences highlight that although TiO_2 and ZnO are commonly co-formulated in products such as sunscreens, their mechanisms of toxicity and impacts on early developmental stages in aquatic organisms are not equivalent and may vary depending on synthesis methods, concentration, and particle properties.

Other studies like (Arabeyyat *et al.*, 2020; Scalisi *et al.*, 2023) were carried out using titanium dioxide and the particle did not affect the embryonic development. Even though the embryo's viability were not compromised, in (Arabeyyat *et al.*, 2020) titanium nanoparticles in the 5–25 nm size range and higher concentrations (of 500 and 1000 mg/L) impacted SOD_2 mRNA expression, indicating oxidative stress response on the embryo chorion surface. In addition, the study of (Scalisi *et al.*, 2023) pointed that TiO_2 alterations in the male reproductive system, acting as potential endocrine disruptors. Additionaly, TiO_2 NPs induced marked

sublethal effects, including reduced larval body length and weight, impaired swimming behavior, and neurodevelopmental alterations such as decreased axonal growth of motor neurons and disrupted central nervous system neurogenesis in transgenic zebrafish lines TG (HuC-GFP) and TG (HB9-GFP) (Zhou *et al.*, 2022).

A study by Aruoja *et al.* (2015) suggests that TiO_2 nanoparticles in the 100 nm size range may not pose significant risks to aquatic organisms at environmentally relevant concentrations, especially when compared to the higher toxicity observed for nanoparticles such as CuO and ZnO. on the other hand, the findings of the present study indicate that TiO_2 may still pose developmental risks, as even at low concentrations, subtle but notable effects were observed in zebrafish embryos.

TiO_2MPs can alter the behavior and toxicity of coexisting organic pollutants in aquatic environments. Bis(2-ethylhexyl)-2,3,4,5-tetrabromophthalate (TBPH), a flame retardant often found alongside TiO_2 NPs, has unclear combined effects with these particles. In zebrafish embryos, co-exposure to TBPH and TiO_2 NPs led to the formation of larger agglomerates, reducing the internal concentrations of both compounds. This interaction mitigated lipid metabolism disorders caused by TBPH alone, suggesting that agglomeration decreases bioavailability and consequently reduces toxicity during early development (Zhou *et al.*, 2022).

These findings underscore the importance of employing complementary imaging techniques, as bright-field microscopy alone may be insufficient to detect all potential toxicological effects. A recent review further emphasizes the diverse impacts of nanomaterials on zebrafish at multiple biological levels, showing that exposure can lead to developmental abnormalities, altered gene expression, and various forms of toxicity (Mutalik *et al.*, 2024).

Advanced methods such as laser scanning confocal microscopy allow for higher-resolution, three-dimensional analysis of morphological and subcellular alterations, providing a more comprehensive assessment of nanoparticle-induced toxicity. This observation is consistent with the study by Tang, Zhang, and Zhu (2019), in which zebrafish embryos exposed to 100 mg/L TiO_2 nanoparticles showed no visible deformities or alterations in hatching rate, suggesting limited observable toxicity under those conditions.

In the confocal microscopy images of zebrafish embryos, both with and without chorion, exposed to TiO_2 nanoparticles (NPs-TiO_2), a difference in green fluorescence emission intensity was observed between individuals stained with acridine orange and those that were not. Zebrafish embryos exhibit inherent autofluorescence and therefore display fluorescence when excited by the microscope laser, even in the absence of acridine orange staining.

Considering that acridine orange is a marker for cell damage, the regions where it binds appear as numerous, distinct, and brightly fluorescent puncta. In the present study, such fluorescence was observed in embryos exposed to TiO_2, indicating apoptosis. Acridine orange is widely used to detect apoptotic cells, as it binds to DNA and emits green fluorescence when excited at wavelengths between 488 and 535 nm (Damas-Souza *et al.*, 2019). This dye permeates all living cells, but its uptake increases when the cytoplasmic membrane is compromised.

Similarly, acridine orange staining was used to demonstrate increased apoptotic cell death in zebrafish larvae exposed to genipin, a compound derived from *Gardenia jasminoides*, commonly used in traditional Chinese medicine. The observed toxicity was dose-dependent and associated with oxidative stress and apoptosis (Xia *et al.* 2021). These parallels reinforce the reliability of acridine orange staining as a sensitive indicator of cell death in developmental toxicity assessments.

This pattern of green bright spots presence was observed (white arrows) in embryos stained at both 24 hpf and 96 hpf, with stronger fluorescence in individuals exposed to different concentrations of NPs-TiO_2 and in the positive control compared to the negative control (Figs. 5 and 6). It was also shown in zebrafish embryos after the exposure to *O*-ethyl-*O*-(4-nitrophenyl) phenylphosphonothioate (EPN) at the concentration of 500 µg/L were examined at 48, 72, and 96 hpf (Choe *et al.*, 2021).

In figure 5, chorion functioned as a barrier to titanium dioxide toxicity because the evidence of cell death appeared just in bigger concentration (5I) and not in 5E and 5G. This result is confirmed by the fact that cell death is present in all the three treatments (5O, 5Q and 5S) in dechorionated individuals. All the samples have their own control showing the embryo's autofluorescence (5B, 5D, 5F, 5H, 5J, 5L, 5N, 5P, 5R, 5T) to prove that the damage is caused by titanium dioxide. In research of chorion function as a barrier to micro and nano plastics and its impact on zebrafish embryos, although micro and nano plastic particles can be efficiently blocked by embryonic chorions, they can still affect the early development of aquatic organisms (Duan *et al.* 2020).

Similarly, in the case of Ag engineered nanomaterials, total silver accumulation was significantly higher in chorionated embryos compared to dechorionated ones indicating that 99.8% of the silver was associated with the chorion, rather than internalized by the embryo ($F_{2,30} = 2.59$, $P = 0.095$). Nevertheless, a small amount of silver (0.2% of the total) was detected inside dechorionated embryos, confirming that internal exposure still occurred (Pereira *et al.*, 2023).

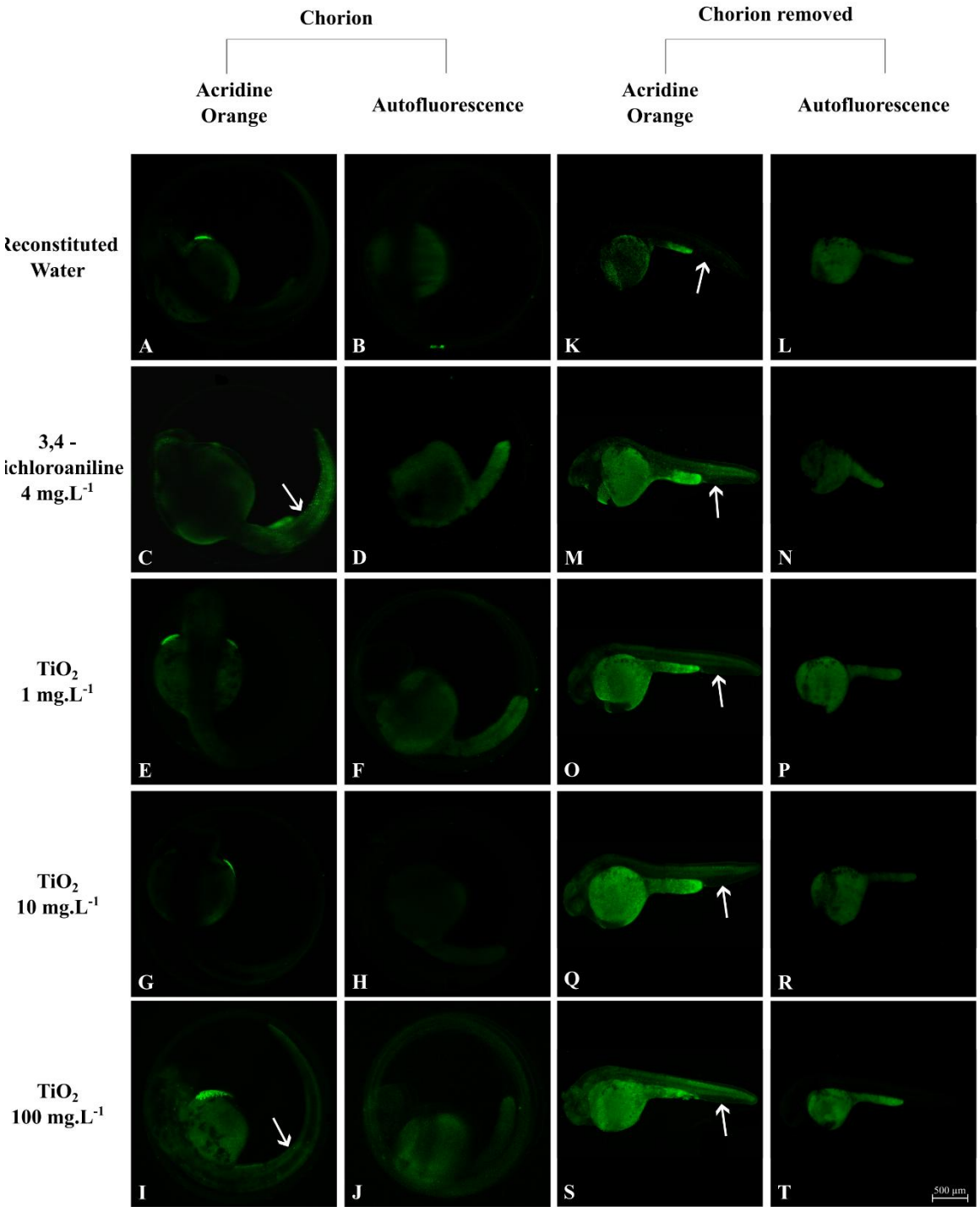

Figure 5. Confocal images of *Danio rerio* embryos at 24 hours post-fertilization (hpf) exposed to different concentrations of TiO_2, under two exposure conditions (with and without chorion), with and without acridine orange staining, including positive and negative controls. A and B show the negative control (reconstituted water), with healthy embryos with chorion and no morphological alterations. C and D correspond to the positive control (3.4-dichloroaniline, 4 mg·L^{-1}), showing apoptotic cells at the posterior region of the yolk sac in embryos with chorion. E and F (1 mg·L^{-1} TiO_2), G and H (10 mg·L^{-1} TiO_2), and I and J (100 mg·L^{-1} TiO_2) show embryos with chorion and no detectable morphological changes. K and L represent negative control without chorion, with healthy embryos and no morphological alterations. M and N correspond to the positive control without chorion, showing cell death at the end of the yolk sac, especially visible in panel M. O and P (1 mg·L^{-1} TiO_2), Q and R (10 mg·L^{-1} TiO_2), and S and T (100 mg·L^{-1} TiO_2) show embryos without chorion, presenting signs of cell death at the posterior region of the yolk sac in panels O, Q, and S, respectively. Scale bar: 500um.

At 96 hpf (Figure 6), all embryos exposed to any concentration of TiO_2MPs showed signs of cell death, as indicated by acridine orange staining. The most intense fluorescent signals were observed in the yolk sac region (white arrows). Similarly, Qian *et al.* (2018) investigated the developmental toxicity mechanisms of boscalid, a pesticide, in zebrafish embryos, and found that sublethal doses induced apoptosis, disrupted lipid metabolism, and altered melanin synthesis and deposition. The apoptotic patterns observed in the confocal images of the present study resemble those reported by Qian *et al.* (2018), with cell death also prominently detected in the yolk sac region.

Among embryos with intact chorion, the highest level of damage was detected at the 10 mg/L (6G) concentration. In dechorionated embryos, apoptotic cells increased progressively (6F and 6H), having a greater effect at 100 mg/L (6J). Each treatment group was accompanied by its respective control, displaying only the natural autofluorescence of the embryos (6B, 6D, 6F, 6H and 6J) thereby confirming that the observed damage was induced by titanium dioxide exposure. In viable cells, fluorescence is faint, whereas early apoptotic cells exhibit a brightly fluorescent green nucleus, indicating chromatin condensation and nuclear fragmentation (Ribble *et al.*, 2005).

Dimethachlor pesticide exposure has been associated with increased apoptosis and oxidative stress in zebrafish embryos (An *et al.*, 2021). In regard of nanomaterials, AgNPs and ZnO NPs introduced into natural water induced significant cellular damage in zebrafish embryos at higher concentrations, including increased production of reactive oxygen species (ROS), activation of autophagy pathways, and apoptosis, which collectively contributed to elevated mortality and delayed hatching (Lee *et al.*, 2022).

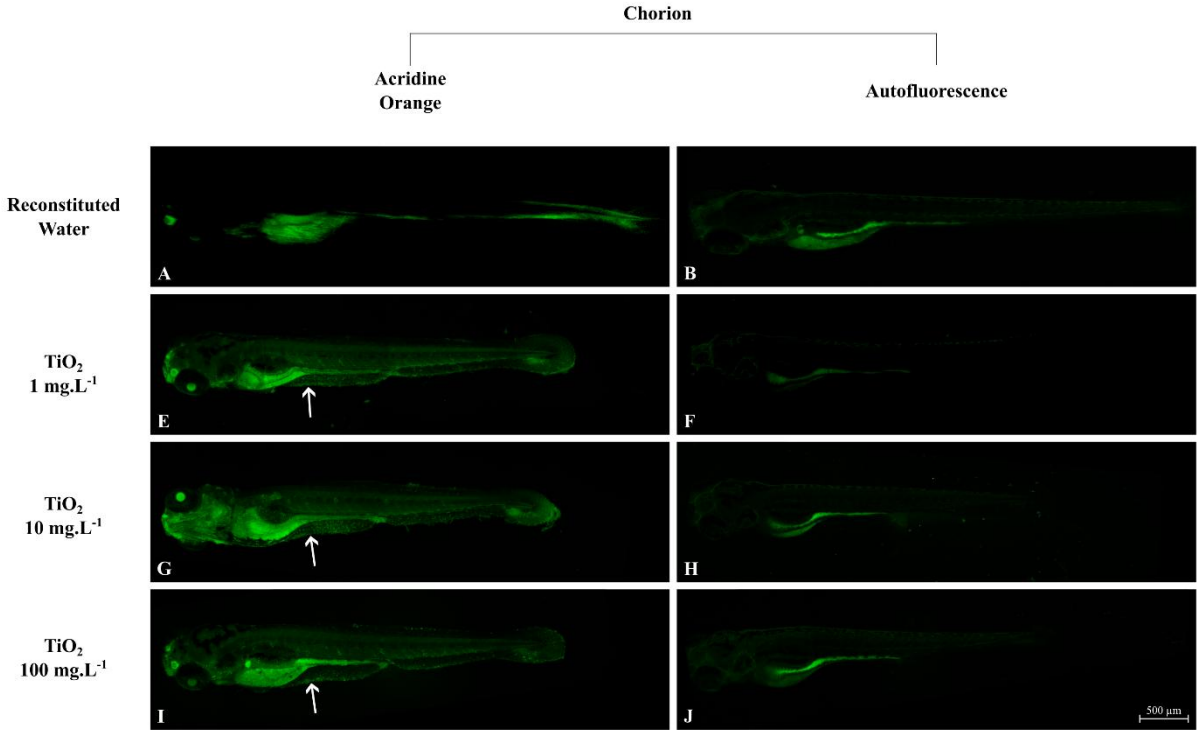

Figure 6. Confocal images of *Danio rerio* embryos at 96 hours post-fertilization (hpf) with chorion, exposed to different concentrations of TiO_2, with and without acridine orange staining, including positive and negative controls. A and B correspond to the negative control (reconstituted water), showing healthy embryos with no morphological alterations. Panels C and D represent the positive control (3.4-dichloroaniline, 4 $mg \cdot L^{-1}$), revealing embryo death prior to hatching. Panels E and F (1 $mg \cdot L^{-1}$ TiO_2), G and H (10 $mg \cdot L^{-1}$ TiO_2), and I and J (100 $mg \cdot L^{-1}$ TiO_2) show signs of cell death at the posterior region of the yolk sac, as indicated by the white arrows. Scale bar: 500 um.

The dechorionated individuals in figure 7 also showed evidence of cell death in yolk sac region. The green bright spots are increasing as well as treatments concentration (Fig. 7O, 7Q, 7S) and they are detailed in figure 8 below indicating with more clarity this damage suffered by the embryos. In 24 hpf images, the 8B and 8D look very similar, revealing the damaged induced by 100 mg/L treatment is closer to the 3,4-dichloroaniline one, but it's also stronger than the figure 8E where the individual had not been dechorionated. This fact expresses that chorion influences the toxicity range of the particle, because in the same concentration, the effects differ in chorion presence or absence. Pereira *et al.* (2023) demonstrated that $CuSO_4$ readily penetrates the chorion, resulting in similar copper accumulation in both chorionated and dechorionated zebrafish embryos. In contrast, CuO nanoparticles exhibited markedly different behavior, with 94.2% of the copper retained on the chorion and only 5.8% detected within the embryo, indicating limited internalization. Nonetheless, the presence of copper in dechorionated embryos confirms effective exposure ($F_{2,\ 33} = 83.37$, $p < 0.001$).

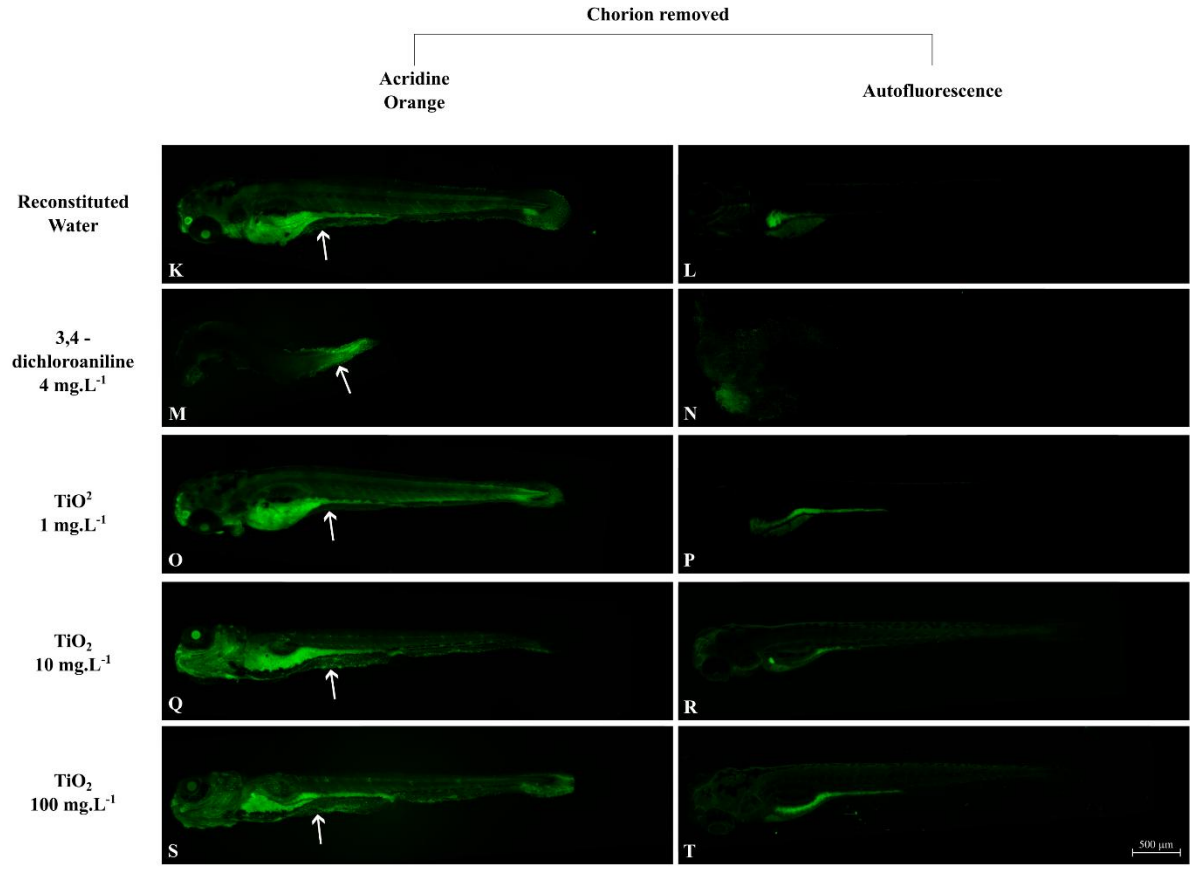

Figure 7. Confocal images of 96 hpf dechorionated zebrafish (*Danio rerio*) embryos exposed to different concentrations of TiO_2 nanoparticles, with and without acridine orange staining. Negative and positive controls are included. A and B show healthy embryos in the negative control group (reconstituted water), with no morphological alterations. C and D represent the positive control (3.4-dichloroaniline at 4 $mg \cdot L^{-1}$), revealing embryo death after hatching. E and F correspond to embryos treated with 1 $mg \cdot L^{-1}$ of TiO_2, showing cell death at the end of the yolk sac (white arrow). G and H depict embryos exposed to 10 $mg \cdot L^{-1}$ of TiO_2, also showing cell death in the yolk sac region (white arrow). I and J illustrate embryos treated with 100 $mg \cdot L^{-1}$ of TiO_2, with visible cell death in the same region (white arrow). Scale bar: 500 um.

In 96hpf exposure, the 3,4-dichloroaniline (8G) was more pronounced compared to the others. When the concentration pairs are compared between 24 and 96hpf (8A and 8E, 8B and 8G, 8C and 8H, 8D and 8I, 8E and 8J) the time difference proves crucial to how aggressive TiO_2 toxic effects will be in the zebrafish embryos. Moreover, the difference in toxicity is due to some factors. Firstly, to exposure time to the contaminant as tested in Ortiz-Román *et al.* (2024) which tested The toxicity of TiO_2 P25 nanoparticles in different concentrations (75, 100, 150, 200, and 250 mg/L TiO_2 P25 NPs) but also, in different exposure times showing stronger effects at 96 hpf than at 48 hpf specifically between the 250 mg/L group and all other groups. Then, the concentration of the treatments according to Jafari *et al.* (2022) where synthesized TiO_2 NPs at high concentrations had relatively high toxicity to zebra fish. Also, due to presence

or absence of the chorion corroborating Chen *et al.* (2025) which demonstrated that the integrity of the chorion significantly influences the bioaccumulation and toxicity of selenium nanoparticles in *Oryzias latipes*, affecting embryonic susceptibility to nanoparticle exposure.

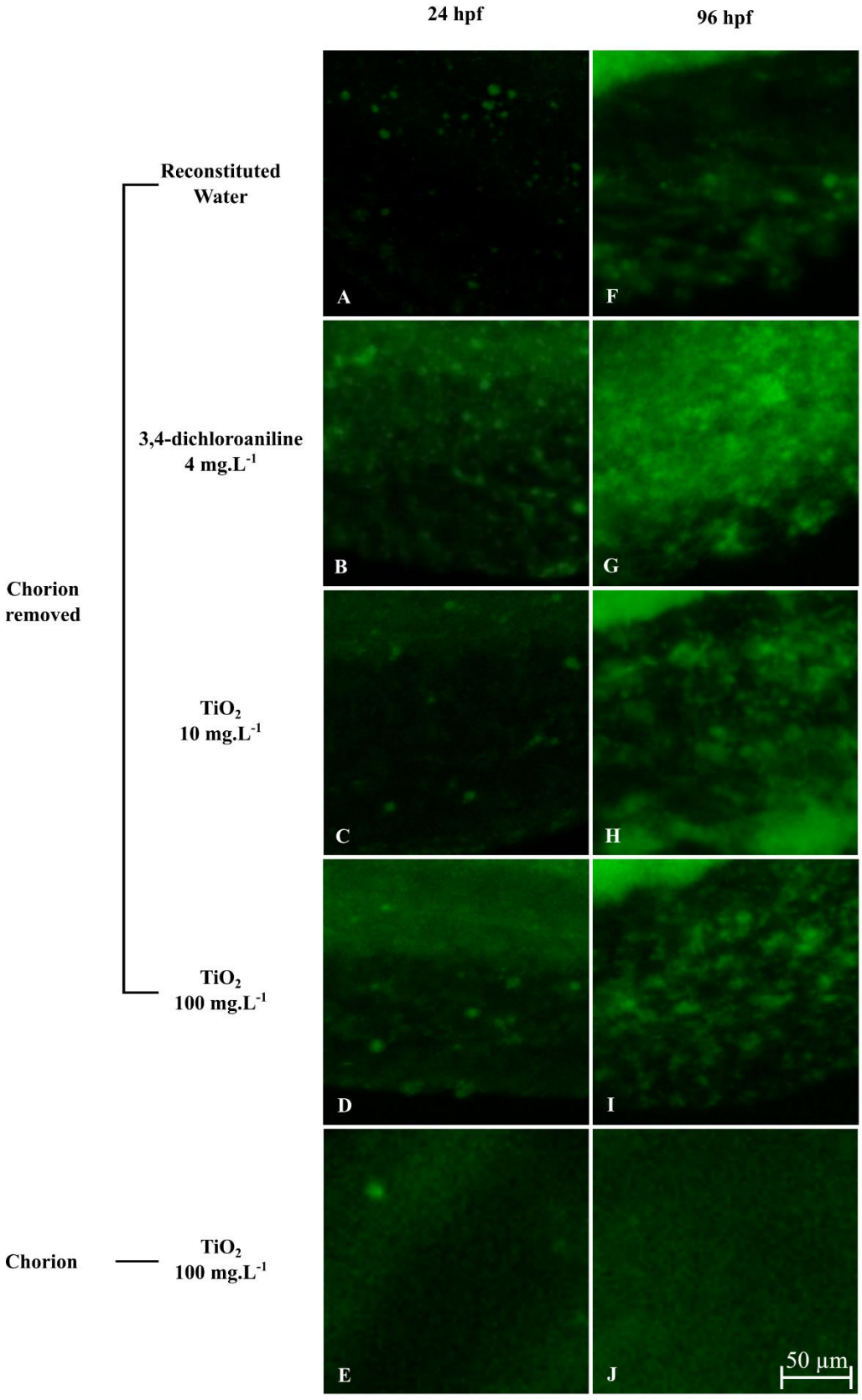

Figure 8. Confocal fluorescence images of *Danio rerio* embryos at 24- and 96-hours post-fertilization (hpf), stained with acridine orange, illustrating representative cases of cell damage under exposure to different concentrations of TiO_2, with and without chorion. A–E correspond to embryos at 24 hpf. A shows the negative control (reconstituted water), with no signs of apoptotic cells. B represents the positive control (3.4-dichloroaniline, 4 $mg \cdot L^{-1}$), revealing intense green fluorescence indicative of cell death. C shows an embryo exposed to 10 $mg \cdot L^{-1}$ of TiO_2, with evidence of apoptotic activity. D and E depict embryos treated with 100 $mg \cdot L^{-1}$ of TiO_2, both showing signs of cell death. F–J correspond to embryos at 96 hpf. Panel F shows negative control without chorion, with signs of apoptotic cells. G, the positive control (3.4-dichloroaniline, 4 $mg \cdot L^{-1}$), reveals prominent green, fluorescent spots associated with cell death. H shows an embryo exposed to 1 $mg \cdot L^{-1}$ of TiO_2, and I to 10 $mg \cdot L^{-1}$, both exhibiting apoptotic cells at the posterior region of the yolk sac. J presents an embryo treated with 100 $mg \cdot L^{-1}$ of TiO_2, also showing localized cell death in the same region.

Besides the concerns of sub-lethal effects of titanium dioxide, other analysis has to be done to guarantee its environmental safety. Additionaly, transgenerational affects should be counted once the particle did not affect the survival or hatching rate, but cause cronical damage, it could be carried out to next generations. As exemple, in tests performed by (Wu *et al.*, 2018) focused on the transgenerational effects of titanium dioxide nanoparticles (n-TiO_2) and microcystin-LR (MCLR), that causes developmental neurotoxicity in zebrafish, on the development of F1 zebrafish offspring, highlighted that parental exposure to titanium dioxide nanoparticles (n-TiO_2) can lead to the transfer of n-TiO_2 to F1 embryos, increasing the accumulation of microcystin-LR (MCLR) in the offspring.

6.1.4 Conclusion

The results of this study demonstrate that TiO_2MPs (1–100 mg/L) did not significantly affect hatching or survival rates of *Danio rerio* embryos, regardless of the presence or absence of the chorion. However, sub-lethal effects were observed, particularly in embryonic growth and cell death responses. In chorion-intact embryos, reduced body length was detected at the highest concentration (100 mg/L), while yolk sac size remained unaffected. Conversely, dechorionated embryos exhibited more pronounced morphological changes and increased apoptosis, especially at higher concentrations, highlighting the protective role of the chorion. Acridine orange staining confirmed cell death at 96 hpf, with stronger fluorescent signals in dechorionated individuals, particularly in the yolk sac region. These findings emphasize that TiO_2MPs toxicity is modulated by factors such as bioavailability, chorion presence, concentration, and exposure duration. While acute toxicity was not evident, the observed

cellular and developmental alterations reinforce the need for further investigation into the long-term environmental safety of TiO_2 nanoparticles.

ACKNOWLEDGMENTS

ECM would like to thank CNPq grant number 312014/2025-2 - Bolsas de Produtividade em Pesquisa - PQ and grant number 313115/2023-0 Chamada CNPq/MCTI Nº 10/2023 - Universal 2023.

ECM acknowledges funding from Universal and Analytical Center-UFC/CT-INFRA-FINEP/Pro-Equipamentos-CAPES/CNPq-SisNano-MCTI 2019 (Grant 442577/ 2019-2). Capes, INCT and FUNCAP. This study was financed in part by the Coordenação de Aperfeiçoamento de Pessoal de Nível Superior - Brasil (CAPES) - Finance Code 001. This work is part of the PhD research of AKML. CNPEM and LIST and GQMat.

AUTHOR CONTRIBUTION

All authors contributed to the study conception and design**.** Developed research (ECM and AKML). Write the manuscript (AKML). Review of the manuscript (ECM). Performed the experiments (AKML; LGVO; JHAV). DLS analysis (RLBSA; ARM; AKML). All authors read and approved of the final manuscript.

CONFLICTS OF INTEREST

The authors declare no conflict of interest.

REFERENCES

ABDEL-LATIF, H. M. R. *et al.* Environmental transformation of n-TiO_2 in the aquatic systems and their ecotoxicity in bivalve mollusks: a systematic review. **Ecotoxicology and Environmental Safety**, v. 200, p. 110776, 2020.

ANDREANI, T. *et al.* The critical role of dispersant agents in nanomaterial ecotoxicity. **Environmental Science and Pollution Research**, v. 27, p. 19845–19857, 2020.

AN, G. *et al.* Developmental toxicity of dimethachlor during zebrafish embryogenesis. **Journal of Animal Reproduction and Biotechnology**, v. 36, n. 1, p. 2–8, 2021.

ARABEYYAT, Z. H. *et al.* Toxicity of polyelectrolyte-functionalized titania nanoparticles in zebrafish (*Danio rerio*) embryos. **SN Applied Sciences**, v. 2, n. 7, 2020.

ARUOJA, V. *et al.* Toxicity of 12 metal-based nanoparticles to algae, bacteria and protozoa. **Environmental Science: Nano**, v. 2, n. 6, p. 630–644, 2015.

ASZTEMBORSKA, M. *et al.* Titanium dioxide nanoparticle circulation in aquatic ecosystems. **Water, Air and Soil Pollution**, v. 229, n. 6, p. 208, 2018.

BAI, C.; TANG, M. Toxicological study of metal nanoparticles in zebrafish. **Journal of Applied Toxicology**, v. 40, n. 1, p. 37–63, 2020.

BARBOSA, J. S. *et al.* Ultrafast sonochemistry-based approach to coat TiO_2 commercial particles for sunscreen formulation. **Ultrasonics Sonochemistry**, v. 48, p. 340–348, 2018.

CEGER, P. *et al.* Current ecotoxicity testing needs among selected US federal agencies. **Regulatory Toxicology and Pharmacology**, v. 133, p. 105195, 2022.

CHEN, H. *et al.* Combined neurotoxicity of DBP and nano-TiO_2 in zebrafish. **Aquatic Toxicology**, v. 269, p. 106881, 2024.

CHEN, H.; WANG, Y.; LIANG, H. The combined neurotoxicity of DBP and nano-TiO_2 in embryonic zebrafish (*Danio rerio*). **Aquatic Toxicology**, v. 269, p. 106881, 2024.

CHEN, H. *et al.* The role of chorion integrity on the bioaccumulation and toxicity of selenium nanoparticles in Japanese medaka (*Oryzias latipes*). **Aquatic Toxicology**, v. 278, p. 107170, 2025.

CHICEA, D. *et al.* Comparative synthesis of silver nanoparticles: evaluation by AFM and DLS. **Materials**, v. 16, n. 15, p. 5244, 2023.

CHOE, H. *et al.* Acute toxicity of the insecticide EPN upon zebrafish (*Danio rerio*) embryos. **Ecotoxicology and Environmental Safety**, v. 222, p. 112544, 2021.

CHOKKATTU, J. J. *et al.* Embryonic toxicology evaluation of ginger- and clove-mediated titanium oxide nanoparticles-based dental varnish with zebrafish. **Journal of Contemporary Dental Practice**, v. 23, n. 11, p. 1157–1162, 2022.

DAMAS-SOUZA, D. M. *et al.* Improved acridine orange staining of DNA/RNA. **Acta Histochemica**, v. 121, p. 450–457, 2019.

DUAN, Z. *et al.* Barrier function of zebrafish embryonic chorions against microplastics. **Journal of Hazardous Materials**, v. 395, p. 122621, 2020.

FIROOZI, A. A. *et al.* Influence of potential nanomaterials for civil engineering projects: a review. **Iranian Journal of Science and Technology, Transactions of Civil Engineering**, v. 45, p. 2057–2068, 2021.

GARCÍA-VALDESPINO, F. *et al.* Captopril's influence on *Danio rerio* embryonic development: unveiling significant toxic outcomes at environmentally relevant concentrations. **Science of the Total Environment**, 2024.

HANIGAN, D. *et al.* Trade-offs in ecosystem impacts from nanomaterial versus organic chemical ultraviolet filters in sunscreens. **Water Research**, v. 139, p. 281–290, 2018.

HAIDER, A. J.; JAMEEL, Z. N.; AL-HUSSAINI, I. H. M. Review on: titanium dioxide applications. **Energy Procedia**, v. 157, p. 17–29, 2019.

HANSJOSTEN, I. *et al.* Surface functionalisation-dependent adverse effects in zebrafish embryos. **Environmental Science: Nano**, v. 9, n. 1, p. 375–392, 2022.

HOWE, K. *et al.* Zebrafish reference genome and relation to human genome. **Nature**, v. 496, n. 7446, p. 498–503, 2013.

HSU, C.-Y. *et al.* Nano titanium oxide: synthesis, properties, and applications. **Case Studies in Chemical and Environmental Engineering**, v. 9, p. 100626, 2024.

HU, S. *et al.* Impact of co-exposure to titanium dioxide nanoparticles and Pb on zebrafish embryos. 2019.

JAFARI, A. *et al.* Toxicity of green synthesized TiO_2 nanoparticles on zebrafish. **Environmental Research**, v. 212, p. 113542, 2022.

JOHNSON, M. S. *Study of the effects of silver ions and silver nanoparticles on embryonic development*. 2019. Tese (Doutorado em Química e Bioquímica) – Old Dominion University.

KIM, R. *et al.* Dechorionated zebrafish embryos improve evaluation of nanotoxicity. **Frontiers in Toxicology**, v. 6, p. 1476110, 2024.

KOCE, J. D. Effects of exposure to nano and bulk sized TiO_2 and CuO in *Lemna minor*. **Plant Physiology and Biochemistry**, v. 119, p. 43–49, 2017.

LACAVE, J. M. *et al.* Effects of metal-bearing nanoparticles on zebrafish embryos. **Nanotechnology**, v. 27, p. 325102, 2016.

LEE, Y. L. *et al.* Toxic effects and mechanisms of silver and zinc oxide nanoparticles. **Nanomaterials**, v. 12, n. 4, p. 717, 2022.

LOJK, J. *et al.* Analysis of the direct and indirect effects of nanoparticle exposure on microglial and neuronal cells in vitro. **International Journal of Molecular Sciences**, v. 21, n. 19, p. 7030, 2020.

LUU, I.; IKERT, H.; CRAIG, P. M. Chronic exposure to anthropogenic and climate-related stressors alters transcriptional responses in zebrafish. **Comparative Biochemistry and Physiology Part C**, v. 240, p. 108918, 2021.

MATĚJOVÁ, L. *et al.* Oxidation of methanol and dichloromethane on TiO_2-based ceramic foams. **Nanomaterials**, v. 13, n. 7, p. 1148, 2023.

MAMBOUNGOU, J. *et al.* Environmental risk of titanium dioxide nanoparticle and cadmium mixture. **Journal of Nanoparticle Research**, v. 24, n. 9, p. 186, 2022.

MISHRA, Y. K. *et al.* Zebrafish (*Danio rerio*) as an ecotoxicological model for nanomaterial-induced toxicity profiling. **Precision Nanomedicine**, v. 4, n. 1, p. 750–782, 2021.

MURUGADOSS, S. *et al.* Agglomeration of titanium dioxide nanoparticles increases toxicological responses. **Particle and Fibre Toxicology**, v. 17, p. 10, 2020.

MURUGADOSS, S. *et al.* Agglomeration state of TiO_2 nanomaterials influences cytotoxic responses. **Nanomaterials**, v. 11, n. 12, p. 3226, 2021.

MUTALIK, C. *et al.* Zebrafish insights into nanomaterial toxicity. **International Journal of Molecular Sciences**, v. 25, n. 3, p. 1926, 2024.

MYLROIE, J. E. *et al.* PFOS-induced toxicity on zebrafish embryos with or without the chorion. **Environmental Toxicology and Chemistry**, v. 40, n. 3, p. 780–791, 2021.

NNAJI, N. D. *et al.* Bioaccumulation for heavy metal removal: a review. **SN Applied Sciences**, v. 5, n. 5, p. 125, 2023.

OECD. *Test No. 236: Fish Embryo Acute Toxicity (FET) Test*. Paris: OECD Publishing, 2025.

ORTIZ-ROMÁN, M. I. *et al.* Ecotoxicological effects of TiO_2 P25 nanoparticles. **Nanomaterials**, v. 14, n. 4, p. 373, 2024.

PAATERO, I. *et al.* Nanotoxicity profiles dependent on surface-functionalization. **Scientific Reports**, v. 7, p. 8423, 2017.

PÉREZ-ATEHORTÚA, M. *et al.* Chorion in fish: synthesis and malformations. **Aquaculture Reports**, v. 30, p. 101590, 2023.

PECORARO, R. *et al.* Toxicity of titanium dioxide–cerium oxide nanocomposites to zebrafish embryos. **Toxics**, v. 11, n. 12, 2023.

PEREIRA, S. P. *et al.* Toxicity and accumulation of metal from copper oxide nanomaterials. **Ecotoxicology and Environmental Safety**, v. 253, p. 114613, 2023.

PEREIRA, S. P. P. *et al.* Toxicity of silver nanomaterials versus silver nitrate in zebrafish. **Chemosphere**, v. 336, p. 139236, 2023.

REICHSTEIN, I. S. *et al.* Improving predictive ability of the FET test using metabolization systems. **Environmental Sciences Europe**, v. 36, n. 1, p. 91, 2024.

RIBBLE, D. *et al.* Technique for quantifying apoptosis in 96-well plates. **BMC Biotechnology**, v. 5, p. 1–7, 2005.

SCALISI, E. M. *et al.* Titanium dioxide nanoparticles: effects on development and male reproductive system. **Nanomaterials**, v. 13, n. 11, 2023.

SEGNER, H. Zebrafish as a model for investigating endocrine disruption. **Comparative Biochemistry and Physiology Part C**, v. 149, n. 2, p. 187–195, 2009.

SENTIS, M. P. *et al.* Dispersibility and stability of TiO_2 by SMLS, DLS, and SEM. **Journal of Nanoparticle Research**, v. 26, n. 3, p. 55, 2024.

SOBANSKA, M. *et al.* Applicability of the FET test (OECD 236) in regulatory contexts. **Environmental Toxicology and Chemistry**, v. 37, n. 3, p. 657–670, 2018.

TANG, T.; ZHANG, Z.; ZHU, X. Toxic effects of TiO_2 NPs on zebrafish. **International Journal of Environmental Research and Public Health**, v. 16, n. 4, 2019.

VALÉRIO, A. *et al.* Are TiO_2 nanoparticles safe for photocatalysis in aqueous media? **Nanoscale Advances**, v. 2, n. 10, p. 4951–4960, 2020.

VASYUKOVA, I. A. *et al.* Toxic effects of metal-based nanomaterials in marine ecosystems. **Nanobiotechnology Reports**, v. 16, p. 138–154, 2021.

VIEIRA, L. R. *et al.* Proteomics analysis of zebrafish larvae exposed to 3,4-dichloroaniline. **Environmental Toxicology**, v. 35, n. 8, p. 849–860, 2020.

WANG, X. *et al.* Nano-TiO_2 adsorption alters bioavailability and toxicity in zebrafish. **Frontiers in Environmental Science**, v. 10, 2022.

WEIR, A. *et al.* Titanium dioxide nanoparticles in food and personal care products. **Environmental Science & Technology**, v. 46, n. 4, p. 2242–2250, 2012.

WU, Q. *et al.* Transgenerational neurotoxicity in zebrafish. **Environmental Pollution**, v. 231, p. 471–478, 2017.

WU, Q. *et al.* Parental transfer of TiO_2 nanoparticles aggravates developmental toxicity. **Environmental Science: Nano**, v. 5, n. 12, p. 2952–2965, 2018.

XIA, Q. *et al.* nrf2-HO-1/JNK-erk signaling in zebrafish developmental toxicity. **Frontiers in Pharmacology**, v. 12, p. 642480, 2021.

YANG, Y. *et al.* Toxic effects of bisphenol AF on zebrafish embryos. **Estuarine, Coastal and Shelf Science**, v. 233, p. 106540, 2020.

ZAVITRI, N. G. *et al.* Toxicity evaluation of zinc oxide nanoparticles green synthesized using papaya extract in zebrafish. **Biomedical Reports**, v. 19, n. 6, p. 1–11, 2023.

ZHOU, Y. *et al.* Effects of nano-TiO_2 on TBPH toxicity in zebrafish. **Chemosphere**, v. 295, p. 133862, 2022.

6.2 MANUSCRIPT 5 – From Prey to Predator: Titanium dioxide MPs trophic transfer in aquatic environment model

Ana Kamila Medeiros Lima[1]; Roberta Laiz Bezerra Santos Albano[1]; Alexia Riquet Martins[1]; João Vinicius Sousa Fernandes[1]; Emilio de Castro Miguel[1*]

[1] Biomaterials Laboratory, Department of Metallurgical Engineering and Materials and Analytical Center, Federal University of Ceará (UFC), Fortaleza, CE, Brazil.

***Corresponding author**

Emilio de Castro Miguel

Federal University of Ceara / Pici Campus

Department of Metallurgical Engineering and Materials (DEMM); Biomaterials Laboratory (BIOMAT)

zip code: 60455-900

Fortaleza - Ceará - Brazil

+85 33669256

emiliomiguel@ufc.br

GRAPHICAL ABSTRACT

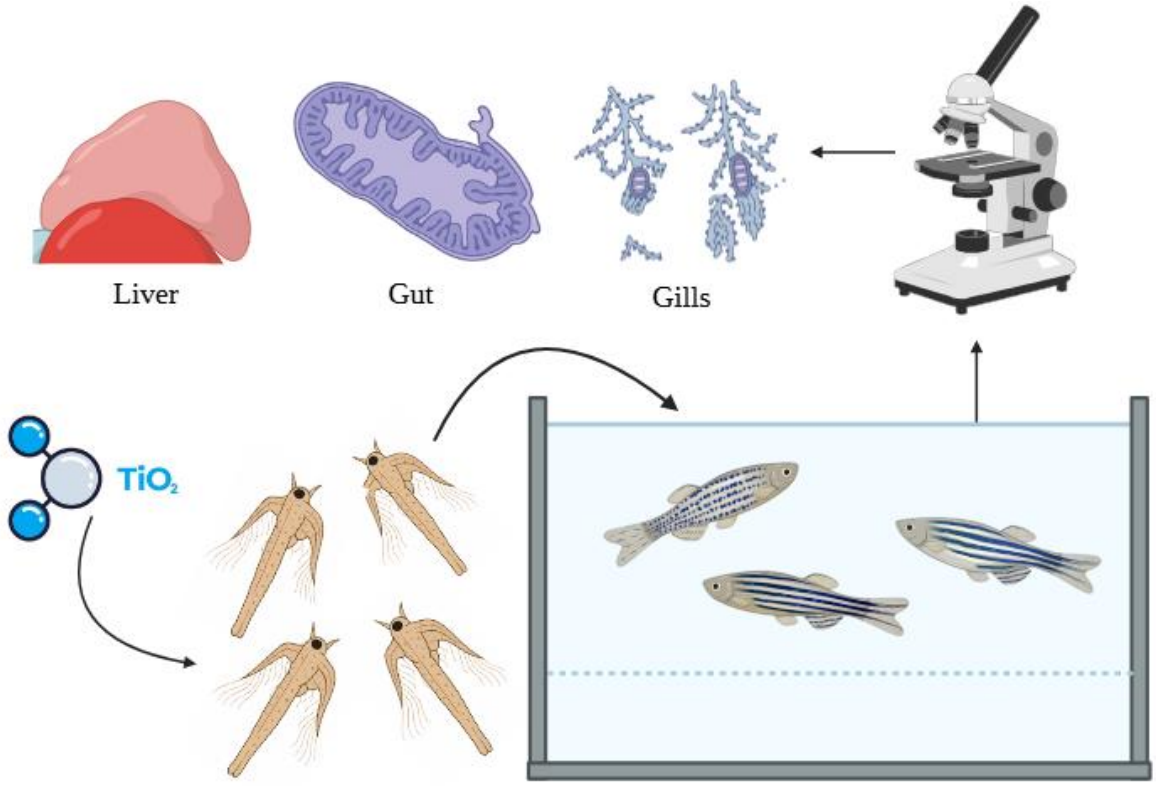

ABSTRACT

Titanium dioxide nanoparticles (TiO_2-NPs) are widely used in a variety of products, including food, cosmetics, and pharmaceuticals, resulting in inevitable human and environmental exposure through inhalation, dermal contact, and ingestion. Due to their versatility and extensive use in consumer goods, TiO_2-NPs can accumulate in the environment and enter the food chain. However, their environmental safety remains under debate among regulatory agencies worldwide. This study aimed to evaluate the toxicity of titanium dioxide in *Danio rerio* through trophic transfer, by feeding the adults with *Artemia salina* nauplii previously exposed to 50 mg/L of TiO_2-MPs. An analytical technique, dynamic light scattering (DLS), was used for microparticle solution behavior. Histological analyses were conducted by sex (male and female) and by organ, including gills, intestine, and liver. No signs of toxicity were observed in the gills; however, toxic effects were identified in intestine and liver. Altogether, the observed lesions support the intestinal and hepatic toxicity potential of TiO_2-NPs, reinforcing concerns regarding their transfer and bioaccumulation through the trophic chain. Although trophic transfer of TiO_2 MPs could not be fully confirmed, the toxic effects caused by particle contact may potentially propagate across trophic levels. These findings highlight the need for further research under more realistic and chronic exposure scenarios to provide stronger evidence for regulatory decisions and ensure environmental and human health safety.

Key words: Titanium dioxide; Nanotoxicity; Trophic transfer; *Danio rerio*; Histopathology

6.2.1 Introduction

Titanium dioxide nanoparticles and microparticles (TiO_2NPs/ TiO_2MPs) are widely used in various products like food, cosmetics, and medications, leading to inevitable human exposure through different routes such as inhalation, dermal penetration, and ingestion (Shabbir et al., 2021). *In vitro* studies have shown that TiO_2-NPs can be cytotoxic and genotoxic, generating reactive oxygen species (ROS) and activating pathways related to inflammation and cell death, indicating potential harm to human health (Bevacqua *et al.*, 2022).

The use of TiO_2-NPs in industrial products and their role in wastewater treatment technologies is increasing (Zahra *et al.*, 2020). TiO_2-based nanocomposites are effective photocatalysts for pollutant removal in wastewater treatment, addressing water pollution issues by degrading pollutants into simpler organic compounds. Although, the composite shows promise in combating white pollution and food waste in the food packaging sector, its controversial use in food processing has led to international disputes (Racovita, 2022).

The European Union banned the use of titanium dioxide in foods in 2022. This decision was made after (European Food Safety Authority (EFSA), 2022) publication concluded its assessment revealing health concerns. As pointed in (Racovita, 2022), balancing the use of nano-TiO_2 as an anticancer agent while considering its cytotoxic potential on healthy cells is crucial for medicinal advancements. Titanium dioxide controverse is also showed by the fact Health Canada's Food Directorate chose not to ban titanium dioxide as a food additive in 2022, although it noted uncertainties in the safety of composite (Health Canada's Food Directorate, 2023).

However, in Brazil, the National Health Surveillance Agency (Anvisa) concluded that titanium dioxide, when used as a food additive in products such as chewing gum, powdered juices, and cookie fillings, does not pose toxicological risks (Brazil, 2023). Anvisa emphasizes that TiO_2 has a long history of safe use and exhibits very low absorption in the human body. Nevertheless, Federal Bill N°. 2257/22, which proposes banning the use of titanium dioxide in food production as well as the importation of products containing this substance, is currently under discussion in the Brazilian Chamber of Deputies (Brazil, 2022).

The research done by (Vijayaraj *et al.*, 2018) highlights the potential risks of titanium dioxide nanoparticles (TiO_2 NPs) in both terrestrial and aquatic ecosystems, demonstrating trophic transfer and toxicity in these environments. Besides, the findings of the study suggest that TiO_2 NPs can have adverse effects on soil microorganisms, plants, and amphibians, indicating the importance of understanding and managing the environmental impact of nanomaterials for ecosystem health.

Regarding environmental effects besides food safety, Lee *et al.*, (2022) demonstrated that silver and zinc oxide nanoparticles spiked in natural waters showed minor toxic effects on zebrafish embryos, indicating potential environmental safety concerns regarding nanoparticle exposure to aquatic ecosystems. Also, the research performed by (Mottola *et al.*, 2022) zebrafish exposed to 10 μg/L TiO_2 nanoparticles showed increased DNA damage and reduced cell viability, indicating potential environmental risks associated with nanoparticle exposure.

The accumulation of nanoparticles in protozoan food vacuoles, even without causing viability effects, indicates a potential risk for food-web transfer and bioaccumulation (Aruoja *et al.*, 2015). The study highlights the complexity of nanoparticle toxicity, influenced by factors like agglomeration, solubility, and ion leaching, emphasizing the need for a quantitative approach to understand aquatic nanoparticle toxicity mechanisms (Aruoja *et al.*, 2015).

Emerging contaminants such as pyrethroids (PYRs) and ultraviolet (UV) filters (UVFs) have been detected in paired mother-fetus samples of dolphins, *Pontoporia blainvillei* (Franciscana) and *Sotalia guianensis* (Guiana dolphin) from the Brazilian coast, revealing their ability to cross the placental barrier. Muscle tissue showed the highest accumulation, suggesting a greater affinity of these compounds for proteins. This was the first study to confirm the placental transfer of PYRs and UVFs in marine mammals, raising concerns about early-life exposure in coastal species (Alonso, *et al.* 2015). Such findings highlight the importance of model organisms capable of reproducing similar exposure and developmental patterns under controlled conditions.

The trophic transfer of titanium dioxide nanoparticles (TiO_2 NPs) has been documented in different experimental food chains, evidencing their capacity to accumulate and influence toxicity across trophic levels. In terrestrial systems, TiO_2 showed higher accumulation than Ag in a lettuce–snail model, with over 70% of Ti retained in the digestive gland, raising concerns about ecological risks (Wu et al., 2021). In aquatic environments, TiO_2 not only accumulated directly in organisms but also modulated the behavior of co-contaminants, as shown by its ability to enhance phenanthrene bioaccumulation and toxicity in *Scophthalmus maximus* after trophic transfer from *Artemia salina* (Lu et al., 2021). Microcosm studies further demonstrated that TiO_2 preferentially accumulated in sediments and biofilms, with sequential low-dose exposures leading to higher bioconcentration in plants and animals, and greater biomagnification in muddy loaches compared to snails (Kim et al., 2016). Biofilm-based food chains also showed that TiO_2 influenced extracellular polymeric substance (EPS) production, altering nanoparticle stabilization and transfer patterns to snails (Cheng et al., 2025). Importantly, nanoparticle modifications can mitigate these effects, as carbon quantum dots (CQDs) doping reduced TiO_2 trophic transfer and bioaccumulation in an algae–daphnia–zebrafish chain by enhancing antioxidant defenses and reducing oxidative stress (Li et al., 2025). Finally, studies with different engineered nanoparticles, including TiO_2, demonstrated that particle properties and transformations, such as sulfidation and surface coatings, strongly influenced uptake, depuration, and toxicity, showing that food web interactions play a critical role in modulating nanoparticle impacts in aquatic ecosystems (Zhao et al., 2025).

Danio rerio models are utilized for evaluating the safety and therapeutic potential of nanoparticles, including environmental implications, due to their innate immune system and embryo's transparency and as well as study beneficial effects of nanoparticles, offering valuable insights about their environmental impact and safety levels (Pensado-López *et al.*, 2021; Yeşilbudak, 2023).

This model is a valuable tool in ecotoxicological studies due to its genetic similarity to other vertebrates and its advantages in environmental ecotoxicity research (Stachurski *et al.*, 2023). They help in meeting the 3Rs (refinement, reduction and replacement) principle in research, enable the discovery of harmful compounds, and reduce the number of animals used in experiments (Singh; Kashyap; Garg, 2021). Acute sublethal effects were observed in zebrafish embryos at different developmental stages, indicating that a completely safe release of TiO_2 nanoparticles into the aquatic environment cannot be guaranteed (Valério *et al.*, 2020).

Zebrafish can be employed to evaluate the toxicological effects of various pollutants in aquatic ecosystems, including metal elements, organic pollutants, nanoparticles, and microplastics, demonstrating their broad applicability in aquatic ecotoxicology research (Li *et al.*, 2023).

The aim of this study was to evaluate titanium dioxide toxicity in *Danio rerio* induced by trophic level transfer feeding adult's zebrafish with *Artemia salina* nauplii exposed to titanium dioxide nanoparticles.

6.2.2 Material and methods

Titanium dioxide

The titanium dioxide microparticles (TiO_2MPs) have this nomenclature in this paper according to new scientific findings of European Comission (EC) and the regulatory experience, adopted an updated definition of nanomaterial. Natural, incidental or manufactured material consisting of solid particles present, either on their own or as identifiable constituent particles in aggregates or agglomerates and one or more external dimensions of the particle are in the size range 1 nm to 100 nm (European Comission, 2022).

The titanium dioxide microparticles (TiO_2MPs) were kindly provided by the Advanced Materials Chemistry Group (GQMat) coordinated by Dr. Pierre Fechine - Department of Analytical Chemistry and Physical Chemistry, Federal University of Ceará – UFC. This particle was characterized in a previous study (Barbosa *et al.* 2018). The particle used underwent a sonochemical process for size reduction and has an average size of 104.4 ± 2.29 nm. The rutile form was used in this study with its zeta potential of −17.36 ± 0.11, its hydrodynamic size value of 297.46 ± 3.66 nm. The solution of 50 mg/L was prepared and sonicated for 15 minutes for the exposure test.

Dynamic Light Scattering (DLS)

To analyze the agglomeration of the TiO_2MPs, scattering readings were taken in the medium using Dynamic Light Scattering (DLS) equipment, (Zetasizer Nano S - Malvern) according to (Chicea *et al.*, 2023). The aliquot tested was 50 mg/L TiO_2, diluted and homogenized. The same concentration used to expose the *Artemia salina* nauplii instar I. The experiment was conducted testing the concentration with artificial seawater and ultrapure water as control. The purpose of repeating the concentration in ultrapure water was to verify whether artificial seawater influences the titanium nanoparticles agglomeration.

Once the dispersion has been diluted and homogenized, 1 ml was placed in a quartz cuvette for DLS analysis. The readings were spaced out at increasing hourly intervals, with the first hour continuous readings (120 total readings) and the following being single readings at 1, 2, 4, 8, 24, 28, 32, 48, 72 and 96 hours after the start of the analysis, gradually monitoring the behavior of the particle in the medium.

Animals maintainance

The breeding fish (*Danio rerio*) are from the vivarium of the Biomaterials Laboratory of the Department of Metallurgical and Materials Engineering at UFC, kept under laboratory conditions (Rack Altamar), with the following parameters: conductivity 650 µS, temperature 28 ºC ± 0.2 and pH 7.0±0.2. Conductivity is maintained using Red Sea Salt® and pH controlled with acid and alkaline buffers. These parameters are automatically maintained by the rack and monitored 24/7 via software.

For spawning, individuals were moved to aquariums with physical dividers and kept without direct contact (six males and three females). The following day the physical barrier was removed from the aquarium and the brooder was kept under lighting. After spawning, the embryos were kept in reconstituted water, prepared in accordance with U.S.EPA68. The procedures used in this study were previously approved by the Ethics Committee on the Use of Animals (CEUA) of the Federal University of Ceará.

Trophic level transfer experiment

The test consisted of a fish feeding experiment for 30 days and a 7-day depuration period, using *Artemia salina* as a food source. The fish used were 6 months old and were fed twice a day, at 8:30 am and 5:00 pm, with 50mL of brine shrimp filtered per aquarium.

A total of 30 fish were used, divided into three groups of 10, with 5 males and 5 females in each group. The groups were subjected to different treatments under the same

experimental conditions: 1. Negative control group fed with commercial food; 2. Negative control group fed with brine shrimp non exposed to TiO_2MPs; 3. Experimental group fed with brine shrimp exposed to TiO_2MPs.

The fish were maintained in six 3L aquariums, with capacity for up to 5 fish per aquarium. Daily, 5 mg of *Artemia salina* cyst were added to artificial seawater to hatch the larvae, which were exposed to the particles for 48 hours after 24 post hatching and then offered to the fish.

Environmental conditions, such as temperature, pH and circadian cycle, were daily monitored. A partial water renewal of 30% was carried out manually every two days, while the aquariums will be cleaned once a week.

At the end of the test, the fish were euthanized with tricaine (MS-222) using an immersion method. They were placed in a solution of MS-222 dissolved in water at a minimum concentration of 250 mg/L. Euthanasia was confirmed by the absence of opercular movement for at least 3 minutes, as determined by the protocol, and subsequently followed by a physical method.

Microscopy Techniques

Light Microscopy (LM) and Transmission Electron Microscopy (TEM)

After euthanasia a dissection procedure was performed to collect and fix the samples. The target organs were fixed in an aqueous solution containing 2.5% glutaraldehyde, 4% formaldehyde, 0.1 M sodium cacodylate buffer, pH 7.2, in room temperature for 24 hours. Thereafter, the material was washed in 0.1M sodium cacodylate buffer three times, each washing lasting 45 minutes. After washing, post-fixation with osmium tetroxide (OsO_4) at 1%, pH 7,02 for two hour follows. Subsequently, three more washes of 40 minutes each were carried out in 0.1M cacodylate buffer. After washing, the material was dehydrated in an increasing series of 50%, 70%, 90% and 3X 100% acetone, each step lasting 40 minutes.

After dehydration, the samples were infiltrated in epoxy resin (Embed 812). After this process, the blocks were assembled and polymerized for 48 hours at 60°C. The ultrathin sections were made with ultramicrotome Leica UC7. The sections were 500nm thick, slides were stained with toluidine blue and hematoxilin-eosin. The visualization of the samples and the respective documentation was finalized in a Zeiss Primo Star equipped with a camera, and the Zen Lite software for the acquisition of images.

6.2.3 Results and discussion

The results indicated that seawater significantly influences the aggregation behavior of TiO_2MPs. In addition to modifying titanium dioxide stability, seawater promoted the formation of agglomerates substantially larger than those observed under control conditions. These pronounced increases in aggregate size, relative to the control, may directly affect particle bioavailability and uptake by exposed organisms. While the control suspensions remained stable throughout the entire experimental period, TiO_2MPs dispersed in seawater exhibited marked temporal variability, characterized by pronounced peaks in aggregate size (Fig. 1).

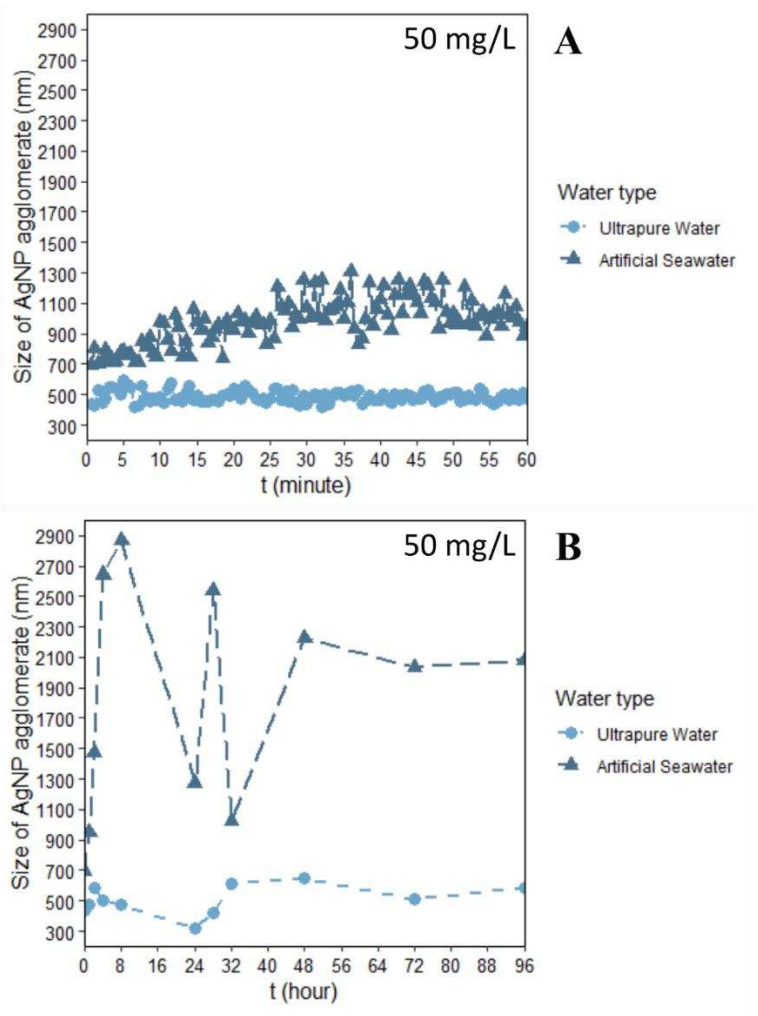

Figure 1. Dynamic light scattering (DLS) analysis of titanium dioxide microparticles (TiO_2MPs) aggregation over 96 h. TiO_2MPs suspensions were maintained in cuvettes and measured automatically at regular time intervals. Artificial seawater promoted a significant increase in aggregate size compared to the control, indicating enhanced agglomeration of TiO_2MPs under saline conditions.

TiO_2 MPs showed increased agglomeration in natural and artificial seawater compared to Milli-Q water. This is due to the presence of ions and organic matter, which bind

to the negatively charged surfaces of the nanoparticles and reduce electrostatic repulsion, allowing van der Waals forces to dominate. As a result, both homo- and hetero-agglomerates form more readily, leading to larger particle sizes and facilitating their sedimentation to benthic layers in marine and estuarine environments (Doyle et al., 2014).

After understanding how the particle behaves in the artificial seawater used for dilution—simulating the environmental conditions in which *Artemia salina* lives—the next analyses focused on histological sections of the three target organs selected for this study: gills, intestine, and liver, following a 30-day feeding period in which adult zebrafish were fed instar II *Artemia salina* nauplii previously exposed to TiO_2 MPs.

The gills were the first organs analyzed (Fig. 2), as they are responsible for gas exchange and are also a primary route of exposure and absorption of toxic agents in fish. In the control group, the gills exhibited tipical morphology, with clearly defined primary and secondary lamellae and intact hyaline cartilage within the primary lamellae, showing no signs of structural alteration (Fig. 2A and 2B). Similarly, the gills of fish from the experimental group fed with *Artemia salina* previously exposed to 50 $mg \cdot L^{-1}$ of TiO_2 displayed normal morphology, with well-preserved tissue structures comparable to the control (Fig. 2C and 2D). The same pattern was observed in the group fed only with *A. salina*, where all gill structures appeared healthy and unaltered (Fig. 2E and 2F).

Signs of toxicity induced by triphenyl phosphate (TPhP) on zebrafish's gills such as tissue structure deformation, and edema of secondary lamellae (Yu *et al.*, 2024) were not observed in our results. These findings align with expectations, considering that the route of TiO_2 MPs exposure in this study was dietary, via contaminated artemias, rather than through direct contact with the gill surface via the respiratory pathway.

Although, the processes involved in the uptake of polystyrene NPs into the intestine may be complex, through either gills (indirect) or ingestion (direct) and nanoplastics, when ingested, can lead to inflammatory responses and structural damage in the gills, as they accumulate and activate immune responses (Wang *et al.*, 2023). This fact reinforces the gills need to be investigated even though it is not the primary target organ of TiO_2 MPs toxicity effects and the results were similar in both sexes. Besides the toxic effects and environmental safety have to be done testing multiples pathway exposures to get reliable results.

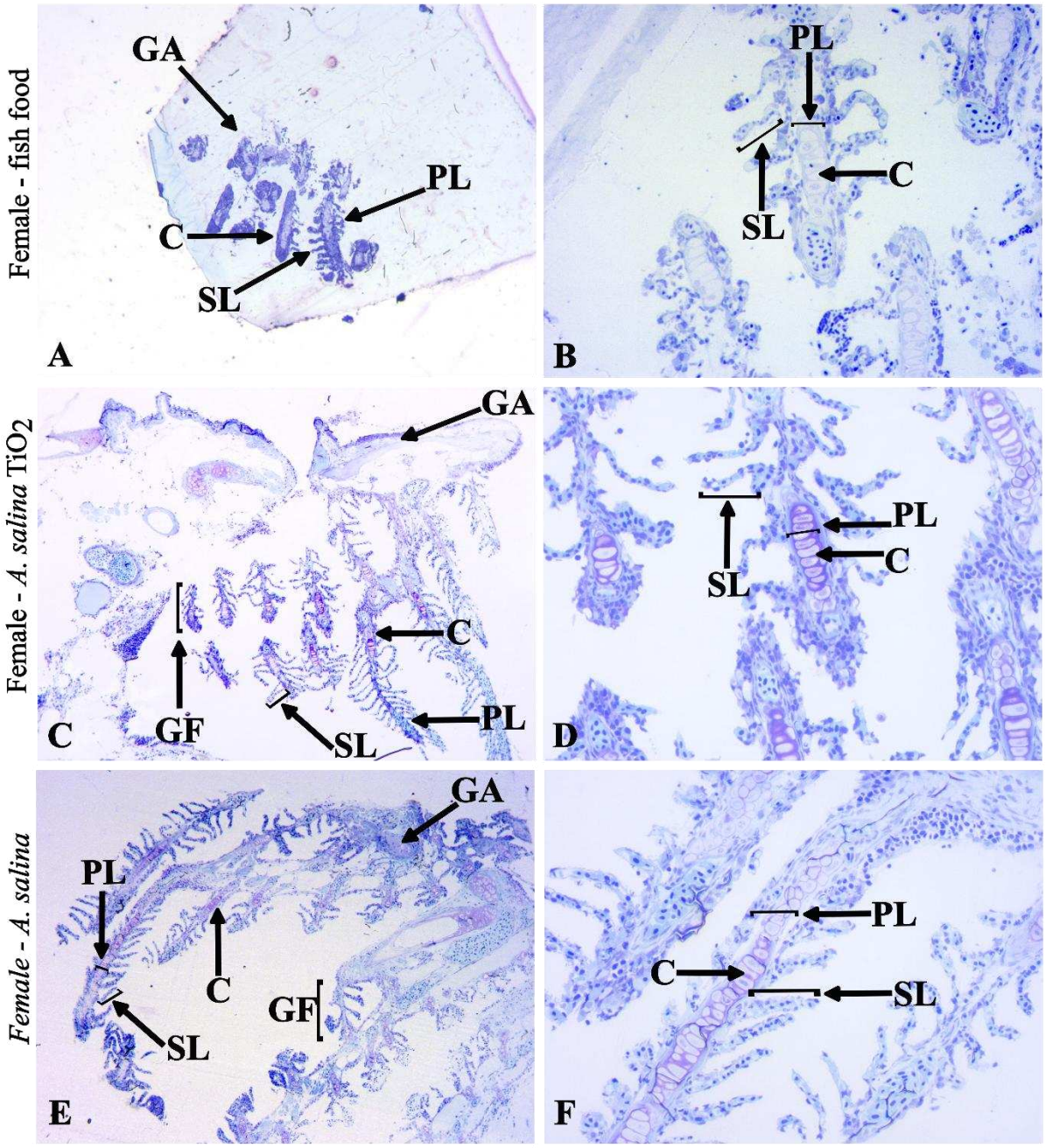

Figure 2. Gills sections of *Danio rerio* female individuals fed with different diets for 30 days. A and B: Control group with healthy gills with fish food diet showing the primary lamellae (PL), secondary lamellae (SL) and hyaline cartilage (C). C and D: Gills of fish fed with *A. salina* exposed to 50mg/L TiO_2 showing conserved histology of gills arch (GA) and gills filament (GF), primary lamellae (PL) and secondary lamellae (SL) and hyaline cartilage (C). E and F: Gills of fish fed with healthy *A. salina* showing conserved histology of gills arch (GA), primary lamellae (PL), secondary lamellae (SL) and hyaline cartilage (C).

The analysis of gill tissues from male individuals (Fig. 3) followed a similar pattern to that observed in females (Fig. 2). Both the control group (Fig. 3A, 3B, and 3G) and the group fed with *Artemia salina* previously exposed to TiO_2MPs (Fig. 3C, 3D, and 3H) exhibited gills with normal morphology based on the evaluated parameters, including filament

structure, presence of lamellar edema, hyperplasia, and inflammatory signs, according to the applied histological techniques. Likewise, fish fed exclusively with non-contaminated *A. salina* (Fig. 3E, 3F, and 3I) showed no signs of gill alteration. These results indicate that dietary exposure, even to TiO_2-contaminated *Artemia* (Fig. 3C, 3D, and 3H), did not pose a detectable risk to gill tissue integrity under the tested conditions.

In contrast, studies with triclosan (TCS)—a broad-spectrum antimicrobial agent widely used in personal care, household, veterinary, medical, and industrial products— reported significant gill damage, including aneurysm, capillary dilation, lamellar disorganization, hyperplasia, epithelial lifting, and desquamation (Arman, 2021). The fact that TiO_2 is also employed in multiple industries reinforces the importance of further investigating its toxicity pathways and mechanisms.

In the study conducted by Rahmani *et al.* (2016), histopathological evaluation of *Carassius auratus* and common carp (*Cyprinus carpio*) exposed to TiO_2 nanoparticles doped with chromium (Cr), iron (Fe), and nickel (Ni) revealed significant tissue damage. The main alterations observed in the gill tissues included aneurysms, lamellar fusion, epithelial degeneration, and hyperplasia. In the intestine, the researchers reported an increased number of blood cells and lymphocytic infiltration, indicating an inflammatory response. These findings suggest that doped TiO_2 nanoparticles can induce notable toxic effects in different fish species, affecting both respiratory and digestive systems.

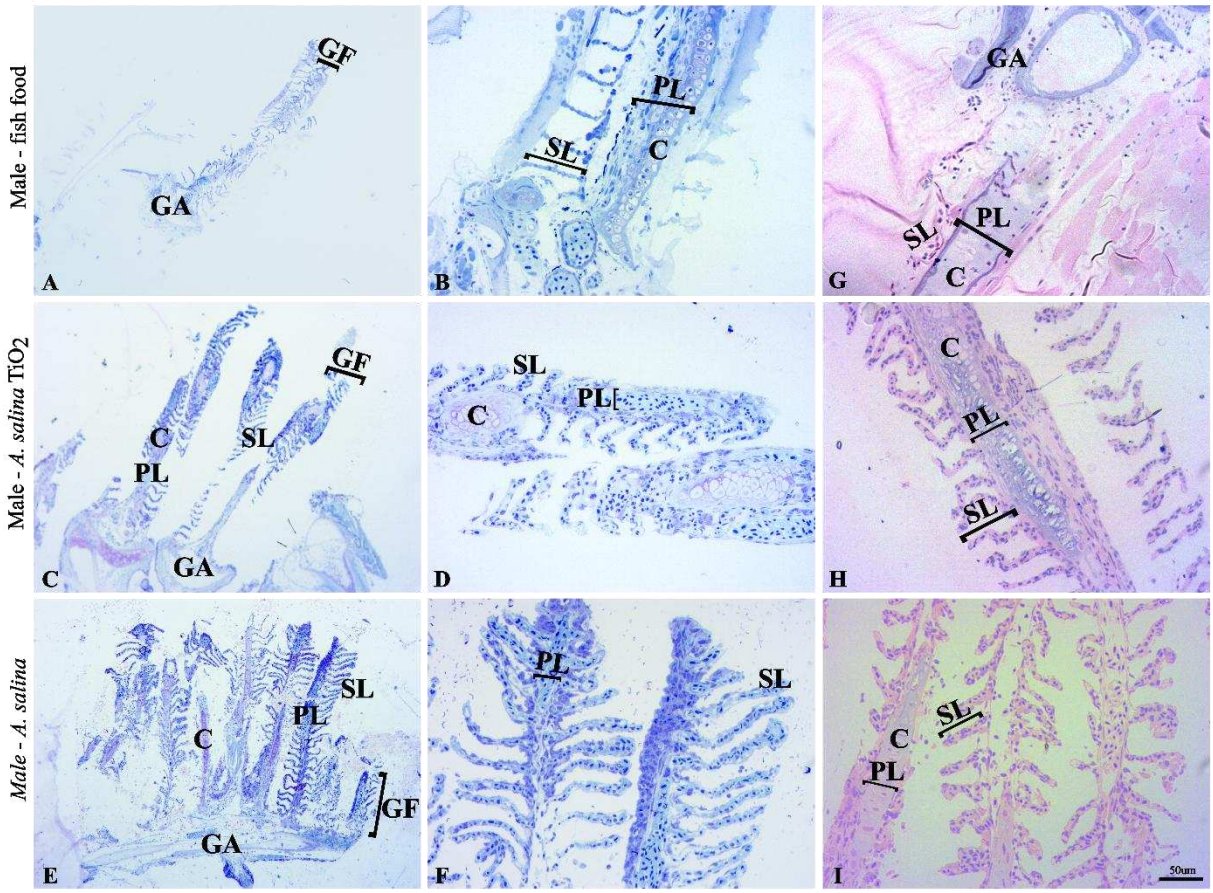

Figure 3. Gills sections of *Danio rerio* male individuals fed with different diets for 30 days. A, B and G: Control group with healthy gills with fish food diet showing gills arch (GA) and gills filament, the primary lamellae (PL), secondary lamellae (SL) and hyaline cartilage (C). C, D and H: Gills of fish fed with *A. salina* exposed to 50mg/L TiO_2 showing conserved histology of gills arch (GA), primary lamellae (PL), secondary lamellae (SL) and hyaline cartilage (C). E, F e I: Gills of fish fed with healthy *A. salina* showing conserved histology of gills arch (GA), primary lamellae (PL), secondary lamellae (SL) and hyaline cartilage (C).

The histological analysis of the intestinal tissue of female *Danio rerio* individuals after 30 days of dietary exposure revealed distinct alterations depending on the diet (Fig. 4). Control samples showed well-preserved gut architecture, with clear identification of goblet cells, lamina propria, columnar enterocytes, muscle layer, and mucosa, confirming healthy tissue structure (Fig. 4A, 4B, and 4G).

In fish fed with *Artemia salina* exposed to 50 mg/L TiO_2, the gut sections showed visible stomach content (Fig. 4C) and significant histopathological changes throughout the intestinal tissue (Fig. 4D and 4H), including villus dissolution, distorted crypt structures, areas of necrosis, and altered goblet cell morphology compared to controls. These damages could be related to Guo *et al.* (2022) who compared the different effects of commercial microplastics (CMPs) and realistic microplastics (RMPs) on zebrafish gut and cell necrosis, hyperchromatic pyknosis and infiltration of inflammatory cells, were found to be some of the toxic effects.

The villus dissolution and distorted crypt structures (Fig. 4D and 4H) are essential for nutrient absorption and tissue renewal and can be related to the development of enteritis or enterocolitis-like pathology (Marjoram; Bagnat, 2015). Normally, they are accompanied by mucosal edema, goblet cell changes, and increased mucus production. Therefore, these damages could be due to TiO_2 NPs contaminated food. To corroborate this hypothesis, the trinitrobenzenesulfonic acid (TNBS) induced model of enterocolitis in adult zebrafish. One of the signs of it is a region showing luminal sloughing of cellular debris in the TNBS-treated intestine (Geiger *et al.*, 2013).

Conversely, fish fed with non-contaminated *A. salina* exhibited preserved intestinal structures (Fig. 4E and 4F), similar to those observed in control animals (Fig. 4G and 4I), with intact mucosa, well-defined columnar enterocytes, and normal globet cells. These findings indicate that ingestion of TiO_2-contaminated prey induces evident toxic effects in the intestinal tissue, while both the control and uncontaminated diet groups maintained the tissue integrity.

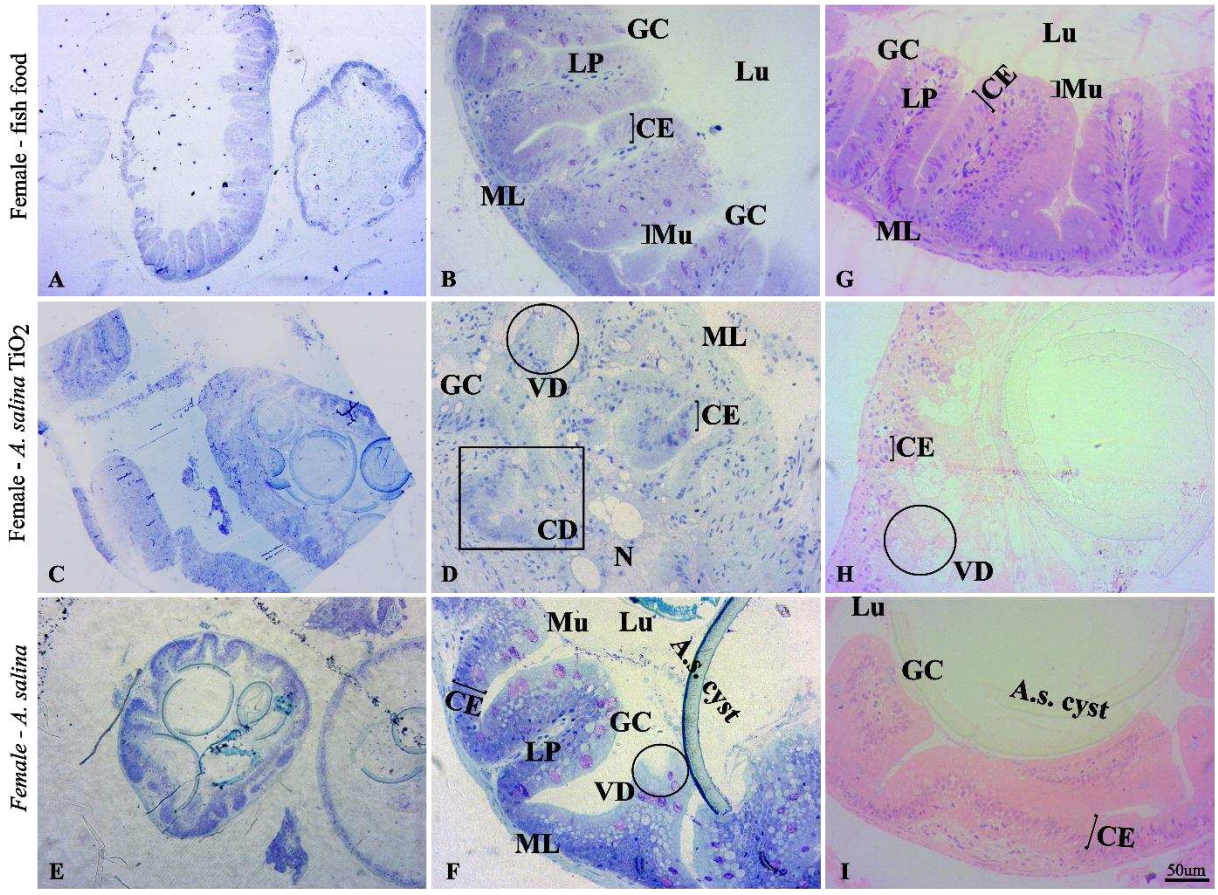

Figure 4. Gut sections of *Danio rerio* female individuals fed with different diets for 30 days. A, B and G: healthy gut histology, tissue structure and its components. Globet cells (GC), lamina propria (LP), columnar enterocyte (CE), muscle layer (ML) and mucosa (Mu). C: Gut showing stomach contents showing feeding with brine shrimp exposed to 50mg/L TiO_2. D and H: Gut of fish fed with *A. salina* exposed to 50mg/L TiO_2 showing toxic effects

in whole tissue. Villus dissolution circled in black (VD), globet cells with different shapes compared to the controls (GC), crypt distortion squared in black (CD), necrosed area (N), columnar enterocyte (CE) and muscle layer (ML). E: Gut showing stomach contents showing feeding with brine shrimp. F and I: columnar enterocyte (CE), muscle layer (ML), globet cells (GC), lamina propria (LP), villus dissolution circled in black (VD) and mucosa (Mu). The panels G, H and I are hematoxilin-eosin stained.

The intestinal histology of male *Danio rerio* individuals after the dietary exposure (Fig. 5) revealed morphological patterns consistent with those observed in females (Fig. 4). Control micrographs presented intact intestinal architecture with preserved goblet cells and enterocytes, indicating healthy tissue structure (Fig. 5A, 5B, and 5G).

In contrast, fish fed with *Artemia salina* previously exposed to 50 mg/L TiO_2 exhibited signs of tissue damage. Gut sections showed visible stomach content (Fig. 5C) and significant alterations, such as villus dissolution, goblet cells with altered morphology compared to controls, and structural disorganization of the enterocytes and the lamina propria (Fig. 5D and 5H). The thickening of the villi as well as increased mucus production and enlarged goblet cells were also found using zebrafish as a model to study intestinal inflammation (Brugman, 2016).

Goblet cells (GCs) are single-cell glands that produce and secrete mucin. The mucin secreted by GCs forms a mucus layer, which plays an important role in resisting the invasion of foreign bacteria and intestinal inherent microorganisms, regulating the immune performance of the body (Zhang; Wu, 2020). The damage to goblet cells observed in this experiment may increase susceptibility to secondary infections, potentially compromising the immune system. Accordingly, signs of toxicity induced by triphenyl phosphate (TPhP) on zebrafish's gut like goblet cell shape deformation, and enteric villus dissolution (Yu *et al.*, 2024).

Additionally, the observed histological damage may reflect broader physiological disturbances beyond structural dysfunction alone, potentially leading to more serious health effects resulting from dietary exposure to titanium dioxide. For instance, exposure to polychlorinated biphenyls (PCBs) has been shown to cause significant histological alterations—including neutropenia, intestinal villus and epithelial damage—alongside oxidative stress and gut inflammation in zebrafish. These effects were also associated with substantial changes in gut microbiota composition and metabolic profiles, particularly involving inflammation and lipid metabolism (Zhu *et al.*, 2022).

On the other hand, individuals fed with non-contaminated *A. salina* displayed normal intestinal histology, with well-preserved cellular components and tissue organization, including clear visualization of the lumen and mucus layer (Fig. 5E, 5F, and 5I). These results support the conclusion that oral exposure to TiO_2 MPs through contaminated prey can induce notable histological damage in the intestine of zebrafish not depending on sex, while exposure to a clean diet maintains gut integrity.

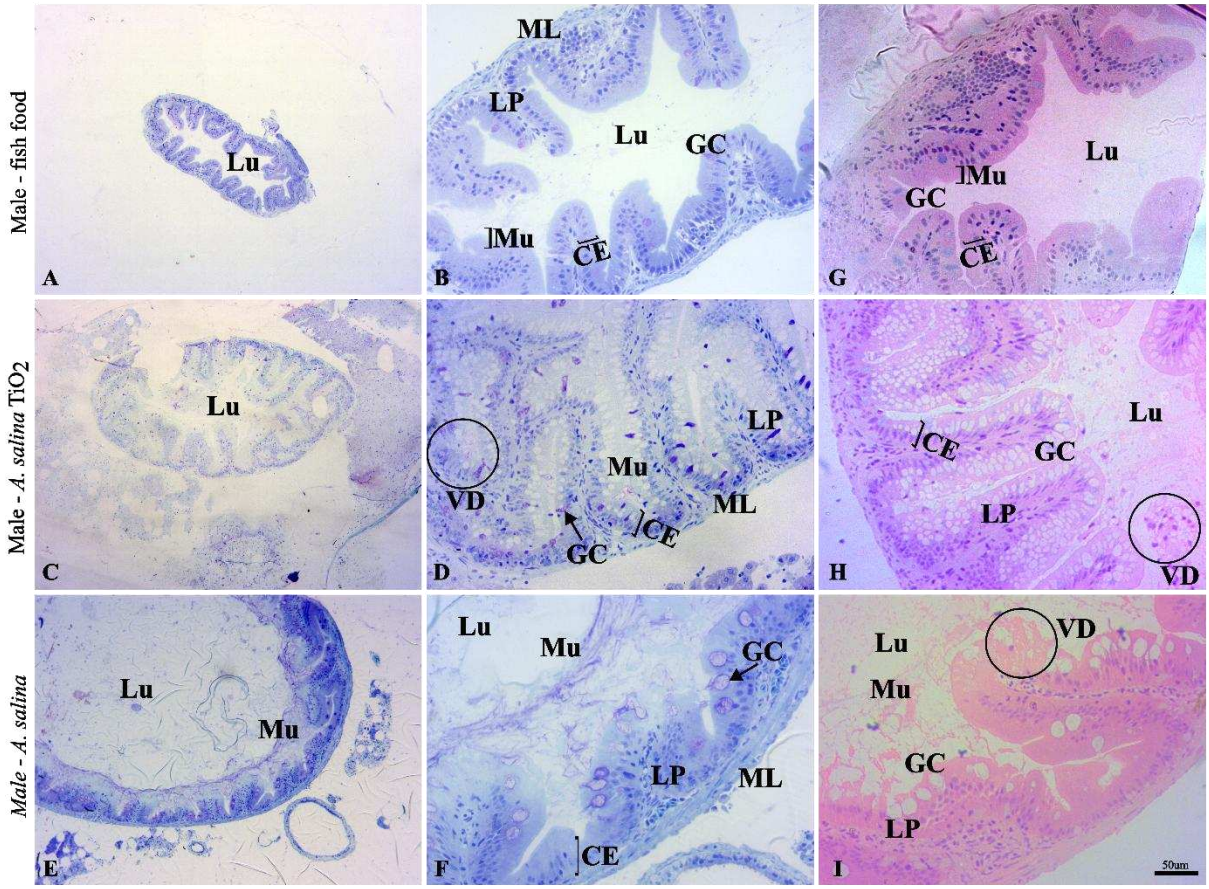

Figure 5. Gut sections of *Danio rerio* male individuals fed with different diets for 30 days. A, B and G: healthy gut histology, tissue structure and its components. Globet cells (GC), lamina propria (LP), columnar enterocyte (CE), muscle layer (ML), mucosa (Mu) and lumen (Lu). C: Gut fed with brine shrimp exposed to 50mg/L TiO_2. D and H: Gut of fish fed with *A. salina* exposed to 50mg/L TiO_2 showing toxic effects in whole tissue. Villus dissolution circled in black (VD), globet cells with different shapes compared to the controls (GC), columnar enterocyte (CE), lamina propria (LP), muscle layer (ML) and mucosa (Mu). E: Gut's fish fed brine shrimp showing the lumen (Lu) and the mucus layer (Mu). F and I: columnar enterocyte (CE), muscle layer (ML), globet cells (GC), lamina propria (LP), mucosa (Mu) and lumen (Lu). The panels A – F are toluidine blue stained. The panels G, H and I are hematoxilin-eosin stained.

The histological analysis of females *Danio rerio* liver after the dietary exposure revealed marked differences between treatment and control groups (Fig. 6). Control individuals displayed normal hepatic architecture, characterized by well-organized hepatocytes, clear blood vessels, preserved sinusoids, and distinct biliary canaliculi (BC), as observed in Fig. 6A, 6B, and 6G.

Similarly to the hepatic alterations observed in zebrafish exposed to *Psychotria carthagenensis* extract—such as karyorrhexis, karyolysis, and megalocytosis at higher concentrations (Nascimento *et al.*, 2024)— and to Wang et al, (2022) where Bisphenol AF (BPAF), an emerging environmental endocrine disruptor that is widely detected in aquatic environments and poses a potential threat to fish health, was tested the exposure to BPAF has been shown to increase hepatic tissue disorganization and reduce spermatid count in fish. The fish fed with *Artemia salina* previously exposed to 50 mg/L TiO_2 also exhibited extensive liver damage. Histological sections revealed severe cytotoxic effects, including vacuolization, inflammatory infiltrates (Smorodinskaya *et al.*, 2023), necrosis, ballooning and degenerated hepatocytes, as well as nuclear fragmentation (Fig. 6C, 6D, and 6H), highlighting the potential of TiO_2 to induce hepatotoxicity through trophic transfer. Also, In triclosan (TCS) testing liver specimens showed sinusoidal dilation, congestion, vacuolization, hepatocellular degeneration, and necrosis (Arman, 2021).

In contrast, fish fed only with uncontaminated *A. salina* maintained healthy liver histology similar to the controls, with intact hepatocytes (Fig. 6E, 6F, and 6I). These findings indicate that oral exposure to TiO_2 MPs via contaminated food can induce significant hepatotoxic effects in adults zebrafish.

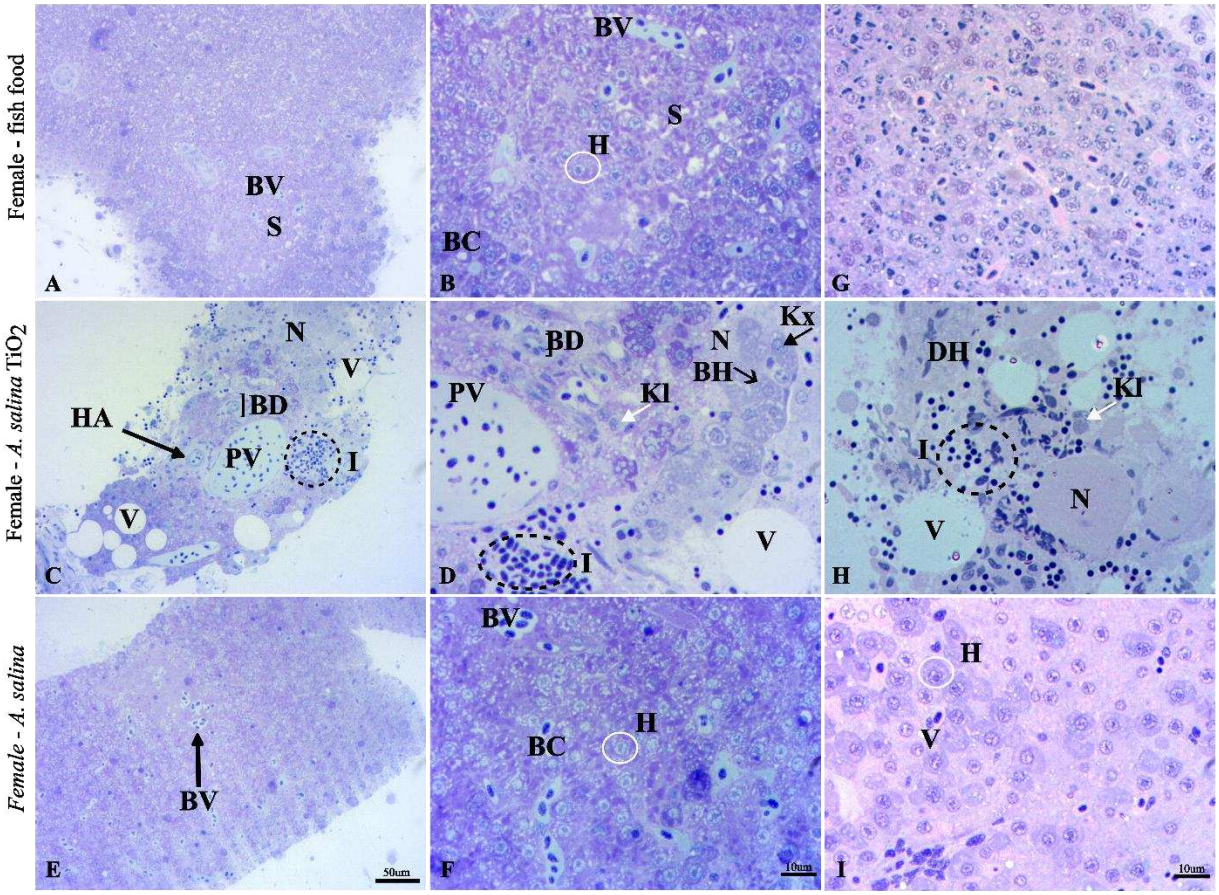

Figure 6. Liver sections of *Danio rerio* female individuals fed with different diets for 30 days. A, B and G: healthy liver histology, tissue structure and its components. Hepatocytes white circled (H), blood vessels (BV), synusoids (S) and biliary canaliculi (BC). C: Liver of fish fed with *A. salina* exposed to 50mg/L TiO_2 showing toxic effects in whole tissue. Portal vein (PV), hepatic artery (HA), biliary duct (BD), vacuolization (V), inflammatory infiltrate (I) and necrosis (N). D and H: Liver of fish fed with *A. salina* exposed to 50mg/L TiO_2 showing toxic effects in whole tissue. Portal vein (PV), biliary duct (BD), inflammatory infiltrate with lymphocytes (I), vacuolization (V), ballooning hepatocytes with thin arrowhead (BH), Necrosis area (N), degenerated hepatocytes (DH), hepatocyte nuclei in the karyorrhexis stage pointed by black arrow (kx) and karyolysis pointed by white arrow (kl). E, F and I: healthy liver histology, tissue structure and its components. Hepatocytes are white circled (H), blood vessels (BV), biliary canaliculi (BC). The panels A – F are toluidine blue stained. The panels G, H and I are hematoxilin-eosin stained.

Histological examination of male *Danio rerio* liver sections fed with different diets, revealed distinct tissue responses across treatment groups (Figure 7). Control animals presented preserved hepatic architecture with normal hepatocytes as shown in 7A, 7B, and 7G.

The histopathological alterations observed in the liver of zebrafish fed with *Artemia salina* exposed to 50 mg/L TiO_2, such as hepatocyte degeneration, extensive vacuolization, necrotic areas, and nuclear fragmentation (karyorrhexis and karyolysis), are consistent with toxic responses reported for other xenobiotics. Similar hepatic injuries, including vacuolation and nuclear necrosis, were described in zebrafish exposed to polychlorinated diphenyl ethers

(PCDEs), where the severity of damage increased with concentration, culminating in nuclear enlargement and diffuse tissue disruption at 50 μg/L (Ye *et al.*, 2022). These effects have been associated with impaired lipid metabolism, inhibition of protein synthesis, and cellular energy depletion (Macêdo *et al.*, 2020). Comparable findings were also reported in zebrafish exposed to fungicides like tebuconazole and difenoconazole, which similarly caused hepatic vacuolization and necrotic degeneration (Jiang *et al.*, 2020). In the present study, deformation of the hepatic artery observed in some individuals further indicates a vascular component of TiO_2 toxicity, likely associated with oxidative stress and inflammatory responses (Smorodinskaya et al., 2023). Collectively, these lesions corroborate the hepatotoxic potential of TiO_2 nanoparticles and reinforce concerns regarding their trophic transfer and bioaccumulation.

Hepatocyte alterations such as cytoplasmic vacuolization are commonly linked to glycogen depletion and lipid accumulation induced by toxic agents, which may compromise liver function. However, glycogen reduction alone does not necessarily indicate toxicity, as zebrafish exhibit high metabolic rates that naturally deplete glycogen during activity. In contrast, nuclear alterations—including vacuolization, atrophy, pyknosis, and fragmentation—are more reliable markers of functional damage and cellular degeneration (Borges *et al.*, 2019). Interestingly, nuclear hypertrophy, also noted in some specimens, may reflect elevated metabolic activity as an adaptive response to toxic stress. In more advanced stages of degeneration, a reduction in nuclear density has been observed, potentially as a protective mechanism against cellular collapse.

Similar hepatic alterations have been reported in zebrafish exposed to 547.64 mg/L fluoride (F) and 435.71 mg/L lead (Pb) contaminated water, with significant increases in vacuolation, atrophy, focal necrosis, and nuclear changes such as pyknosis and karyolysis, especially in males, suggesting a sex-specific sensitivity to toxicants (Wang *et al.*, 2022). After 45 and 90 days of exposure, both male and female zebrafish exhibited liver degeneration and impaired tissue architecture, along with disrupted oxidative balance and immune function. Changes in antioxidant enzymes (CAT, SOD, GPx), oxidative markers (ROS, MDA, GSH), and immune-related gene expression further reinforced the systemic impact of these contaminants on hepatic physiology.

However, unlike the findings reported by Wang *et al.* (2022), where sex-related differences in liver toxicity were observed following exposure to fluoride (F) and lead (Pb), no such variation was detected in the present study. The results suggest that titanium-induced

toxicity via trophic transfer does not differ between male and female zebrafish in any of the analyzed organs.

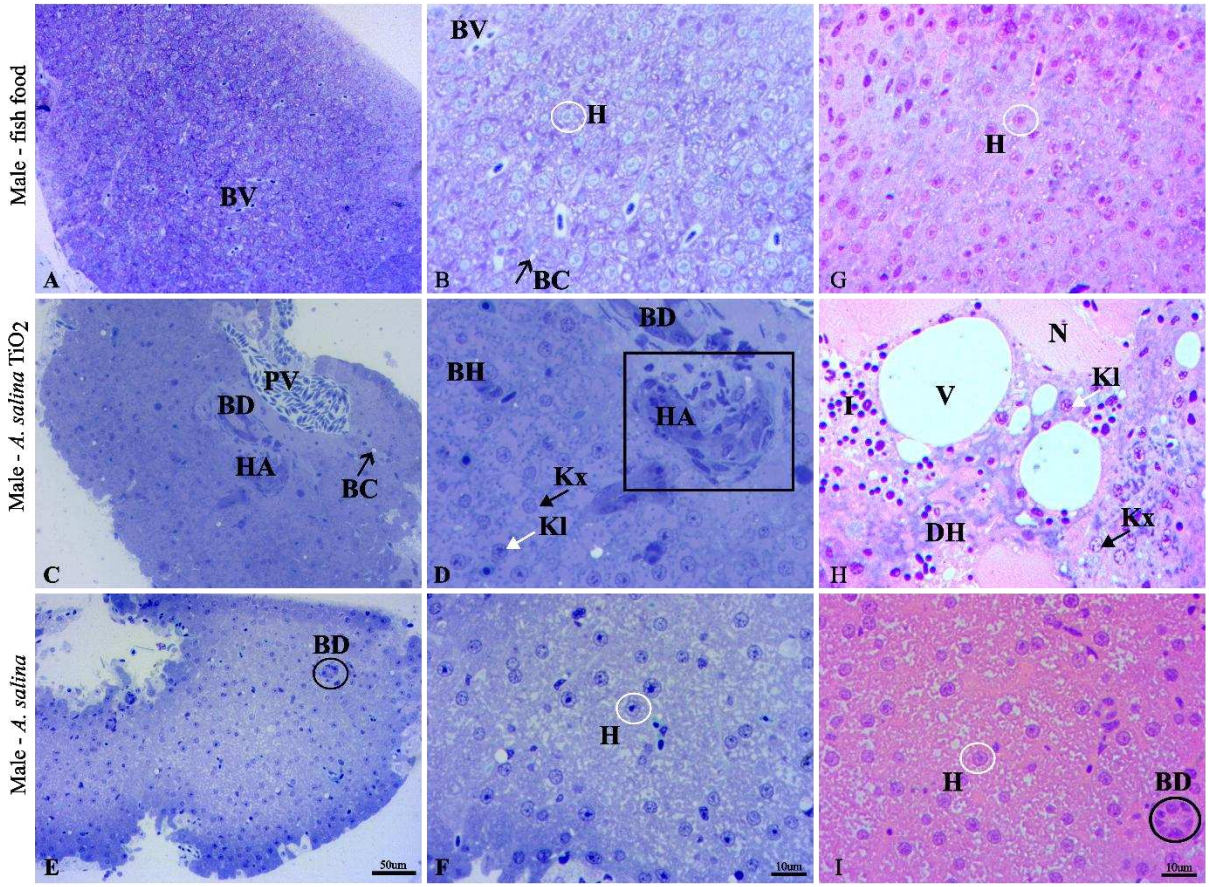

Figure 7. Liver sections of *Danio rerio* male individuals fed with different diets for 30 days. A, B and G: healthy liver histology, tissue structure and its components. Hepatocytes are white circled (H), blood vessels (BV), and biliary canaliculi pointed by thin black arrowhead (BC). C: Liver of fish fed with *A. salina* exposed to 50mg/L TiO_2 showing toxic effects in whole tissue. Portal vein (PV), hepatic artery (HA), biliary duct (BD), and biliary canaliculi pointed by thin black arrowhead (BC). D and H: Liver of fish fed with *A. salina* exposed to 50mg/L TiO_2 showing toxic effects in whole tissue. Biliary duct (BD), deformed hepatic artery highlighted by black square (HA), hepatocyte nuclei in the karyorrhexis stage pointed by black arrow (kx) and karyolysis pointed by white arrow (kl), vacuolization (V), necrosis (N) and degenerated hepatocytes (DH). E, F and I: healthy liver histology, tissue structure and its components. Hepatocytes are white circled (H), and biliary duct are black circled (BC). The images A, C and E have a 40x zoom. The images B, D, F, G, H and I have a 100x zoom. The panels A – F are toluidine blue stained. The panels G, H and I are hematoxilin-eosin stained.

Finally, the group fed only with uncontaminated *A. salina* displayed well-preserved liver morphology, as seen in fig. 7E, 7F, and 7I. These findings are mirroring the alterations observed in females and confirming the liver as a sensitive target of nanoparticle toxicity and impact the organs analyzed without difference between sex.

The fact that titanium dioxide is an insoluble particle in aqueous environments, and that no direct evidence of particle absorption was observed in the present study—only toxic effects associated with exposure—raises important environmental concerns. These findings

suggest that the mere contact with TiO_2 MPs, even in the absence of systemic absorption, may be sufficient to trigger cellular and histopathological damage. This aligns with the study by Ferraris *et al.* (2023), which demonstrated that food-grade TiO_2 (E171) particles exhibit high resistance to dissolution under gastrointestinal and lysosomal conditions. Their persistence in these biological environments not only challenges previous assumptions of extensive agglomeration and neutralization during digestion but also highlights their potential for bioaccumulation and transference through trophic levels. The stability and dispersion of TiO_2 under such conditions support the hypothesis that its toxic effects may propagate in aquatic systems even without full cellular uptake, thereby posing long-term risks to aquatic food webs.

Vignard *et al.* (2023) reinforce the potential for food-grade titanium dioxide (TiO_2) particles to translocate across biological barriers and enter cells, either as isolated particles or as small aggregates, regardless of their nominal size (nanometric or submicron). Using high-resolution imaging techniques such as confocal microscopy, TEM, and SIMS, the authors demonstrated cellular internalization of TiO_2 in buccal mucosa, suggesting that epithelial tissues may be directly exposed to particle-induced genotoxic effects. These results align with the present study, which, although not directly visualizing particle uptake, observed histopathological alterations consistent with cellular stress and damage—indicating that even in the absence of complete absorption or systemic distribution, the contact of TiO_2 with epithelial surfaces, including the gut lining, may be sufficient to induce toxicity.

6.2.4 Conclusion

The aggregation behavior of TiO_2 nanoparticles stabilized around 48 hours, coinciding with the exposure period of *Artemia salina* prior to being used as prey. No histological damage was observed in the gills of either sex, which is consistent with the dietary route of exposure rather than direct contact via the respiratory pathway. Nevertheless, gill analysis remains important in multi-route exposure assessments. In contrast, significant histopathological changes were identified in the intestine, including villus dissolution, altered goblet cell morphology, and enterocyte disorganization, indicating intestinal toxicity independent of sex. Similarly, the liver showed severe alterations such as hepatocyte degeneration, vacuolization, necrosis, and nuclear fragmentation. These findings highlight the toxic potential of titanium dioxide nanoparticles when transferred through the food chain, reinforcing concerns about their bioaccumulation and ecological impact.

Environmental safety of titanium dioxide cannot yet be confirmed. Further research under more realistic conditions and chronic exposure scenarios is essential to understand not only the immediate, but also long-term toxic effects of this compound. Such investigations are critical to provide clearer evidence for regulatory decisions, ensuring both environmental protection and consumer safety. Although trophic transfer of TiO_2 MPs could not be confirmed in the present study, it was demonstrated that toxic effects were caused by direct contact with the particles, and such effects may potentially propagate across trophic levels.

ACKNOWLEDGMENTS

ECM acknowledges funding from Universal and Analytical Center-UFC/CT-INFRA-FINEP/Pro-Equipamentos-CAPES/CNPq-SisNano-MCTI 2019 (Grant 442577/ 2019-2). Capes, INCT and FUNCAP. This work is part of the PhD research of AKML. CNPEM and LIST and GQMat.

AUTHOR CONTRIBUTION

All authors contributed to the study conception and design**.** Developed research (Emilio de Castro Miguel and Ana Kamila Medeiros Lima). Write the manuscript (Ana Kamila Medeiros Lima). Performed the experiments (Ana Kamila Medeiros Lima and João Vinicius Sousa Fernandes). All authors read and approved of the final manuscript.

CONFLICTS OF INTEREST

The authors declare no conflict of interest.

REFERENCES

ALONSO, Mariana B. *et al.* Toxic heritage: Maternal transfer of pyrethroid insecticides and sunscreen agents in dolphins from Brazil. **Environmental Pollution**, v. 207, p. 391–402, 2015.

ARMAN, S. Effects of acute triclosan exposure on gill and liver tissues of zebrafish (*Danio rerio*). **Annales de Limnologie – International Journal of Limnology**, v. 57, p. 6, 2021.

ARUOJA, Villem *et al.* Toxicity of 12 metal-based nanoparticles to algae, bacteria and protozoa. **Environmental Science: Nano**, v. 2, n. 6, p. 630–644, 2015.

BARBOSA, J. S.; NETO, D. M. A.; FREIRE, R. M.; ROCHA, J. S.; FECHINE, L. M. U. D.; DENARDIN, J. C. *et al.* Ultrafast sonochemistry-based approach to coat TiO_2 commercial particles for sunscreen formulation. **Ultrasonics Sonochemistry**, v. 48, p. 340–348, 2018. DOI: https://doi.org/10.1016/j.ultsonch.2018.06.015.

BEVACQUA, Emilia *et al.* TiO_2-NPs toxicity and safety: An update of the findings published over the last six years. **Mini-Reviews in Medicinal Chemistry**, v. 23, n. 9, p. 1050–1057, 2022.

BORGES, R. S. *et al.* Histopathology of zebrafish (*Danio rerio*) in nonclinical toxicological studies of new drugs. In: **Zebrafish in Biomedical Research**. London: IntechOpen, 2019.

BRASIL. Agência Nacional de Vigilância Sanitária. Nota Técnica nº 30/2021/SEI/GEARE/GGALI/DIRE2/ANVISA – Processo nº 25351.919622/2021-97. Brasília: ANVISA, 2023.

BRASIL. Câmara dos Deputados. Projeto proíbe uso de dióxido de titânio na produção de alimentos. **Agência Câmara de Notícias**, 2022. Disponível em: https://www.camara.leg.br/noticias/925401-projeto-proibe-uso-de-dioxido-de-titanio-na-producao-de-alimentos/. Acesso em: 11 jul. 2025.

CHENG, Yu *et al.* Diet dependent trophic transfer of nanoparticles (ZnO and TiO_2) along the "photic biofilm–snail" food chain. **Journal of Hazardous Materials**, v. 489, p. 137657, 2025.

CHICEA, Dan *et al.* Comparative synthesis of silver nanoparticles: Evaluation by AFM and DLS. **Materials**, v. 16, n. 15, p. 5244, 2023.

DOYLE, J. J.; PALUMBO, V.; HUEY, B. D.; WARD, J. E. Behavior of titanium dioxide nanoparticles in three aqueous media samples: Agglomeration and implications for benthic deposition. **Water, Air, and Soil Pollution**, v. 225, n. 9, p. 2106, 2014. DOI: https://doi.org/10.1007/s11270-014-2106-7.

EUROPEAN FOOD SAFETY AUTHORITY (EFSA). Commission Regulation (EU) 2022/63. [S.l.: s.n.], 2022.

FERRARIS, F. *et al.* Agglomeration behavior and fate of food-grade titanium dioxide in human gastrointestinal digestion and in the lysosomal environment. **Nanomaterials**, v. 13, n. 13, p. 1908, 2023. DOI: https://doi.org/10.3390/nano13131908.

GEIGER, B. M. *et al.* Intestinal upregulation of melanin-concentrating hormone in TNBS-induced enterocolitis in adult zebrafish. **PLoS ONE**, v. 8, n. 12, e83194, 2013.

GUO, X. *et al.* The distinct toxicity effects between commercial and realistic polystyrene microplastics on microbiome and histopathology of gut in zebrafish. **Journal of Hazardous Materials**, v. 434, p. 128874, 2022.
HEALTH CANADA'S FOOD DIRECTORATE. Titanium dioxide (TiO_2) as a food additive: Current science report. [S.l.: s.n.]. Disponível em: https://www.canada.ca/en/health-canada/services/food-nutrition/reports-.

JIANG, Jinhua *et al.* Effects of difenoconazole on hepatotoxicity, lipid metabolism and gut microbiota in zebrafish (*Danio rerio*). **Environmental Pollution**, v. 265, p. 114844, 2020.

KIM, Jung In *et al.* Trophic transfer of nano-TiO_2 in a paddy microcosm: A comparison of single-dose versus sequential multi-dose exposures. **Environmental Pollution**, v. 212, p. 316–324, 2016.

LEE, Yen Ling *et al.* Toxic effects and mechanisms of silver and zinc oxide nanoparticles on zebrafish embryos in aquatic ecosystems. **Nanomaterials**, v. 12, n. 4, 2022.

LI, Huiqi *et al.* Research progress of zebrafish model in aquatic ecotoxicology. **Water (Switzerland)**, 2023.

LI, Mingyang *et al.* Carbon quantum dots modification reduces TiO_2 nanoparticle toxicity in an aquatic food chain. **Journal of Hazardous Materials**, v. 486, p. 137115, 2025.

LU, Jing *et al.* TiO_2 nanoparticles enhanced bioaccumulation and toxic performance of PAHs via trophic transfer. **Journal of Hazardous Materials**, v. 407, p. 124834, 2021.

MACÊDO, Anderson Kelvin Saraiva *et al.* Histological and molecular changes in gill and liver of fish (*Astyanax lacustris* Lütken, 1875) exposed to water from the Doce basin after the rupture of a mining tailings dam. **Science of the Total Environment**, v. 735, p. 139505, 2020.

MARJORAM, L.; BAGNAT, M. Infection, inflammation and healing in zebrafish: Intestinal inflammation. **Current Pathobiology Reports**, v. 3, n. 2, p. 147–153, 2015.

MOTTOLA, Filomena *et al.* Evaluation of zebrafish DNA integrity after individual and combined exposure to TiO_2 nanoparticles and lincomycin. **Toxics**, v. 10, n. 3, 2022.

NASCIMENTO, G. C. Z. *et al.* Acute exposure of zebrafish (*Danio rerio*) adults to *Psychotria carthagenensis* leaf extracts. **Drug and Chemical Toxicology**, v. 47, n. 6, p. 1358–1368, 2024.

PENSADO-LÓPEZ, Alba *et al.* Zebrafish models for the safety and therapeutic testing of nanoparticles with a focus on macrophages. **Nanomaterials**, 2021.

RACOVITA, Anca Diana. Titanium dioxide: Structure, impact, and toxicity. **International Journal of Environmental Research and Public Health**, 2022.

RAHMANI, R. *et al.* Histopathological alterations in the gill of zebrafish (*Danio rerio*) exposed to Cr and Ba doped TiO_2 nanoparticles. 2016. Disponível em: http://eprints.iums.ac.ir/3379/. Acesso em: 8 jul. 2025.

SHABBIR, Samina *et al.* Toxicological consequences of titanium dioxide nanoparticles and their jeopardy to human population. **Bionanoscience**, v. 11, n. 2, p. 621–632, 2021.

SINGH, Kalpana; KASHYAP, Satyendra Kumar; GARG, Vandana. Use of zebrafish (*Danio rerio*) as a model for research in toxicological studies. **Journal of Applied and Natural Science**, 2021.

SMORODINSKAYA, Svetlana *et al.* Effects of acute bisphenol A toxicity on zebrafish (*Danio rerio*). **Animals**, v. 13, n. 23, p. 3685, 2023.

STACHURSKI, Piotr *et al.* A short review of the toxicity of dentifrices—zebrafish model. **International Journal of Molecular Sciences**, 2023.

VALÉRIO, Alexsandra *et al.* Are TiO_2 nanoparticles safe for photocatalysis in aqueous media? **Nanoscale Advances**, v. 2, n. 10, p. 4951–4960, 2020.

VIGNARD, Julien *et al.* Food-grade titanium dioxide translocates across the buccal mucosa in pigs. **Nanotoxicology**, v. 17, n. 4, p. 289–309, 2023.

VIJAYARAJ, Vinita *et al.* Transfer and ecotoxicity of titanium dioxide nanoparticles. **Environmental Science & Technology**, v. 52, n. 21, p. 12757–12764, 2018.

WANG, G. *et al.* Sex-specific effects of fluoride and lead exposures in zebrafish (*Danio rerio*). **Ecotoxicology**, v. 31, n. 3, p. 396–414, 2022.

WANG, Xueran *et al.* Nanoparticles in plants: Uptake, transport and physiological activity. **Materials**, v. 16, n. 8, p. 3097, 2023.

WU, Juan *et al.* Trophic transfer and toxicity of Ag and TiO_2 nanoparticles. **Environmental Science & Technology**, v. 55, n. 24, p. 16563–16572, 2021.

YE, C. *et al.* Biomarker responses in zebrafish (*Danio rerio*). **Frontiers in Physiology**, v. 13, p. 907906, 2022.

YEŞİLBUDAK, Burcu. Toxicological aspects and bioanalysis of nanoparticles. **Open Journal of Nano**, v. 8, n. 1, p. 22–35, 2023.

YU, F. *et al.* Toxicity of TPhP on zebrafish intestines. **Science of the Total Environment**, v. 908, p. 168212, 2024.

ZAHRA, Zahra *et al.* Exposure route of TiO_2 NPs and impacts on agro-environment. **Nanomaterials**, 2020.

ZHANG, M.; WU, C. Relationship between intestinal goblet cells and immune response. **Bioscience Reports**, v. 40, n. 10, p. BSR20201471, 2020.

ZHAO, Xingchen *et al.* Trophic transfer of metal nanoparticles diminishes toxicity disparities. **Environmental Science & Technology**, v. 59, n. 13, p. 6812–6824, 2025.

ZHU, D. H. *et al.* Effects of Aroclor 1254 on zebrafish immunity. **Frontiers in Nutrition**, v. 9, p. 929925, 2022.

7 CONSIDERAÇÕES FINAIS

O conjunto de resultados desta tese demonstra que a toxicidade das micropartículas de dióxido de titânio (TiO_2MPs) é modulada pela concentração, pelo tempo de exposição e pelo modelo biológico avaliado. Mesmo na ausência de absorção celular confirmada, o contato direto com as partículas foi suficiente para induzir danos celulares e estruturais em diferentes organismos, incluindo plantas e animais.

Em embriões de *Danio rerio*, o córion desempenhou um papel fundamental como barreira protetora, atenuando os efeitos tóxicos e evidenciando sua importância na modulação da biodisponibilidade e da sensibilidade embrionária aos nanomateriais. Em organismos adultos de *Danio rerio*, a exposição por via trófica evidenciou o intestino e o fígado como os principais órgãos-alvo da toxicidade, reforçando o potencial do TiO_2 em causar efeitos adversos ao longo da cadeia alimentar. A exposição prolongada resultou em alterações morfológicas, inflamatórias e apoptóticas, indicando riscos ecológicos relevantes e possíveis impactos cumulativos nos ecossistemas.

Dessa forma, os achados ressaltam a necessidade de estudos crônicos e conduzidos sob condições ambientais mais realistas, a fim de compreender de maneira mais precisa os efeitos de longo prazo do TiO_2 e subsidiar avaliações de risco ambiental e decisões regulatórias mais robustas.

REFERÊNCIAS

ABDEL-LATIF, H. M. R. et al. Environmental transformation of n-TiO_2 in aquatic systems and ecotoxicity in bivalve mollusks: a systematic review. **Ecotoxicology and Environmental Safety**, v. 200, p. 110776, 2020.

AGHDAM, Mohammad Taieb Baiazidi; MOHAMMADI, Hamid; GHORBANPOUR, Mansour. Effects of nanoparticulate anatase titanium dioxide on physiological and biochemical performance of *Linum usitatissimum* under well-watered and drought stress conditions. **Brazilian Journal of Botany**, v. 39, p. 139–146, 2016.

AL-JARYAN, Sara Khalid; ABD AL-REZZAQ, Adi Jassim; AL-AMARI, Moayed J. Y. Using algae and brine shrimp as food chain model for bioaccumulation and biomagnification of lead and cadmium. **Journal of Applied & Natural Science**, v. 16, n. 2, 2024.

ALONSO, Mariana B. et al. Toxic heritage: Maternal transfer of pyrethroid insecticides and sunscreen agents in dolphins from Brazil. **Environmental Pollution**, v. 207, p. 391–402, 2015.

AN, G. et al. Developmental toxicity of dimethachlor during zebrafish embryogenesis. **Journal of Animal Reproduction and Biotechnology**, v. 36, n. 1, p. 2–8, 2021.

AN, H. J. et al. Comparative toxicity of silver nanoparticles and silver nanowires on saltwater microcrustacean *Artemia salina*. **Comparative Biochemistry and Physiology Part C**, v. 218, p. 62–69, 2019.

ANDERSEN, C. P. et al. Germination and early plant development of ten plant species exposed to titanium dioxide and cerium oxide nanoparticles. **Environmental Toxicology and Chemistry**, v. 35, p. 2223–2229, 2016.

ANDREANI, T. et al. The critical role of dispersant agents in the preparation and ecotoxicity of nanomaterial suspensions. **Environmental Science and Pollution Research**, v. 27, p. 19845–19857, 2020.

ARABEYYAT, Z. H. et al. Toxicity of polyelectrolyte-functionalized titania nanoparticles in zebrafish embryos. **SN Applied Sciences**, v. 2, n. 7, 2020.

ARMAN, S. Effects of acute triclosan exposure on gill and liver tissues of zebrafish (*Danio rerio*). **Annales de Limnologie – International Journal of Limnology**, v. 57, p. 6, 2021.

ARUOJA, V. et al. Toxicity of 12 metal-based nanoparticles to algae, bacteria and protozoa. **Environmental Science: Nano**, v. 2, n. 6, p. 630–644, 2015.

ASZTEMBORSKA, M. et al. Titanium dioxide nanoparticle circulation in aquatic ecosystems. **Water, Air, and Soil Pollution**, v. 229, n. 6, p. 208, 2018.

ATES, M. et al. Effects of aqueous suspensions of titanium dioxide nanoparticles on *Artemia salina*. **Environmental Monitoring and Assessment**, v. 185, p. 3339–3348, 2013.

ATES, M. et al. Comparative evaluation of Zn and ZnO nanoparticles toxicity in brine shrimp. **Environmental Science: Processes & Impacts**, v. 15, p. 225–233, 2013.

ATES, M. et al. Assessment of oxidative stress on *Artemia salina* and *Daphnia magna* after Zn and ZnO nanoparticles exposure. **Bulletin of Environmental Contamination and Toxicology**, v. 104, p. 206–214, 2020.

BAI, C.; TANG, M. Toxicological study of metal nanoparticles in zebrafish. **Journal of Applied Toxicology**, v. 40, n. 1, p. 37–63, 2020.

BARANOVA, E. N. et al. Targeted protection of mitochondria of mesophyll cells in transgenic tobacco under salt stress. **Proceedings of the Latvian Academy of Sciences**, p. 334–340, 2018.

BARBOSA, J. S. et al. Ultrafast sonochemistry-based approach to coat TiO_2 commercial particles for sunscreen formulation. **Ultrasonics Sonochemistry**, v. 48, p. 340–348, 2018.

BARRENA, R. et al. Evaluation of the ecotoxicity of model nanoparticles. **Chemosphere**, v. 75, n. 7, p. 850–857, 2009.

BEVACQUA, E. et al. TiO_2-NPs toxicity and safety: an update of the findings published over the last six years. **Mini-Reviews in Medicinal Chemistry**, v. 23, n. 9, p. 1050–1057, 2022.

BERGAMI, E. et al. Nano-sized polystyrene affects feeding and physiology of *Artemia franciscana*. **Ecotoxicology and Environmental Safety**, v. 123, p. 18–25, 2016.

BORAN, H. et al. Hg^{2+} association with TiO_2 nanoparticles and bioavailability to zebrafish. **Aquatic Toxicology**, v. 174, p. 242–246, 2016.

BORGES, R. S. et al. Histopathology of zebrafish in nonclinical toxicological studies. In: **Zebrafish in Biomedical Research**. London: IntechOpen, 2019.

BRAND, W. et al. Possible effects of titanium dioxide particles on human tissues after oral exposure. **Nanotoxicology**, v. 14, n. 7, p. 985–1007, 2020.

BRASIL. Agência Nacional de Vigilância Sanitária. Nota Técnica nº 30/2021. Brasília: ANVISA, 2023.

BRASIL. Câmara dos Deputados. Projeto proíbe uso de dióxido de titânio na produção de alimentos. Agência Câmara de Notícias, 2022.

BUNDSCHUH, M. et al. Nanoparticles in the environment: Where do we come from, where do we go to? **Environmental Sciences Europe**, v. 30, p. 1–17, 2018.

CASTIGLIONE, M. R. et al. Root responses to different types of TiO_2 nanoparticles in *Vicia faba*. **Environmental and Experimental Botany**, v. 130, p. 11–21, 2016.

CEGER, P. et al. Current ecotoxicity testing needs among US federal agencies. **Regulatory Toxicology and Pharmacology**, v. 133, p. 105195, 2022.

CHAHARDOLI, A.; KARIMI, N.; SHARIFIAN, H. Phytotoxic endpoints of titanium dioxide nanoparticles in *Dracocephalum* species. **Chemosphere**, v. 370, p. 143853, 2025.

CHEN, H. et al. Combined neurotoxicity of DBP and nano-TiO_2 in zebrafish. **Aquatic Toxicology**, v. 269, p. 106881, 2024.

CHENG, Y. et al. Diet-dependent trophic transfer of ZnO and TiO_2 nanoparticles. **Journal of Hazardous Materials**, v. 489, p. 137657, 2025.

CHICEA, D. et al. Comparative synthesis of silver nanoparticles evaluated by AFM and DLS. **Materials**, v. 16, n. 15, p. 5244, 2023.

CLEMENT, L.; HUREL, C.; MARMIER, N. Toxicity of TiO_2 nanoparticles to aquatic organisms and plants. **Chemosphere**, v. 90, n. 3, p. 1083–1090, 2013.

CORSI, I.; DESIMONE, M. F.; CAZENAVE, J. Building the bridge from aquatic nanotoxicology to safety by design silver nanoparticles. **Frontiers in Bioengineering and Biotechnology**, 2022.

COX, A. et al. Silver and titanium dioxide nanoparticle toxicity in plants: a review. **Plant Physiology and Biochemistry**, v. 110, p. 33–49, 2017.

DAMAS-SOUZA, D. M. et al. Improved acridine orange staining of DNA/RNA. **Acta Histochemica**, v. 121, p. 450–457, 2019.

DE PAIVA PINHEIRO, S. K. et al. Acute toxicity of titanium dioxide microparticles in *Artemia* nauplii. **Microscopy Research and Technique**, v. 86, n. 6, p. 636–647, 2023.

DOYLE, J. J. et al. Behavior of titanium dioxide nanoparticles in aqueous media. **Water, Air, and Soil Pollution**, v. 225, n. 9, p. 2106, 2014.

DUAN, Z. et al. Barrier function of zebrafish embryonic chorions against microplastics. **Journal of Hazardous Materials**, v. 395, p. 122621, 2020.

DUTTA, P. et al. Nanoparticles: the plant saviour under abiotic stresses. **Nanomaterials**, v. 12, n. 21, p. 3915, 2022.

EGLER, S. G. et al. Phytotoxicity of rare earth elements in *Lactuca sativa*. **Ecotoxicology**, v. 33, n. 10, p. 1193–1209, 2024.

EMAMVERDIAN, A. et al. Physiological responses of bamboo to TiO_2 nanoparticles under heavy metal toxicity. **Forests**, v. 12, n. 6, 2021.

EUROPEAN COMMISSION. Commission recommendation of 10.06.2022 on the definition of nanomaterial. Brussels, 2022.

EUROPEAN FOOD SAFETY AUTHORITY (EFSA). Commission Regulation (EU) 2022/63. 2022.

FARAHI, S. M. M. et al. Effects of TiO_2 nanoparticles on *Vitex agnus-castus*. **Heliyon**, v. 9, n. 11, 2023.

FARRÉ, M. et al. Ecotoxicity and analysis of nanomaterials in aquatic environments. **Analytical and Bioanalytical Chemistry**, v. 393, p. 81–95, 2009.

FERRARIS, F. et al. Agglomeration behavior of food-grade titanium dioxide. **Nanomaterials**, v. 13, n. 13, p. 1908, 2023.

FIROOZI, A. A. et al. Influence of nanomaterials for civil engineering projects. **Iranian Journal of Science and Technology**, v. 45, p. 2057–2068, 2021.

FLOR, J.; DAVOLOS, M. R.; CORREA, M. A. Protetores solares. **Revista Brasileira de Medicina**, v. 65, p. 6–11, 2008.

FRENCH, R. A. et al. Aggregation kinetics of titanium dioxide nanoparticles. **Environmental Science & Technology**, v. 43, n. 5, p. 1354–1359, 2009.

GAMBardella, C. et al. Effects of metal oxide nanoparticles on *Artemia salina*. **Environmental Monitoring and Assessment**, 2014.

GARAVENTA, F. et al. Swimming speed alteration as a sublethal endpoint. **Ecotoxicology**, v. 19, p. 512–519, 2010.

GARCÍA-SÁNCHEZ, S. et al. Early response to nanoparticles in *Arabidopsis*. **BMC Genomics**, v. 16, 2015.

GEIGER, B. M. et al. Intestinal responses in zebrafish enterocolitis. **PLoS ONE**, v. 8, n. 12, e83194, 2013.

GUTSCH, A. et al. Cadmium exposure effects on plant cell walls. **BMC Plant Biology**, v. 19, p. 271, 2019.

HANIGAN, D. et al. Ecosystem impacts of nanomaterial versus organic UV filters. **Water Research**, v. 139, p. 281–290, 2018.

HANSJOSTEN, I. et al. Surface functionalisation-dependent adverse effects in zebrafish embryos. **Environmental Science: Nano**, v. 9, n. 1, p. 375–392, 2022.

HAYNES, V. N. et al. Photocatalytic effects of titanium dioxide nanoparticles. **Aquatic Toxicology**, v. 185, p. 138–148, 2017.

HOWE, K. et al. Zebrafish reference genome. **Nature**, v. 496, p. 498–503, 2013.

HU, J. et al. TiO_2 nanoparticle exposure effects on *Lactuca sativa*. **Environmental Science: Nano**, v. 7, n. 2, p. 501–513, 2020.

HUANG, D. et al. Uptake and transformation of silver nanoparticles in plants. **Environmental Science: Nano**, v. 9, n. 1, p. 12–39, 2022.

IANNONE, M. F. et al. Impact of magnetite nanoparticles on wheat development. **Environmental and Experimental Botany**, v. 131, p. 77–88, 2016.

JAFARI, A. et al. Toxicity of green synthesized TiO_2 nanoparticles in zebrafish. **Environmental Research**, v. 212, p. 113542, 2022.

JOHARI, S. A. et al. ISO/TS 20787 aquatic toxicity assessment using *Artemia*. **Toxicology Mechanisms and Methods**, v. 29, p. 95–109, 2019.

JUNG, M.; CHOI, H.; MUN, J. Y. Autophagy research in electron microscopy. **Applied Microscopy**, v. 49, n. 1, p. 11, 2019.

KACHENTON, S. et al. Cytotoxicity of titanium nanoparticles in *Artemia salina*. **Environmental Science and Pollution Research**, v. 26, p. 14706–14711, 2019.

KHAN, A. R. et al. ZnO nanoparticles effects in rice seedlings. **Ecotoxicology and Environmental Safety**, v. 226, p. 112844, 2021.

KHAN, M. N. et al. Role of nanomaterials in plants under stress. **Plant Physiology and Biochemistry**, v. 110, p. 194–209, 2017.

KRISHNA, R. et al. Toxicological effects of metal nanoparticles in biomedicine. **Macromolecular Symposia**, v. 413, n. 1, 2024.

LACAVE, J. M. et al. Dietary transfer of silver nanoparticles from *Artemia* to zebrafish. **Comparative Biochemistry and Physiology Part C**, v. 199, p. 69–80, 2017.

LARUE, C. et al. Foliar exposure of *Lactuca sativa* to silver nanoparticles. **Journal of Hazardous Materials**, v. 264, p. 98–106, 2014.

LEE, Y. L. et al. Toxic effects of silver and zinc oxide nanoparticles. **Nanomaterials**, v. 12, n. 4, p. 717, 2022.

LI, S. et al. Auxin and nitric oxide regulation in *Arabidopsis thaliana*. **Planta**, v. 259, n. 3, p. 52, 2024.

LIMA, A. K. M. et al. Effect of TiO_2 microparticles in lettuce. **Bulletin of Environmental Contamination and Toxicology**, v. 110, n. 6, 2023.

LIU, Y. et al. Combined toxicity of Cu and ZnO nanoparticles. **Environmental Science & Technology**, v. 50, n. 10, p. 5328–5337, 2016.

LUO, Z. et al. Rethinking nano-TiO_2 safety. **Small**, v. 16, n. 36, p. 2002019, 2020.

MA, H. et al. Oxidative stress and genotoxicity induced by titanium dioxide nanoparticles in zebrafish (*Danio rerio*). **Environmental Toxicology**, v. 33, n. 5, p. 534–543, 2018. DOI: 10.1002/tox.22540.

MAGDOLENOVA, Z. et al. Can standard genotoxicity tests be applied to nanoparticles? **Journal of Toxicology and Environmental Health, Part A**, v. 75, n. 13–15, p. 800–806, 2012. DOI: 10.1080/15287394.2012.690793.

MAKOWEJ, A. T.; ORZECHOWSKA, A.; SZYMAŃSKA, R. Hormetic effect of titanium dioxide nanoparticles on plants. **Science of the Total Environment**, v. 910, p. 168669, 2024.

MALHOTRA, N. et al. Titanium dioxide nanoparticles induce oxidative stress and genotoxicity in human liver cells. **Journal of Biomedical Nanotechnology**, v. 12, n. 6, p. 1196–1208, 2016.

MARTINS, N. et al. Toxicity of engineered nanoparticles in aquatic organisms. **Environmental Pollution**, v. 193, p. 56–63, 2014.

MATTOS, J. J. et al. Avaliação citogenotóxica de contaminantes ambientais utilizando *Allium cepa*. **Revista Brasileira de Toxicologia**, v. 29, n. 2, p. 45–52, 2016.

MCNEIL, S. E. Nanoparticle characterization and exposure assessment. **Wiley Interdisciplinary Reviews: Nanomedicine and Nanobiotechnology**, v. 3, n. 4, p. 373–382, 2011.

MELETIADIS, S. et al. Nanoparticle dispersion stability and biological effects. **Nanotoxicology**, v. 14, n. 6, p. 726–741, 2020.

MENEZES, A. P. et al. Phytotoxicity of metal oxide nanoparticles in lettuce (*Lactuca sativa*). **Ecotoxicology and Environmental Safety**, v. 148, p. 648–655, 2018.

MISHRA, V. et al. Interaction of nanoparticles with plant cell walls. **Plant Physiology and Biochemistry**, v. 110, p. 59–69, 2017.

MONTEIRO, R. T. R. Ecotoxicologia de organismos aquáticos. São Paulo: Blucher, 2016.

MORAES, B. S. et al. Toxic effects of nanomaterials on aquatic biota. **Aquatic Toxicology**, v. 170, p. 1–8, 2016.

MORGAN, A. M. et al. Uptake and toxicity of titanium dioxide nanoparticles in zebrafish embryos. **Chemosphere**, v. 152, p. 233–240, 2016.

NAMDEO, M.; SAXENA, S.; TANKHIWALE, R.; BAJPAI, M.; MOHAN, Y. M.; BAJPAI, S. K. Magnetic nanoparticles for drug delivery applications. **Journal of Nanoscience and Nanotechnology**, v. 8, n. 7, p. 3247–3271, 2008. DOI: 10.1166/jnn.2008.399.

NASCIMENTO, G. C. Z. et al. Acute exposure of zebrafish (*Danio rerio*) adults to

Psychotria carthagenensis leaf extracts. **Drug and Chemical Toxicology**, v. 47, n. 6, p. 1358–1368, 2024.

NEWMAN, M. D.; STOTLAND, M.; ELLIS, J. I. The safety of nanosized particles in titanium dioxide- and zinc oxide-based sunscreens. **Journal of the American Academy of Dermatology**, v. 61, n. 4, p. 685–692, 2009. DOI: 10.1016/j.jaad.2009.02.051.

NICOLÁS-ÁLVAREZ, D. E. et al. Effects of TiO_2 nanoparticles in tomato roots. **Nanomaterials**, v. 11, n. 5, p. 1127, 2021.

NNAJI, N. D. et al. Bioaccumulation for heavy metal removal: a review. **SN Applied Sciences**, v. 5, n. 5, p. 125, 2023.

NOHYNEK, G. J.; DUFOUR, E. K.; ROBERTS, M. S. Nanotechnology, cosmetics and the skin: Is there a health risk? **Skin Pharmacology and Physiology**, v. 21, n. 3, p. 136–149, 2008. DOI: 10.1159/000131078.

NOWACK, B.; BUCHELI, T. D. Occurrence, behavior and effects of nanoparticles in the environment. **Environmental Pollution**, v. 150, p. 5–22, 2007. DOI: 10.1016/j.envpol.2007.06.006.

NUNES, B. S.; CARVALHO, F. D.; GUILHERMINO, L. M.; VAN STAPPEN, G. Use of the genus *Artemia* in ecotoxicity testing. **Environmental Pollution**, v. 144, p. 453–462, 2006. DOI: 10.1016/j.envpol.2005.12.037.

O'BRIEN, T. P.; FEDER, N.; MCCULLY, M. E. Polychromatic staining of plant cell walls by toluidine blue O. **Protoplasma**, v. 59, n. 2, p. 368–373, 1964.

OCARANZA-JOYA, V. S. et al. Sensitivity of different stages of *Artemia franciscana* to potassium dichromate. **Pan-American Journal of Aquatic Sciences**, v. 14, p. 8–12, 2019.

OECD. **Guideline for the testing of chemicals**. Paris: OECD Publishing, 2004. DOI: 10.1787/9789264069947-en.

OECD. **Test No. 236: Fish Embryo Acute Toxicity (FET) Test**. Paris: OECD Publishing, 2025.

OKUMU, M. O. et al. *Artemia salina* as an animal model for the preliminary evaluation of snake venom-induced toxicity. **Toxicon: X**, v. 12, 2021.

OLIVER, A. L. S. et al. Bioaccumulation of ionic titanium and titanium dioxide nanoparticles in zebrafish eleutheroembryos. **Nanotoxicology**, v. 9, n. 7, p. 835–842, 2015.

ONDRASEK, G. et al. Zinc and cadmium mapping in radish tissues. **International Journal of Environmental Research and Public Health**, v. 16, n. 3, p. 373, 2019.

ORTIZ-ROMÁN, M. I. et al. Ecotoxicological effects of TiO_2 P25 nanoparticles. **Nanomaterials**, v. 14, n. 4, p. 373, 2024.

OST, A. D. et al. The Ionmaster magSIMS. 2024.

OZKAN, Y.; ALTINOK, I.; ILHAN, H.; SOKMEN, M. Determination of TiO_2 and $AgTiO_2$ nanoparticles in *Artemia salina*. **Bulletin of Environmental Contamination and Toxicology**, v. 96, p. 36–42, 2016. DOI: 10.1007/s00128-015-1634-1.

PAATERO, I. et al. Nanotoxicity profiles dependent on surface-functionalization. **Scientific Reports**, v. 7, p. 8423, 2017.

PECORARO, R. et al. *Artemia salina*: a microcrustacean to assess engineered nanoparticles toxicity. **Microscopy Research and Technique**, v. 84, p. 531–536, 2021. DOI: 10.1002/jemt.23609.

PECORARO, R. et al. Toxicity of titanium dioxide–cerium oxide nanocomposites to zebrafish embryos. **Toxics**, v. 11, n. 12, 2023.

PENSADO-LÓPEZ, A. et al. Zebrafish models for the safety and therapeutic testing of nanoparticles. **Nanomaterials**, 2021.

PÉREZ-ATEHORTÚA, M. et al. Chorion in fish: synthesis and malformations. **Aquaculture Reports**, v. 30, p. 101590, 2023.

PEREIRA, S. P. et al. Toxicity and accumulation of metal from copper oxide nanomaterials. **Ecotoxicology and Environmental Safety**, v. 253, p. 114613, 2023.

PEREIRA, S. P. P. et al. Toxicity of silver nanomaterials versus silver nitrate in zebrafish. **Chemosphere**, v. 336, p. 139236, 2023.

PINO, M. R. et al. Phytotoxicity of pharmaceuticals on *Lactuca sativa*. **Environmental Science and Pollution Research**, v. 23, n. 22, p. 22530–22541, 2016.

PINHEIRO, S. K. de P. et al. Assessing toxicity mechanism of silver nanoparticles using *Artemia salina*. **Chemosphere**, v. 347, 2024.

POLISCHUK, S. D. et al. Reasons for different environmental effects of technogenic nanoparticles. 2022.

RACOVITA, A. D. Titanium dioxide: structure, impact, and toxicity. **International Journal of Environmental Research and Public Health**, 2022.

RAHMANI, R. et al. Histopathological alterations in the gill of zebrafish (*Danio rerio*) exposed to Cr and Ba doped TiO_2 nanoparticles. 2016. Disponível em: http://eprints.iums.ac.ir/3379/. Acesso em: 8 jul. 2025.

RAJAKARUNA, T. P. B. et al. Nonhazardous process for extracting pure titanium dioxide nanorods from geogenic ilmenite. **ACS Omega**, v. 5, n. 26, p. 16176–16182, 2020.

RALIA, R. et al. Mechanistic evaluation of translocation and physiological impact of titanium dioxide and zinc oxide nanoparticles on tomato plants (*Solanum lycopersicum* L.). **Metallomics**, v. 12, p. 1584–1594, 2015.

RAO, M. J.; ZHENG, B. Polyphenols in abiotic stress tolerance. **Antioxidants**, v. 14, n. 1, p. 74, 2025.

RASTOGI, A. et al. Impact of metal and metal oxide nanoparticles on plants: a critical review. **Frontiers in Chemistry**, v. 5, p. 1–16, 2017. DOI: 10.3389/fchem.2017.00078.

REICHSTEIN, I. S. et al. Improving predictive ability of the FET test using metabolization systems. **Environmental Sciences Europe**, v. 36, n. 1, p. 91, 2024.

REKULAPALLY, R. et al. Toxicity of TiO_2, SiO_2, ZnO, CuO, Au and Ag engineered nanoparticles on *Artemia* sp. **PeerJ**, e6138, 2019. DOI: 10.7717/peerj.6138.

RIBBLE, D.; GOLDSTEIN, N. B.; NORRIS, D. A.; SHELLMAN, Y. G. A simple technique for quantifying apoptosis in 96-well plates. **BMC Biotechnology**, v. 5, p. 1–7, 2005. DOI: 10.1186/1472-6750-5-12.

RODRÍGUEZ-GONZÁLEZ, V.; TERASHIMA, C.; FUJISHIMA, A. Applications of photocatalytic titanium dioxide-based nanomaterials in sustainable agriculture. **Journal of Photochemistry and Photobiology C**, v. 40, p. 49–67, 2019.

SADRIEH, N.; WOKOVICH, A. M.; GOPEE, N. V.; ZHENG, J.; HAINES, D.; PARMITER, D.; SIITONEN, P. H.; COZART, C. R.; PATRI, A. K.; MCNEIL, S. E.; HOWARD, P. C.; DOUB, W. H.; BUHSE, L. F. Lack of significant dermal penetration of titanium dioxide from sunscreen formulations containing nano- and submicron-size TiO_2 particles. **Toxicological Sciences**, v. 115, n. 1, p. 156–166, 2010. DOI: 10.1093/toxsci/kfq041.

SALA, F. C.; COSTA, C. P. da. Retrospectiva e tendência da alfacicultura brasileira. **Horticultura Brasileira**, v. 30, n. 2, p. 187–194, 2012. DOI: 10.1590/S0102-05362012000200002.

SÁNCHEZ-FORTÚN, S.; SANZ, F.; BARAHONA, M. V. Acute toxicity of several organophosphorous insecticides on *Artemia salina* larvae. **Archives of Environmental Contamination and Toxicology**, v. 31, p. 391–398, 1996. DOI: 10.1007/BF00212678.

SANTOS FILHO, R. et al. Genotoxicity of titanium dioxide nanoparticles and triggering of defense mechanisms in *Allium cepa*. **Genetics and Molecular Biology**, v. 42, p. 425–435, 2019. DOI: 10.1590/1678-4685-GMB-2018-0205.

SARKHEIL, M. et al. Acute toxicity, uptake, and elimination of ZnO nanoparticles in *Artemia franciscana*. **Environmental Toxicology and Pharmacology**, v. 57, p. 181–188, 2018. DOI: 10.1016/j.etap.2017.12.018.

SCALISI, E. M. et al. Titanium dioxide nanoparticles: effects on development and male reproductive system. **Nanomaterials**, v. 13, n. 11, 2023.

SCHWAB, F. et al. Barriers, pathways and processes for uptake and accumulation of nanomaterials in plants. **Nanotoxicology**, v. 10, p. 257–278, 2016. DOI: 10.3109/17435390.2015.1048326.

SEGNER, H. Zebrafish as a model for investigating endocrine disruption. **Comparative Biochemistry and Physiology Part C**, v. 149, n. 2, p. 187–195, 2009.

SENDRA, M. et al. Effects of TiO_2 nanoparticles and sunscreens on coastal marine microalgae. **Environment International**, v. 98, p. 62–68, 2017. DOI: 10.1016/j.envint.2016.09.024.

SENTIS, M. P. et al. Investigation of nanoparticle dispersibility and stability based on TiO_2 analysis by SMLS, DLS, and SEM. **Journal of Nanoparticle Research**, v. 26, n. 3, p. 55, 2024.

SERVIN, A. D. et al. Uptake and translocation of TiO_2 nanoparticles in *Cucumis sativus*. **Environmental Science & Technology**, v. 46, n. 14, p. 7637–7643, 2012.

SHABBIR, S. et al. Toxicological consequences of titanium dioxide nanoparticles. **Bionanoscience**, v. 11, n. 2, p. 621–632, 2021.

SHI, H. et al. Titanium dioxide nanoparticles: a review of current toxicological data. **Particle and Fibre Toxicology**, v. 10, p. 1–33, 2013. DOI: 10.1186/1743-8977-10-15.

SHELKE, D. B. et al. Mycogenic nanoparticles in crops. **Biocatalysis and Agricultural Biotechnology**, v. 52, p. 102805, 2023.

SINGH, A. et al. Plant–nanoparticle interaction. **Environmental Chemistry Letters**, v. 13, p.

429–441, 2015.

SINGH, K.; KASHYAP, S. K.; GARG, V. Use of zebrafish (*Danio rerio*) as a toxicological model. **Journal of Applied and Natural Science**, 2021.

SIROTIKIN, A. V. et al. Toxic influence of silver and titanium dioxide nanoparticles on ovarian granulosa cells. **Reproductive Biology**, v. 21, p. 100467, 2021.

SMIJS, T. G.; PAVEL, S. Titanium dioxide and zinc oxide nanoparticles in sunscreens. **Nanotechnology, Science and Applications**, 2011.

SMORODINSKAYA, S. et al. Acute bisphenol A toxicity in zebrafish. **Animals**, v. 13, n. 23, p. 3685, 2023.

SOBANSKA, M. et al. Applicability of the FET test (OECD 236). **Environmental Toxicology and Chemistry**, v. 37, n. 3, p. 657–670, 2018.

SORGELOOS, P.; REMICHE-VAN DER WIELEN, C.; PERSOONE, G. The use of *Artemia* nauplii for toxicity tests. **Ecotoxicology and Environmental Safety**, v. 2, p. 249–255, 1978.

STACHURSKI, P. et al. Toxicity of dentifrices: zebrafish model. **International Journal of Molecular Sciences**, 2023.

TANG, T.; ZHANG, Z.; ZHU, X. Toxic effects of TiO_2 nanoparticles on zebrafish. **International Journal of Environmental Research and Public Health**, v. 16, n. 4, 2019.

TENHAKEN, R. Cell wall remodeling under abiotic stress. **Frontiers in Plant Science**, v. 5, p. 771, 2015.

TOMBULOGLU, H. et al. Impact of $MnFe_2O_4$ nanoparticles on barley. **Environmental Pollution**, v. 243, p. 872–881, 2018.

TRELA-MAKOWEJ, A.; ORZECHOWSKA, A.; SZYMAŃSKA, R. Hormetic effect of TiO_2 nanoparticles on plants. **Science of the Total Environment**, v. 910, p. 168669, 2024.

TRIPATHI, S. et al. Interaction of silver nanoparticles with plants. **Plant Nano Biology**, p. 100082, 2024.

TYULKOVA, E. G. Anatomical structure of wood plant leaves under VOC exposure. **Ecology and Noospherology**, v. 31, n. 1, p. 52–58, 2020.

VALÉRIO, A. et al. Are TiO_2 nanoparticles safe for photocatalysis in aqueous media? **Nanoscale Advances**, v. 2, n. 10, p. 4951–4960, 2020.

VAN DOORN, W. G. et al. Morphological classification of plant cell deaths. **Cell Death & Differentiation**, v. 18, n. 8, p. 1241–1246, 2011.

VASYUKOVA, I. A. et al. Toxic effects of metal-based nanomaterials in marine ecosystems. **Nanobiotechnology Reports**, v. 16, p. 138–154, 2021.

VIEIRA, C.; MARCON, C.; DROSTE, A. Phytotoxic and cytogenotoxic effects of glyphosate on *Lactuca sativa*. **Brazilian Journal of Biology**, v. 84, 2024.

VIEIRA, L. R. et al. Proteomics of zebrafish larvae exposed to 3,4-dichloroaniline. **Environmental Toxicology**, v. 35, n. 8, p. 849–860, 2020.

VIGNARD, J. et al. Food-grade titanium dioxide translocates across the buccal mucosa. **Nanotoxicology**, v. 17, n. 4, p. 289–309, 2023.

VIJAYARAJ, V. et al. Transfer and ecotoxicity of TiO_2 nanoparticles. **Environmental Science & Technology**, v. 52, n. 21, p. 12757–12764, 2018.

VISHNU, D. et al. Structural and ultrastructural changes in nanoparticle-exposed plants. 2019.

WAKABAYASHI, K. et al. Cell wall modification under lead stress. **Life**, v. 13, n. 2, 2023.

WANG, C. et al. Toxicity of α-Fe_2O_3 nanoparticles in *Artemia salina*. **Science of the Total Environment**, v. 598, p. 847–855, 2017.

WANG, G. et al. Sex-specific effects of fluoride and lead in zebrafish. **Ecotoxicology**, v. 31, n. 3, p. 396–414, 2022.

WANG, L. F. et al. Copper release from nanoparticles. **Water Research**, v. 68, p. 12–23, 2015.

WANG, X. et al. Nano-TiO_2 adsorption alters bioavailability and toxicity in zebrafish. **Frontiers in Environmental Science**, v. 10, 2022.

WEIR, A. et al. Titanium dioxide nanoparticles in food and personal care products. **Environmental Science & Technology**, v. 46, n. 4, p. 2242–2250, 2012.

WU, J. et al. Trophic transfer and toxicity of Ag and TiO_2 nanoparticles. **Environmental Science & Technology**, v. 55, n. 24, p. 16563–16572, 2021.

WU, Q. et al. Parental transfer of TiO_2 nanoparticles aggravates developmental toxicity. **Environmental Science: Nano**, v. 5, n. 12, p. 2952–2965, 2018.

WU, Q. et al. Transgenerational neurotoxicity in zebrafish. **Environmental Pollution**, v. 231, p. 471–478, 2017.

XIA, Q. et al. NRF2-HO-1/JNK-ERK signaling in zebrafish developmental toxicity. **Frontiers in Pharmacology**, v. 12, p. 642480, 2021.

YADAV, V. et al. Structural modifications of plant organs by metals. **Plant Physiology and Biochemistry**, 2021.

YANG, Y. et al. Toxic effects of bisphenol AF on zebrafish embryos. **Estuarine, Coastal and Shelf Science**, v. 233, p. 106540, 2020.

YE, C. et al. Biomarker responses in zebrafish. **Frontiers in Physiology**, v. 13, p. 907906, 2022.

YEŞİLBUDAK, B. Toxicological aspects and bioanalysis of nanoparticles. **Open Journal of Nano**, v. 8, n. 1, p. 22–35, 2023.

YU, F. et al. Toxicity of TPhP on zebrafish intestines. **Science of the Total Environment**, v. 908, p. 168212, 2024.

ZAHRA, Z. et al. Exposure route of TiO_2 nanoparticles and agro-environment impacts. **Nanomaterials**, 2020.

ZAVITRI, N. G. et al. Toxicity of ZnO nanoparticles in zebrafish. **Biomedical Reports**, v. 19, n. 6, p. 1–11, 2023.

ZHANG, M.; WU, C. Intestinal goblet cells and immune response. **Bioscience Reports**, v. 40, n. 10, p. BSR20201471, 2020.

ZHANG, P. et al. Species-specific toxicity of ceria nanoparticles to *Lactuca*. **Nanotoxicology**, v. 9, n. 1, p. 1–8, 2015.

ZHANG, W. et al. Uptake and toxicity of magnetic TiO_2 nanophotocatalysts. **Chemosphere**, v. 224, p. 658–667, 2019.

ZHAO, X. et al. Trophic transfer of metal nanoparticles. **Environmental Science & Technology**, v. 59, n. 13, p. 6812–6824, 2025.

ZHOU, Y. et al. Effects of nano-TiO_2 on TBPH toxicity. **Chemosphere**, v. 295, p. 133862, 2022.

ZHU, D. H. et al. Effects of Aroclor 1254 on zebrafish immunity. **Frontiers in Nutrition**, v. 9, p. 929925, 2022.

ZHU, S. et al. Toxicity of graphene oxide in *Artemia salina*. **Science of the Total Environment**, v. 595, p. 101–109, 2017.